THE ROLE OF THE BASAL GANGLIA IN SOMATOSENSORY-MOTOR INTERACTIONS: EVIDENCE FROM NEUROPHYSIOLOGY AND BEHAVIOR

EDITED BY: Matt J. N. Brown, Antonella Macerollo, Martijn Beudel and Robert Chen

PUBLISHED IN: Frontiers in Human Neuroscience, Frontiers in Systems Neuroscience and Frontiers in Neurology

frontiers Research Topics

frontiers

ISSN 1664-8714
ISBN 978-2-88963-475-0
DOI 10.3389/978-2-88963-475-0

About Frontiers

Frontiers is more than just an open-access publisher of scholarly articles: it is a pioneering approach to the world of academia, radically improving the way scholarly research is managed. The grand vision of Frontiers is a world where all people have an equal opportunity to seek, share and generate knowledge. Frontiers provides immediate and permanent online open access to all its publications, but this alone is not enough to realize our grand goals.

Frontiers Journal Series

The Frontiers Journal Series is a multi-tier and interdisciplinary set of open-access, online journals, promising a paradigm shift from the current review, selection and dissemination processes in academic publishing. All Frontiers journals are driven by researchers for researchers; therefore, they constitute a service to the scholarly community. At the same time, the Frontiers Journal Series operates on a revolutionary invention, the tiered publishing system, initially addressing specific communities of scholars, and gradually climbing up to broader public understanding, thus serving the interests of the lay society, too.

Dedication to Quality

Each Frontiers article is a landmark of the highest quality, thanks to genuinely collaborative interactions between authors and review editors, who include some of the world's best academicians. Research must be certified by peers before entering a stream of knowledge that may eventually reach the public - and shape society; therefore, Frontiers only applies the most rigorous and unbiased reviews.
Frontiers revolutionizes research publishing by freely delivering the most outstanding research, evaluated with no bias from both the academic and social point of view. By applying the most advanced information technologies, Frontiers is catapulting scholarly publishing into a new generation.

What are Frontiers Research Topics?

Frontiers Research Topics are very popular trademarks of the Frontiers Journals Series: they are collections of at least ten articles, all centered on a particular subject. With their unique mix of varied contributions from Original Research to Review Articles, Frontiers Research Topics unify the most influential researchers, the latest key findings and historical advances in a hot research area! Find out more on how to host your own Frontiers Research Topic or contribute to one as an author by contacting the Frontiers Editorial Office: researchtopics@frontiersin.org

THE ROLE OF THE BASAL GANGLIA IN SOMATOSENSORY-MOTOR INTERACTIONS: EVIDENCE FROM NEUROPHYSIOLOGY AND BEHAVIOR

Topic Editors:
Matt J. N. Brown, California State University, Sacramento, United States
Antonella Macerollo, University College London, United Kingdom
Martijn Beudel, University Medical Center Amsterdam, Netherlands
Robert Chen, University of Toronto, Canada

Citation: Brown, M. J. N., Macerollo, A., Beudel, M., Chen, R., eds. (2020). The Role of the Basal Ganglia in Somatosensory-Motor Interactions: Evidence from Neurophysiology and Behavior. Lausanne: Frontiers Media SA.
doi: 10.3389/978-2-88963-475-0

Table of Contents

frontiers in Human Neuroscience

EDITORIAL
published: 08 January 2020
doi: 10.3389/fnhum.2019.00451

Editorial: The Role of the Basal Ganglia in Somatosensory-Motor Interactions: Evidence From Neurophysiology and Behavior

Martijn Beudel[1]*, *Antonella Macerollo*[2], *Matt J. N. Brown*[3] and *Robert Chen*[4]

[1] Department of Neurology, Amsterdam Neuroscience Institute, Amsterdam University Medical Centre, Amsterdam, Netherlands, [2] School of Psychology, University of Liverpool, Liverpool, United Kingdom, [3] Department of Kinesiology, California State University Sacramento, Sacramento, CA, United States, [4] Division of Neurology, Department of Medicine, University of Toronto, Toronto, ON, Canada

Keywords: basal ganglia, deep brain stimulation, Parkinson's disease, dystonia, oscillations, somatosensory, motor

Editorial on the Research Topic

The Role of the Basal Ganglia in Somatosensory-Motor Interactions: Evidence From Neurophysiology and Behavior

Sensory-motor interactions offer critical mechanisms for how we move. Somatosensory information, from cutaneous, muscle, joint, and tendon receptors, are known to provide the central nervous system (CNS) with information about the body and the environment (e.g., objects). In turn, somatosensory input provided to the CNS can be relayed to motor areas to assist in the preparation, execution, and correction of movements.

The basal ganglia are known to receive input from both cortical somatosensory and motor areas, but the significance and the contribution of these interactions for various aspects of human movement remains enigmatic. A variety of different neurophysiological techniques have been used to investigate the role of the basal ganglia in somatosensory-motor interactions including electroencephalography (EEG), magnetoencephalography (MEG), magnetic resonance imaging (MRI), recordings from deep brain stimulation (DBS) electrodes, and combining DBS with transcranial magnetic stimulation (TMS) over the cortex.

Much of what is currently known about somatosensory-motor interactions has been derived from research combining neurophysiological techniques with behavioral measures of movement. In addition, behavioral and neurophysiology measurements in clinical populations affecting the basal ganglia, such as Parkinson's disease (PD), Huntington's disease (HD), and dystonia have been critical in advancing our understanding. Determining how somatosensory-motor interactions contribute to specific aspects of movements (e.g., initiation, inhibition, force production, timing) will help in understanding the role that these mechanisms contribute to sensorimotor pathophysiology of neurological disorders affecting the basal ganglia. Both animal and human research is critical to developing a thorough understanding of this topic. Furthermore, computational methods that consider the sensory-motor and connected biological system as a whole, including peripheral sensory receptor physiology, are integral to advancing knowledge on this topic.

In the Frontiers Research Topic, 12 papers (**Table 1**) have been published. Both from a methodological as well as from a theoretical view, many exciting contributions were published. The heterogeneity of the applied methods, e.g., movement analysis, diffusion tensor imaging (DTI), MEG, and non-invasive brain stimulation (NIBS), show how sophisticated the toolbox of the current neuroscience community is. In order to see how the frontier of the field has moved forward,

OPEN ACCESS

Edited and reviewed by:
Mingzhou Ding,
University of Florida, United States

***Correspondence:**
Martijn Beudel
m.beudel@amsterdamumc.nl

Specialty section:
This article was submitted to Brain Imaging and Stimulation, a section of the journal Frontiers in Human Neuroscience

Received: *13 November 2019*
Accepted: *06 December 2019*
Published: *08 January 2020*

Citation:
Beudel M, Macerollo A, Brown MJN and Chen R (2020) Editorial: The Role of the Basal Ganglia in Somatosensory-Motor Interactions: Evidence From Neurophysiology and Behavior. Front. Hum. Neurosci. 13:451. doi: 10.3389/fnhum.2019.00451

TABLE 1 | Summary of the published papers.

References	Type	(Brief) Title	(Unique) Technique	Disease
Beudel et al.	Perspective	Linking pathological oscillations to altered temporal processing in PD		PD
Cao et al.	Original	Dystonia cortico-subcortico coherence	LFP/MEG	Dystonia
Dubbioso et al.	Perspective	Fast intracortical sensorimotor integration	NIBS	PD
Feller et al.	Original	Sensory re-weighting for postural control in PD	Movement analysis	PD
Filip et al.	Original	Disruption of distinctive neural networks associated with ICD in PD	fMRI	PD
Filyushkina et al.	Original	Hyperactivity BGGL in PD during internally guided voluntary movements	fMRI	PD
Hirschmann et al.	Original	Longitudinal recordings reveal transient increase of alpha low beta in the STN	LFP/EEG	PD
Lee et al.	Original	Abnormal phase coupling in PD	EEG, NIBS	PD
Macerollo et al.	Original	Da modulation of sensory attenuation in PD	SSEP	PD
Martino et al.	Original	Motor timing in Tourette	DTI	Tourette
Milardi et al.	Review	CTX—BGGL—cerebellar circuitry		
Saxena et al.	Original	Modulation of GPi activity during hand movement	MER non-human primate	

PD, Parkinson's Disease; ICD, impulse control disorder; BGGL, basal ganglia; STN, subthalamic nucleus; CTX, cortex; GPi, internal part of the globus pallidus; LFP, local field potentials; MEG, magnetoencephalography; fMRI, functional MRI; NIBS, non-invasive brain stimulation; SSEP, somatosensory evoked potentials; DTI, diffusion tensor imaging; MER, microelectrode recordings.

one could ask oneself to which extent a contribution could have been realized 10 years ago. To answer this question, it is not only of relevance whether the method (hardware/software) was available 10 years ago but also whether the work builds on new ideas about the understanding of the role of the basal ganglia in health and disease.

One clear novelty in the field, that was not available 10 years ago, is the use of fully implantable DBS devices that not only can stimulate but can also record local field potentials (LFP's). The use of these devices as described by Hirschmann et al. gives an outstanding example of how these new technological advances can make invasive recordings from deep brain nuclei endlessly more easy, comfortable, and more comprehensive. The most important reason for this is that it is no longer necessary to perform LFP recordings in the intra- or immediate post-operative phase but that it is possible to conduct these recordings at any moment. Given the frailty of patients in the intra- or immediate post-operative after DBS implantation, conducting LFP research will be far less demanding from a patient perspective. One other crucial difference is that longitudinal recordings can be performed where changes in somatosensory-motor interactions can be studied over longer periods which might become a powerful tool to assess the efficacy of DBS or to develop biomakers, i.e., "physiomarkers" (Kühn and Volkmann, 2017) for adjusting DBS. The latter is called adaptive DBS (aDBS) and is currently a subject of intense inquiry (Habets et al., 2018).

Another development is the perception of the relevance of basal ganglia pathways beyond the direct, indirect and hyperdirect pathways as described by Milardi et al. Next to these "traditional" pathways, the traditional view that cerebellum and basal ganglia communicate via the cerebral cortex no longer holds and more relevant pathways exist between cerebellum and basal ganglia. These bilateral connections, i.e., cerebellum to basal ganglia and vice versa, have been revealed by state of art imaging methods like optogenetics showing short-latency activation (10 ms) of the basal ganglia after optogenetic stimulation of the cerebellum (Chen et al., 2014). These novel findings can be attributed to the sophistication of these new techniques over the last decade and would not have been possible 10 years ago. For this example, it is clear that new technologies clearly add to our understanding of the basal ganglia and restore concepts that have previously been discarded (Caligiore et al., 2017). Furthermore, the evidence for functional significance of the basal ganglia-cerebellar connections, and how these connections facilitate co-operation is growing and opens an entirely new perspective on the pathophysiology of movement disorders, like dystonia (Darby et al., 2019; Fung and Peall, 2019). Finally, these basal-ganglia cerebellar connections can now be functionally restored using DBS of the subthalamic nucleus (STN), leading to improved (sensori) motor learning (de Almeida Marcelino et al., 2019).

Next to the technological developments and new neuro-anatomical insights, a third recent and important development is the further understanding of the neural computations performed in the basal ganglia. In the contribution of Saxena et al. new physiological insights of the role of the basal ganglia in action selection have been provided. Traditionally, the way in which basal ganglia exerted their influence on each other or adjacent structures was thought to be based on the firing rate of individual neurons. This firing rate model was, however, challenged by the evidence that making a lesion can yield the same effect as stimulating the same structure using DBS and DBS of the same structure with the same stimulation characteristics can improve both hypokinetic (e.g., Parkinson's disease) and hyperkinetic (e.g., dystonia) movement disorders. In their paper, Saxena et al. showed that during movement planning and execution information encoding in the basal ganglia occurs in a highly localized manner via sudden emergence and suppression of oscillatory activities. More specifically, during movement oscillations in the gamma band (35–90 Hz) emerge and beta (13–30 Hz) oscillations decrease. This experimental

evidence is in line with recent conceptions that neural activity in the basal ganglia is not strictly inhibitory or excitatory based on the firing rate but more on the firing pattern. In PD, strong evidence is available that shows abnormal oscillatory activity in this beta band that is correlated with the severity of motor symptoms (Ray et al., 2008). As such, the role of DBS might be more one of disruption of pathological oscillatory activity instead of simple inhibition or excitation (Chiken and Nambu, 2016).

This evident progress in both technology, basal ganglia connectivity and computational processing will find its way to clinical practice and will open up a plethora of research possibilities in the coming decade.

AUTHOR CONTRIBUTIONS

All authors have contributed to the editorial and critically reflected on the successive versions.

REFERENCES

Caligiore, D., Pezzulo, G., Baldassarre, G., Bostan, A. C., Strick, P. L., Doya, K., et al. (2017). Consensus paper: towards a systems-level view of cerebellar function: the interplay between cerebellum, basal ganglia, and cortex. *Cerebellum* 16, 203–229. doi: 10.1007/s12311-016-0763-3

Chen, C. H., Fremont, R., Arteaga-Bracho, E. E., and Khodakhah, K. (2014). Short latency cerebellar modulation of the basal ganglia. *Nat. Neurosci.* 17, 1767–1775. doi: 10.1038/nn.3868

Chiken, S., and Nambu, A. (2016). Mechanism of deep brain stimulation: inhibition, excitation, or disruption? *Neuroscientist* 22, 313–322. doi: 10.1177/1073858415581986

Darby, R. R., Joutsa, J., and Fox, M. D. (2019). Network localization of heterogeneous neuroimaging findings. *Brain* 142, 70–79. doi: 10.1093/brain/awy292

de Almeida Marcelino, A. L., Horn, A., Krause, P., Kühn, A. A., and Neumann, W.-J. (2019). Subthalamic neuromodulation improves short-term motor learning in Parkinson's disease. *Brain* 142, 2198–2206. doi: 10.1093/brain/awz152

Fung, W. K. W., and Peall, K. J. (2019). What is the role of the cerebellum in the pathophysiology of dystonia? *J. Neurol.* 266, 1549–1551. doi: 10.1007/s00415-019-09344-7

Habets, J. G. V., Heijmans, M., Kuijf, M. L., Janssen, M. L. F., Temel, Y., and Kubben, P. L. (2018). An update on adaptive deep brain stimulation in Parkinson's disease. *Mov. Disord.* 33, 1834–1843. doi: 10.1002/mds.115

Kühn, A. A., and Volkmann, J. (2017). Innovations in deep brain stimulation methodology. *Mov. Disord.* 32, 11–19. doi: 10.1002/mds.26703

Ray, N. J., Jenkinson, N., Wang, S., Holland, P., Brittain, J. S., Joint, C., et al. (2008). Local field potential beta activity in the subthalamic nucleus of patients with Parkinson's disease is associated with improvements in bradykinesia after dopamine and deep brain stimulation. *Exp. Neurol.* 213, 108–113. doi: 10.1016/j.expneurol.2008.05.008

Conflict of Interest: The authors declare that the research was conducted in the absence of any commercial or financial relationships that could be construed as a potential conflict of interest.

frontiers in Human Neuroscience

ORIGINAL RESEARCH
published: 21 November 2018
doi: 10.3389/fnhum.2018.00462

Disruption of Multiple Distinctive Neural Networks Associated With Impulse Control Disorder in Parkinson's Disease

Pavel Filip[1,2*], *Pavla Linhartová*[3], *Pavlína Hlavatá*[3], *Rastislav Šumec*[1], *Marek Baláž*[1], *Martin Bareš*[1,4] *and Tomáš Kašpárek*[3]

[1] First Department of Neurology, Faculty of Medicine, Masaryk University and University Hospital of St. Anne, Brno, Czechia, [2] Center for Magnetic Resonance Research (CMRR), University of Minnesota, Minneapolis, MN, United States, [3] Department of Psychiatry, Faculty of Medicine, Masaryk University and University Hospital Brno, Brno, Czechia, [4] Department of Neurology, School of Medicine, University of Minnesota, Minneapolis, MN, United States

The phenomenon of impulsivity in Parkinson's disease appears as an arduous side effect of dopaminergic therapy with potentially detrimental consequences for the life of the patients. Although conceptualized as a result of non-physiologic chronic dopaminergic stimulation, recent advances speculate on combined disruption of other networks as well. In the search for neuroanatomical correlates of this multifaceted disturbance, this study employs two distinct, well-defined tasks of close association to motor inhibition and decision-making impulsivity, Go/No Go and Delay discounting. The fMRI and functional connectivity analysis in 21 Parkinson's disease patients, including 8 patients suffering from severe impulse control disorder, and 28 healthy controls, revealed in impulsive Parkinson's disease patients not only decreased fMRI activation in the dorsolateral prefrontal cortex and bilateral striatum, but also vast functional connectivity changes of both caudate nuclei as decreased connectivity to the superior parietal cortex and increased connectivity to the insular area, clearly beyond the commonly stated areas, which indicates that orbitofronto-striatal and mesolimbic functional disruptions are not the sole mechanisms underlying impulse control disorder in Parkinson's disease. Ergo, our results present a refinement and synthesis of gradually developing ideas about the nature of impulsive control disorder in Parkinson's disease—an umbrella term encompassing various behavioral deviations related to distinct neuronal networks and presumably neurotransmitter systems, which greatly exceed the previously envisioned dopaminergic pathways as the only culprit.

Keywords: impulse control disorder, Parkinson's disease, fMRI, functional connectivity, Go/No Go task, delay discounting task

OPEN ACCESS

Edited by:
Martijn Beudel, University Medical Center Groningen, Netherlands

Reviewed by:
Federico Giove, Centro Fermi—Museo storico della fisica e Centro studi e ricerche Enrico Fermi, Italy
Michele Poletti, Azienda Sanitaria Unità Locale di Reggio Emilia, Italy

***Correspondence:**
Pavel Filip
pvlfilip@gmail.com

Received: *06 June 2018*
Accepted: *01 November 2018*
Published: *21 November 2018*

Citation:
Filip P, Linhartová P, Hlavatá P, Šumec R, Baláž M, Bareš M and Kašpárek T (2018) Disruption of Multiple Distinctive Neural Networks Associated With Impulse Control Disorder in Parkinson's Disease. Front. Hum. Neurosci. 12:462. doi: 10.3389/fnhum.2018.00462

INTRODUCTION

While considered a mere movement disorder in the times past, Parkinson's disease (PD) is now generally seen as a complex dimension of multiple motor, cognitive, and behavioral components, with neuropsychiatric affections as depression, apathy, and impulse control disorders (ICDs) being the most salient of the non-motor symptoms (Cooney and Stacy, 2016). Impulsivity, commonly defined as the lack of behavioral inhibition and/or premature decision making, entails compulsive

or repetitive engagement in certain activities, closely associated with the inability to foresee or learn from negative outcomes. Specifically in PD, a diverse spectrum of maladaptive behaviors is included in ICDs such as pathological gambling, paraphilias, excessive shopping, or binge eating, with the list sometimes extended by closely related phenomena and purposeless, repetitive behaviors as punding, hoarding, and hobbyism (Weintraub et al., 2015). Given the paucity of therapeutic options and potentially devastating consequences, inter alia, financial ruin, divorce, or loss of employment, the recognition of these aberrant behaviors in routine clinical practice and the delineation of precise neurobiological correlates and causes are of paramount importance.

ICDs are thought to be triggered by the interaction of chronic dopaminergic medication, especially dopamine agonist therapy (Garcia-Ruiz et al., 2014), and pathophysiological vulnerabilities, either pre-existing before the onset of the disease, or associated directly with neurodegeneration in progressing PD (Vriend, 2018), as occurrence of ICDs in treatment-naïve PD patients is very similar to the general population (Weintraub et al., 2013). The underlying neuropathology of ICD probably involves not only the overstimulation of dopaminergic reward-related pathways, hence assigning excessive salience to incentives (Robinson and Berridge, 1993), but also the interference in D2-signaling pauses in the ventral striatum (Frank et al., 2004; Vriend, 2018), which impairs the encoding of harmful behavior, i.e., prevents negative-feedback learning, and leaves D1-receptor-facilitated positive reinforcement intact. Moreover, dopamine receptor abnormities (Steeves et al., 2009; Vriend et al., 2014) support the hypothesis of PD pathology being a direct predisposition to ICD.

The previous body of MRI research in ICD has firmly established disturbances not only in the striatal regions (Gescheidt et al., 2012), but also in the limbic cortex during tasks associated with visual sexual cues (Politis et al., 2013), probabilistic learning (Voon et al., 2010), and risk taking (Voon et al., 2011a), also suggesting the dysregulation of mesolimbic dopaminergic pathways. Nonetheless, this hypothesis was partially countered by structural MRI (Biundo et al., 2015), perfusion SPECT imaging (Cilia et al., 2011), tracers with high affinity for extrastriatal D2/D3 receptors (Buckholtz et al., 2010; Ray et al., 2012) uncovering dysfunctions beyond the sole disturbance of the mesolimbic system and striatum.

With this discrepancy in mind, the presented cross-sectional study used a multimodal approach encompassing behavioral, fMRI activation and functional connectivity analysis in two distinctive tasks reflecting various aspects of impulsivity to elucidate the neurobiology underlying ICD in PD further—specifically motor response inhibition in a Go/No Go (GNG) task and decision-making impulsivity in a Delay Discounting (DD) task. Moreover, only PD patients with truly detrimental effects of ICD were selected to avoid borderline effects for activities, which may be considered not genuinely abnormal or deviant from premorbid behavior. Our premise anticipated not only affections in the striatum and mesolimbic system, but also the recruitment and connectivity changes from the striatum to other cortical areas beyond the dopamine regulated network in both tasks. Furthermore, we intended to evaluate eventual overlap of neuroanatomical signatures of impulsivity-eliciting stimuli in ICD-PD patients in both tasks to delineate the truly common nodes for distinctive, albeit impulse-control-oriented activity types.

Abbreviations: MRI, magnetic resonance imaging; fMRI, functional magnetic resonance imaging; BOLD, blood-oxygen-level dependent; SPECT, Single-photon emission computed tomography; PD, Parkinson's disease; ICD, impulse control disorder; GNG, Go/No Go task; DD, Delay Discounting task.

METHODS

Subjects

A total of twenty-eight PD patients were recruited at the 1st Department of Neurology, University Hospital of St. Anne, Brno, Czech Republic, based on the UK Brain Bank Criteria (Hughes et al., 1992). This cohort included specifically selected ten PD patients with significant signs of ICD affecting their day-to-day lives. Demographic (gender, age) and neurologic data [Hoehn & Yahr stage (Hoehn and Yahr, 1967), age at the onset of the disease, disease duration, L-dopa equivalent dose (Tomlinson et al., 2010)] were recorded, complemented with depression and impulsivity evaluation [Montgomery-Asberg Depression Scale (MADRS) (Montgomery and Asberg, 1979) and Barratt scale (Patton et al., 1995), respectively; see the **Table 1**]. All the assessments of PD patients, including the fMRI acquisition, were performed on medication. Additionally, we recruited twenty-nine healthy controls, who underwent the same MRI, and neuropsychological protocols as PD patients.

We did not include individuals with conspicuous cognitive impairment [defined as Mini-mental state examination score of <27 (Folstein et al., 1975)], comorbid psychotic, affective or autistic spectrum disorder, and MRI contraindications. Furthermore, subjects with evidence of significant vascular or space occupying lesions in MRI scans and head motion beyond 3.0 mm during fMRI acquisition were excluded as well, leaving 13 non-impulsive PD patients, 8 ICD-PD patients, and 28 healthy controls.

The study was approved by the Institutional Review Board of the University Hospital of St. Anne, Brno, Czech Republic. A written informed consent was provided by each subject in accordance with the Declaration of Helsinki.

Tasks

Before entering the MRI system, the subjects underwent a training session in both tasks to avoid misunderstanding of the instructions and the interference of eventual learning effects in the fMRI results. The subjects responded to stimuli by pressing a button with the dominant hand.

Go/No Go

The task began with either a red or a green fixation cross displayed for the period of 2–6 s. The subjects were notified in advance that the green fixation cross (1/3 of runs) would always be followed by the Go stimulus, thus removing the need for alertness in this case. The runs with the red fixation cross (2/3

TABLE 1 | Demographics, neurologic, neuropsychologic and behavioral data of PD subgroups and healthy controls.

	Non-impulsive PD ($n = 13$)	ICD-PD ($n = 8$)	Healthy controls ($n = 28$)
Gender (M/F)	5/8	6/2	14/14
Age (years)	71.0 [4.0]	65.0 [5.7]	66.4 [6.9]
NEUROLOGIC DATA			
H&Y stage	2.23 [0.60]	2.25 [0.53]	–
Age at the onset	65.39 [5.44]	55.25 [6.20]	–
Disease duration	5.62 [3.64]	9.75 [3.99]	–
L-dopa equivalent dose	926.67 [209.38]	1061.88 [270.70]	–
NEUROPSYCHOLOGIC DATA			
MADRS	3.31 [4.09]	1.63 [3.11]	0.28 [0.76]
Barratt score	53.54 [4.98]	60.88 [8.89]	55.00 [6.10]
GNG TASK–SUCCESS RATES			
Green cross-Go	0.89 [0.27]	0.96 [0.02]	0.93 [0.11]
Red cross-Go	0.99 [0.03]	0.89 [0.24]	0.95 [0.10]
Red cross-No Go	0.94 [0.04]	0.89 [0.11]	0.95 [0.05]
GNG TASK – REACTION TIMES[s]			
Green cross - Go	0.39 [0.15]	0.41 [0.09]	0.42 [0.11]
Red cross - Go	0.50 [0.07]	0.45 [0.16]	0.48 [0.09]
DD TASK			
Control success rate	0.95 [0.03]	0.85 [0.17]	0.97 [0.02]
Easy - immediate vs. delayed response ratio	0.44 [0.22]	0.43 [0.26]	0.47 [0.25]
Hard - immediate vs. delayed response ratio	0.41 [0.37]	0.37 [0.35]	0.48 [0.36]

The values are stated in the format average [standard deviation]. DD, Delay Discounting task; F, female; GNG, Go/No Go task; H&Y, Hoehn & Yahr; ICD, impulse control disorder; M, male; PD, Parkinson's disease.

of cases) could be followed by either the Go stimulus (letter "A" displayed in the middle of the screen, presented in 1/3 of all the cases) or the No Go stimulus (letter "B" displayed in the middle of the screen, presented also in 1/3 of all the cases). The stimulus duration was 0.2 s, succeeded by a 2 s empty screen. The subject was supposed to press or avoid pressing a key based on the stimulus type. The whole task consisted of 4 blocks, each with 54 stimuli [18 Green cross–Go (GcG), 18 Red cross–Go (RcG), 18 Red cross–No Go (RcNG) runs]. The blocks were divided by short breaks.

Delay discounting

During this task, the subject was shown two options—an immediate and a delayed reward, with random arrangement at the left or the right side. The task included 3 types of questions: (I) difficult questions, with rewards of similar subjective value as determined in the pre-acquisition training part utilizing a well-documented and widely accepted approach (Mazur, 1987); (II) easy questions with options of distinctive subjective value, and (III) control questions, where one of the responses was associated with significant objective advantage over the other (4 types: naught now vs. some reward later; some reward now vs. naught later; the same reward now and later; higher reward now than later). The options were shown for 7 s, followed by a 1-second-long blank screen. The subject was required to press a key corresponding to the chosen option, highlighting the desired response. The whole task consisted of three blocks, each with 48 stimuli (16 questions of each type). The blocks were divided by short breaks.

MRI Data Acquisition

MRI scanning was performed using a 3 Tesla whole body MRI scanner SIEMENS MAGNETOM Prisma syngo (Siemens Medical Systems, Erlangen, Germany) at the Central European Institute of Technology, Brno, Czech Republic. At the beginning, a high-resolution anatomical T1-weighted scan was acquired with the following parameters: magnetization-prepared rapid gradient-echo (MPRAGE) sequence [repetition time (TR) = 2,300 ms, echo time (TE) = 2.34 ms, flip angle (FA) = 8°, voxel size 1.00 × 1.00 × 1.00 mm, slice thickness 1.00 mm, matrix 240 × 224 × 224]. Subsequently, whole brain fMRI was performed with the parameters: TR = 2280 ms, TE = 35.0 ms, FA = 75°, voxel size 3 × 3 × 3 mm, 39 sagittal slices, field of view 192 × 192 mm, total number of volumes 153 per one block of the GNG task (i.e., 612 volumes in total) and 175 per one block of the DD task (i.e., 525 volumes in total).

Analysis of Demographic and Behavioral Data

Firstly, equivalence analysis [two-one-sided test (Schuirmann, 1987)] was used to confirm the absence of significant differences in basic demographic parameters between PD patients and healthy controls (gender, age). Furthermore, where we expected the subgroups to differ, analysis of variance (ANOVA) was used to evaluate the parameters in the individual groups (MADRS, Barratt score).

In the behavioral analysis of the performance in the two tasks, the primary parameters of interest in the GNG task included the

success rate and reaction times in individual stimuli variants and in the DD task, the percentage of correct responses in the control trials, and immediate vs. delayed responses for easy and hard trials. The average success rates and reaction/response times were determined for each subject in order to use parametric statistical analyses. ANOVA was used to compare the individual subject groups—non-impulsive PD, ICD-PD and healthy controls. All the analyses were performed using Statistica 13 (Statsoft Inc., Oklahoma, USA).

Analysis of fMRI Data

MRI data were processed and analyzed using SPM12 (Wellcome Department of Cognitive Neurology, London, UK) implemented in Matlab R2017b (Mathworks Inc., Natick, MA, USA). The preprocessing of fMRI images included the realignment to correct for the movements of the subject's head. As stated in the section Subjects, the threshold of 3 mm shift and 3° rotation in any direction was implemented, excluding 8 subjects in total. Subsequently, co-registration of functional and anatomical images and interpolation in time were performed, followed by the spatial normalization into the stereotactic Montreal Neurological Institute (MNI) space and spatial smoothing (isotropic Gaussian kernel of 8 mm full-width at half-maximum). The data were high-pass filtered with a Gaussian kernel filter of 128 s.

The first level general linear model of BOLD activations in the GNG task included the time windows between the stimulus presentation (letter "A" or "B" distinguishing the Go and No Go runs) and key press by the subject. The individual design matrix for each subject distinguished the GcG runs, RcG runs, and RcNG runs, including the accuracy of the response (key pressed correctly in the Go task and key not pressed in the No Go task) and the head movements in all the directions as nuisance covariates, thus providing three contrast maps. These were then submitted to the second level full factorial design (3 × 3) with the following factors: subject subgroups (non-impulsive PD, ICD-PD, healthy controls) and 3 run types (GcG, RcG, RcNG), and the age and gender as covariates of non-interest.

In the DD task, the first level general linear model consisted of the time windows between the stimulus presentation (2 windows with 2 options to choose from) and the subject's key press. The design matrix of individual subjects included the control, easy and hard task types, with the head movements as nuisance covariates. Once again, the three generated contrast maps were submitted to the second level full factorial design (3 × 3) analysis with the following factors: subject subgroups (non-impulsive PD, ICD-PD, healthy controls) and 3 run types (control, easy and hard), and the age and gender as covariates of non-interest.

Furthermore, we analyzed the differences in the individual sub-groups in the task-related connectivity. The analysis of psychophysiological interactions [PPI (Friston et al., 1997)] focused on the connectivity of striatum bilaterally, specifically the caput of the caudate nuclei, as defined by the Automated Anatomical Labeling (AAL) atlas (Tzourio-Mazoyer et al., 2002; Maldjian et al., 2003), repeatedly emerging in the previous activation analysis. The time course of these two individual seeds (the caput of the left and the right caudate nucleus) was extracted as the average over the atlas-defined volume of interest in both tasks. The two created first level models consisted of the extracted series, the run type regressor (GcG, RcG, and RcNG in the GNG task and control, easy and hard in the DD task), the PPI regressor, and the head movements in all the directions as nuisance covariates, thus providing three individual t-contrasts. These were then submitted to the two subsequent second level analyses with the full factorial designs corresponding to the constructs in the activation analysis, i.e., subject groups (non-impulsive PD, ICD-PD, healthy controls) and 3 run types (GcG, RcG, RcNG, and control, easy and hard in the GNG and DD tasks, respectively). Furthermore, age and gender were included as nuisance variables.

Statistical Thresholds

Due to the relative paucity of data points, the behavioral and demographic results are presented at the significance level of $p < 0.05$. Secondly, the activation analysis results were considered significant at $p < 0.05$, family-wise error (FWE)-corrected for multiple comparisons at the voxel level (with the cluster threshold of 40 contiguous voxels). And because of the nature and utilized contrasts, the PPI analysis adopted a less stringent threshold of $p < 0.05$, FWE-corrected for multiple comparisons at the cluster level (voxel-wise threshold of $p < 0.001$, uncorrected, small volume correction, cluster threshold of 40 contiguous voxels).

RESULTS

Characteristics of the Subjects and Behavioral Performance

The two-one-sided test showed no difference in age ($p = 0.045$) and gender ($p = 0.035$) between the PD patients and controls (with 5-year and 25% mean difference considered clinically relevant for the age and the gender, respectively). However, implementing the same hypothesized mean differences, the subgroups of ICD-PD patients and non-impulsive PD patients cannot be considered equivalent ($p > 0.2$ for both age and gender). As for the clinical data, the ICD-PD and non-impulsive PD groups had similar modified Hoehn & Yahr stage ($p < 0.001$) and L-dopa equivalent dose ($p = 0.37$; with 1 stage and 300 mg L-dopa equivalent dose mean difference considered clinically relevant). Nonetheless, there was a significant difference in both the age at the PD onset and disease duration ($p > 0.20$ for both comparisons, with 5-year and 2-year difference considered clinically relevant, respectively).

Moreover, ANOVA revealed significant differences among the subgroups in both MADRS [$F_{(2,47)} = 6.64$, $p = 0.003$] and Barratt scale [$F_{(2,47)} = 3.57$, $p = 0.036$], with the highest depression scores found in the non-impulsive PD group, and, the highest impulsivity scores, as expected, in the ICD-PD group.

ANOVA in the GNG task found no significant between-group differences in the success rates [$F_{(2,47)} = 0.46$, 1.42 and 2.06 in the GcG, RcG, and RcNG tasks, respectively, with p >0.10 for all the comparisons) and reaction times [$F_{(2,47)} = 0.24$ and 0.62 for GcG and RcG tasks, respectively, with $p > 0.50$ for both comparisons]. No group differences were revealed also in the analysis of the immediate vs. delayed response ratios in the easy and hard stimuli

types in the DD task [$F_{(2,47)}$ =0.12 and 0.39 for easy and hard, respectively, with p >0.50 for both comparisons]. Nonetheless, a significant distinction was found in the ratio of correct responses to the control task [$F_{(2,47)} = 8.10$, $p = 0.001$], with lower success rate in the ICD-PD patients. For more information, see the **Table 1**.

Activation and Connectivity Analysis

Due to the sheer extent of acquired results, only data relevant for ICD-PD patients are reported to avoid the dilution of consequential outcomes.

Between-group contrasts revealed the following differences in the combined outcome of all stimuli types (not distinguishing between the Go and No Go runs in the GNG task, and control, easy and hard stimuli in the DD task):

A. **All PD patients > Healthy controls**—As illustrated in the **Figure 1A** and detailed in the **Table 1**, PD patients had significantly higher activation in various cortical areas in both tasks, including the left supplementary motor cortex, bilateral fusiform gyrus (GNG task), and vast cortical areas around the left central sulcus, in both thalami and both lobuli VI of the cerebellum (DD task).

B. **Healthy controls > All PD patients**—PD patients showed lower activity in both caudate nuclei and angular gyri (GNG task) and left middle temporal gyrus and anterior cingulate (DD task; see **Figure 1B**, **Table 1**).

C. **Non-impulsive PD patients > ICD-PD patients**—Right Brodmann area 8 (GNG task) and right caudate (DD task) were less active in ICD-PD patients (see **Figure 1C**, **Table 1**). The effects of the reverse contrast failed to reach the predetermined significance thresholds.

D. **Healthy controls > ICD-PD patients**—The hypoactivity of caudate nuclei was also implicated in this contrast in PD-ICD patients (left-side in the GNG task, right side in the DD task). Moreover, right dorsolateral prefrontal cortex (DLPFC) and left middle temporal lobe were less active in PD-ICD patients (see **Figure 1D**, **Table 1**). Again, effects of the reverse contrast were not significant.

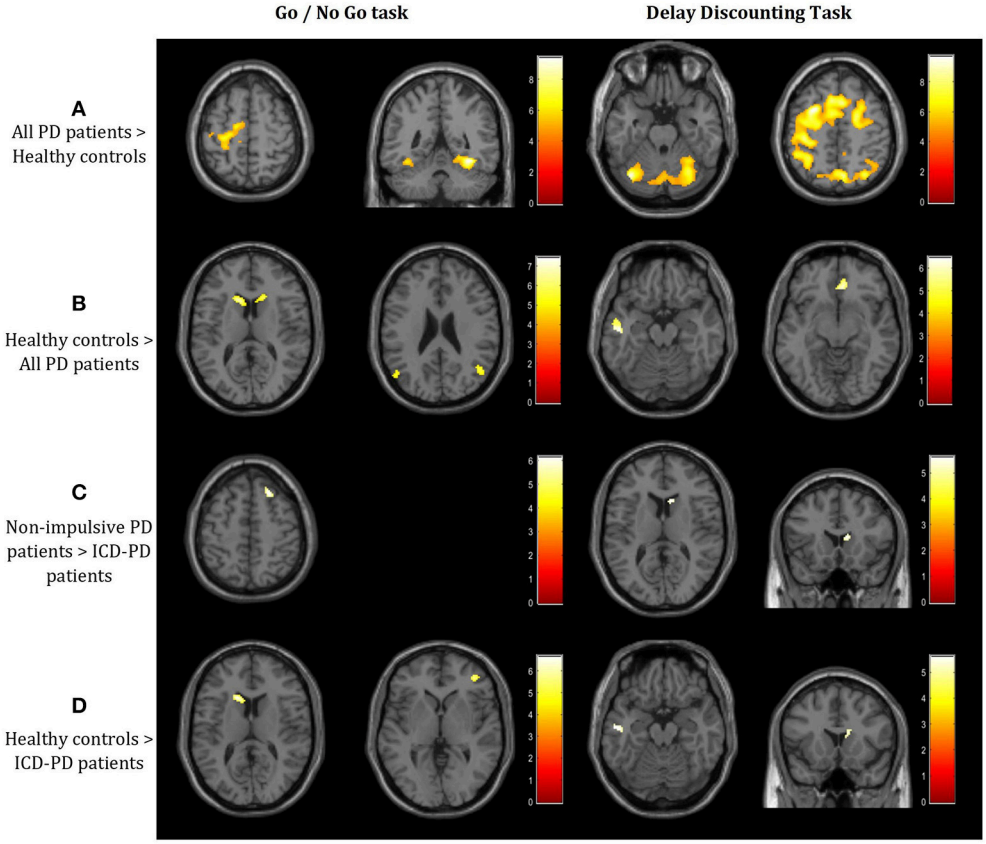

FIGURE 1 | Results of the 3 × 3 full factorial design (3 subgroups vs. 3 stimuli types) in 2 tasks – Go/No Go (GNG) and Delay Discounting (DD; $p < 0.05$, FWE-corrected at the voxel level; T-contrasts, threshold T = 4.73 for both GNG and DD tasks). (**A**) Increased activation in the right precentral, both fusiform gyri, cerebellum, and vast precentral and postcentral areas, including the dorsolateral prefrontal cortex in the whole cohort of Parkinson's disease (PD) patients when compared to healthy controls. (**B**) Decreased activation in bilateral caudate, angular gyri, left middle temporal and right cingulate gyrus. **(C)** Decreased activation in the superior frontal gyrus and right striatum in ICD-PD patients when compared to non-impulsive PD patients. (**D**) Decreased activation in both left and right caudate and the right dorsolateral prefrontal cortex in PD patients with impulsivity when compared to healthy controls. Laterality conventions with the right side in the figure corresponding to the right side of the scanned area were implemented. See **Table 2** for detailed statistical results and anatomical localization of clusters.

TABLE 2 | Anatomical localization of clusters in the activation analysis in the Go/No Go and Delay Discounting tasks.

	Anatomical regions	Brodmann area	Side	Volume (in voxels)	p-value (SVC)	T-score of local max	MNI coordinates of local maxima		
Go/No go task	**ALL PD PATIENTS > HEALTHY CONTROLS**								
	Fusiform gyrus	BA 37	R	434	<0.001	9.42	34	−48	−14
	SMA	BA 6	L	927	<0.001	7.16	−8	−14	48
	Precentral gyrus	BA 6	L	117	<0.001	6.44	−54	0	42
	Fusiform gyrus	BA 37	L	103	<0.001	6.40	−38	−50	−16
	SMA, middle cingulate	BA 32, 6	L	141	<0.001	6.36	−12	10	42
	SMA	BA 6	R	86	<0.001	6.18	12	16	44
	Postcentral gyrus		L	143	<0.001	6.10	−34	−20	40
	Calcarine sulcus		L	52	0.002	5.62	−10	−68	10
	Supramarginal gyrus	BA 40	L	58	0.002	5.57	−48	−40	32
	Calcarine sulcus		R	75	0.002	5.56	14	−72	12
	Cuneus		R	73	0.002	5.51	−10	−88	28
	Precentral gyrus	BA 6	R	55	0.003	5.47	36	4	46
	HEALTHY CONTROLS > ALL PD PATIENTS								
	Inferior occipital lobe	BA 18	L	76	<0.001	7.45	−28	−90	−6
	Inferior occipital lobe	BA 18	R	82	<0.001	7.03	34	−84	−6
	Caudate		L	97	<0.001	6.82	−12	20	14
	Caudate		R	43	<0.001	6.18	18	24	14
	Angular gyrus	BA 39	R	50	0.002	5.60	48	−60	24
	Angular gyrus	BA 39	L	46	0.002	5.43	−50	−70	26
	NON-IMPULSIVE PD PATIENTS > ICD-PD PATIENTS								
	Frontal superior gyrus	BA 8	R	60	<0.001	6.16	22	28	56
	HEALTHY CONTROLS > ICD-PD PATIENTS								
	Superior frontal gyrus	BA 8	R	70	<0.001	6.68	22	28	54
	Caudate		L	62	<0.001	6.38	−14	20	14
	DLPFC	BA 10	R	48	0.001	5.67	40	46	4
Delay Discounting Task	**ALL PD PATIENTS > HEALTHY CONTROLS**								
	Precentral gyrus, SMA	BA 6	L	17,823	<0.001	9.72	−26	8	50
	Thalamus		L	1,756	<0.001	9.08	−10	−18	4
	Thalamus		R				14	−16	2
	Cerebellum, lobule VI		R	2,361	<0.001	8.85	24	−92	−4
	Cerebellum, lobule VI		L				−36	−68	−24
	Cingulate gyrus	BA 31	R	152	<0.001	6.64	10	−40	46
	Supramarginal gyrus	BA 40	L	52	0.001	5.76	−54	−44	24
	Cerebellum, vermis III		R	65	0.001	5.75	2	−44	−18
	Dorsolateral prefrontal cortex	BA 46	R	54	0.002	5.60	50	46	6
	HEALTHY CONTROLS > ALL PD PATIENTS								
	Middle temporal gyrus	BA 21	L	145	<0.001	6.48	−50	−14	−20
	Dorsal anterior cingulate area	BA 32	R	40	<0.001	6.10	6	34	−10
	NON-IMPULSIVE PD PATIENTS > ICD-PD PATIENTS								
	Caudate		R	45	0.003	5.51	12	18	12
	ICD-PD PATIENTS > HEALTHY CONTROLS								
	Middle frontal lobe	BA 6	L	217	<0.001	7.25	−26	8	50
	Thalamus		L	640	<0.001	6.75	−8	−16	2
	Thalamus		R				10	−26	−4
	Lingual gyrus	BA 30	L	789	<0.001	6.73	−22	−70	6
	Precentral gyrus	BA 6	R	81	<0.001	6.37	50	0	34
	Precentral gyrus	BA 6	R	216	<0.001	6.36	22	−2	48

(Continued)

TABLE 2 | Continued

Anatomical regions	Brodmann area	Side	Volume (in voxels)	p-value (SVC)	T-score of local max	MNI coordinates of local maxima		
Fusiform gyrus		R	85	<0.001	6.33	36	−64	−10
Precentral gyrus	BA 6	L	262	<0.001	6.16	−36	−12	34
Inferior parietal lobe	BA 40	L	154	0.001	5.69	−28	−48	32
Lingual gyrus	BA 30	L	63	0.008	5.22	−16	−52	2
HEALTHY CONTROLS > ICD-PD PATIENTS								
Caudate		R	59	0.002	5.63	14	14	20
Middle temporal lobe	BA 21	L	50	0.002	5.60	−50	−14	−18

Clusters significant at $p < 0.05$, FWE-corrected for multiple comparisons at the voxel level (with the cluster threshold of 40 contiguous voxels). Abbreviations: BA, Brodmann area; DD, Delay Discounting task; DLPFC, dorsolateral prefrontal cortex; few, family-wise error; GNG, Go/No Go task; ICD, Impulse control disorder; L, left; MNI, Montreal Neurological Institute; PD, Parkinson's disease; R, right; SMA, supplementary motor area.

Further contrasts of PD-ICD patients, including interaction analyses with the task types, failed to reveal any significant clusters at the predetermined threshold.

The seeds for the PPI analysis were localized in the striatum, with more precise focus on both the heads of nuclei caudate based on the activation analysis results above. As the more relevant contrasts using stimuli supposedly associated with higher impulse control requirements provided far more significant and pertinent results, only these outcomes (i.e., RcNG stimulus and the difference of RcNG > RcG in the GNG task, and Easy choice (EC) and the difference of Easy choice > Control stimuli (EC > CS) in the DD task) are reported.

A. **GNG task–Healthy controls > All PD patients:** This comparison revealed decreased connectivity in PD patients dominantly to the right-side postcentral cortical areas from both the right and the left seed in both the contrasts (simple RcNG, and RcNG > RcG), furthermore to the left precentral gyrus (from the left caudate in the RcNG > RcG contrast) and the left cerebellar lobule VI (from the right caudate in the RcNG contrast), when compared with healthy controls (see **Figure 2A**, **Table 3**).

B. **GNG task–Non-impulsive PD patients > ICD-PD patients:** This analysis yielded decreased connectivity in ICD-PD patients to the left DLPFC (from the contralateral caudate) and decreased connectivity from the left caudate to the right superior parietal cortex in both the used contrasts and to the right cingulate gyrus in the RcNG >RcG contrast (see **Figure 2B**, **Table 3**).

C. **GNG task–Healthy controls > ICD-PD patients:** ICD-PD patients showed decreased connectivity of the right caudate to the right superior parietal cortex in both contrasts and decreased connectivity of the left caudate to the ipsilateral DLPFC (see **Figure 2C**, **Table 3**).

D. **DD task–Healthy controls > All PD patients:** Decreased connectivity of both caudate nuclei to the contralateral putamina was found in the pooled PD patient group in the simple EC contrast. Furthermore, PD patients had decreased connectivity of caudate nuclei to ipsilateral superior temporal gyri and both the left (simple EC contrast) and the right (EC > CS contrast) medial frontal cortex from the left caudate (see **Figure 2D**, **Table 3**).

E. **DD task–ICD-PD patients > Non-impulsive PD patients:** The simple EC contrast revealed increased connectivity of the right caudate to bilateral calcarine cortices and increased connectivity of the left caudate to the ipsilateral insula in ICD-PD patients (see **Figure 2E**, **Table 3**).

No clusters survived the reverse contrasts to the above stated outcomes at the same threshold.

DISCUSSION

This study is the first to investigate the neural substrates of ICD in PD using two distinct, impulse-control-related fMRI tasks in the same patient population, with a specific focus on cases of severe ICD significantly impacting the quality of life. Neuroimaging analyses revealed not only decreased fMRI activation in the striatum in ICD-PD patients in keeping with the previous research reports (Napier et al., 2015; Vriend, 2018), but also vast connectivity changes beyond the commonly stated areas, indicating that fronto-striatal and mesolimbic functional disruptions are not the sole mechanisms underlying ICD in PD patients.

While ICD-PD patients did not perform differently from healthy controls and non-impulsive PD patients in the behavioral aspect of GNG and DD tasks, the inclusion of both decision-making impulsivity as a measure of mapping future actions into rewards in PD (Averbeck et al., 2013), and motor response inhibition tests (Nombela et al., 2014) proved of paramount importance in the fMRI analysis, with distinct patterns of concurrence in the cortical areas around the central sulcus recruited in both tasks generally less in the PD population. Moreover, the emergence of bilateral supplementary motor area hypoactivity in PD patients during the GNG task, previously proven of critical importance for the selection of appropriate responses and the inhibition of the inappropriate ones, and fronto-parietal cortices is in accord with processes implicated in motor response inhibition (Simmonds et al., 2008) and clearly shows the encroachment of neurodegeneration processes to a wide-spread network of distinctive neural nodes. Frontal and parietal areas partly share one inhibitory-attentional network associated with action withholding and interference

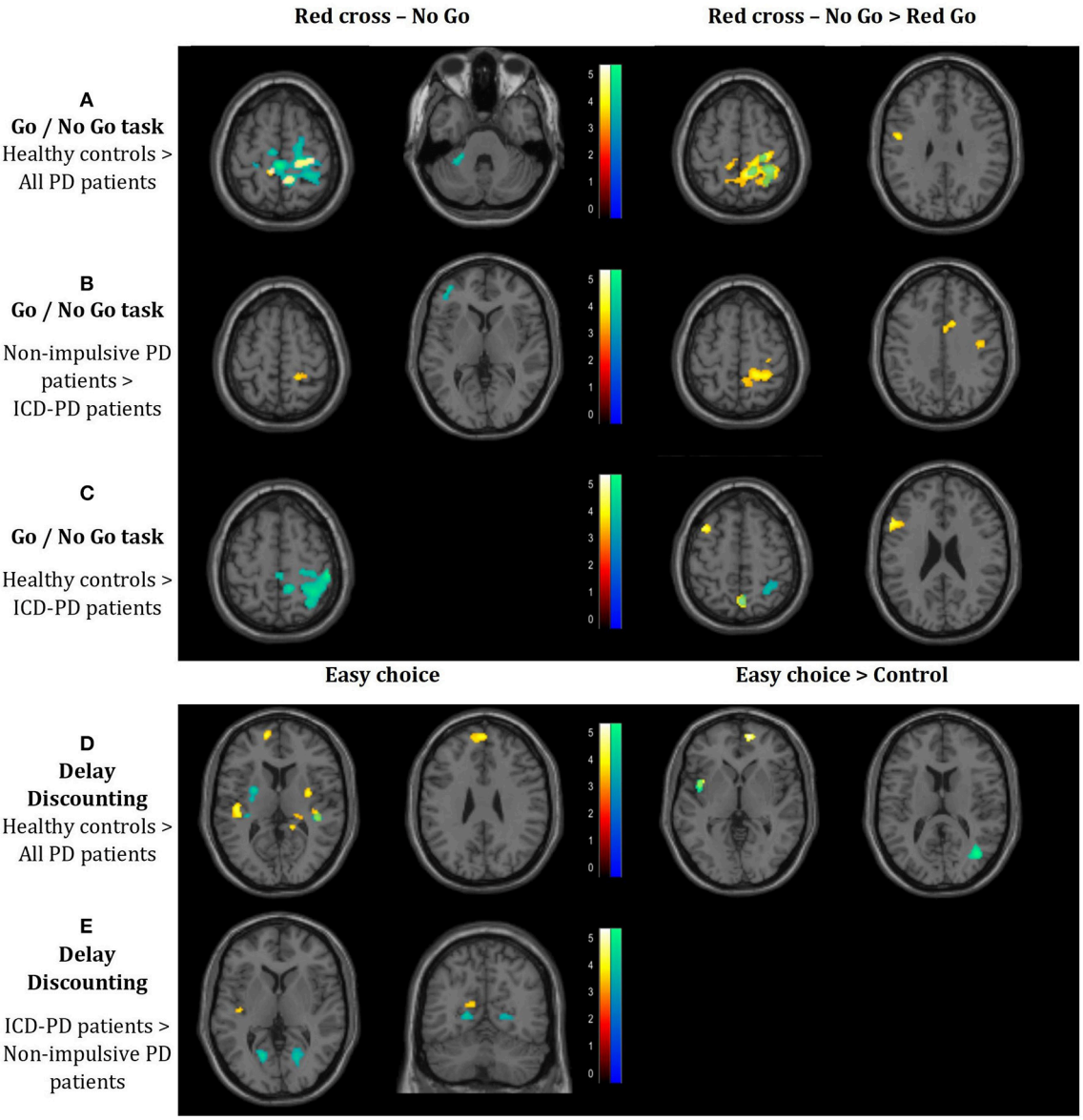

FIGURE 2 | Results of the connectivity analysis ($p < 0.05$) FWE-corrected at the cluster level ($p < 0.001$ uncorrected at the voxel level; threshold $T = 3.16$ for all the reported results). The results of the functional connectivity of the seed in the left caudate head and in the right caudate head are denoted by red-to-yellow and blue-to-green spectrum, respectively. Results of the connectivity analysis in the Go/No Go task: **(A)** Decreased connectivity in the whole cohort of Parkinson's disease (PD) patients to the right-side postcentral cortical areas, left precentral gyrus and left cerebellar lobule VI, when compared with healthy controls. **(B)** Decreased connectivity in PD patients with impulse control disorder (ICD) vs. non-impulsive PD patients to the left dorsolateral prefrontal cortex, cingulate gyrus and right-side postcentral cortical areas. **(C)** Decreased connectivity in ICD-PD patients vs. healthy controls to the right-side postcentral cortical areas and left dorsolateral prefrontal cortex. Results of the connectivity analysis in the Delay Discounting task. **(D)** Decreased connectivity in the whole cohort of PD patients to both putamina (each contralateral to the respective seed), both superior temporal gyri (each ipsilateral to the respective seed) and left medial frontal cortex, when compared with healthy controls. **(E)** Increased connectivity in ICD-PD patients vs. non-impulsive PD patients to the left insula and bilateral calcarine cortices. Laterality conventions with the right side in the figure corresponding to the right side of the scanned area were implemented. See **Table 3** for detailed statistical results and anatomical localization of clusters.

inhibition (Levy and Wagner, 2011; Sebastian et al., 2013), with substantial involvement of the fronto-striatal pathways mainly in the inhibition of already initiated actions (Jahfari et al., 2011). The fronto-parietal recruitment changes in non-PD gamblers, supposedly reflecting the cue-induced addiction memory network (Miedl et al., 2010), may mirror processes comparable to the dysfunctions presented in this study.

Nonetheless, the abundance of relevant research findings seems clearly to show dominant association of ICD in PD with hyperdopaminergic state and relevant structures. However, the

TABLE 3 | Anatomical localization of clusters in the connectivity analysis in the Go/No Go and Delay Discounting tasks.

	Anatomical regions	Brodmann area	Side	Volume (in voxels)	*p*-value (SVC)	T-score of local max	MNI coordinates of local maxima		
Go/No go task	**RED CROSS NO GO IN HEALTHY CONTROLS > ALL PD PATIENTS**								
	Seed in the left caudate head								
	Precentral gyrus	BA 4	R	154	0.002	4.02	26	−28	64
	Precuneus	BA 5	R	106	0.003	3.84	8	−46	62
	Precuneus		L	44	0.003	3.70	−8	−36	62
	Seed in the right caudate head								
	Postcentral gyrus Precentral gyrus	BA 6, 40, 4	R	2,055	0.001	5.76	22	−28	66
	Paracentral lobule	BA 6	L	77	0.002	4.38	−8	−18	64
	Cerebellum, lobule VI		L	55	0.007	4.06	−34	−46	−34
	Postcentral gyrus	BA 3, 4	L	57	0.003	3.94	−20	−32	68
	RED CROSS NO GO IN NON-IMPULSIVE PD PATIENTS > ICD-PD PATIENTS								
	Seed in the left caudate head								
	Postcentral gyrus	BA 3	R	55	0.003	3.66	20	−40	60
	Seed in the right caudate head								
	DLPFC	BA 10	L	62	0.004	3.94	−38	50	4
	RED CROSS NO GO IN HEALTHY CONTROLS > ICD-PD PATIENTS								
	Seed in the right caudate head								
	Postcentral gyrus	BA 40, 7	R	1,223	0.001	4.66	22	−28	66
	Precuneus	BA 5	R	254	0.001	4.44	10	−46	62
	Precuneus	BA 7	R	61	0.003	3.95	8	−60	52
	Postcentral gyrus	BA 4	L	45	0.004	3.66	−22	−30	66
	RED CROSS NO GO > RED CROSS GO IN HEALTHY CONTROLS > ALL PD PATIENTS								
	Seed in the left caudate head								
	Postcentral, precuneus	BA 5, 7	R	1,266	<0.001	4.53	28	−26	62
	Superior parietal lobe	BA 7	L	67	0.003	4.41	−20	−80	46
	Precentral gyrus	BA 6	L	82	0.002	3.90	−10	−36	64
	Middle temporal lobe	BA 22	L	70	0.003	3.79	−50	−4	30
	Seed in the right caudate head								
	Postcentral gyrus	BA 40, 7	R	246	0.001	4.11	32	−40	60
	Postcentral gyrus	BA 4	R	129	0.002	4.04	26	−28	62
	Postcentral gyrus	BA 5	R	60	0.002	3.89	14	−42	60
	RED CROSS NO GO > RED CROSS GO IN NON-IMPULSIVE PD PATIENTS > ICD-PD PATIENTS								
	Seed in the left caudate head								
	Caudate		R	47	0.003	4.18	16	−20	26
	Postcentral gyrus	BA 5	R	441	0.001	3.97	28	−40	64
	Cingulate gyrus	BA 24	R	61	0.004	3.73	12	10	36
	Precentral gyrus	BA 6	R	58	0.003	3.69	44	−14	34
	RED CROSS NO GO > RED CROSS GO IN HEALTHY CONTROLS > ICD-PD PATIENTS								
	Seed in the left caudate head								
	Precuneus	BA 7	C	106	0.001	4.60	2	−64	56
	Superior parietal lobe	BA 7	L	73	0.004	4.50	−20	−78	48
	Angular gyrus	BA 40	L	55	0.004	4.44	−46	−66	46
	DLPFC	BA 9	L	285	0.002	4.23	−54	20	26
	Middle frontal gyrus	BA 6	L	74	0.004	4.22	−40	16	54
	Seed in the right caudate head								
	Superior parietal gyrus	BA 40	R	129	0.002	3.89	30	−54	58
	Precuneus	BA 7	R	47	0.003	3.84	4	−64	56

(Continued)

TABLE 3 | Continued

	Anatomical regions	Brodmann area	Side	Volume (in voxels)	*p*-value (SVC)	T-score of local max	MNI coordinates of local maxima		
Delay discounting task	**EASY STIMULUS IN HEALTHY CONTROLS > ALL PD PATIENTS**								
	Seed in the left caudate head								
	Thalamus		R	395	0.001	4.57	20	−28	14
	Superior temporal gyrus	BA 41	L	117	0.002	4.48	−44	−24	12
	Superior temporal gyrus	BA 41	R	162	0.001	4.19	44	−30	14
	Medial frontal cortex	BA 10	L	42	0.004	4.12	−12	58	10
	Putamen		R	43	0.004	3.92	32	−4	10
	Medial frontal gyrus	BA 9, 10	C	97	0.003	3.89	0	56	28
	Seed in the right caudate head								
	Putamen		L	137	0.003	4.06	−28	−24	6
	Superior temporal gyrus	BA 41	R	90	0.002	3.93	42	−32	10
	EASY STIMULUS IN ICD-PD PATIENTS > NON-IMPULSIVE PD PATIENTS								
	Seed in the left caudate head								
	Insula	BA 13	L	47	0.003	3.74	−42	−18	8
	Calcarine		L	44	0.004	3.61	−12	−60	16
	Seed in the right caudate head								
	Calcarine	BA 30	L	91	0.002	4.20	−16	−66	4
	Calcarine	BA 30	R	95	0.002	3.85	20	−66	4
	EASY STIMULUS > CONTROL STIMULUS IN HEALTHY CONTROLS > ALL PD PATIENTS								
	Seed in the left caudate head								
	Medial frontal cortex	BA 10	R	59	0.003	4.07	12	56	0
	Insula	BA 13	L	41	0.004	3.41	−40	8	2
	Seed in the right caudate head								
	Middle temporal gyrus		R	128	0.001	4.01	38	−68	14
	Insula	BA 13	L	70	0.002	3.83	−42	6	2

Clusters significant at $p < 0.05$, FWE-corrected for multiple comparisons at the cluster level (voxel-wise threshold of $p < 0.001$, uncorrected, small volume correction). BA, Brodmann area; C, central; DD, Delay Discounting task; DLPFC, dorsolateral prefrontal cortex; few, family-wise error; GNG, Go/No Go task; ICD, Impulse control disorder; L, left; MNI, Montreal Neurological Institute; PD, Parkinson's disease; R, right; SVC, small volume correction.

extent, to which the function of ventral striatum, one of the core nodes implicated in ICD in PD patients, is disrupted remains equivocal, despite the mounting evidence in various studies—both increased striatal fMRI activation, in pathological gambling (Frosini et al., 2010) and hyperlibidinous deviations (Politis et al., 2013), and decreased neural activity in this area in risk taking activities (Rao et al., 2010; Voon et al., 2011a) in ICD-PD patients. Connectivity studies provide further prima facie evidence, with the reports of absence of connectivity differences in ICD-PD of the ventral striatum, but of decreased connectivity of the associative striatum to various frontal cortical areas (Carriere et al., 2015), even underlined by structural analyses in general PD population (Rae et al., 2012). Moreover, despite the surmised relevance of the associative striatum to cognition, primarily executive functions (Monchi et al., 2006; O'Callaghan et al., 2014), the studies concentrating on this realm in PD-ICD provided largely negative outcomes (Djamshidian et al., 2011; Antonini et al., 2017). The decreased GNG task connectivity of both caudate nuclei to the left DLPFC and of the left caudate to the cingulate gyrus in ICD-PD patients presented in our study seems to resonate well with these findings, but the suggested overall striatal connectivity decline in ICD-PD is countered by the elevation of DD-task connectivity to the salience-associated left insular regions implicated also in addiction and several neuropsychiatric disorders (Uddin, 2015). Hence, these results support the recent gradual opinion shift from simplistic views of striatal hypoactivity and hypoconnectivity to more open, structural and functional changes in the dopaminergic system in ICD-PD, where different aspects of inhibition control stem from distinct networks (Antonelli et al., 2014; Napier et al., 2015) and impulsivity is truly taken as an umbrella term encompassing multiple different behaviors and neuronal nodes (Vriend, 2018).

Indeed, the progressing PD pathology eventually affects also other neurotransmitter systems beyond the dopaminergic network—particularly noradrenaline and serotonin producing neurons (Braak et al., 2003), with suggested distinct effects also on impulsive behaviors (Vriend, 2018). This hypothesis is supported by neuroimaging of selective serotonin reuptake inhibitor (SSRI) induced modulation of response inhibition in PD patients (Ye et al., 2014) and the behavioral effects of SSRI, albeit ranging from the reduction of impulsive actions (Homberg et al., 2007; Baarendse and Vanderschuren, 2012)

to the absence of effect in other impulsivity subdomains (Bari et al., 2009; Baarendse and Vanderschuren, 2012). Moreover, the atomoxetine-induced facilitation of noradrenergic signaling has been reported to reduce decision-making impulsivity and risk taking in PD patients (Kehagia et al., 2014), similarly with hypothesized dependence on impulsive behavior subtypes (Bari et al., 2009), and opioid receptor antagonists, despite the lack of clinically relevant effect in ICD-PD patients (Papay et al., 2014), are able to reduce pathological gambling (Grant et al., 2008) and improve symptoms in the impulsive-compulsive spectrum disorders (Piquet-Pessôa and Fontenelle, 2016) in PD-unrelated impulsivity.

And likewise, different aspects of impulse control may be differentially sensitive to dopamine concentration decline and pharmacologic supplementation (Voon et al., 2011a). There is an ample and growing body of research on the escalated reward-related striatal dopaminergic activity as the primary pathophysiological basis of ICD in PD, be it dominantly due to the "overdose" theory postulating excessive dopamine stimulation of the relatively preserved ventral striatum (Voon et al., 2011b), denervation-induced D3 receptor hypersensitivity in the same area (Prieto et al., 2011) or the interference in D2-signaling pauses in the ventral striatum impairing the encoding of harmful behaviors (Frank et al., 2004; Vriend, 2018). However, as a large proportion of PD patients do not develop impulsivity problems, it is less evident whether or not this specific hypodopaminergic condition and hence the increased vulnerability to ICD is wrought by antecedent neural or genetic traits, plastic structural changes in the reward system (Biundo et al., 2015) or merely a maladaptive response to non-physiological chronic dopaminergic stimulation, thus adding to the high heterogeneity of PD (Lewis et al., 2005; Farrer, 2006; van Balkom et al., 2016).

These multifaceted aspects of impulsivity and PD in general partly hamper clear-cut interpretation of the outcomes of this study, as the high diversity of impulsivity profiles and, indeed, probable subtypes of PD itself, undoubtedly interfered with the results, but the small number of ICD-PD subjects in our sample prevented any meaningful separate analyses. The low numbers of subjects presumably also contributed to the absence of significant between-group differences in the behavioral analysis, even though the simple numerical comparison seems to show at least a trend toward lower performance and the correlates of higher impulsivity in the ICD-PD group. This was primarily incurred by our deliberate decision to include only PD patients with ICD severity of detrimental extent for their day-to-day life (e.g., substantial financial losses due to gambling). Even though the prevalence of ICD in PD patients is usually reported at the level of ∼15%, with non-negligible dependence on cultural factors and gender (Perez-Lloret et al., 2012; Santangelo et al., 2013; Maloney et al., 2017), ICD of the level deliberately chosen for this study is rather rare, making the recruitment of larger cohorts of severe ICD PD patients virtually impossible. As the symptoms widely range in severity, subclinical ICD symptom screenings yield significantly higher rates (Joutsa et al., 2012; Vriend et al., 2014), but these behaviors should generally be considered a disorder only when becoming harmful to the patient or interfering with the daily functioning as a significant deviation from premorbid behavior. Interestingly, most patients and caregivers do not consider their ICD a severe problem (Garcia-Ruiz et al., 2014). Ergo, the recruitment of these "borderline" patients could induce unwelcome interference in the outcomes. Secondly, the difference in age and gender between the ICD-PD and non-impulsive PD group, even though in accord with the previous body of research on risk factors of ICD (Ceravolo et al., 2009), calls also for caution in the further interpretation of differences between these two subgroups due to possible confounding. Furthermore, physiological noise, not accounted for in our study, might have led to potential distortion of the connectivity analysis outcomes, even though the analysis itself was purely task based. And lastly, our study shares the problem of all the cross-sectional research projects comparing ICD-PD and non-impulsive PD patients, as it is virtually impossible to delineate the true cause of neurobiological differences, i.e., antecedent characteristics or true alterations associated with ICD. Nonetheless, prospective fMRI study capable of recruiting a satisfactory number of high-severity ICD-PD patients is highly impractical, if feasible at all, and the general character of our hypotheses allows reasonable confidence in the outcomes.

In conclusion, our results present a refinement and synthesis of gradually developing ideas about the nature of ICD in PD—an umbrella term encompassing various behavioral deviations related to distinct neuronal networks, which greatly exceed the previously envisioned fronto-striatal and mesolimbic pathways. The significance of these differences in the context of disruptions to neurotransmitter systems beyond the dopaminergic component is far from elucidated, and although speculative, the neuroanatomical correlation and relevance of these signaling alterations are an important topic for further investigation, with possible highly-sought-after therapeutic implications for the clinical practice.

AUTHOR CONTRIBUTIONS

PF, PL, PH, MBal, MBar, and TK participated in designing the project and defining the aims and hypotheses. PF, RŠ, MBal, and MBar were responsible for patient recruitment and neurological examinations. PL and PH performed neuropsychological testing. PF performed the data analysis and wrote the manuscript draft. All co-authors provided their comments to the manuscript draft.

FUNDING

This work was supported by the EU H2020 Marie Skłodowska RISE project #691110 (MICROBRADAM), Ministry of Health of the Czech Republic grant nr. 15-30062A, Ministry of Health of the Czech Republic Development of Research Organization grant FNBr 65269705.

ACKNOWLEDGMENTS

The authors are grateful to the patients and their families for their support of research activities.

REFERENCES

Antonelli, F., Ko, J. H., Miyasaki, J., Lang, A. E., Houle, S., Valzania, F., et al. (2014). Dopamine-agonists and impulsivity in Parkinson's disease: impulsive choices vs. impulsive actions. *Hum. Brain Mapp.* 35, 2499–2506. doi: 10.1002/hbm.22344

Antonini, A., Barone, P., Bonuccelli, U., Annoni, K., Asgharnejad, M., and Stanzione, P. (2017). ICARUS study: prevalence and clinical features of impulse control disorders in Parkinson's disease. *J. Neurol. Neurosurg. Psychiatr.* 88, 317–324. doi: 10.1136/jnnp-2016-315277

Averbeck, B. B., Djamshidian, A., O'Sullivan, S. S., Housden, C. R., Roiser, J. P., and Lees, A. J. (2013). Uncertainty about mapping future actions into rewards may underlie performance on multiple measures of impulsivity in behavioral addiction: evidence from Parkinson's disease. *Behav. Neurosci.* 127:245. doi: 10.1037/a0032079

Baarendse, P. J. J., and Vanderschuren, L. J. M. J. (2012). Dissociable effects of monoamine reuptake inhibitors on distinct forms of impulsive behavior in rats. *Psychopharmacology* 219, 313–326. doi: 10.1007/s00213-011-2576-x

Bari, A., Eagle, D. M., Mar, A. C., Robinson, E. S. J., and Robbins, T. W. (2009). Dissociable effects of noradrenaline, dopamine, and serotonin uptake blockade on stop task performance in rats. *Psychopharmacology* 205, 273–283. doi: 10.1007/s00213-009-1537-0

Biundo, R., Weis, L., Facchini, S., Formento-Dojot, P., Vallelunga, A., Pilleri, M., et al. (2015). Patterns of cortical thickness associated with impulse control disorders in Parkinson's disease. *Mov. Disord.* 30, 688–695. doi: 10.1002/mds.26154

Braak, H., Del Tredici, K., Rüb, U., De Vos, R. A. I., Steur, E. N. H. J., and Braak, E. (2003). Staging of brain pathology related to sporadic Parkinson's disease. *Neurobiol. Aging* 24, 197–211. doi: 10.1016/S0197-4580(02)00065-9

Buckholtz, J. W., Treadway, M. T., Cowan, R. L., Woodward, N. D., Li, R., Ansari, M. S., et al. (2010). Dopaminergic network differences in human impulsivity. *Science* 329:532. doi: 10.1126/science.1185778

Carriere, N., Lopes, R., Defebvre, L., Delmaire, C., and Dujardin, K. (2015). Impaired corticostriatal connectivity in impulse control disorders in Parkinson disease. *Neurology* 84, 2116–2123. doi: 10.1212/WNL.0000000000001619

Ceravolo, R., Frosini, D., Rossi, C., and Bonuccelli, U. (2009). Impulse control disorders in Parkinson's disease: definition, epidemiology, risk factors, neurobiology and management. *Parkinsonism Relat. Disord.* 15:S111–S5. doi: 10.1016/S1353-8020(09)70847-8

Cilia, R., Cho, S. S., van Eimeren, T., Marotta, G., Siri, C., Ko, J. H., et al. (2011). Pathological gambling in patients with Parkinson's disease is associated with fronto-striatal disconnection: a path modeling analysis. *Mov. Disord.* 26, 225–233. doi: 10.1002/mds.23480

Cooney, J. W., and Stacy, M. (2016). Neuropsychiatric issues in Parkinson's disease. *Curr Neurol Neurosci Rep* 16, 49. doi: 10.1007/s11910-016-0647-4

Djamshidian, A., O'Sullivan, S. S., Lees, A., and Averbeck, B. B. (2011). Stroop test performance in impulsive and non impulsive patients with Parkinson's disease. *Parkinsonism Relat. Disord.* 17, 212–214. doi: 10.1016/j.parkreldis.2010.12.014

Farrer, M. J. (2006). Genetics of Parkinson disease: paradigm shifts and future prospects. *Nat. Rev. Genet.* 7:306. doi: 10.1038/nrg1831

Folstein, M. F., Folstein, S. E., and McHugh, P. R. (1975). "Mini-mental state": a practical method for grading the cognitive state of patients for the clinician. *J. Psychiatr. Res.* 12, 189–198.

Frank, M. J., Seeberger, L. C., and O'Reilly, R. C. (2004). By carrot or by stick: cognitive reinforcement learning in parkinsonism. *Science* 306, 1940–1943. doi: 10.1126/science.1102941

Friston, K. J., Buechel, C., Fink, G. R., Morris, J., Rolls, E., and Dolan, R. J. (1997). Psychophysiological and modulatory interactions in neuroimaging. *Neuroimage* 6, 218–229. doi: 10.1006/nimg.1997.0291

Frosini, D., Pesaresi, I., Cosottini, M., Belmonte, G., Rossi, C., Dell'Osso, L., et al. (2010). Parkinson's disease and pathological gambling: results from a functional MRI study. *Mov. Disord.* 25, 2449–2453. doi: 10.1002/mds.23369

Garcia-Ruiz, P. J., Castrillo, J. C. M., Alonso-Canovas, A., Barcenas, A. H., Vela, L., Alonso, P. S., et al. (2014). Impulse control disorder in patients with Parkinson's disease under dopamine agonist therapy: a multicentre study. *J. Neurol. Neurosurg. Psychiatr.* 85, 840–844. doi: 10.1136/jnnp-2013-306787

Gescheidt, T., Czekóová, K., Urbánek, T., Mareček, R., Mikl, M., Kubíková, R., et al. (2012). Iowa Gambling Task in patients with early-onset Parkinson's disease: strategy analysis. *Neurol. Sci.* 33, 1329–1335. doi: 10.1007/s10072-012-1086-x

Grant, J. E., Suck, W. K., and Hartman, B. K. (2008). A double-blind, placebo-controlled study of the opiate antagonist naltrexone in the treatment of pathological gambling urges. *J. Clin. Psychiatry* 69, 783–789. doi: 10.4088/JCP.v69n0511

Hoehn, M. M., and Yahr, M. D. (1967). Parkinsonism onset, progression, and mortality. *Neurology* 17:427. doi: 10.1212/WNL.17.5.427

Homberg, J. R., Pattij, T., Janssen, M. C. W., Ronken, E., De Boer, S. F., Schoffelmeer, A. N. M., et al. (2007). Serotonin transporter deficiency in rats improves inhibitory control but not behavioural flexibility. *Eur. J. Neurosci.* 26, 2066–2073. doi: 10.1111/j.1460-9568.2007.05839.x

Hughes, A. J., Daniel, S. E., Kilford, L., and Lees, A. (1992). J. Accuracy of clinical diagnosis of idiopathic Parkinson's disease: a clinico-pathological study of 100 cases. *J. Neurol. Neurosurg. Psychiatry* 55, 181–4. doi: 10.1136/jnnp.55.3.181

Jahfari, S., Waldorp, L., van den Wildenberg, W. P. M., Scholte, H. S., Ridderinkhof, K. R., and Forstmann, B. U. (2011). Effective connectivity reveals important roles for both the hyperdirect (fronto-subthalamic) and the indirect (fronto-striatal-pallidal) fronto-basal ganglia pathways during response inhibition. *J. Neurosci.* 31, 6891–6899. doi: 10.1523/JNEUROSCI.5253-10.2011

Joutsa, J., Martikainen, K., Vahlberg, T., Voon, V., and Kaasinen, V. (2012). Impulse control disorders and depression in Finnish patients with Parkinson's disease. *Parkinsonism Relat. Disord.* 18, 155–160. doi: 10.1016/j.parkreldis.2011.09.007

Kehagia, A. A., Housden, C. R., Regenthal, R., Barker, R. A., Müller, U., Rowe, J., et al. (2014). Targeting impulsivity in Parkinson's disease using atomoxetine. *Brain* 137, 1986–1997. doi: 10.1093/brain/awu117

Levy, B. J., and Wagner, A. D. (2011). Cognitive control and right ventrolateral prefrontal cortex: reflexive reorienting, motor inhibition, and action updating. *Ann. N. Y. Acad. Sci.* 1224, 40–62. doi: 10.1111/j.1749-6632.2011.05958.x

Lewis, S. J. G., Foltynie, T., Blackwell, A. D., Robbins, T. W., Owen, A. M., and Barker, R. A. (2005). Heterogeneity of Parkinson's disease in the early clinical stages using a data driven approach. *J. Neurol. Neurosurg. Psychiatr.* 76, 343–348. doi: 10.1136/jnnp.2003.033530

Maldjian, J. A., Laurienti, P. J., Kraft, R. A., and Burdette, J. H. (2003). An automated method for neuroanatomic and cytoarchitectonic atlas-based interrogation of fMRI data sets. *Neuroimage* 19, 1233–1239. doi: 10.1016/S1053-8119(03)00169-1

Maloney, E. M., Djamshidian, A., and O'Sullivan, S. S. (2017). Phenomenology and epidemiology of impulsive-compulsive behaviours in Parkinson's disease, atypical Parkinsonian disorders and non-Parkinsonian populations. *J. Neurol. Sci.* 374:47–52. doi: 10.1016/j.jns.2016.12.058

Mazur, J. E. (1987). "An adjusting procedure for studying delayed reinforcement," in *Quantitative Analyses of Behavior, Vol. 5. The Effect of Delay and of Intervening Events on Reinforcement Value,* M. L. Commons, J. E. Mazur, J. A. Nevin (Hillsdale, NJ: Lawrence Erlbaum Associates, Inc.), 55–73.

Miedl, S. F., Fehr, T., Meyer, G., and Herrmann, M. (2010). Neurobiological correlates of problem gambling in a quasi-realistic blackjack scenario as revealed by fMRI. *Psychiatry Res.* 181, 165–173. doi: 10.1016/j.pscychresns.2009.11.008

Monchi, O., Petrides, M., Mejia-Constain, B., and Strafella, A. P. (2006). Cortical activity in Parkinson's disease during executive processing depends on striatal involvement. *Brain* 130, 233–244. doi: 10.1093/brain/awl326

Montgomery, S. A., and Asberg, M. (1979). A new depression scale designed to be sensitive to change. *Br. J. Psychiatry* 134, 382–389. doi: 10.1192/bjp.134.4.382

Napier, T. C., Corvol, J. C., Grace, A. A., Roitman, J. D., Rowe, J., Voon, V., et al. (2015). Linking neuroscience with modern concepts of impulse control disorders in Parkinson's disease. *Mov. Disord.* 30, 141–149. doi: 10.1002/mds.26068

Nombela, C., Rittman, T., Robbins, T. W., and Rowe, J. B. (2014). Multiple modes of impulsivity in Parkinson's disease. *PLoS ONE* 9:e85747. doi: 10.1371/journal.pone.0085747

O'Callaghan, C., Bertoux, M., and Hornberger, M. (2014). Beyond and below the cortex: the contribution of striatal dysfunction to cognition and behaviour in neurodegeneration. *J. Neurol. Neurosurg. Psychiatr.* 85, 371–378. doi: 10.1136/jnnp-2012-304558

Papay, K., Xie, S. X., Stern, M., Hurtig, H., Siderowf, A., Duda, J. E., et al. (2014). Naltrexone for impulse control disorders in Parkinson disease A placebo-controlled study. *Neurology* 83, 826–833. doi: 10.1212/WNL.0000000000000729

Patton, J. H., Stanford, M. S., and Barratt, E. S. (1995). Factor structure of the Barratt impulsiveness scale. *J. Clin. Psychol.* 51, 768–74. doi: 10.1002/1097-4679(199511)51:6<768::AID-JCLP2270510607>3.0.CO;2-1

Perez-Lloret, S., Rey, M. V., Fabre, N., Ory, F., Spampinato, U., Brefel-Courbon, C., et al. (2012). Prevalence and pharmacological factors associated with impulse-control disorder symptoms in patients with Parkinson disease. *Clin. Neuropharmacol.* 35, 261–265. doi: 10.1097/WNF.0b013e31826e6e6d

Piquet-Pessôa, M., and Fontenelle, L. F. (2016). Opioid antagonists in broadly defined behavioral addictions: a narrative review. *Expert Opin. Pharmacother.* 17, 835–844. doi: 10.1517/14656566.2016.1145660

Politis, M., Loane, C., Wu, K., O'Sullivan, S. S., Woodhead, Z., Kiferle, L., et al. (2013). Neural response to visual sexual cues in dopamine treatment-linked hypersexuality in Parkinson's disease. *Brain* 136, 400–411. doi: 10.1093/brain/aws326

Prieto, G. A., Perez-Burgos, A., Palomero-Rivero, M., Galarraga, E., Drucker-Colin, R., and Bargas, J. (2011). Upregulation of D2-class signaling in dopamine-denervated striatum is in part mediated by D3 receptors acting on CaV2. 1 channels via PIP2 depletion. *J. Neurophysiol.* 105, 2260–74. doi: 10.1152/jn.00516.2010

Rae, C. L., Correia, M. M., Altena, E., Hughes, L. E., Barker, R. A., and Rowe, J. B. (2012). White matter pathology in Parkinson's disease: the effect of imaging protocol differences and relevance to executive function. *Neuroimage* 62, 1675–1684. doi: 10.1016/j.neuroimage.2012.06.012

Rao, H., Mamikonyan, E., Detre, J. A., Siderowf, A. D., Stern, M. B., Potenza, M. N., et al. (2010). Decreased ventral striatal activity with impulse control disorders in Parkinson's disease. *Mov. Disord.* 25, 1660–1669. doi: 10.1002/mds.23147

Ray, N. J., Miyasaki, J. M., Zurowski, M., Ko, J. H., Cho, S. S., Pellecchia, G., et al. (2012). Extrastriatal dopaminergic abnormalities of DA homeostasis in Parkinson's patients with medication-induced pathological gambling: a [11C] FLB-457 and PET study. *Neurobiol. Dis.* 48, 519–525. doi: 10.1016/j.nbd.2012.06.021

Robinson, T. E., and Berridge, K. C. (1993). The neural basis of drug craving: an incentive-sensitization theory of addiction. *Brain Res. Rev.* 18, 247–291. doi: 10.1016/0165-0173(93)90013-P

Santangelo, G., Barone, P., Trojano, L., and Vitale, C. (2013). Pathological gambling in Parkinson's disease. *A comprehensive review. Parkinsonism Relat. Disord.* 19, 645–653. doi: 10.1016/j.parkreldis.2013.02.007

Schuirmann, D. J. (1987). A comparison of the two one-sided tests procedure and the power approach for assessing the equivalence of average bioavailability. *J. Pharmacokinet. Biopharm.* 15, 657–680. doi: 10.1007/BF01068419

Sebastian, A., Pohl, M. F., Klöppel, S., Feige, B., Lange, T., Stahl, C., et al. (2013). Disentangling common and specific neural subprocesses of response inhibition. *Neuroimage* 64:601–615. doi: 10.1016/j.neuroimage.2012.09.020

Simmonds, D. J., Pekar, J. J., and Mostofsky, S. H. (2008). Meta-analysis of Go/No-go tasks demonstrating that fMRI activation associated with response inhibition is task-dependent. *Neuropsychologia* 46, 224–232. doi: 10.1016/j.neuropsychologia.2007.07.015

Steeves, T. D. L., Miyasaki, J., Zurowski, M., Lang, A. E., Pellecchia, G., Van Eimeren, T., et al. (2009). Increased striatal dopamine release in Parkinsonian patients with pathological gambling: a [11C] raclopride PET study. *Brain* 132, 1376–1385. doi: 10.1093/brain/awp054

Tomlinson, C. L., Stowe, R., Patel, S., Rick, C., Gray, R., and Clarke, C. E. (2010). Systematic review of levodopa dose equivalency reporting in Parkinson's disease. *Mov. Disord.* 25, 2649–2653. doi: 10.1002/mds.23429

Tzourio-Mazoyer, N., Landeau, B., Papathanassiou, D., Crivello, F., Etard, O., Delcroix, N., et al. (2002). Automated anatomical labeling of activations in SPM using a macroscopic anatomical parcellation of the MNI MRI single-subject brain. *Neuroimage* 15, 273–289. doi: 10.1006/nimg.2001.0978

Uddin, L. Q. (2015). Salience processing and insular cortical function and dysfunction. *Nat. Rev. Neurosci.* 16:55. doi: 10.1038/nrn3857

van Balkom, T. D., Vriend, C., Berendse, H. W., Foncke, E. M. J., van der Werf, Y. D., van den Heuvel, O. A., et al. (2016). Profiling cognitive and neuropsychiatric heterogeneity in Parkinson's disease. *Parkinsonism Relat. Disord.* 28:130–136. doi: 10.1016/j.parkreldis.2016.05.014

Voon, V., Gao, J., Brezing, C., Symmonds, M., Ekanayake, V., Fernandez, H., et al. (2011a). Dopamine agonists and risk: impulse control disorders in Parkinson's; disease. *Brain* 134, 1438–1446. doi: 10.1093/brain/awr080

Voon, V., Mehta, A. R., and Hallett, M. (2011b). Impulse control disorders in Parkinson's disease: recent advances. *Curr. Opin. Neurol.* 24:324. doi: 10.1097/WCO.0b013e3283489687

Voon, V., Pessiglione, M., Brezing, C., Gallea, C., Fernandez, H. H., Dolan, R. J., et al. (2010). Mechanisms underlying dopamine-mediated reward bias in compulsive behaviors. *Neuron* 65, 135–142. doi: 10.1016/j.neuron.2009.12.027

Vriend, C. (2018). The neurobiology of impulse control disorders in Parkinson's disease: from neurotransmitters to neural networks. *Cell Tissue Res.* 373, 327–336. doi: 10.1007/s00441-017-2771-0

Vriend, C., Nordbeck, A. H., Booij, J., van der Werf, Y. D., Pattij, T., Voorn, P., et al. (2014). Reduced dopamine transporter binding predates impulse control disorders in Parkinson's disease. *Mov. Disord.* 29, 904–911. doi: 10.1002/mds.25886

Weintraub, D., David, A. S., Evans, A. H., Grant, J. E., and Stacy, M. (2015). Clinical spectrum of impulse control disorders in Parkinson's disease. *Mov Disord.* 30, 121–127. doi: 10.1002/mds.26016

Weintraub, D., Papay, K., Siderowf, A., and Parkinson's Progression Markers, I. (2013). Screening for impulse control symptoms in patients with *de novo* Parkinson disease A case-control study. *Neurology* 80, 176–180. doi: 10.1212/WNL.0b013e31827b915c

Ye, Z., Altena, E., Nombela, C., Housden, C. R., Maxwell, H., Rittman, T., et al. (2014). Selective serotonin reuptake inhibition modulates response inhibition in Parkinson's disease. *Brain* 137, 1145–1155. doi: 10.1093/brain/awu032

Conflict of Interest Statement: The authors declare that the research was conducted in the absence of any commercial or financial relationships that could be construed as a potential conflict of interest.

frontiers in Neurology

ORIGINAL RESEARCH
published: 07 March 2019
doi: 10.3389/fneur.2019.00145

Longitudinal Recordings Reveal Transient Increase of Alpha/Low-Beta Power in the Subthalamic Nucleus Associated With the Onset of Parkinsonian Rest Tremor

Jan Hirschmann[1], Omid Abbasi[1†], Lena Storzer[1†], Markus Butz[1], Christian J. Hartmann[1,2], Lars Wojtecki[1,2] and Alfons Schnitzler[1,2]*

[1] Medical Faculty, Institute of Clinical Neuroscience and Medical Psychology, Heinrich Heine University, Düsseldorf, Germany, [2] Medical Faculty, Center for Movement Disorders and Neuromodulation, Heinrich Heine University, Düsseldorf, Germany

Functional magnetic resonance imaging studies suggest that different subcortico-cortical circuits control different aspects of Parkinsonian rest tremor. The basal ganglia were proposed to drive tremor onset, and the cerebellum was suggested to be responsible for tremor maintenance ("dimmer-switch" hypothesis). Although several electrophysiological correlates of tremor have been described, it is currently unclear whether any of these is specific to tremor onset or maintenance. In this study, we present data from a single patient measured repeatedly within 2 years after implantation of a deep brain stimulation (DBS) system capable of recording brain activity from the target. Local field potentials (LFPs) from the subthalamic nucleus and the scalp electroencephalogram were recorded 1 week, 3 months, 6 months, 1 year, and 2 years after surgery. Importantly, the patient suffered from severe rest tremor of the lower limbs, which could be interrupted voluntarily by repositioning the feet. This provided the unique opportunity to record many tremor onsets in succession. We found that tremor onset and tremor maintenance were characterized by distinct modulations of subthalamic oscillations. Alpha/low-beta power increased transiently immediately after tremor onset. In contrast, beta power was continuously suppressed during tremor maintenance. Tremor maintenance was additionally associated with subthalamic and cortical power increases around individual tremor frequency. To our knowledge, this is the first evidence of distinct subthalamic LFP modulations in tremor onset and tremor maintenance. Our observations suggest the existence of an acceleration signal for Parkinsonian rest tremor in the basal ganglia, in line with the "dimmer-switch" hypothesis.

Keywords: tremor, subthalamic nucleus, neuronal oscillations, local field potentials, Parkinson's disease

OPEN ACCESS

Edited by:
Martijn Beudel, University Medical Center Amsterdam, Netherlands

Reviewed by:
Rick Helmich, Radboud University Nijmegen Medical Centre, Netherlands
Gertrud Tamas, Semmelweis University, Hungary

****Correspondence:***
Jan Hirschmann
jan.hirschmann@med.uni-duesseldorf.de

†Present Address:
Omid Abbasi, Institute for Biomagnetism and Biosignalanalysis, University of Münster, Münster, Germany
Lena Storzer, Klinik für Psychiatrie, Psychotherapie und Psychosomatik, Sana Kliniken, Duisburg, Germany

Specialty section:
This article was submitted to Movement Disorders, a section of the journal Frontiers in Neurology

Received: *23 November 2018*
Accepted: *05 February 2019*
Published: *07 March 2019*

Citation:
Hirschmann J, Abbasi O, Storzer L, Butz M, Hartmann CJ, Wojtecki L and Schnitzler A (2019) Longitudinal Recordings Reveal Transient Increase of Alpha/Low-Beta Power in the Subthalamic Nucleus Associated With the Onset of Parkinsonian Rest Tremor. Front. Neurol. 10:145. doi: 10.3389/fneur.2019.00145

INTRODUCTION

Tremor is one of the cardinal symptoms of Parkinson's disease (PD). Parkinsonian tremor occurs primarily at rest, although a combination with postural and/or kinetic tremor is common (1). It affects about 75% of the PD patient population (2) and can range from mild to disabling. In case tremor cannot be sufficiently suppressed by pharmacological treatment, deep brain stimulation (DBS) of the subthalamic nucleus (STN) (3) or the ventral intermediate nucleus of the thalamus (4) is a commonly chosen treatment option.

Recently, it has been argued that continuous DBS, which is the standard today, may not be optimal for tremor control, since tremor is a dynamic symptom waxing and waning spontaneously. Adaptive systems capable of detecting tremor and stimulating on demand might be a more suitable alternative (5). Adaptive systems can use peripheral recordings for tremor detection (6, 7) or electrophysiological signals recorded by the DBS electrode. In fact, several studies have revealed patterns in brain activity associated with tremor, which might serve as a control signal in adaptive DBS systems. These include features of local field potential (LFP) oscillations in the STN, such as power and coherence at individual tremor frequency (8–10), beta power (13–30 Hz) (11, 12), low gamma power (31–45 Hz) (13, 14), and high frequency oscillations (>200 Hz) (15, 16).

While these signals are known to be associated with tremor, it is unclear whether they relate to tremor onset or to tremor maintenance specifically. These two processes are believed to be controlled by different subcortico-cortical circuits, according to a recently proposed model of tremor, called the "dimmer-switch" hypothesis (17). This hypothesis is based on a functional magnetic resonance imaging study showing that tremor amplitude is correlated with thalamic and cerebellar activity, whereas *changes* in tremor amplitude are correlated with pallidal activity (18). Thus, the authors proposed that the basal ganglia drive changes in the tremor state (the "switch") whereas the cerebello-thalamo-cortical circuit maintains tremor and modulates its amplitude (the "dimmer"). According to this model, tremor onset should be associated with basal ganglia activity. This prediction can be validated by electrophysiology, which offers the appropriate temporal resolution to investigate tremor onset specifically.

The search for a specific marker of tremor onset is complicated by the fact that tremor appears and disappears on a very slow timescale. Intra- and perioperative, invasive recordings in patients, however, are usually time-constrained, such that most patients either exhibit continuous tremor during the measurement or no tremor at all. Here, we sought to overcome this problem by measuring many tremor onsets in a patient with the ability to interrupt tremor voluntarily. The measurements were obtained in several sessions within a period of 2 years using an implanted DBS system capable of LFP recording (Activa PC+S^{TM}, Medtronic, USA). The longitudinal design allowed us to (i) collect a larger number of tremor onsets and (ii) to monitor movement-related brain signals over a long period of time. For the latter part, we aimed at investigating the robustness of subcortico-cortical activity associated with a set of standard motor tasks and to relate the temporal development of this activity to the development of symptoms.

MATERIALS AND METHODS

Patient

We report results from a single patient diagnosed with idiopathic Parkinson's disease of the tremor-dominant sub-type. The patient gave written informed consent and the study was approved by the local ethics committee (study no. 4326).

The patient (age range: 42–48 y) first noticed rest and action tremor in 2000, starting in the right leg and spreading to the other extremities, later accompanied by hypokinesia. Reduced dopamine transporter density was confirmed by single photon emission computed tomography. The patient showed a clear response to levodopa (MDS-UDPRS III Medication OFF/Medication ON: 43/28; highest score possible: 132) and no cognitive deficit (Mattis Dementia Rating Scale: 142/144, Montreal Cognitive Assessment: 30/30). Tremor, however, was only slightly improved by levodopa (pre-surgical daily dose: 600 mg) and did not respond to beta-blockers, primidone, clozapine, or topiramate. The patient was implanted with an Activa PC+S^{TM} DBS system (Medtronic, USA) in 2015. DBS led to marked symptom suppression (MS-UDPRS III Medication OFF– DBS OFF/ Medication OFF—DBS ON: 50/25), including tremor, and initially allowed for a complete discontinuation of medication. Two years later, at the time of the last measurement, reemerging lower limb tremor required treatment with 50 mg of levodopa and 2 mg of rotiogotin in addition to DBS.

In Medication OFF/DBS OFF, the patient suffered from severe bilateral leg tremor when resting. Importantly for this study, the patient was able to interrupt leg tremor for several seconds by repositioning the feet.

Experimental Paradigm

LFP and EEG signals were measured 1 week, 3 months, 6 months, 1 year, and 2 years after surgery. In order to limit battery usage, each LFP recording was constrained to 15 min. Anti-parkinsonian medication, if any, was withdrawn >12 h before the recordings started and DBS was turned off between 30 and 60 min before the recording started. Each session consisted of four motor tasks, referred to as REST, HOLD, MOVE, and TREMOR in the following. In the REST condition, the patient sat relaxed and quietly with eyes open for 2 min. In the HOLD condition, the patient elevated both forearms to 45° angle relative to the body's frontal plane and spread the fingers for 3 min. In the MOVE condition, the patient opened and closed the right fist (contralateral to LFP recording) in a self-paced fashion with a frequency of ∼1 Hz for 3 min. In the TREMOR condition (7 min), the patient repeatedly interrupted bilateral rest tremor of the legs by repositioning the feet. Tremor reemerged spontaneously and was interrupted again after 20 s, upon verbal instruction of the experimenter. All sessions were recorded on video.

Data Acquisition

The Activa PC+S^{TM} system allows for chronic recordings from the DBS target site in addition to therapeutic stimulation (19). We used this system for longitudinal, bipolar LFP recordings from the left STN (contact 0 vs. contact 3). We used the first and the last electrode contact to record the largest area possible, thus reducing the risk of missing relevant subthalamic activity. The sampling rate was 794 Hz. In addition to the subthalamic LFPs, we recorded from eight scalp EEG electrodes (Cz, Fz, Pz, C3, Oz, FC2, P3, and P4) using a portable amplifier (Porti, TMSi, The Netherlands), and measured the vertical and the horizontal electrooculogram (EOG), the electrocardiogram (ECG), and the electromyogram (EMG) of the lower arms and of the lower legs on both body sides. These signals were sampled at 2,048 Hz. Before each recording, a transcutaneous, biphasic electric pulse with 5 mA amplitude and 2 ms duration was applied by an Osiris stimulator (Inomed, Germany). The pulse served as a common temporal marker visible in both the LFP and the EEG trace, and was used to align the signals in time during offline analysis (see below). It was delivered via two surface EMG electrodes, one attached to the neck and one above the subcutaneous cable connecting the DBS electrodes to the implanted pulse generator.

Data Preprocessing

All analyses were carried out with Matlab (The Mathworks, USA) and the Matlab-based toolbox FieldTrip (20). The EEG was re-referenced to the average of all scalp EEG channels and band-stop filters were applied to remove 50 Hz line noise and its harmonics. EMG data were high-pass filtered at 10 Hz and rectified. EOG and ECG signals were demeaned. Subsequently, these signals were temporally aligned with the LFP signal, using the transcutaneous pulse as a common temporal marker. Next, bad channels and epochs with strong artifacts were removed. The EEG signal was decomposed using FASTICA (21), components reflecting heart beat and eye movements were deselected manually and the signal was back-transformed.

Spectral Analysis

For the computation of epoch-average spectra, data were cut into segments of 1 s duration and 50% overlap. Segments were convolved with a Hanning taper and subjected to Fourier transformation. The Fourier coefficients were used to compute power and coherence spectra. For the computation of time-frequency representations (TFRs), Fourier coefficients were computed for each time-frequency bin using Morlet wavelets with a width of 7. TFRs were baseline-corrected (−0.5 to −0.15 s relative to tremor onset).

Although we analyzed the data up to the highest frequency possible (397 Hz), we only show spectra up to 45 Hz in this report because tremor-specific effects occurred in this range. Furthermore, we opted to represent the cortical signal by the Cz-electrode, which showed the strongest coherence with the LFP.

Epoch Selection

Tremor Onset

Although we recorded about 100 attempted tremor arrests in total, we included only those 38 trials in the analyses with a clearly identifiable onset. The latter was not always observable because voluntary tremor arrest was not always successful. Tremor onsets were identified by first screening leg EMG traces and right leg EMG power between 3 and 8 Hz, as obtained by Hilbert transformation, and by marking all potential leg tremor onsets. The band limits for EMG power were chosen to accommodate both the individual tremor frequency (3.5 Hz) and its first harmonic (7 Hz). Following the labeling of candidate onsets, we checked whether leg tremor was suppressed and the muscle was relaxed for at least 500 ms. If this was the case, we searched the right leg EMG power trace for the last local minimum before tremor reemergence and defined this sample as tremor onset (**Figure 1**). Onset times were confirmed by visual inspection of the time-domain EMG signal. For spectral and statistical analysis, tremor onsets from all sessions were pooled to maximize statistical power.

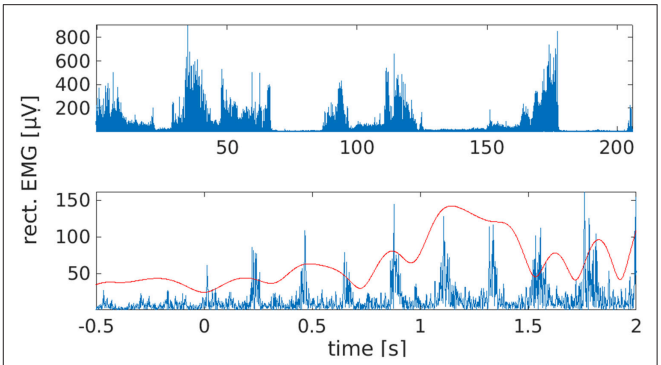

FIGURE 1 | Waxing and waning of leg tremor. **(Top)** Rectified EMG trace from right lower leg. Note the presence of transient tremor arrests/reductions. These were induced by the patient by repositioning the feet. **(Bottom)** Example of a tremor onset episode. Time 0 marks the time of tremor onset, as estimated by inspection of the right leg EMG trace (blue) and EMG power between 3 and 8 Hz (red).

Information on onset detection for voluntary movements (feet repositioning and fist-clenching) is provided in the **Supplementary Material**.

Tremor Episodes and Tremor-Free Episodes

To investigate subthalamic and cortical signals during tremor maintenance, we inspected the EMG recording of the right lower leg and marked tremor episodes and tremor-free episodes. The other EMG signals were disregarded, but the left and the right leg were equally affected by tremor. Hence, the terms "tremor episode" and "tremor-free episode" relate to leg tremor, but not to tremor in other body parts. Again, episodes from all sessions were pooled to maximize statistical power. Note that the lower leg musculature was relaxed during tremor-free episodes, i.e., these episodes do not reflect tremor suppression through muscle contraction.

Statistics

Spectra were compared using FieldTrip's cluster-based permutation approach (22), which corrects for testing at multiple frequencies or time-frequency bins. In each comparison, the number of epochs/trials was equalized across experimental conditions by deleting the last samples from the longer condition.

REST vs. HOLD vs. MOVE

For each session, logarithmic power and coherence in the conditions REST, HOLD, and MOVE were compared pairwise using a *t*- (power) and a *z*-statistic (coherence) (23) for independent samples, respectively. The resulting *p*-values, already corrected for testing at multiple frequencies, were further corrected for comparing at multiple dates using False Discovery Rate.

Pre-onset vs. Post-onset

TFRs of logarithmic LFP and EEG power were compared between the pre-onset baseline (−0.65 to −0.15 relative to tremor onset) and the post-onset phase using the "activation vs. baseline *t*-statistic" (22). For this method to work, the baseline and the post-onset epoch need to have equal length. The length of the baseline epoch was dictated by the shortest tremor-free episode (500 ms). Hence, we set the post-onset epoch to 500 ms and shifted this window by 500 ms four times, thus probing a 2 s period following tremor onset in four separate tests. We did not test coherence this way because a corresponding statistic for coherence is not available. We do, however, provide time-resolved plots of coherence to give an impression of phase difference consistency across tremor onsets for each time-frequency bin.

Tremor vs. Rest

Tremor and tremor-free episodes were compared in the same way as REST, HOLD, and MOVE. We did not apply False Discovery Rate, however, since data were pooled over sessions, i.e., we did not perform separate comparisons at each date.

RESULTS

Longitudinal Measurements of Subcortico-Cortical Activity in Different Motor Tasks

Clinically, DBS surgery resulted in a marked, transient symptom reduction (stun effect), particularly of tremor (**Figure 2**). Three months before surgery, the UPDRS III sum-score for Medication OFF/DBS OFF was 43. It decreased to 29 one week after surgery, and increased again to 57 three months after surgery. Thereafter, it remained on a comparable level (six months: 52, one year: 50, two years: 50). Interestingly, STN beta power underwent a different temporal development. It was strongest 1 week after surgery, when tremor was suppressed due to the stun-effect, but diminished over time.

With respect to electrophysiology, the HOLD condition was repeatedly associated with more power than REST and MOVE in a variable frequency range. This difference was most prominent for the alpha peaks observed in the first-week and sixth-month recordings. The most robust electrophysiological feature was a peak in STN-cortex coherence around 10 Hz, which was visible in all sessions.

Note that differences between motor tasks were only observable up to 6 months after surgery in the LFP signal, indicating a possible decrease of the signal-to-noise-ratio over time. We evaluated the available data on contact impedance

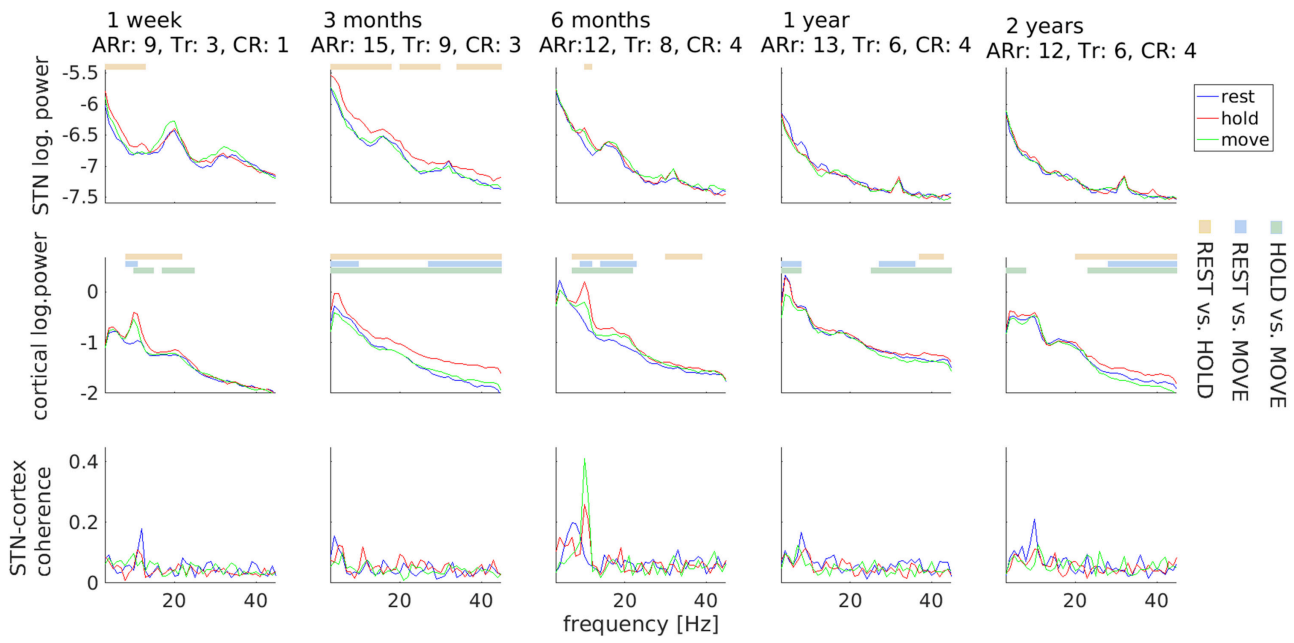

FIGURE 2 | Temporal stability of subthalamic and cortical oscillations. Motor tasks are color-coded. Horizontal lines mark significant differences and comparisons are coded by another color scheme (see legends on the right). Values underneath the row titles indicate body side-specific scores for akinesia/rigidity (ARr; UPDRS III items 3.3–3.8) and for tremor (Tr: UPDRS III items 3.17) for the right body side, i.e., contralateral to local field potential recordings, and for the constancy of rest tremor (CR: UPDRS III item 3.18). Clinical scores obtained 3 months before surgery: ARr: 10, Tr: 8, CR: 3.

and observed an increase occurring earlier than 6 months. The impedance of contact L03 was 1726 Ω at the day of stimulator implantation, 4,261 Ω 3 months after surgery, and 3,153 Ω 2 years after surgery. In other words, the loss of LFP beta peaks after 1 year was not accompanied by a corresponding increase in impedance.

Tremor Onset

Following tremor onset, we observed a significant increase of STN power between 8 and 15 Hz compared to pre-onset baseline (**Figure 3**; $p = 0.009$). This increase occurred between 150 to 520 ms after tremor onset. At this stage, tremor had not evolved to full amplitude in most of the epochs yet, as indicated by the dynamics of leg EMG power (**Figure 3**, lowermost plot). Cortical beta power between 16 and 20 Hz decreased compared to pre-onset baseline at 1.15–1.4 s relative to tremor onset ($p = 0.019$). Furthermore, we observed an increase of STN-cortex coherence at 5 Hz, following the occurrence of the transient alpha/low-beta power increase in the STN.

We tested the tremor-specificity of the STN power increase between 8 and 15 Hz by examining STN power changes around two types of voluntary movement: feet repositioning and repetitive fist-clenching. Feet repositioning was associated with a post-movement increase of beta-band power around 20 Hz, possibly related to tremor arrest (**Figure S1** of the Supplementary Material). A power increase between 8 and 15 Hz was not observed. Repetitive fist-clenching showed a pattern of power changes that was in part reminiscent of tremor onset, including signs of an alpha/low-beta power increase around 300 ms after movement onset (**Figure S3**). This change, however, was not significant ($p = 0.33$) and much weaker than for tremor onset.

Tremor Maintenance

In contrast to tremor onset, tremor maintenance was associated with a decrease, not an increase, in subthalamic beta oscillations. This decrease was observed for beta peaks in the low (20–25 Hz; $p < 0.001$) and the high beta/low gamma band (32–36 Hz; $p < 0.001$), as illustrated in **Figure 4**. In addition, we detected an increase of STN power between 4 and 7 Hz ($p = 0.003$), and increases of cortical power between 7 and 10 Hz ($p < 0.001$) and 16 and 18 Hz ($p = 0.004$). STN-cortex coherence did not change significantly, but exhibited several peaks below 20 Hz in the tremor condition only.

DISCUSSION

A New Maker of Tremor Onset

We have revealed an electrophysiological, subthalamic marker of tremor onset, suggesting that the basal ganglia mediate the emergence of tremulous movements, as proposed by the "dimmer-switch" hypothesis (17). Interestingly, the "dimmer-switch" hypothesis does not specify whether the STN is part of

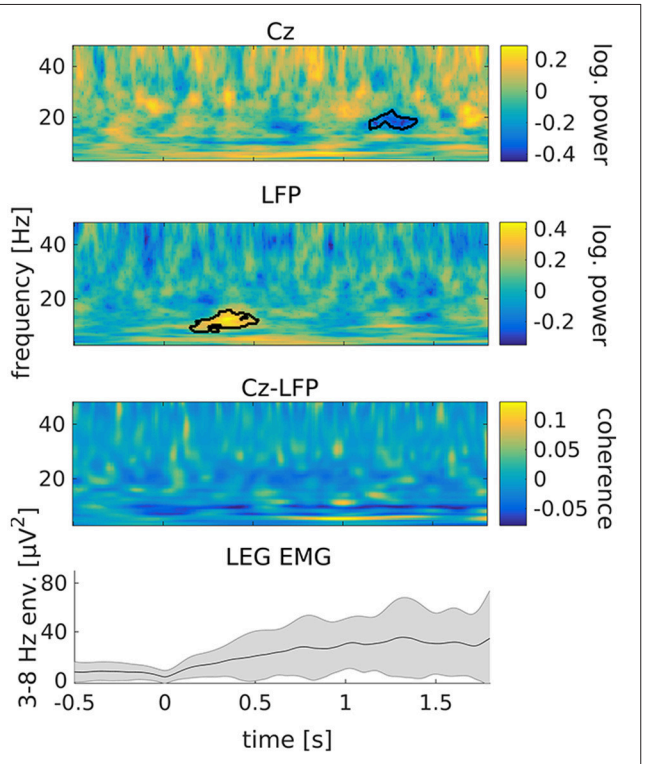

FIGURE 3 | Tremor onset is associated with a transient increase of subthalamic power at alpha/low beta frequencies. From top to bottom: cortical power, STN power, STN-cortex coherence and leg EMG power between 3 and 8 Hz. Time 0 marks tremor onset. Colors indicate the difference to baseline (−0.65 to −0.15 s relative to tremor onset). The black outline marks significant differences. The gray shading in the lowermost plot illustrates the standard deviation across tremor epochs.

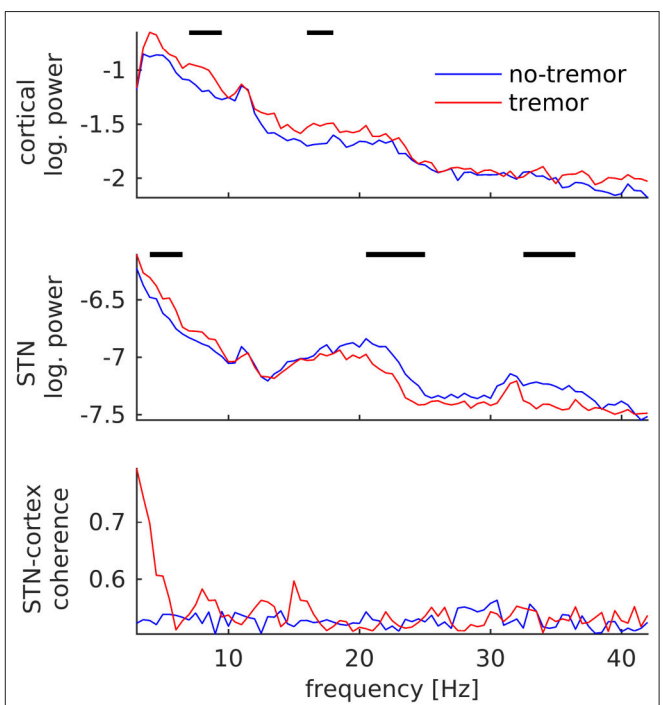

FIGURE 4 | Changes of subthalamic and cortical signals during tremor maintenance. Cortical **(Top)** and subthalamic **(Middle)** power averaged over all tremor (red) and no-tremor segments (blue). **(Bottom)** STN-cortex coherence. Vertical bars mark significant differences.

the "dimmer" (cerebello-thalamo-cortical loop) or the "switch" (striato-pallidal loop). This is because the STN is part of the basal ganglia but also receives projections from and sends projections to the cerebellum (24). Indeed, the current results implicate a dual role for the STN. Subthalamic beta power was found to be modulated both at tremor onset and during tremor maintenance, albeit in opposite directions. These observations suggest that distinct processes are at work during tremor onset and tremor maintenance, and the STN is involved in both of them.

In addition to revealing a new marker of tremor onset, the current results confirm beta power suppression and increases at individual tremor frequency and/or its harmonics as basic markers of tremor maintenance (10–12, 25). Note that the current results differ partly from our own previous work on Parkinsonian rest tremor (10), which investigated consistent patterns of power and coherence in 11 PD patients. This work had revealed an increase of STN power at individual tremor frequency occurring about 1 s after tremor onset and lasting for the entire epoch under investigation (9 s), but it had not detected the 8–15 Hz increase reported here. In light of the current findings, we interpret the late and sustained increase of subthalamic power at individual tremor frequency as a correlate of tremor maintenance, which is reflected in the 4–7 Hz increase in the STN power spectrum in this study (**Figure 4**, upper row). The transient 8–15 Hz increase might have been missed in our previous study due the higher variability introduced by sampling from different patients. The current study, in turn, did not find a significant increase of STN-cortex coherence during tremor, but the pattern observed here matches our previous results on a qualitative level. Finally, we observed a tremor-associated increase in cortical oscillations in the beta band and below, although previous studies reported a beta power decrease (12). This discrepancy might be due to tremor-related EEG artifacts in the data at hand, which can arise during severe tremor (several seconds after tremor onset) and are difficult to remove completely.

In addition to beta oscillations and oscillations at individual tremor frequency, high-frequency oscillations (HFOs; >200 Hz) were found to reliably reflect the tremor state of PD patients (15, 16, 25). Unfortunately, we did not find any HFO peaks in the data at hand, most likely because the amplitude of HFOs is too low for detection by the PC+S^{TM} system.

Insights From Longitudinal Recordings

To our knowledge, this is the first longitudinal, invasive recording of tremor-related patterns in power and coherence in the STN of PD patients. Previous studies on PD have utilized the Activa PC+S^{TM} system for recording changes of STN power associated with voluntary or passive movements in patients (26–28) and in non-human primates (29, 30), and for investigating the effects of DBS on STN power (31, 32). In addition, Swann and colleagues have revealed a relationship between dyskinesia and gamma oscillations in the STN and motor cortex (33). Finally, a recent report made use of PC+S^{TM} data to fit a computational model of LFP rhythm generation (34).

The longest time range investigated in any of the previous patient studies was 12 months. Here, we performed measurements up to 24 months after surgery and found a 10 Hz peak in STN-coherence in all sessions, indicating that relevant, physiological signals remain measurable within this time frame. The fact that differences in STN power between motor tasks were only observed up to 6 months, however, suggests that the signal-to-noise ratio may have decreased over time. A similar decrease has been described in a previous study on cortical LFPs in non-human primates, using sub-dural electrodes (30). In this case, the deterioration of signal quality was associated with a dramatic increase of contact impedance and was found to be caused by regrowth of the dura. In our case, the loss of STN beta peaks observed at 1 year after surgery and thereafter was not accompanied by a corresponding increase in contact impedance, suggesting a minor role of tissue reorganization at the electrode-tissue interface.

A noteworthy finding of the longitudinal analysis is that a prominent beta power peak was visible in the first week after surgery but vanished over time. During the first week, the patient experienced a strong, transient reduction of motor symptoms caused by electrode insertion (stun effect). The stun effect has previously been used to explain the lack of beta peaks in some PD patients (31, 35). This study suggests that the stun effect can also lead to an increase rather than a disappearance of beta peaks, associated with tremor suppression. In agreement with this idea, the constancy of rest item of the UPDRS and STN beta power underwent antagonistic developments (**Figure 2**). Alternatively, the decline of power at beta frequencies might be a general marker of disease progression (36) or might be caused by a decrease in the signal-to-noise ratio not accompanied by increased impedance (see above). It could also be an after-effect of chronic DBS (32).

Clinical Relevance

Electrophysiological markers of PD symptoms are clinically relevant because they might be used to control adaptive DBS systems applying stimulation based on the current clinical state rather than continuously. The Activa PC+S^{TM} system, for example, can be incorporated into such systems (37). Adaptive stimulation can either be controlled by brain signals measured by the DBS electrodes or by external signals, such as accelerometers (6, 7). Studies using prototypes of adaptive, systems conditioned on brain activity suggest increased clinical benefit (38–40) and reduced occurrence of side-effects (5, 41) as compared to conventional DBS. The robustness of the relevant electrophysiological symptom markers is a prerequisite for the application of adaptive DBS systems (42), and longitudinal measurements, as performed in the current study, can provide information about their long-term stability.

This study adds a short, transient increase of subthalamic alpha/low-beta power to the list of potential markers of tremor. The short latency (∼150 ms) of this signal relative to the first noticeable sign of tremor in the EMG might enable adaptive systems to prevent tremor manifestation at an early stage, possibly before the patient is aware of tremor and certainly before tremor is noticed by others or interferes with

voluntary movements. Of course, noticing the brief alpha/low-beta power increase would require a very sensitive detector. Detector specificity, on the other hand, would depend on whether STN alpha/low-beta power undergoes comparable changes in situations other than tremor onset. Although the current study cannot provide a final answer to this question, we have not seen increases of alpha/low-beta power at comparable strength in voluntary foot or hand movements, suggesting that tremor-specificity is achievable.

Limitations

With only a single patient, the current study is not representative of the PD patient population. In particular, the patient under study suffered from severe leg tremor in addition to upper limb tremor, which is not the most common symptomatology. Future experiments need to investigate to what degree the results generalize to other muscles, to other patients, and to other types of tremor.

Furthermore, although we have been very careful in the definition of tremor onset, inspection of EMG traces cannot provide unequivocal onset times. Hence, the onset times and the latencies reported here need to be understood as estimates rather than precise measurements.

ETHICS STATEMENT

The patient gave written informed consent and the study was approved by the local ethics committee (study no. 4326).

AUTHOR CONTRIBUTIONS

AS and LW designed the experiment. LS and CH collected clinical data. OA, LS, JH, and MB recorded the electrophysiological data. JH analyzed the data and wrote the first draft of the manuscript. AS, MB, LW, OA, and CH reviewed and edited the manuscript.

FUNDING

Medtronic provided the PC+S device and technical support. It did neither influence data acquisition, analysis, interpretation nor publication.

ACKNOWLEDGMENTS

We would like to thank the patient for participating in this study. Further, we thank Medtronic for providing the Activa PC+S^{TM} system, and Ayse Bovet, Scott Stanslaski, and Gaetano Leogrande for technical support. Finally, we are thankful to Max Betz for screening and organizing the data.

SUPPLEMENTARY MATERIAL

The Supplementary Material for this article can be found online at: https://www.frontiersin.org/articles/10.3389/fneur.2019.00145/full#supplementary-material

REFERENCES

1. Deuschl G, Raethjen J, Baron R, Lindemann M, Wilms H, Krack P. The pathophysiology of parkinsonian tremor: a review. *J Neurol.* (2000) 247:V33–48. doi: 10.1007/PL00007781
2. Hughes AJ, Daniel SE, Blankson S, Lees AJ. A clinicopathologic study of 100 cases of Parkinson's disease. *Arch Neurol.* (1993) 50:140–8. doi: 10.1001/archneur.1993.00540020018011
3. Kumar R, Lozano AM, Kim YJ, Hutchison WD, Sime E, Halket E, et al. Double-blind evaluation of subthalamic nucleus deep brain stimulation in advanced Parkinson's disease. *Neurology*. (1998) 51:850–5.
4. Benabid AL, Pollak P, Hoffmann D, Gervason C, Hommel M, Perret JE, et al.. Long-term suppression of tremor by chronic stimulation of the ventral intermediate thalamic nucleus. *Lancet*. (1991) 337:403–6. doi: 10.1016/0140-6736(91)91175-T
5. Priori A, Foffani G, Rossi L, Marceglia S. Adaptive deep brain stimulation (aDBS) controlled by local field potential oscillations. *Exp Neurol.* (2013) 245:77–86. doi: 10.1016/j.expneurol.2012.09.013
6. Cagnan H, Pedrosa D, Little S, Pogosyan A, Cheeran B, Aziz T, et al. Stimulating at the right time: phase-specific deep brain stimulation. *Brain*. (2017) 140:132–45. doi: 10.1093/brain/aww286
7. Malekmohammadi M, Herron J, Velisar A, Blumenfeld Z, Trager MH, Chizeck HJ, et al. Kinematic adaptive deep brain stimulation for resting tremor in Parkinson's disease. *Mov Disord.* (2016) 31:426–28. doi: 10.1002/mds.26482
8. Timmermann L, Gross J, Dirks M, Volkmann J, Freund HJ, Schnitzler A. The cerebral oscillatory network of parkinsonian resting tremor. *Brain*. (2003) 126:199–212. doi: 10.1093/brain/awg022
9. Muthuraman M, Heute U, Arning K, Anwar AR, Elble R, Deuschl G, et al. Oscillating central motor networks in pathological tremors and voluntary movements. What makes the difference? *Neuroimage*. (2012) 60:1331–9. doi: 10.1016/j.neuroimage.2012.01.088
10. Hirschmann J, Hartmann CJ, Butz M, Hoogenboom N, Özkurt TE, Elben S, et al. A direct relationship between oscillatory subthalamic nucleus-cortex coupling and rest tremor in Parkinson's disease. *Brain*. (2013) 136:3659–70. doi: 10.1093/brain/awt271
11. Wang SY, Aziz TZ, Stein JF, Liu X. Time-frequency analysis of transient neuromuscular events: dynamic changes in activity of the subthalamic nucleus and forearm muscles related to the intermittent resting tremor. *J Neurosci Methods*. (2005) 145:151–8. doi: 10.1016/j.jneumeth.2004.12.009
12. Qasim SE, de Hemptinne C, Swann N, Miocinovic S, Ostrem JL, Starr PA. Electrocorticography reveals beta desynchronization in the basal ganglia-cortical loop during rest tremor in Parkinson's disease. *Neurobiol Dis.* (2016) 86:177–86. doi: 10.1016/j.nbd.2015.11.023
13. Weinberger M, Hutchison WD, Lozano AM, Hodaie M, Dostrovsky JO. Increased gamma oscillatory activity in the subthalamic nucleus during tremor in Parkinson's disease patients. *J Neurophysiol.* (2009) 101:789–802. doi: 10.1152/jn.90837.2008
14. Beudel M, Little S, Pogosyan A, Ashkan K, Foltynie T, Limousin P, et al. Tremor reduction by deep brain stimulation is associated with gamma power suppression in Parkinson's disease. *Neuromodulation*. (2015) 18:349–54. doi: 10.1111/ner.12297
15. Hirschmann J, Butz M, Hartmann CJ, Hoogenboom N, Özkurt TE, Vesper J, et al. Parkinsonian rest tremor is associated with modulations of subthalamic high-frequency oscillations. *Mov Disord.* (2016) 31:1551–9. doi: 10.1002/mds.26663
16. Telkes I, Viswanathan A, Jimenez-Shahed J, Abosch A, Ozturk M, Gupte A, et al. Local field potentials of subthalamic nucleus contain electrophysiological footprints of motor subtypes of Parkinson's disease. *Proc Natl Acad Sci USA*. (2018) 115:E8567–76. doi: 10.1073/pnas.1810589115

17. Helmich RC, Hallett M, Deuschl G, Toni I, Bloem BR. Cerebral causes and consequences of parkinsonian resting tremor: a tale of two circuits? *Brain*. (2012) 135:3206–26. doi: 10.1093/brain/aws023
18. Helmich RC, Janssen MJR, Oyen WJG, Bloem BR, Toni I. Pallidal dysfunction drives a cerebellothalamic circuit into Parkinson tremor. *Ann Neurol.* (2011) 69:269–81. doi: 10.1002/ana.22361
19. Stanslaski S, Afshar P, Cong P, Giftakis J, Stypulkowski P, Carlson D, et al. Design and validation of a fully implantable, chronic, closed-loop neuromodulation device with concurrent sensing and stimulation. *IEEE Trans Neural Syst Rehabil Eng.* (2012) 20:410–21. doi: 10.1109/TNSRE.2012.2183617
20. Oostenveld R, Fries P, Maris E, Schoffelen J-M. FieldTrip: Open source software for advanced analysis of MEG, EEG, and invasive electrophysiological data. *Comput Intell Neurosci.* (2011) 2011:1–9. doi: 10.1155/2011/156869
21. Hyvarinen A. Fast and robust fixed-point algorithms for independent component analysis. *IEEE Trans Neural Netw.* (1999) 10:626–34. doi: 10.1109/72.761722
22. Maris E, Oostenveld R. Nonparametric statistical testing of EEG- and MEG-data. *J Neurosci Methods*. (2007) 164:177–90. doi: 10.1016/j.jneumeth.2007.03.024
23. Maris E, Schoffelen JM, Fries P. Nonparametric statistical testing of coherence differences. *J Neurosci Methods*. (2007) 163:161–75. doi: 10.1016/j.jneumeth.2007.02.011
24. Bostan AC, Dum RP, Strick PL. The basal ganglia communicate with the cerebellum. *Proc Natl Acad Sci USA*. (2010) 107:8452–6. doi: 10.1073/pnas.1000496107
25. Hirschmann J, Schoffelen JM, Schnitzler A, van Gerven MAJ. Parkinsonian rest tremor can be detected accurately based on neuronal oscillations recorded from the subthalamic nucleus. *Clin Neurophysiol.* (2017) 128:2029–36. doi: 10.1016/j.clinph.2017.07.419
26. Hanrahan S, Nedrud J, Davidson B, Farris S, Giroux M, Haug A, et al. Long-term task- and dopamine-dependent dynamics of subthalamic local field potentials in Parkinson's disease. *Brain Sci.* (2016) 6:57. doi: 10.3390/brainsci6040057
27. Quinn EJ, Blumenfeld Z, Velisar A, Koop MM, Shreve LA, Trager MH, et al. Beta oscillations in freely moving Parkinson's subjects are attenuated during deep brain stimulation. *Mov Disord.* (2015) 30:1750–8. doi: 10.1002/mds.26376
28. Canessa A, Pozzi NG, Arnulfo G, Brumberg J, Reich MM, Pezzoli G, et al. Striatal dopaminergic innervation regulates subthalamic beta-oscillations and cortical-subcortical coupling during movements: preliminary evidence in subjects with Parkinson's disease. *Front Hum Neurosci.* (2016) 10:611. doi: 10.3389/fnhum.2016.00611
29. Connolly AT, Muralidharan A, Hendrix C, Johnson L, Gupta R, Stanslaski S, et al. Local field potential recordings in a non-human primate model of Parkinsons disease using the Activa PC + S neurostimulator. *J Neural Eng.* (2015) 12:066012. doi: 10.1088/1741-2560/12/6/066012
30. Ryapolova-Webb E, Afshar P, Stanslaski S, Denison T, de Hemptinne C, Bankiewicz K, et al. Chronic cortical and electromyographic recordings from a fully implantable device: preclinical experience in a nonhuman primate. *J Neural Eng.* (2014) 11:16009. doi: 10.1088/1741-2560/11/1/016009
31. Neumann WJ, Staub F, Horn A, Schanda J, Mueller J, Schneider GH, et al. Deep brain recordings using an implanted pulse generator in Parkinson's disease. *Neuromodulation*. (2016) 19:20–3. doi: 10.1111/ner.12348
32. Trager MH, Koop MM, Velisar A, Blumenfeld Z, Nikolau JS, Quinn EJ, et al. Subthalamic beta oscillations are attenuated after withdrawal of chronic high frequency neurostimulation in Parkinson's disease. *Neurobiol Dis.* (2016) 96:22–30. doi: 10.1016/J.NBD.2016.08.003
33. Swann NC, de Hemptinne C, Miocinovic S, Qasim S, Wang SS, Ziman N, et al. Gamma oscillations in the hyperkinetic state detected with chronic human brain recordings in Parkinson's disease. *J Neurosci.* (2016) 36:6445–58. doi: 10.1523/JNEUROSCI.1128-16.2016
34. Maling N, Lempka SF, Blumenfeld Z, Bronte-Stewart H, McIntyre CC. Biophysical basis of subthalamic local field potentials recorded from deep brain stimulation electrodes. *J Neurophysiol.* (2018) 120:1932–44. doi: 10.1152/jn.00067.2018
35. Eusebio A, Brown P. Synchronisation in the beta frequency-band - The bad boy of parkinsonism or an innocent bystander? *Exp Neurol.* (2009) 217:1–3. doi: 10.1016/j.expneurol.2009.02.003
36. Connolly AT, Jensen AL, Bello EM, Netoff TI, Baker KB, Johnson MD, et al. Modulations in oscillatory frequency and coupling in globus pallidus with increasing parkinsonian severity. *J Neurosci.* (2015) 35:6231–40. doi: 10.1523/JNEUROSCI.4137-14.2015
37. Afshar P, Khambhati A, Stanslaski S, Carlson D, Jensen R, Linde D, et al. A translational platform for prototyping closed-loop neuromodulation systems. *Front Neural Circuits*. (2013) 6:117. doi: 10.3389/fncir.2012.00117
38. Rosin B, Slovik M, Mitelman R, Rivlin-Etzion M, Haber SN, Israel Z, et al. Closed-loop deep brain stimulation is superior in ameliorating parkinsonism. *Neuron*. (2011) 72:370–84. doi: 10.1016/j.neuron.2011.08.023
39. Little S, Pogosyan A, Neal S, Zavala B, Zrinzo L, Hariz M, et al. Adaptive deep brain stimulation in advanced Parkinson disease. *Ann Neurol.* (2013) 74:449–57. doi: 10.1002/ana.23951
40. Piña-Fuentes D, Little S, Oterdoom M, Neal S, Pogosyan A, Tijssen MAJ, et al. Adaptive DBS in a Parkinson's patient with chronically implanted DBS: a proof of principle. *Mov Disord.* (2017) 32:1253–4. doi: 10.1002/mds.26959
41. Little S, Tripoliti E, Beudel M, Pogosyan A, Cagnan H, Herz D, et al. Adaptive deep brain stimulation for Parkinson's disease demonstrates reduced speech side effects compared to conventional stimulation in the acute setting. *J Neurol Neurosurg Psychiatry*. (2016) 87:1388–9. doi: 10.1136/jnnp-2016-313518
42. Arlotti M, Marceglia S, Foffani G, Volkmann J, Lozano AM, Moro E, et al. Eight-hours adaptive deep brain stimulation in patients with Parkinson disease. *Neurology*. (2018) 90:e971–6. doi: 10.1212/WNL.0000000000005121

Conflict of Interest Statement: AS and LW have received consultant/speaker fees from Boston Scientific, Medtronic, Inomed, and/or Abbott.

The remaining authors declare that the research was conducted in the absence of any commercial or financial relationships that could be construed as a potential conflict of interest.

frontiers in Human Neuroscience

ORIGINAL RESEARCH
published: 03 April 2019
doi: 10.3389/fnhum.2019.00118

Abnormal Phase Coupling in Parkinson's Disease and Normalization Effects of Subthreshold Vestibular Stimulation

Soojin Lee[1,2], Aiping Liu[2,3], Z. Jane Wang[1,4] and Martin J. McKeown[2,5]*

[1] School of Biomedical Engineering, University of British Columbia, Vancouver, BC, Canada, [2] Pacific Parkinson's Research Centre, Vancouver, BC, Canada, [3] Department of Electronic Science and Technology, University of Science and Technology of China, Hefei, China, [4] Department of Electrical and Computer Engineering, University of British Columbia, Vancouver, BC, Canada, [5] Department of Medicine (Neurology), University of British Columbia, Vancouver, BC, Canada

The human brain is a highly dynamic structure requiring dynamic coordination between different neural systems to perform numerous cognitive and behavioral tasks. Emerging perspectives on basal ganglia (BG) and thalamic functions have highlighted their role in facilitating and mediating information transmission among cortical regions. Thus, changes in BG and thalamic structures can induce aberrant modulation of cortico-cortical interactions. Recent work in deep brain stimulation (DBS) has demonstrated that externally applied electrical current to BG structures can have multiple downstream effects in large-scale brain networks. In this work, we identified EEG-based altered resting-state cortical functional connectivity in Parkinson's disease (PD) and examined effects of dopaminergic medication and electrical vestibular stimulation (EVS), a non-invasive brain stimulation (NIBS) technique capable of stimulating the BG and thalamus through vestibular pathways. Resting EEG was collected from 16 PD subjects and 18 age-matched, healthy controls (HC) in four conditions: *sham* (no stimulation), EVS1 (4–8 Hz multisine), EVS2 (50–100 Hz multisine) and EVS3 (100–150 Hz multisine). The mean, variability, and entropy were extracted from time-varying phase locking value (PLV), a non-linear measure of pairwise functional connectivity, to probe abnormal cortical couplings in the PD subjects. We found the mean PLV of Cz and C3 electrodes were important for discrimination between PD and HC subjects. In addition, the PD subjects exhibited lower variability and entropy of PLV (mostly in theta and alpha bands) compared to the controls, which were correlated with their clinical characteristics. While levodopa medication was effective in normalizing the mean PLV only, all EVS stimuli normalized the mean, variability and entropy of PLV in the PD subject, with the exact extent and duration of improvement a function of stimulus type. These findings provide evidence demonstrating both low- and high-frequency EVS exert widespread influences on cortico-cortical connectivity, likely via subcortical activation. The improvement observed in PD in a stimulus-dependent manner suggests that EVS with optimized parameters may provide a new non-invasive means for neuromodulation of functional brain networks.

Keywords: Parkinson's disease, electrical vestibular stimulation, EEG, phase locking value, cortical oscillations, sample entropy, sparse discriminant analysis

OPEN ACCESS

Edited by:
Matt J. N. Brown,
California State University, Sacramento, United States

Reviewed by:
Görsev Yener,
Dokuz Eylül University, Turkey
Antonio Ivano Triggiani,
University of Foggia, Italy

***Correspondence:**
Aiping Liu
aipingl@ece.ubc.ca

Received: *22 November 2018*
Accepted: *19 March 2019*
Published: *03 April 2019*

Citation:
Lee S, Liu A, Wang ZJ and McKeown MJ (2019) Abnormal Phase Coupling in Parkinson's Disease and Normalization Effects of Subthreshold Vestibular Stimulation. Front. Hum. Neurosci. 13:118. doi: 10.3389/fnhum.2019.00118

INTRODUCTION

Parkinson's disease (PD), the second most common neurodegenerative disease (Scandalis et al., 2001), is characterized by motor symptoms such as bradykinesia, tremor, rigidity and impaired balance and gait as well as non-motor complications, resulting primarily from degeneration of dopaminergic neurons in the substantia nigra pars compacta (SNc) (Davie, 2008). Several electrophysiology studies using local field potential (LFP) recordings demonstrated that, in the dopamine-deficient state, the neuronal synchronization in the basal ganglia (BG) is exaggerated at frequencies in the beta range (13–30 Hz) (Brown and Williams, 2005; Eusebio et al., 2009; Litvak et al., 2012; Oswal et al., 2013). These beta oscillations are also highly synchronized with sensorimotor areas (Brown et al., 2001; Marsden et al., 2001; Cassidy et al., 2002; Williams et al., 2002) as well as muscle activity of upper limbs during movement (Marsden et al., 2001). This excessive beta synchronization is considered to be, in part, responsible for the Parkinsonian symptoms and thus reducing the abnormal synchronization with deep brain stimulation (DBS) has shown to be an effective therapy.

Recent fMRI findings have highlighted that large-scale cortical resting-state functional connectivity (rsFC) is altered in PD, possibly as a result of BG impairment effects on cortical-BG networks (Helmich et al., 2010). The striatum, a subcortical region significantly affected with dopamine depletion in PD, has altered FC with inferior parietal, temporal, and motor cortices (Helmich et al., 2010), which supports that PD-induced connectivity changes can be seen beyond local subcortical regions. In addition to effects on BG-cortical FC, impairment in the BG can also alter cortico-cortical connectivity. Diminished interhemispheric connectivity in sensorimotor cortical regions (Seibert et al., 2012) and reduced rsFC in widespread regions including inferior frontal, superior parietal, and occipital regions (Dubbelink et al., 2014) have been shown to be implicated with disease duration and cognitive dysfunctions in PD.

Inferring pathological cortico-cortical connectivity in PD solely based on evidence from fMRI alone may not provide a complete picture, as fMRI has limited temporal resolution. Electrophysiology can provide complementary information as it measures spontaneous synchronous activity of a large population of neurons occurring on a millisecond time scale. A simultaneous LFP-electroencephalography (EEG) study reported that the dynamics of LFP synchrony in STN is related to the dynamics of cortical synchrony (Ahn et al., 2015), and BG DBS modulates cortical phase coupling measured with EEG (Silberstein et al., 2005; Smolders et al., 2013).

One of the most widely-used method to quantify the couplings between oscillatory signals recorded at pairs of electrodes placed on the scalp in EEG is to look at their phase relationships (Klimesch et al., 2008; Fell and Axmacher, 2011). If cortical activities at two different regions are coupled, their phase angle differences tend to be consistent across time. Phase locking value (PLV) quantifies the strength of the phase coupling between two oscillatory signals, bounded between zero and one indicating a completely random and perfectly coupled relationship, respectively. Interregional phase synchronization has been shown to reflect specific neural activity coding different cognitive functions (Klimesch et al., 2001; Hanslmayr et al., 2005), motor behaviors (Andres and Gerloff, 1999; for a review, see Sauseng and Klimesch, 2008) and pathological brain states (Spencer et al., 2004; Sakkalis et al., 2007; Vakorin et al., 2016). However, to date, only a few studies have examined phase-based rsFC across broad cortical regions and different frequency bands in PD (Silberstein et al., 2005; Moazami-Goudarzi et al., 2008; George et al., 2013; He et al., 2017).

Most of the EEG connectivity studies to date have employed magnitude squared coherence. PD subjects exhibit excessive EEG coherence (Silberstein et al., 2005; George et al., 2013), especially in the beta band, in the off-medication condition that is decreased by medication (George et al., 2013). For PD subjects on-medication, enhanced coherence in the frontal regions in the theta (4–6 Hz), beta (12–18 Hz), and gamma (30–45 Hz) (Moazami-Goudarzi et al., 2008) and altered interhemispheric beta coherences in the midtemporal and frontal areas (He et al., 2017) can be observed, indicating the multifarious role of dopamine in the control of oscillatory activity, in and beyond the BG. However, coherence is different from PLV in that it relies on the assumption of linearity and stationarity in the signals and is calculated independently for each frequency, which is then scaled by the amplitudes of the signals. PLV-based connectivity, which do not rely on the strict assumptions underlying coherence, might be more suitable for non-linear and non-stationary dynamics of neural oscillations, and sheds a new light on pathophysiological brain networks as it has not been explored yet in PD.

Recent progress in non-invasive brain stimulation (NIBS) has demonstrated its capability to modulate cortical oscillations (Helfrich et al., 2014; Vossen et al., 2015; Amengual et al., 2017) and interregional couplings, indicating its potential applications as an effective therapeutic technique for PD. Electrical vestibular stimulation (EVS) is a NIBS technique that delivers weak current to the mastoid processes and modulates firing rates of vestibular afferents, which then activates various cortical and subcortical regions including the BG and thalamus (Bense et al., 2001; Utz et al., 2010; Lopez et al., 2012). Similar to transcranial electrical stimulation (tES), EVS stimuli can take the form of direct current (DC), alternating current (AC), or random noise (RN) and stimulation effects vary according to stimulus types. While DC-EVS perturbs perception of orientation and locomotion and has been widely utilized in postural balance control research (St George and Fitzpatrick, 2011), RN-EVS has demonstrated its efficacy in motor functions (Yamamoto et al., 2005; Pan et al., 2008; Lee et al., 2015) and modulation of EEG oscillatory rhythms across broad cortical regions in PD (Kim et al., 2013). It is conceivable, therefore, that EVS may be able to modulate cortical couplings, which has not been explored yet.

To establish the potential of EVS as a therapeutic intervention to modulate abnormal cortical couplings in PD, we investigated whether resting-state cortical couplings, as measured as PLV, were altered in unmedicated PD subjects, and determined if EVS had any normalizing effects. Specifically, we applied three novel EVS stimuli, each restricted to a specific frequency band, to PD and healthy subjects and examined how the different stimuli

affected both the strength and temporal variation of aberrant couplings in PD.

MATERIALS AND METHODS

Participants

Twenty PD patients and 22 age- and gender-matched healthy controls (HC) participated in this study. Patients with atypical parkinsonism or other neurological disorders were excluded from the study, and all included PD patients were classified as having mild to moderate stage PD (Hoehn and Yahr Stage 1–2). Four PD and four HC subjects were excluded in the data analysis due to severe muscle artifacts in their EEG recordings. Therefore, 16 PD (7 males; age: 67.3 ± 6.5 years) and 18 HC (9 males; age: 67.6 ± 8.9 years) subjects were included in the analysis (**Table 1**). All subjects did not have any reported vestibular or auditory disorders and were right-handed. The study protocol was approved by the Clinical Research Ethics Board at the University of British Columbia (UBC) and the recruitment was conducted at the Pacific Parkinson's Research Centre (PPRC) in UBC. All subjects gave a written informed consent prior to participation.

Study Protocol

As individuals have inherently subjective perception of EVS, we utilized systematic procedures that have been previously used in determining subliminal current level (Lee et al., 2015). The measured individual threshold level was in the range of 0.23–1.1 mA. After the threshold was determined, the subjects were comfortably seated in front of a computer screen and were instructed to focus their gaze on a continuously displayed fixed target while EEG was being recorded. EEG was first recorded without stimulation for 20 s and EVS were then delivered for a fixed duration of 60 s, followed by an EVS-off period for 20 s (post-stimulation). During the stimulation period, EVS was applied at 90% of the individual threshold level.

EEG was recorded from the subjects in 4 different conditions: *Sham* (no stimulation), EVS1, EVS2 and EVS3 (for details, see section EVS). EEG recording was first performed in the *sham* condition and the EVS conditions were randomly ordered. We allowed a 2 min break between each condition to prevent any potential post-stimulation effects carried over from the previous EVS conditions.

The HC subjects performed the protocol once, whereas PD subjects performed it twice in off-medication (PDMOFF) and on-medication (PDMON) conditions on the same day. The PD subjects stopped taking their normal L-dopa medication at least 12 h, and any dopamine agonists 18 h prior to the EEG recording. United Parkinson's Disease Rating Scale (UPDRS) Parts II and III were assessed in the off-medication condition. Immediately after finishing the EEG acquisition, they took their regular dose of L-dopa medication and rested for 1 h. After the break, EEG was recorded in the on-medication condition.

TABLE 1 | Demographic and clinical characteristics of the patients with Parkinson's disease (PD) and healthy controls (HC).

	PD	HC
Age (years), mean (SD)	67.3 (6.5)	67.6 (8.9)
Gender, n (male/female)	7/9	9/9
Disease duration (years), mean (SD)	7.4 (4.3)	–
[a]UPDRS II, mean (SD)	14.8 (8.1)	–
[b]UPDRS III, mean (SD)	22.1 (8.9)	–
Hoehn and Yahr scale, mean (range)	1.3 (1–2)	–
Levodopa equivalent daily dose (mg), mean (SD) (Tomlinson et al., 2010)	635.9 (356.4)	–

[a]*Motor aspects of experiences of daily living.* [b]*Motor symptoms.*

EVS

EVS was delivered through pre-gelled Ag/AgCl electrodes (BIOPAC Systems Inc., CA, United States) placed in bilateral, bipolar fashion over the mastoid process behind each ear. Nuprep^{TM} skin prep gel was used to clean skin for better electrode contact and to reduce resistance during stimulation. Stimulation waveforms were generated on a computer using MATLAB (R2018a, MathWorks, MA, United States) and converted to an analog signal using a NI USB-6221 BNC digital acquisition module (National Instruments, TX, United States). The analog voltage signals were then passed to a constant current stimulator (DS5, Digitimer, United Kingdom), which was connected to the stimulating electrodes.

Three multisine signals in different frequency bands (EVS1: 4–8 Hz; EVS2: 50–100 Hz; EVS3: 100–150 Hz) were used (**Figure 1A**). Multisine signals are designed to concentrate power at a precise number of frequencies within the bandwidth of interest, which is advantageous compared to other excitation signals (e.g., a white noise or swept sine) as there is no spectral leakage. Each multisine signals were designed to have the frequencies of sinusoids (f_i) uniformly distributed every 0.2 Hz and the phases (ϕ_i) chosen to minimize the crest factor using a clipping algorithm (Van der Ouderaa et al., 1988) in order to generate a flat amplitude of the signal and thus improve subject's comfort:

$$x(t, \phi) = a \cdot \sum_{i=1}^{n} \cos\left(2\pi f_i t + \phi_i\right)$$

where $x(t,\phi)$ is the multisine, a is the amplitude, f_i and ϕ_i are the frequency and phase, and i is the index of each sinusoidal component (e.g., $f_1, f_2, \ldots, f_n =$ 4.0, 4.2, . . ., 8.0 Hz for EVS1).

EEG Recording

Data were recorded from 27 scalp electrodes using a 64-channel EEG cap (Neuroscan, VA, United States) and a Neuroscan SynAmps2 acquisition system (Neuroscan, VA, United States) at a sampling rate of 1 kHz. Recording electrodes were positioned according to the International 10–20 placement standard with one ground and one reference electrode located between Cz and CPz (**Figure 1B**). Impedances were kept below 15 k**Ω** using

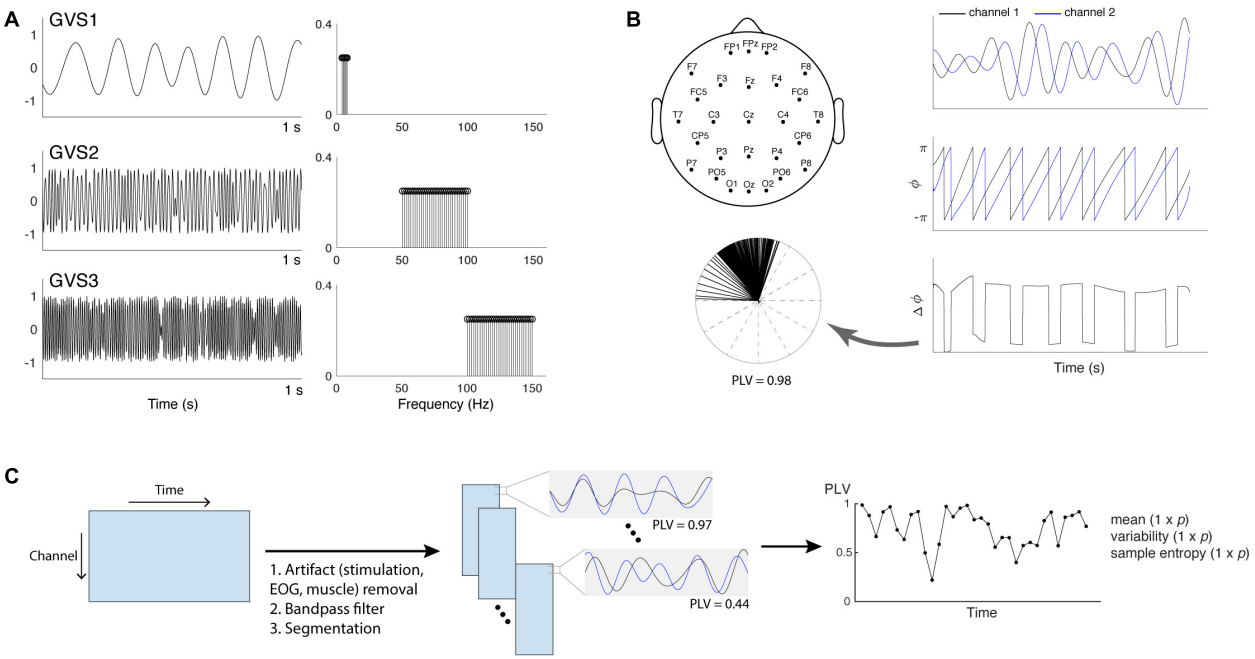

FIGURE 1 | (A) Time and frequency plots of the three types of multisine stimulus given at 90% individual threshold level (EVS1: 4–8 Hz; EVS2: 50–100 Hz; EVS3: 100–150 Hz). **(B)** Placement of 27 EEG electrodes and PLV calculation. Hilbert transform is applied to the two signals to extract the instantaneous phases. The phase differences calculated at each time point are represented into unit vectors in the complex plane and PLV is computed to evaluate the spread of the distribution (Lachaux et al., 1999; Mormann et al., 2000). **(C)** The procedure to extract phase locking value (PLV) time series. For each subject, preprocessing steps were first applied to the raw EEG data in order to remove high-voltage stimulation artifacts as well as cardinal artifacts caused by eye movements [electrooculography (EOG)] or muscle movement. The cleaned data were bandpass filtered into four different frequency bands (theta: 4–8 Hz; alpha: 8–13 Hz; beta: 13–30 Hz; gamma: 30–45 Hz) and segmented into epochs. PLV between a pair of electrodes in each epoch was computed to generate the time series, and its mean, variability, and sample entropy were calculated. Each subject has a 1 × p vector for the mean, variability and sample entropy (p = 1,404 = 351 pairs × 4 frequency bands).

Electro-Gel (Electrode-Cap International, OH, United States). No clipping of EEG was observed during stimulation.

EEG Preprocessing

The EEG data were bandpass filtered between 3 and 45 Hz using a two-way finite impulse response (FIR) filter (the "eegfilt" function in EEGLAB). High-voltage stimulation artifacts during EVS2 and EVS3 were removed using the digital filters. The artifacts during EVS1 were removed using a quadrature-IVA method (Lee et al., 2019). Data were then re-referenced to the average reference (linked earlobe) and ocular artifacts (EOG) were corrected based on cross-correlation with the reference EOG channels using the AAR toolbox included in EEGLAB. The cleaned EEG data were bandpass filtered into four conventional EEG frequency bands (Groppe et al., 2013): theta (4–8 Hz), alpha (8–13 Hz), beta (13–30 Hz), and gamma (30–45 Hz). The bandpass-filtered data were then segmented into non-overlapping epochs. Epoch sizes were determined such that the epochs include around four cycles at a center frequency of the selected bandwidth (Martin and Schröder, 2016), resulting in epoch sizes of 600, 400, 200, and 100 ms for the theta, alpha, beta, and gamma bands.

Phase Locking Value (PLV)

PLV evaluates the spread of the distribution of phase angle differences between pairs of electrodes over time (Lachaux et al., 1999; Mormann et al., 2000; **Figure 1B**). The connectivity is measured from this spread such that strongly clustered phase differences between two electrodes result in the PLV value close to one, indicating a strong connectivity between the signals. If there is no phase dependence, PLV value becomes zero.

To calculate the PLV, instantaneous phase angles were obtained by applying the Hilbert transformation to the bandpass-filtered data. Then, the PLV between two signals A and B was computed as Bruña et al. (2018):

$$PLV_{A,B} = \frac{1}{T}\left|\sum_{t=1}^{T} e^{-i(\varphi_A(t) - \varphi_B(t))}\right|$$

where T is the number of time points and $\varphi(t)$ is the instantaneous phase angles of each EEG signal. The PLV was computed for each epoch, resulting in times series of the PLV computed from all pairs of 27 electrodes and the four frequency bands (1,404 time series in total). Three temporal features were extracted from each PLV time series for further analysis: the mean, variability (standard deviation), and sample entropy. Sample entropy is a non-linear measure to quantify the degree of complexity in a time series (Richman and Moorman, 2000), and has been applied to EEG data for clinical application such as classification (Bruce et al., 2009; Kumar et al., 2012) and epilepsy

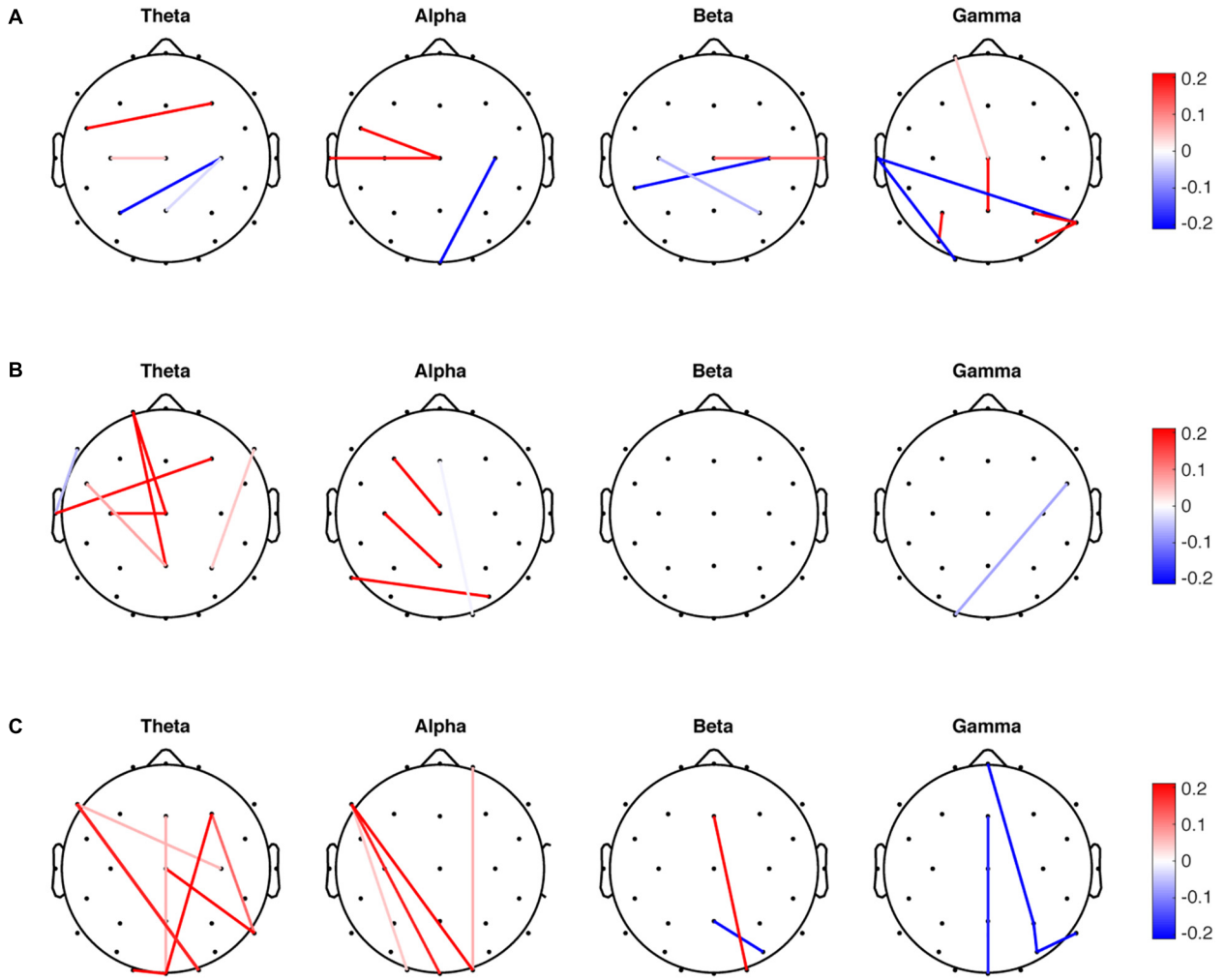

FIGURE 2 | Non-zero features selected by sparse discriminant analysis (SDA). SDA was applied to the mean, variability and entropy data sets, respectively, to discriminate the PDMOFF and HC groups. The non-zero weights in the sparse discriminant vectors are presented in the scalp maps. **(A)** Weights for the 17 selected features from the mean PLV data set. **(B)** Weights for the 12 selected features from the PLV variability data set. **(C)** Weights for the 17 selected features from the PLV entropy data set.

detection (Song et al., 2012). Tolerance (r) and window length (m) were specified to be 0.3 and 2, respectively, to compute the sample entropy based on Lake et al. (2002) and characteristics of our data sets.

Sparse Discriminant Analysis

Linear discriminant analysis (LDA) is a classical supervised classification technique that finds the most discriminative projections of a $N \times p$ data in a p-dimensional space such that the data projected into the low-dimensional subspace can be well partitioned into k classes (Mai, 2013). In biomedical research, it has become an increasingly important topic to perform a classification with a high-dimensional data where the number of variables far exceeds the number of samples. In such high-dimensional settings, LDA cannot be applied directly because of singularity of the sample covariance matrix. To overcome this limitation, various regularized versions of LDA have been proposed (Safo and Long, 2018). Sparse discriminant analysis (SDA) was proposed by Clemmensen et al. (2011) where an elastic net penalty and optimal scoring framework are applied to a high-dimensional data to generate a sparse discriminant vector. The authors demonstrated that SDA outperforms other regularized methods such as shrunken centroids regularized discriminant analysis and sparse partial least squares regression. The details of the algorithm can be found in Clemmensen et al. (2011).

Here, we aim to classify the PDMOFF and HC groups in the baseline resting state (i.e., the *sham* condition) using the PLV features obtained above. The three data sets (mean, variability and sample entropy) have the same high-dimensional settings as each data set has the number of variables (p = 1,404) much greater than the number of samples (i.e., subjects). Therefore, we applied SDA to each data set to infer from the sparse discriminant vectors which combination of the electrode pairs and frequency bands are the most important features for the classification of

the two groups. As in Clemmensen et al. (2011), we created the training set consisted of 26 subjects (12 PDMOFF and 14 HC) and the test set of eight subjects (4 PDMOFF and 4 HC subjects) and the tuning parameters for SDA (i.e., λ and γ for regularization penalties) were chosen using leave-one-out cross-validation (LOOCV) on the training data. The models with the selected parameters were evaluated on the test data.

In the subsequent analyses, we investigated effects of L-dopa medication on the PLV features by applying the sparse discriminant vectors obtained from the above SDA to the data sets of the PDMON group in the *sham* condition. In the same manner, effects of EVS on the PLV features were evaluated by applying the same sparse discriminant vectors to the data sets in the EVS conditions.

Statistical Analysis

A one-way ANOVA was performed to compare the PLV features between groups followed by *post hoc* Tukey's honestly significant difference (HSD) test for multiple comparison correction. To evaluate effects of EVS on the PLV features within a group, a repeated measures (rm) ANOVA, with stimulation condition (*sham*, EVS1, EVS2, and EVS3) as the within-subject factor, was performed followed by *post hoc* Tukey's HSD test for multiple comparison correction. The rm ANOVA analysis was performed for online and after-effect conditions, respectively.

RESULTS

SDA Classification Results and Selected Features

SDA was performed for the mean, variability, and entropy PLV data sets independently to discriminate the PDMOFF and HC groups. Since there are two classes in the data, only one discriminant vector was obtained from each SDA. For the mean PLV data set, LOOCV on the training data resulted in the selection of 17 non-zero features (1.2%) out of total 1,404 features (**Figure 2A**). There were both negative and positive weights for the selected features in each frequency band. Since the transformed PLV mean was greater for the PDMOFF (**Figure 3A**) than the HC group, the positive weights were interpreted as cortical couplings exaggerated in the PDMOFF group. 35% of the selected features were associated with Cz over a broad frequency bandwidth, and the PDMOFF group had a stronger coupling strength for the features. In contrast, the features related to C4 had negative weights, indicating that these couplings are attenuated in the PDMOFF group. In the gamma band, decreased long-distance connectivity in the left temporal region (T7-O1 and T7-P8) and increased short-distance connectivity in the parietal region (P3-PO5, P8-P4, and P8-PO6) were found to be related to the PDMOFF group. The training and test classification accuracy (fraction of correctly classified) were both 100%.

For the PLV variability data set, 12 non-zero features (0.85%) were selected and the largest number of the selected features was found in the theta band (**Figure 2B**), followed by the alpha and gamma bands. Note that positive weights are associated with the lower connectivity variability of the PDMOFF group because the transformed variability is lower for the PDMOFF group (**Figure 3A**). Decreased variability in the PDMOFF group was mostly associated with the frontal electrodes in the theta band and with F3-Cz, C3-Pz, and P7-PO6 in the alpha band. The classification accuracy for the training and test data sets were 100 and 87.5%, respectively.

The SDA on the PLV entropy data set selected 17 non-zero features (1.2%) and most of them were long-distance connectivity. Note that positive weights are associated with the connectivity with lower entropy for the PDMOFF group. In the theta and alpha bands, the entropy of the selected features was lower whereas in the gamma band the entropy was higher for the PDMOFF group compared to the HC group. In the beta band, the PDMOFF group had a lower entropy for Fz-O2 and higher entropy for Pz-PO6 than the HC group. The training and test classification accuracy were 96 and 87.5%, respectively.

Group Comparison of Baseline PLV Features

The SDA discriminant vectors were applied to the data sets obtained from the PDMON group, and the group means of the transformed data are compared in **Figure 3A**. Significant group differences were found for the PLV features [PLV mean: $F(2, 47) = 41.68$, $P < 0.001$; PLV variability: $F(2, 47) = 23.46$, $P < 0.001$; PLV entropy: $F(2, 47) = 60.59$, $P < 0.001$]. The PLV mean for the PDMOFF group was significantly higher than the HC group ($P < 0.001$), which was decreased by L-dopa medication ($P < 0.01$). The PLV variability was significantly lower in the PDMOFF compared to the HC group ($P < 0.001$), and the lower variability was associated with higher UPDRS2 scores (i.e., more severe difficulties of daily motor activities) ($r = -0.56$, $P = 0.025$; **Figure 3B**). The medication slightly improved the variability in the PD subjects but the changes did not reach statistical significance ($P = 0.096$). The entropy of the PDMOFF group was lower than the HC group ($P < 0.001$) and the lower entropy was related to a longer disease duration ($r = -0.51$, $P = 0.038$; **Figure 3B**). The medication did not improve the PLV entropy ($P = 0.41$).

Online- and After-Effects of EVS

Next, EVS effects on the PLV features were investigated. Specifically, we examined whether the effects are dependent on the stimulus types and sustained even after the stimulation ceases. **Figures 4A–C** show changes in the PLV mean for each group induced by EVS1, EVS2, and EVS3, respectively. The PLV mean was significantly modulated during stimulation in PDMOFF [$F(3, 45) = 11.16$, $P < 0.001$] and HC [$F(3, 51) = 3.81$, $P < 0.05$] groups. All stimuli decreased the PLV mean in the PDMOFF group compared to the *sham* condition (EVS1: $P < 0.001$; EVS2: $P < 0.01$; EVS3: $P < 0.01$), making it closer to the HC group, and the effects lasted in the post-stimulation period. EVS1 decreased the mean PLV greater than the other two stimuli and there was no continuing decrease in the post-stimulation period whereas EVS3 decreased the mean PLV less than EVS1 during stimulation and the effect continued in the post-stimulation period. In contrast, we found the opposite EVS effects for the HC group where EVS

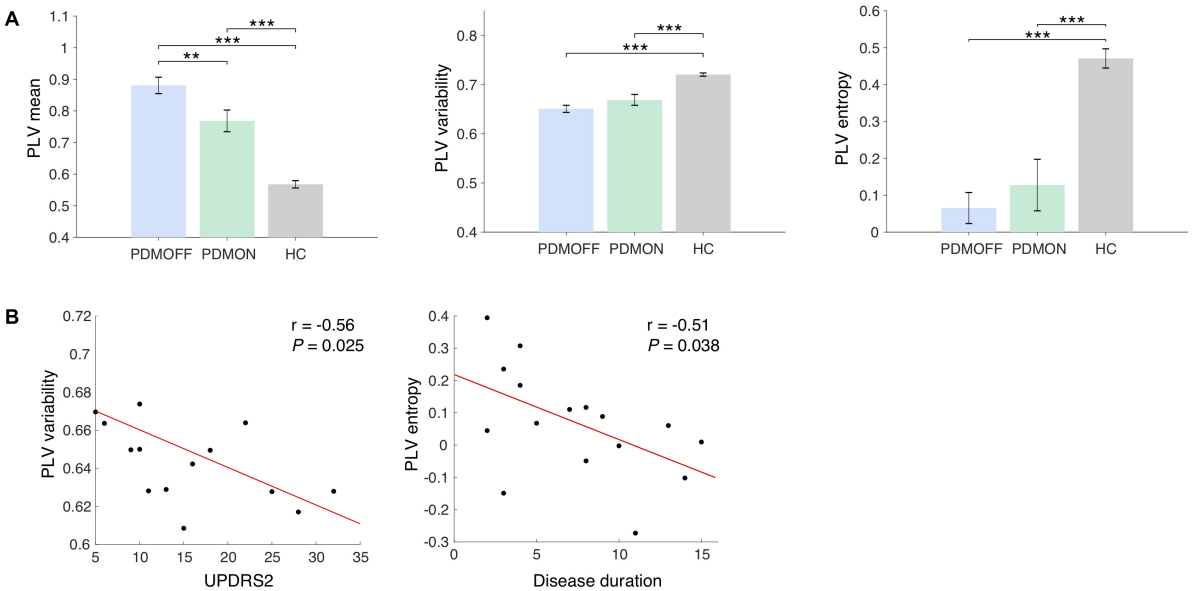

FIGURE 3 | (A) Group comparison of the discriminant component obtained from the SDA. The discriminant components were obtained by multiplying the discriminant vectors to the data sets from the *sham* condition. Bars and error bars indicate group means and s.e. Significant *P*-values from one-way ANOVA with *post hoc* Tukey's HSD test are indicated (**$P < 0.01$; ***$P < 0.001$). **(B)** Pearson correlations with clinical scores. The PLV variability and entropy of the PDMOFF subjects are significantly correlated with UPDRS2 and disease duration, respectively.

increased the PLV mean (EVS2: $P < 0.05$; EVS3: $P < 0.01$). No significant effects of EVS were found in the PDMON group.

EVS effects on the PLV variability are presented in **Figures 5A–C**. There were significant online effects of stimulation on the PLV variability in PDMOFF [$F(3, 45) = 4.43$, $P < 0.01$] and HC [$F(3, 51) = 4.62$, $P < 0.01$] groups. EVS1 and EVS2 were found to have positive effects on the PDMOFF group, increasing the variability during stimulation (EVS1: $P < 0.01$; EVS2: $P < 0.05$). Similar to the effects on the PLV mean, EVS1 induced the greatest increase in the variability during stimulation and the increased value tends to return to the baseline after the stimulation ceased whereas the effects of EVS2 and 3 were less during stimulation but lasted longer than that of EVS1. In the HC group, we found decreases in the PLV variability induced by EVS (EVS1: $P < 0.01$; EVS2: $P < 0.05$; EVS3: $P < 0.05$). EVS1 decreased the variability during the stimulation and the effect lasted in the post-stimulation period. EVS2 and EVS3 appeared to further decrease the variability in the post-stimulation period. For the PDMON group, all stimuli increased the PLV variability but the effects did not reach the statistical significance.

Figures 6A–C show EVS effects on the PLV entropy. The PLV entropy was significantly modulated during stimulation in PDMOFF [$F(3, 45) = 4.65$, $P < 0.01$], PDMON [$F(3, 45) = 3.12$, $P < 0.05$], and HC [$F(3, 51) = 4.25$, $P < 0.01$] groups. We found that all stimuli increased the entropy significantly in the PDMOFF group (EVS1: $P < 0.01$; EVS2: $P < 0.05$; EVS3: $P < 0.05$), bring it closer to the HC group. The effects were greatest during stimulation and diminished in the post-stimulation period, and EVS1 increased the largest amount of the entropy. For the PDMON group, EVS1 ($P < 0.05$) and EVS2 ($P < 0.05$) increased the entropy significantly. While not statistically significant, increases in the entropy were also found during and post-EVS3 compared to the *sham* condition. The PLV entropy of the HC group changed in the opposite direction by EVS compared to the PD groups. Significant decreases in the entropy was observed with all stimuli [EVS1 ($P < 0.01$), EVS2 ($P < 0.05$) and EVS3 ($P < 0.01$)].

DISCUSSION

We investigated phase-based cortical connectivity in resting EEG in PD. To our knowledge, this is the first study that examined connectivity dynamics in PD by characterizing temporally fluctuating cortico-cortical couplings over broad frequency bands. The results from the current study on the time-varying connectivity provide novel insights into altered cortical dynamics derived from pathological BG changes in PD.

Disrupted Cortical Coupling Strength in the Motor Regions

We found most changes in cortical coupling strength associated with PD (**Figure 2A**; 11 out of 17) were in key motor and parietal regions, including over the primary motor cortex (M1), supplementary motor area (SMA), premotor area (PMA), and superior parietal regions, which was in line with previous findings (Otten et al., 2012). Typically, a common finding of pathological synchronization in PD is hypersynchronization of the cortical regions in the beta range (Silberstein et al., 2005; George et al., 2013; Pollok et al., 2013). This appears to be related to exaggerated beta synchronization within the BG and between the BG and

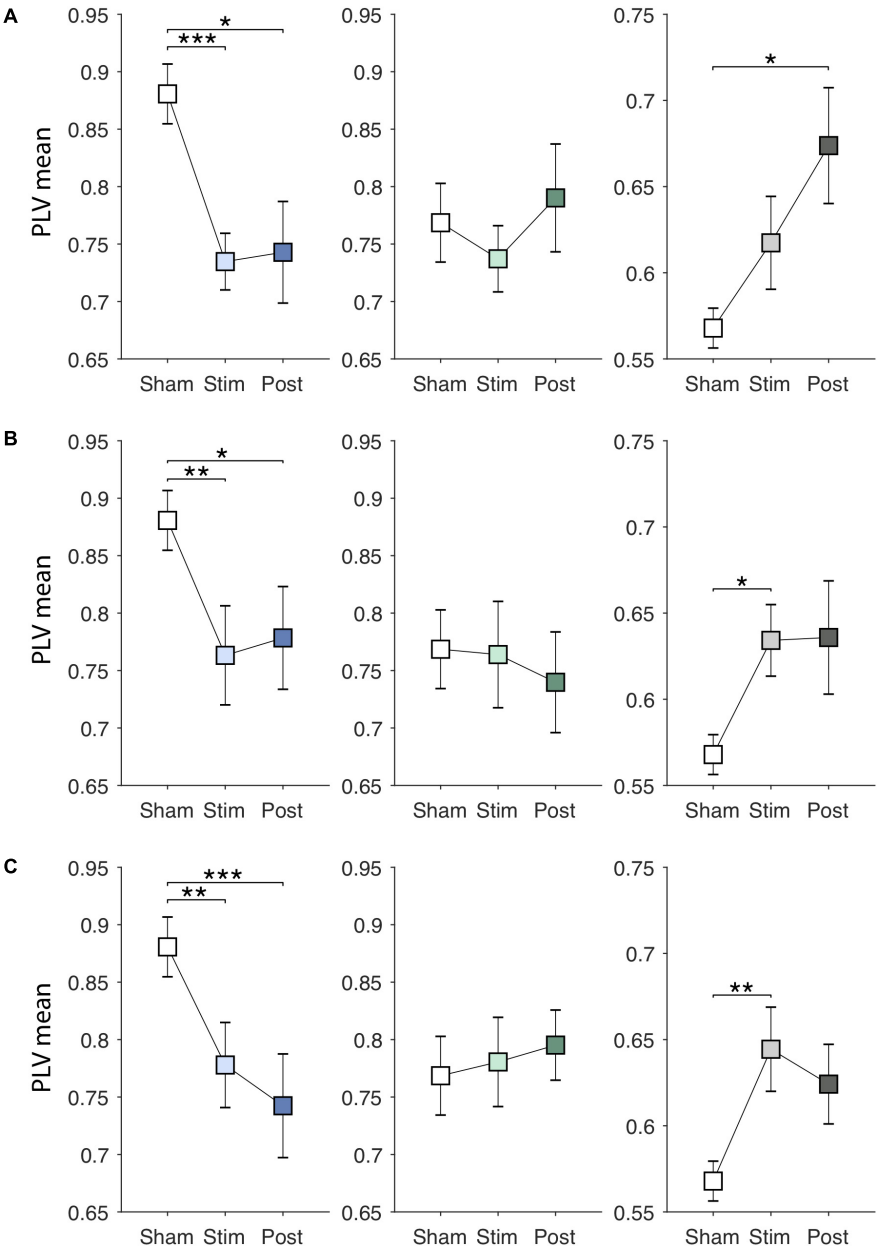

FIGURE 4 | Effects of EVS on the PLV mean. The PLV mean values in the *sham* condition are identical to those in **Figure 3A**. The PLV mean values in the stimulation (60 s) and post-stimulation period (20 s) were obtained in the same manner by multiplying the discriminant vector to the corresponding data sets. In each row, from the left, the results for the PDMOFF (blue), PDMON (green), and HC (gray) groups are presented in each panel. Significant *P*-values from repeated measures ANOVA with *post hoc* Tukey's HSD test are indicated (*$P < 0.05$; **$P < 0.01$; ***$P < 0.001$). **(A)** EVS1 effects. **(B)** EVS2 effects. **(C)** EVS3 effects.

motor cortical regions (Brown, 2007; Jenkinson and Brown, 2011; Brittain and Brown, 2014). However, growing evidence indicates that PD has more complex influences on motor networks beyond excessive beta synchronization (Wu et al., 2009, 2011). There is altered cortical oscillatory activity in other bands beside beta (Bosboom et al., 2006; Stoffers et al., 2007). On the other hand, there is substantial agreement that therapeutic DBS (Pollok et al., 2013) and dopaminergic medication (Wu et al., 2009; Heinrichs-Graham et al., 2014; Tahmasian et al., 2015) have normalizing effects on rsFC of motor networks in PD. Consistent with these findings, our results demonstrated that the altered connectivity found in the PDMOFF group was normalized by both medication and EVS to a similar extent.

Variability and Entropy of PLV in the Theta Band

The altered variability and entropy of PLV in the PD group were mostly found in the theta band (**Figures 2B,C**), which may reflect abnormalities in thalamocortical dynamics. The

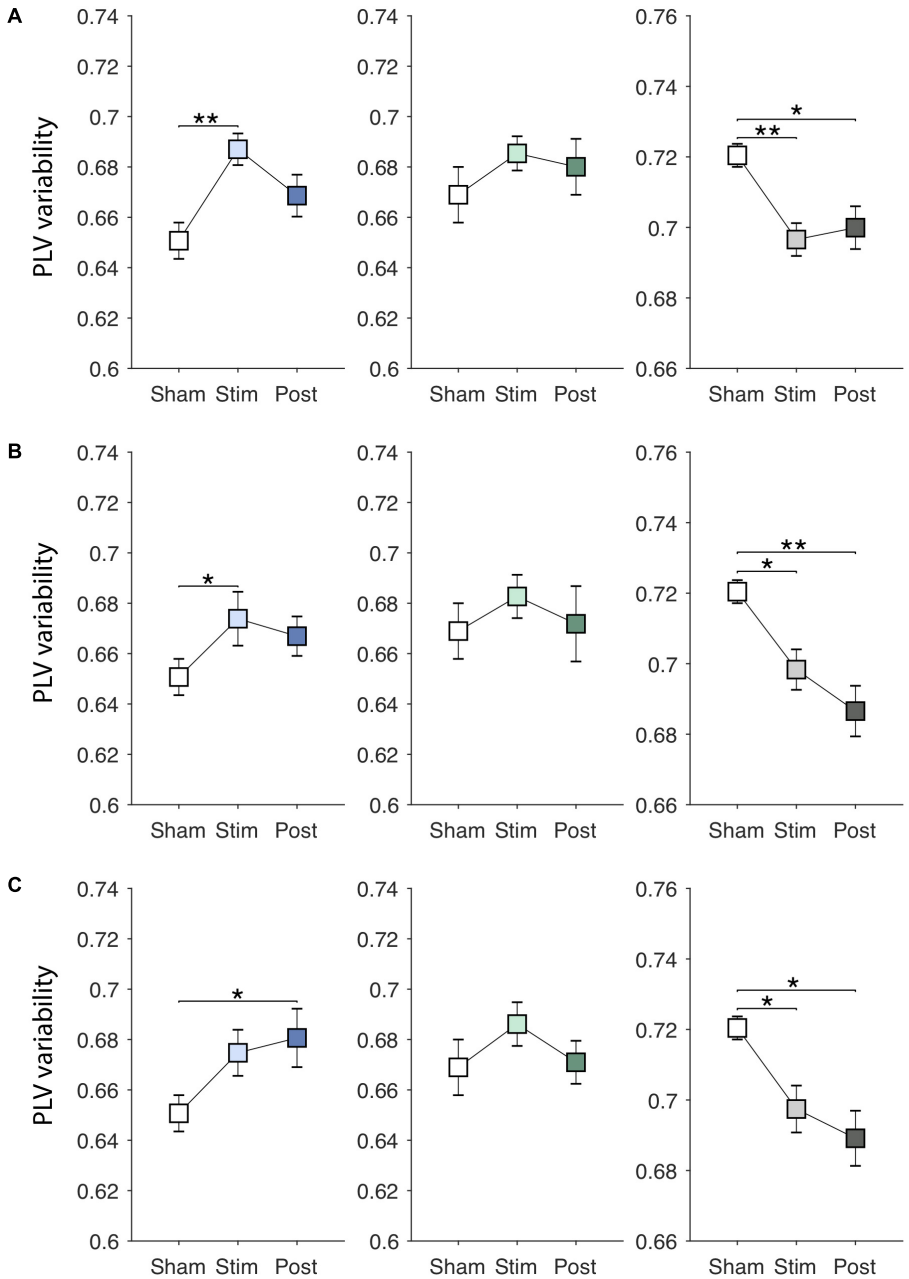

FIGURE 5 | Effects of EVS on the PLV variability. The PLV variability values in the *sham* condition are identical to those in **Figure 3A**. Descriptions for the arrangement of the plots and statistical significance are same as in the **Figure 4**. **(A)** EVS1 effects. **(B)** EVS2 effects. **(C)** EVS3 effects.

ventral anterior (VA) and anterior part of ventral lateral (VLa) thalamic nuclei are the major recipients from the globus pallidus internus (GPi) via pallidothalamic tracts that are crucially involved in motor disorders such as PD (Gallay et al., 2008). Simultaneously-recorded LFP in the VA and VLa nuclei and EEG on the scalp from PD subjects demonstrated the highest coherence in the theta band (4–9 Hz), in particular in the frontal region of both hemispheres (Sarnthein and Jeanmonod, 2007). Thalamocortical interaction may thus be a major influence in generation of frontal theta activity in PD, and possibly also healthy controls, but we typically do not have LFP recordings from healthy subjects. Multimodal functional imaging studies in healthy human and animal models suggest that the thalamus is critically involved in generating and modulating activities in the cortex (Klimesch, 1999; Schreckenberger et al., 2004; Hughes and Crunelli, 2005; Klimesch et al., 2007). The enhanced synchronization in the theta band of the thalamus and frontal cortical region may be reflective of pathological changes in PD. Together, we conjecture that the increased mean and reduced variability in theta that we observed in PD

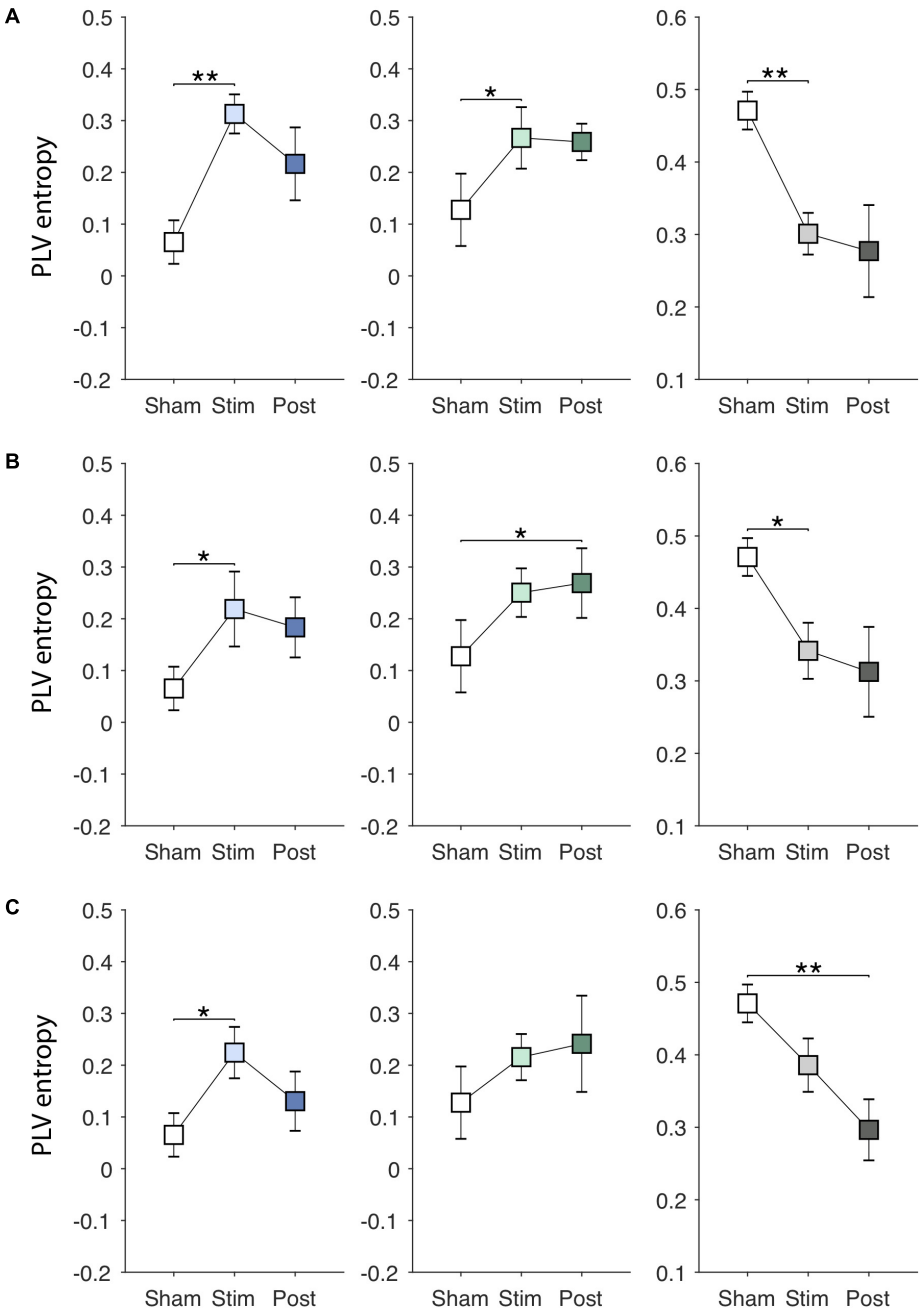

FIGURE 6 | Effects of EVS on the PLV entropy. The PLV entropy values in the *sham* condition are identical to those in **Figure 3A**. Descriptions for the arrangement of the plots and statistical significance are same as in the **Figure 4**. **(A)** EVS1 effects. **(B)** EVS2 effects. **(C)** EVS3 effects.

subjects was a consequence of excessive synchronization between thalamocortical structures.

Variability and Entropy of PLV in the Alpha Band

The dominant frequency in the human EEG under rest is in the alpha frequency band (8–13 Hz). Alpha oscillations are known to be affected by visual and auditory stimuli (Hari et al., 1997) and change during voluntary movement (Pfurtscheller et al., 2006). A large body of evidence has also demonstrated the critical role of alpha rhythms in attention as well as various cognitive functions (Klimesch, 1999). The dynamic change of alpha activity reflects a variability of states with enhanced and reduced cortical excitability, facilitating the brain's responses to surrounding stimuli (Garrett et al., 2013). Several studies have shown that brain signal variability/complexity can serve as an important discriminator for clinical comparisons. For example,

EEG entropy is related to brain maturity, as adults have higher entropy compared to children and adolescents (Lippe et al., 2009). Higher entropy is also correlated with better performance on a working memory task (McIntosh et al., 2008). Schlee et al. (2014) found reduced variability of alpha activity during rest over the temporal cortex for subjects with tinnitus compared to controls. Similarly, the reduced variability and complexity of the cortical couplings of the PD groups we observed may be related to diminished motor and cognitive adaptability, as executive cognitive functions such as set shifting, divided or alternating attention and dual tasking (e.g., combining walking with another task) are impaired in PD (Muslimovic et al., 2007; Aarsland et al., 2010; Watson and Leverenz, 2010). Although the mechanisms responsible for these symptoms have not been fully accounted for, dopaminergic depletion in the striatum disrupts the parallel organization of cortico-striatal circuits, resulting in more widespread instead of domain-specific involvement of striatal activity and loss of the normally segregated circuits (Bergman et al., 1998; Calabresi et al., 2015; Nieuwhof et al., 2017). Our results together with the close relationships between cortico-striatal circuits and cortical alpha oscillations (Laufs et al., 2003; Slagter et al., 2017) warrant future studies to further elucidate the functional implications of the impaired alpha dynamic couplings we have demonstrated here.

PLV Sample Entropy Is Higher in the Long-Range Gamma Activity in PD

We found that the connectivity in the gamma band was more irregular in the PD group than the HC group (**Figure 2C**). The binding of cortical regions together via synchronization of gamma oscillations between neuronal populations, is implicated in numerous cognitive processes (Fries, 2009; Sohal, 2012). In voluntary movement, for example, synchronization of cortical gamma oscillations prior to movement onset has been described as representing active information processing (Pfurtscheller et al., 1993; Salenius et al., 1996) and considered to serve as a prokinetic signal (Brittain and Brown, 2014). Abnormal gamma oscillations in the motor cortex in PD have been reported (Litvak et al., 2012; Nowak et al., 2018). However, resting-state gamma oscillations and connectivity in PD remain largely unknown. The mechanism underlying generation of the gamma oscillations are known to be critically involved with excitatory post-synaptic potentials (EPSPs) of gamma-aminobutyric acid (GABA)ergic interneurons and their intact function of fast-spiking (Fuchs et al., 2001; Vreugdenhil et al., 2003; Hajos et al., 2004). Thus, alterations in function of GABAergic interneurons could be inferenced from gamma-band oscillations at the macroscopic level. The fast-spiking interneurons are modulated by neurotransmitters including acetylcholine (Fries, 2009; Teles-Grilo Ruivo and Mellor, 2013; Tremblay et al., 2016) and serotonin (Fries, 2009; Puig et al., 2010), and there is robust evidence demonstrating deficits in the cholinergic and serotoninergic systems in PD contributing to various aspects of parkinsonian pathophysiology including motor symptoms, gait dysfunction, cognitive decline, autonomic dysfunction (for review, see Perez-Lloret and Barrantes, 2016). Therefore, it is likely that the disrupted neurotransmitter systems in PD cause alterations in the activities of fast-spiking interneurons, subsequently resulting in pathological cortical couplings in the gamma band in PD.

Normalizing Effects of EVS and Potential Mechanisms

In this study, we demonstrated that EVS normalizes the mean, variability and entropy of PLV in PD subjects during stimulation and the extent and duration of the effects were dependent on the stimulation frequencies (**Figures 4–6**). Modulatory effects of EVS on the cortical oscillatory activity were reported in prior EEG studies that noisy stimulus (pink noise in 0.1–10 Hz) decreased gamma oscillatory activity in the lateral regions and increased the beta and gamma activity in the frontal region (Kim et al., 2013), and altered interhemispheric coherence (Lee et al., 2017). To our knowledge, effects of high-frequency multisine EVS (>50 Hz) on cortical activity have not been explored yet in humans and the results presented in this study provide valuable information on how the effects would differ from low-frequency EVS that has been used in prior behavior and neuroimaging studies. We found two characteristics of effects induced by EVS2 and EVS3 on PLV. First, their effects were similar to EVS1 in the sense that the direction of changes (i.e., increase or decrease in the PLV features) was the same. We did not find a frequency specific increase or decrease in the PLV value in both the PD and HC groups. Second, the extent of changes was less compared to EVS1 during the high-frequency stimulation but lasted longer in the post-stimulation period. This was observed in the PDMOFF group for all the PLV measures and in the HC group for the variability and entropy. For the PDMON group, the EVS effects were less significant, indicating the processing of vestibular inputs in the thalamus and BG (Lopez and Blanke, 2011; Stiles and Smith, 2015; Wijesinghe et al., 2015) is dependent on the dopaminergic level of the BG.

Modulation of firing rates of vestibular afferents by externally applied electrical current will alter directly the vestibular nuclei activities in the brain stem, and eventually multiple cortical areas through the thalamocortical vestibular system. Thus, understanding vestibular information processing regarding varying frequency contents at the vestibular nuclei and thalamus is critical to comprehend above findings. A prior study that examined spiking rates of the guinea pig medial vestibular nuclei (MVN) reported that two types of neurons having different characteristics of afterpotentials responded to current inputs differentially according to the frequency content (1–30 Hz) (Ris et al., 2001). It was shown that spontaneous firing rates of type A neurons was well modulated by only low-frequency (<10 Hz) current inputs and the spiking rates become irrelevant to the current input at high frequencies whereas type B neurons tended to fire in synchrony better when the stimulation frequency was higher, which demonstrates existence of signal transformation at the vestibular nuclei level to a certain extent in that type A neurons act like a low-pass filter (du Lac and Lisberger, 1995; Ris et al., 2001) whereas type B neurons act as signal detectors with greater sensitivity to external stimuli at high frequencies.

Considering functional roles of the thalamic nuclei playing integrative and modulatory roles in sensorimotor processing (Tyll et al., 2011), it is likely that further transformation of the modified signal transmitted from the vestibular nuclei occurs in the thalamus. The VA, VL, ventral posterior lateral (VPL), ventral posterior medial (VPM), intraminar nuclei and geniculate bodies of the thalamus receive primary afferents from the vestibular nuclei and play a critical role in processing vestibular information (Bucher et al., 1998; Bense et al., 2001; Stephan et al., 2005; Meng et al., 2007; Wijesinghe et al., 2015). These thalamic nuclei also receive a range of different afferents from peripheral sensory, subcortical, and cortical regions, and process the different types of information before sending the refined signals to the cortex. This may also explain the interaction between EVS and L-dopa medication as observed in the PDMOFF and PDMON groups as the thalamic nuclei processing vestibular information would be receiving differential inputs from the BG according to dopamine levels. Together, unlike the transcranial electrical or magnetic stimulation that directly target cortical regions of interest, influences of EVS on cortical activities are much more indirect. Our results suggest that although the frequency contents of current input to the peripheral vestibular nerve vary considerably, alterations of the refined higher-level multisensory information transmitted from the thalamic nuclei to the broad cortical regions may be relatively consistent.

Limitations

In the current work, the post-stimulation effects were only evaluated for the first 20 s after stimulation ceased and there may be potential confounding effects if the after effects persist much longer. Aftereffects of EVS on cortical activation have not been fully investigated yet. Delayed responses in the beta and gamma power in frontal regions was reported to appear 20–25 s after 72-s EVS, but lasted only for several seconds. Based on prior studies reporting aftereffects of invasive (Wingeier et al., 2006) and non-invasive stimulation (Strüber et al., 2015) and the short duration of weak current EVS used here, we concluded that the break time and randomly-ordered trials were sufficient to avoid confounding effects.

CONCLUSION

In conclusion, in this resting-state EEG study, we demonstrated that connectivity strengths in the sensorimotor region, and variability and complexity of the time-varying cortico-cortical connectivity are affected in PD, and improved by subthreshold EVS. Furthermore, the magnitude and duration of the improvement was found to vary depending on the stimulation frequency and the subjects' dopamine level. The findings from the current study provide valuable information that thalamic functions of integrating subcortical afferent inputs and thalamocortical projections to the cortex play a critical role in the mechanism of the EVS effects, and warrant further investigation of EVS as a potential therapy in PD.

DATA AVAILABILITY

The raw data supporting the conclusions of this manuscript will be made available by the authors, without undue reservation, to any qualified researcher.

AUTHOR CONTRIBUTIONS

SL and MM designed the study. SL conducted the study, performed the data analysis, and wrote the first draft of the manuscript. AL and ZW contributed to interpretation of data for the work. All authors contributed to manuscript revision, read, and approved the submitted version.

FUNDING

This work was partly funded by the Pacific Parkinson's Research Institute (PPRI)/UBC chair in Parkinson's disease (MM) and a generous gift from the Mottershead Foundation. This material was partly based upon work supported by National Natural Science Foundation of China (61701158).

ACKNOWLEDGMENTS

We would like to thank Christy Jones for assisting recruiting participants, and are enormously grateful to the participants in this study for generous support.

REFERENCES

Aarsland, D., Bronnick, K., Williams-Gray, C., Weintraub, D., Marder, K., Kulisevsky, J., et al. (2010). Mild cognitive impairment in Parkinson disease: a multicenter pooled analysis. *Neurology* 75, 1062–1069. doi: 10.1212/WNL.0b013e3181f39d0e

Ahn, S., Zauber, S. E., Worth, R. M., Witt, T., and Rubchinsky, L. L. (2015). Interaction of synchronized dynamics in cortex and basal ganglia in Parkinson's disease. *Eur. J. Neurosci.* 42, 2164–2171. doi: 10.1111/ejn.12980

Amengual, J. L., Vernet, M., Adam, C., and Valero-Cabré, A. (2017). Local entrainment of oscillatory activity induced by direct brain stimulation in humans. *Sci. Rep.* 7:41908. doi: 10.1038/srep41908

Andres, F. G., and Gerloff, C. (1999). Coherence of sequential movements and motor learning. *J. Clin. Neurophysiol.* 16, 520–527. doi: 10.1097/00004691-199911000-00004

Bense, S., Stephan, T., Yousry, T. A., Brandt, T., and Dieterich, M. (2001). Multisensory cortical signal increases and decreases during vestibular galvanic stimulation (fMRI). *J. Neurophysiol.* 85, 886–899. doi: 10.1152/jn.2001.85.2.886

Bergman, H., Feingold, A., Nini, A., Raz, A., Slovin, H., Abeles, M., et al. (1998). Physiological aspects of information processing in the basal ganglia of normal and parkinsonian primates. *Trends Neurosci.* 21, 32–38. doi: 10.1016/S0166-2236(97)01151-X

Bosboom, J. L., Stoffers, D., Stam, C. J. J., van Dijk, B. W. W., Verbunt, J., Berendse, H. W. W., et al. (2006). Resting state oscillatory brain dynamics in Parkinson's

disease: an MEG study. *Clin. Neurophysiol.* 117, 2521–2531. doi: 10.1016/j.clinph.2006.06.720

Brittain, J.-S., and Brown, P. (2014). Oscillations and the basal ganglia: motor control and beyond. *Neuroimage* 85(Pt 2), 637–647. doi: 10.1016/j.neuroimage.2013.05.084

Brown, P. (2007). Abnormal oscillatory synchronisation in the motor system leads to impaired movement. *Curr. Opin. Neurobiol.* 17, 656–664. doi: 10.1016/j.conb.2007.12.001

Brown, P., Oliviero, A., Mazzone, P., Insola, A., Tonali, P., and Di Lazzaro, V. (2001). Dopamine dependency of oscillations between subthalamic nucleus and pallidum in Parkinson's disease. *J. Neurosci.* 21, 1033–1038. doi: 10.1523/JNEUROSCI.21-03-01033.2001

Brown, P., and Williams, D. (2005). Basal ganglia local field potential activity: character and functional significance in the human. *Clin. Neurophysiol.* 116, 2510–2519. doi: 10.1016/j.clinph.2005.05.009

Bruce, E. N., Bruce, M. C., and Vennelaganti, S. (2009). Sample entropy tracks changes in electroencephalogram power spectrum with sleep state and aging. *J. Clin. Neurophysiol.* 26, 257–266. doi: 10.1097/WNP.0b013e3181b2f1e3

Bruña, R., Maestú, F., and Pereda, E. (2018). Phase locking value revisited: teaching new tricks to an old dog. *J. Neural Eng.* 15:056011. doi: 10.1088/1741-2552/aacfe4

Bucher, S. F., Dieterich, M., Wiesmann, M., Weiss, A., Zink, R., Yousry, T. A., et al. (1998). Cerebral functional magnetic resonance imaging of vestibular, auditory, and nociceptive areas during galvanic stimulation. *Ann. Neurol* 44, 120–125. doi: 10.1002/ana.410440118

Calabresi, P., Ghiglieri, V., Mazzocchetti, P., Corbelli, I., and Picconi, B. (2015). Levodopa-induced plasticity: a double-edged sword in Parkinson's disease? *Philos. Trans. R. Soc. B Biol. Sci.* 370:20140184. doi: 10.1098/rstb.2014.0184

Cassidy, M., Mazzone, P., Oliviero, A., Insola, A., Tonali, P., Di Lazzaro, V., et al. (2002). Movement-related changes in synchronization in the human basal ganglia. *Brain* 125, 1235–1246. doi: 10.1093/brain/awf135

Clemmensen, L., Hastie, T., Witten, D., and Ersbøll, B. (2011). Sparse Discriminant Analysis. *Technometrics* 53, 406–413. doi: 10.1198/TECH.2011.08118

Davie, C. A. (2008). A review of Parkinson's disease. *Br. Med. Bull.* 86, 109–127. doi: 10.1093/bmb/ldn013

du Lac, S., and Lisberger, S. G. (1995). Cellular processing of temporal information in medial vestibular nucleus neurons. *J. Neurosci.* 15, 8000–8010. doi: 10.1523/JNEUROSCI.15-12-08000.1995

Dubbelink, K. T. O., Schoonheim, M. M., Deijen, J. B., Twisk, J. W. R., Barkhof, F., Berendse, H. W., et al. (2014). Functional connectivity and cognitive decline over 3 years in Parkinson disease. *Neurology* 83, 2046–2053. doi: 10.1212/WNL.0000000000001020

Eusebio, A., Pogosyan, A., Wang, S., Averbeck, B., Gaynor, L. D., Cantiniaux, S., et al. (2009). Resonance in subthalamo-cortical circuits in Parkinson's disease. *Brain* 132, 2139–2150. doi: 10.1093/brain/awp079

Fell, J., and Axmacher, N. (2011). The role of phase synchronization in memory processes. *Nat. Rev. Neurosci.* 12, 105–118. doi: 10.1038/nrn2979

Fries, P. (2009). Neuronal gamma-band synchronization as a fundamental process in cortical computation. *Annu. Rev. Neurosci.* 32, 209–224. doi: 10.1146/annurev.neuro.051508.135603

Fuchs, E. C., Doheny, H., Faulkner, H., Caputi, A., Traub, R. D., Bibbig, A., et al. (2001). Genetically altered AMPA-type glutamate receptor kinetics in interneurons disrupt long-range synchrony of gamma oscillation. *Proc. Natl. Acad. Sci. U.S.A.* 98, 3571–3576. doi: 10.1073/pnas.051631898

Gallay, M. N., Jeanmonod, D., Liu, J., and Morel, A. (2008). Human pallidothalamic and cerebellothalamic tracts: anatomical basis for functional stereotactic neurosurgery. *Brain Struct. Funct.* 212, 443–463. doi: 10.1007/s00429-007-0170-0

Garrett, D. D., Samanez-Larkin, G. R., MacDonald, S. W. S., Lindenberger, U., McIntosh, A. R., and Grady, C. L. (2013). Moment-to-moment brain signal variability: a next frontier in human brain mapping? *Neurosci. Biobehav. Rev.* 37, 610–624. doi: 10.1016/j.neubiorev.2013.02.015

George, J. S., Strunk, J., Mak-McCully, R., Houser, M., Poizner, H., and Aron, A. R. (2013). Dopaminergic therapy in Parkinson's disease decreases cortical beta band coherence in the resting state and increases cortical beta band power during executive control. *Neuroimage Clin.* 3, 261–270. doi: 10.1016/j.nicl.2013.07.013

Groppe, D. M., Bickel, S., Keller, C. J., Jain, S. K., Hwang, S. T., Harden, C., et al. (2013). Dominant frequencies of resting human brain activity as measured by the electrocorticogram. *Neuroimage* 79, 223–233. doi: 10.1016/j.neuroimage.2013.04.044

Hajos, N., Pálhalmi, J., Mann, E. O., Németh, B., Paulsen, O., and Freund, T. F. (2004). Spike timing of distinct types of GABAergic interneuron during hippocampal gamma oscillations in vitro. *J. Neurosci.* 24, 9127–9137. doi: 10.1523/JNEUROSCI.2113-04.2004

Hanslmayr, S., Klimesch, W., Sauseng, P., Gruber, W., Doppelmayr, M., Freunberger, R., et al. (2005). Visual discrimination performance is related to decreased alpha amplitude but increased phase locking. *Neurosci. Lett.* 375, 64–68. doi: 10.1016/j.neulet.2004.10.092

Hari, R., Salmelin, R., Mäkelä, J. P., Salenius, S., and Helle, M. (1997). Magnetoencephalographic cortical rhythms. *Int. J. Psychophysiol.* 26, 51–62. doi: 10.1016/S0167-8760(97)00755-1

He, X., Zhang, Y., Chen, J., Xie, C., Gan, R., Yang, R., et al. (2017). The patterns of EEG changes in early-onset Parkinson's disease patients. *Int. J. Neurosci.* 127, 1028–1035. doi: 10.1080/00207454.2017.1304393

Heinrichs-Graham, E., Kurz, M. J., Becker, K. M., Santamaria, P. M., Gendelman, H. E., and Wilson, T. W. (2014). Hypersynchrony despite pathologically reduced beta oscillations in patients with Parkinson's disease: a pharmaco-magnetoencephalography study. *J. Neurophysiol.* 112, 1739–1747. doi: 10.1152/jn.00383.2014

Helfrich, R. F. F., Schneider, T. R. R., Rach, S., Trautmann-Lengsfeld, S. A. A., Engel, A. K. K., and Herrmann, C. S. S. (2014). Entrainment of brain oscillations by transcranial alternating current stimulation. *Curr. Biol.* 24, 333–339. doi: 10.1016/j.cub.2013.12.041

Helmich, R. C., Derikx, L. C., Bakker, M., Scheeringa, R., Bloem, B. R., and Toni, I. (2010). Spatial remapping of cortico-striatal connectivity in Parkinson's disease. *Cereb. Cortex* 20, 1175–1186. doi: 10.1093/cercor/bhp178

Hughes, S. W., and Crunelli, V. (2005). Thalamic mechanisms of EEG alpha rhythms and their pathological implications. *Neuroscientist* 11, 357–372. doi: 10.1177/1073858405277450

Jenkinson, N., and Brown, P. (2011). New insights into the relationship between dopamine, beta oscillations and motor function. *Trends Neurosci.* 34, 611–618. doi: 10.1016/j.tins.2011.09.003

Kim, D. J., Yogendrakumar, V., Chiang, J., Ty, E., Wang, Z. J., and McKeown, M. J. (2013). Noisy galvanic vestibular stimulation modulates the amplitude of EEG synchrony patterns. *PLoS One* 8:e69055. doi: 10.1371/journal.pone.0069055

Klimesch, W. (1999). EEG alpha and theta oscillations reflect cognitive and memory performance: a review and analysis. *Brain Res. Rev.* 29, 169–195. doi: 10.1016/S0165-0173(98)00056-3

Klimesch, W., Doppelmayr, M., Yonelinas, A., Kroll, N. E., Lazzara, M., Röhm, D., et al. (2001). Theta synchronization during episodic retrieval: neural correlates of conscious awareness. *Brain Res. Cogn. Brain Res.* 12, 33–38. doi: 10.1016/S0926-6410(01)00024-6

Klimesch, W., Freunberger, R., Sauseng, P., and Gruber, W. (2008). A short review of slow phase synchronization and memory: evidence for control processes in different memory systems? *Brain Res.* 1235, 31–44. doi: 10.1016/J.BRAINRES.2008.06.049

Klimesch, W., Sauseng, P., and Hanslmayr, S. (2007). EEG alpha oscillations: the inhibition–timing hypothesis. *Brain Res. Rev.* 53, 63–88. doi: 10.1016/j.brainresrev.2006.06.003

Kumar, Y., Dewal, M. L., and Anand, R. S. (2012). "Features extraction of EEG signals using approximate and sample entropy," in *Proceedings of the 2012 IEEE Students' Conference on Electrical, Electronics and Computer Science (IEEE); 2012 March 1–2*, Bhopal, 1–5. doi: 10.1109/SCEECS.2012.6184830

Lachaux, J. P., Rodriguez, E., Martinerie, J., and Varela, F. J. (1999). Measuring phase synchrony in brain signals. *Hum. Brain Mapp.* 8, 194–208. doi: 10.1002/(SICI)1097-0193(1999)8:4<194::AID-HBM4>3.0.CO;2-C

Lake, D. E., Richman, J. S., Griffin, M. P., and Moorman, J. R. (2002). Sample entropy analysis of neonatal heart rate variability. *Am. J. Physiol. Integr. Comp. Physiol.* 283, R789–R797. doi: 10.1152/ajpregu.00069.2002

Laufs, H., Kleinschmidt, A., Beyerle, A., Eger, E., Salek-Haddadi, A., Preibisch, C., et al. (2003). EEG-correlated fMRI of human alpha activity. *Neuroimage* 19, 1463–1476. doi: 10.1016/S1053-8119(03)00286-6

Lee, S., Kim, D., and McKeown, M. J. (2017). "Galvanic Vestibular Stimulation (GVS) effects on impaired interhemispheric connectivity in Parkinson's Disease," in *Proceedings of the 2017 39th Annual International Conference of the IEEE Engineering in Medicine and Biology Society (IEEE); 2017 July 11–15*, Jeju, 2109–2113. doi: 10.1109/EMBC.2017.8037270

Lee, S., Kim, D. J., Svenkeson, D., Parras, G., Oishi, M. M. K., and McKeown, M. J. (2015). Multifaceted effects of noisy galvanic vestibular stimulation on manual tracking behavior in Parkinson's disease. *Front. Syst. Neurosci.* 9:5. doi: 10.3389/fnsys.2015.00005

Lee, S., McKeown, M. J., Wang, Z. J., and Chen, X. (2019). Removal of high-voltage brain stimulation artifacts from simultaneous EEG recordings. *IEEE Trans. Biomed. Eng.* 66, 50–60. doi: 10.1109/TBME.2018.2828808

Lippe, S., Kovacevic, N., and McIntosh, A. R. (2009). Differential maturation of brain signal complexity in the human auditory and visual system. *Front. Hum. Neurosci.* 3:48. doi: 10.3389/neuro.09.048.2009

Litvak, V., Eusebio, A., Jha, A., Oostenveld, R., Barnes, G., Foltynie, T., et al. (2012). Movement-related changes in local and long-range synchronization in Parkinson's disease revealed by simultaneous magnetoencephalography and intracranial recordings. *J. Neurosci.* 32, 10541–10553. doi: 10.1523/JNEUROSCI.0767-12.2012

Lopez, C., and Blanke, O. (2011). The thalamocortical vestibular system in animals and humans. *Brain Res. Rev.* 67, 119–146. doi: 10.1016/j.brainresrev.2010.12.002

Lopez, C., Blanke, O., and Mast, F. W. (2012). The human vestibular cortex revealed by coordinate-based activation likelihood estimation meta-analysis. *Neuroscience* 212, 159–179. doi: 10.1016/j.neuroscience.2012.03.028

Mai, Q. (2013). A review of discriminant analysis in high dimensions. *Wiley Interdiscip. Rev. Comput. Stat.* 5, 190–197. doi: 10.1002/wics.1257

Marsden, J. F., Limousin-Dowsey, P., Ashby, P., Pollak, P., and Brown, P. (2001). Subthalamic nucleus, sensorimotor cortex and muscle interrelationships in Parkinson's disease. *Brain* 124, 378–388. doi: 10.1093/brain/124.2.378

Martin, K. A. C., and Schröder, S. (2016). Phase locking of multiple single neurons to the local field potential in cat V1. *J. Neurosci.* 36, 2494–2502. doi: 10.1523/JNEUROSCI.2547-14.2016

McIntosh, A. R., Kovacevic, N., and Itier, R. J. (2008). Increased brain signal variability accompanies lower behavioral variability in development. *PLoS Comput. Biol.* 4:e1000106. doi: 10.1371/journal.pcbi.1000106

Meng, H., May, P. J., Dickman, J. D., and Angelaki, D. E. (2007). Vestibular signals in primate thalamus: properties and origins. *J. Neurosci.* 27, 13590–13602. doi: 10.1523/JNEUROSCI.3931-07.2007

Moazami-Goudarzi, M., Sarnthein, J., Michels, L., Moukhtieva, R., and Jeanmonod, D. (2008). Enhanced frontal low and high frequency power and synchronization in the resting EEG of Parkinsonian patients. *Neuroimage* 41, 985–997. doi: 10.1016/j.neuroimage.2008.03.032

Mormann, F., Lehnertz, K., David, P., and Elger, C. (2000). Mean phase coherence as a measure for phase synchronization and its application to the EEG of epilepsy patients. *Phys. D Nonlinear Phenom.* 144, 358–369. doi: 10.1016/S0167-2789(00)00087-7

Muslimovic, D., Schmand, B., Speelman, J. D., and De Haan, R. J. (2007). Course of cognitive decline in Parkinson's disease: a meta-analysis. *J. Int. Neuropsychol. Soc.* 13, 920–932. doi: 10.1017/S1355617707071160

Nieuwhof, F., Bloem, B. R., Reelick, M. F., Aarts, E., Maidan, I., Mirelman, A., et al. (2017). Impaired dual tasking in Parkinson's disease is associated with reduced focusing of cortico-striatal activity. *Brain* 140, 1384–1398. doi: 10.1093/brain/awx042

Nowak, M., Zich, C., and Stagg, C. J. (2018). Motor cortical gamma oscillations: What have we learnt and where are we headed?. *Curr. Behav. Neurosci. Rep.* 5, 136–142. doi: 10.1007/s40473-018-0151-z

Oswal, A., Brown, P., and Litvak, V. (2013). Synchronized neural oscillations and the pathophysiology of Parkinson's disease. *Curr. Opin. Neurol.* 26, 662–670. doi: 10.1097/WCO.0000000000000034

Otten, M. L., Mikell, C. B., Youngerman, B. E., Liston, C., Sisti, M. B., Bruce, J. N., et al. (2012). Motor deficits correlate with resting state motor network connectivity in patients with brain tumours. *Brain* 135, 1017–1026. doi: 10.1093/brain/aws041

Pan, W., Soma, R., Kwak, S., and Yamamoto, Y. (2008). Improvement of motor functions by noisy vestibular stimulation in central neurodegenerative disorders. *J. Neurol.* 255, 1657–1661. doi: 10.1007/s00415-008-0950-3

Perez-Lloret, S., and Barrantes, F. J. (2016). Deficits in cholinergic neurotransmission and their clinical correlates in Parkinson's disease. *NPJ Park. Dis.* 2:16001. doi: 10.1038/npjparkd.2016.1

Pfurtscheller, G., Brunner, C., Schlögl, A., and Lopes da Silva, F. H. (2006). Mu rhythm (de)synchronization and EEG single-trial classification of different motor imagery tasks. *Neuroimage* 31, 153–159. doi: 10.1016/J.NEUROIMAGE.2005.12.003

Pfurtscheller, G., Neuper, C., and Kalcher, J. (1993). 40-Hz oscillations during motor behavior in man. *Neurosci. Lett.* 164, 179–182. doi: 10.1016/0304-3940(93)90886-P

Pollok, B., Kamp, D., Butz, M., Wojtecki, L., Timmermann, L., Südmeyer, M., et al. (2013). Increased SMA–M1 coherence in Parkinson's disease — Pathophysiology or compensation? *Exp. Neurol.* 247, 178–181. doi: 10.1016/j.expneurol.2013.04.013

Puig, M. V., Watakabe, A., Ushimaru, M., Yamamori, T., and Kawaguchi, Y. (2010). Serotonin modulates fast-spiking interneuron and synchronous activity in the rat prefrontal cortex through 5-HT1A and 5-HT2A receptors. *J. Neurosci.* 30, 2211–2222. doi: 10.1523/JNEUROSCI.3335-09.2010

Richman, J. S., and Moorman, J. R. (2000). Physiological time-series analysis using approximate entropy and sample entropy. *Am. J. Physiol. Circ. Physiol.* 278, H2039–H2049. doi: 10.1152/ajpheart.2000.278.6.H2039

Ris, L., Hachemaoui, M., Vibert, N., Godaux, E., Vidal, P. P., and Moore, L. E. (2001). Resonance of spike discharge modulation in neurons of the guinea pig medial vestibular nucleus. *J. Neurophysiol.* 86, 703–716. doi: 10.1152/jn.2001.86.2.703

Safo, S. E., and Long, Q. (2018). Sparse linear discriminant analysis in structured covariates space. *Stat. Anal. Data Min.* 2018, 1–14. doi: 10.1002/sam.11376

Sakkalis, V., Tsiaras, V., Zervakis, M., and Tollis, I. (2007). "Optimal brain network synchrony visualization: application in an alcoholism paradigm," in *Proceedings of the 2007 29th Annual International Conference of the IEEE Engineering in Medicine and Biology Society (IEEE); 2007 August 22–26*, Lyon, 4285–4288. doi: 10.1109/IEMBS.2007.4353283

Salenius, S., Salmelin, R., Neuper, C., Pfurtscheller, G., and Hari, R. (1996). Human cortical 40 Hz rhythm is closely related to EMG rhythmicity. *Neurosci. Lett.* 213, 75–78. doi: 10.1016/0304-3940(96)12796-8

Sarnthein, J., and Jeanmonod, D. (2007). High thalamocortical theta coherence in patients with Parkinson's disease. *J. Neurosci.* 27, 124–131. doi: 10.1523/JNEUROSCI.2411-06.2007

Sauseng, P., and Klimesch, W. (2008). What does phase information of oscillatory brain activity tell us about cognitive processes? *Neurosci. Biobehav. Rev.* 32, 1001–1013. doi: 10.1016/j.neubiorev.2008.03.014

Scandalis, T. A., Bosak, A., Berliner, J. C., Helman, L. L., and Wells, M. R. (2001). Resistance training and gait function in patients with Parkinson's disease. *Am. J. Phys. Med. Rehabil.* 80, 38–43. doi: 10.1097/00002060-200101000-00011

Schlee, W., Schecklmann, M., Lehner, A., Kreuzer, P. M., Vielsmeier, V., Poeppl, T. B., et al. (2014). Reduced variability of auditory alpha activity in chronic tinnitus. *Neural Plast.* 2014:436146. doi: 10.1155/2014/436146

Schreckenberger, M., Lange-Asschenfeldt, C., Lange-Asschenfeld, C., Lochmann, M., Mann, K., Siessmeier, T., et al. (2004). The thalamus as the generator and modulator of EEG alpha rhythm: a combined PET/EEG study with lorazepam challenge in humans. *Neuroimage* 22, 637–644. doi: 10.1016/j.neuroimage.2004.01.047

Seibert, T. M., Murphy, E. A., Kaestner, E. J., and Brewer, J. B. (2012). Interregional correlations in parkinson disease and parkinson-related dementia with resting functional MR imaging. *Radiology* 263, 226–234. doi: 10.1148/radiol.12111280

Silberstein, P., Pogosyan, A., Kühn, A. A., Hotton, G., Tisch, S., Kupsch, A., et al. (2005). Cortico-cortical coupling in Parkinson's disease and its modulation by therapy. *Brain* 128, 1277–1291. doi: 10.1093/brain/awh480

Slagter, H. A., Mazaheri, A., Reteig, L. C., Smolders, R., Figee, M., Mantione, M., et al. (2017). Contributions of the ventral striatum to conscious perception: an intracranial eeg study of the attentional blink. *J. Neurosci.* 37, 1081–1089. doi: 10.1523/JNEUROSCI.2282-16.2016

Smolders, R., Mazaheri, A., van Wingen, G., Figee, M., de Koning, P. P., and Denys, D. (2013). Deep brain stimulation targeted at the nucleus accumbens decreases the potential for pathologic network communication. *Biol. Psychiatry* 74, e27–e28. doi: 10.1016/j.biopsych.2013.03.012

Sohal, V. S. (2012). Insights into cortical oscillations arising from optogenetic studies. *Biol. Psychiatry* 71, 1039–1045. doi: 10.1016/j.biopsych.2012.01.024

Song, Y., Crowcroft, J., and Zhang, J. (2012). Automatic epileptic seizure detection in EEGs based on optimized sample entropy and extreme learning machine. *J. Neurosci. Methods* 210, 132–146. doi: 10.1016/J.JNEUMETH.2012.07.003

Spencer, K. M., Nestor, P. G., Perlmutter, R., Niznikiewicz, M. A., Klump, M. C., Frumin, M., et al. (2004). Neural synchrony indexes disordered perception and cognition in schizophrenia. *Proc. Natl. Acad. Sci. U.S.A.* 101, 17288–17293. doi: 10.1073/pnas.0406074101

St George, R. J., and Fitzpatrick, R. C. (2011). The sense of self-motion, orientation and balance explored by vestibular stimulation. *J. Physiol.* 589, 807–813. doi: 10.1113/jphysiol.2010.197665

Stephan, T., Deutschländer, A., Nolte, A., Schneider, E., Wiesmann, M., Brandt, T., et al. (2005). Functional MRI of galvanic vestibular stimulation with alternating currents at different frequencies. *Neuroimage* 26, 721–732. doi: 10.1016/j.neuroimage.2005.02.049

Stiles, L., and Smith, P. F. (2015). The vestibular–basal ganglia connection: balancing motor control. *Brain Res.* 1597, 180–188. doi: 10.1016/J.BRAINRES.2014.11.063

Stoffers, D., Bosboom, J. L. W., Deijen, J. B., Wolters, E. C., Berendse, H. W., and Stam, C. J. (2007). Slowing of oscillatory brain activity is a stable characteristic of Parkinson's disease without dementia. *Brain* 130, 1847–1860. doi: 10.1093/brain/awm034

Strüber, D., Rach, S., Neuling, T., and Herrmann, C. S. (2015). On the possible role of stimulation duration for after-effects of transcranial alternating current stimulation. *Front. Cell. Neurosci.* 9:311. doi: 10.3389/fncel.2015.00311

Tahmasian, M., Bettray, L. M., van Eimeren, T., Drzezga, A., Timmermann, L., Eickhoff, C. R., et al. (2015). A systematic review on the applications of resting-state fMRI in Parkinson's disease: Does dopamine replacement therapy play a role? *Cortex* 73, 80–105. doi: 10.1016/j.cortex.2015.08.005

Teles-Grilo Ruivo, L. M., and Mellor, J. R. (2013). Cholinergic modulation of hippocampal network function. *Front. Synaptic Neurosci.* 5:2. doi: 10.3389/fnsyn.2013.00002

Tomlinson, C. L., Stowe, R., Patel, S., Rick, C., Gray, R., and Clarke, C. E. (2010). Systematic review of levodopa dose equivalency reporting in Parkinson's disease. *Mov. Disord.* 25, 2649–2653. doi: 10.1002/mds.23429

Tremblay, R., Lee, S., and Rudy, B. (2016). GABAergic interneurons in the neocortex: from cellular properties to circuits. *Neuron* 91, 260–292. doi: 10.1016/j.neuron.2016.06.033

Tyll, S., Budinger, E., and Noesselt, T. (2011). Thalamic influences on multisensory integration. *Commun. Integr. Biol.* 4, 378–381. doi: 10.4161/cib.4.4.15222

Utz, K. S., Dimova, V., Oppenländer, K., and Kerkhoff, G. (2010). Electrified minds: Transcranial direct current stimulation (tDCS) and Galvanic Vestibular Stimulation (GVS) as methods of non-invasive brain stimulation in neuropsychology—A review of current data and future implications. *Neuropsychologia* 48, 2789–2810. doi: 10.1016/j.neuropsychologia.2010.06.002

Vakorin, V. A., Doesburg, S. M., da Costa, L., Jetly, R., Pang, E. W., and Taylor, M. J. (2016). Detecting mild traumatic brain injury using resting state magnetoencephalographic connectivity. *PLoS Comput. Biol.* 12:e1004914. doi: 10.1371/JOURNAL.PCBI.1004914

Van der Ouderaa, E., Schoukens, J., and Renneboog, J. (1988). Peak factor minimization of input and output signals of linear systems. *IEEE Trans. Instrum. Meas.* 37, 207–212. doi: 10.1109/19.6053

Vossen, A., Gross, J., and Thut, G. (2015). Alpha power increase after transcranial alternating current stimulation at alpha frequency (α-tACS) reflects plastic changes rather than entrainment. *Brain Stimul.* 8, 499–508. doi: 10.1016/j.brs.2014.12.004

Vreugdenhil, M., Jefferys, J. G. R., Celio, M. R., and Schwaller, B. (2003). Parvalbumin-deficiency facilitates repetitive IPSCs and gamma oscillations in the hippocampus. *J. Neurophysiol.* 89, 1414–1422. doi: 10.1152/jn.00576.2002

Watson, G. S., and Leverenz, J. B. (2010). Profile of cognitive impairment in Parkinson's disease. *Brain Pathol.* 20, 640–645. doi: 10.1111/j.1750-3639.2010.00373.x

Wijesinghe, R., Protti, D. A., and Camp, A. J. (2015). Vestibular interactions in the thalamus. *Front. Neural Circuits* 9:79. doi: 10.3389/fncir.2015.00079

Williams, D., Tijssen, M., Van Bruggen, G., Bosch, A., Insola, A., Di Lazzaro, V., et al. (2002). Dopamine-dependent changes in the functional connectivity between basal ganglia and cerebral cortex in humans. *Brain* 125, 1558–1569. doi: 10.1093/brain/awf156

Wingeier, B., Tcheng, T., Koop, M. M., Hill, B. C., Heit, G., and Bronte-Stewart, H. M. (2006). Intra-operative STN DBS attenuates the prominent beta rhythm in the STN in Parkinson's disease. *Exp. Neurol.* 197, 244–251. doi: 10.1016/j.expneurol.2005.09.016

Wu, T., Long, X., Wang, L., Hallett, M., Zang, Y., Li, K., et al. (2011). Functional connectivity of cortical motor areas in the resting state in Parkinson's disease. *Hum. Brain Mapp.* 32, 1443–1457. doi: 10.1002/hbm.21118

Wu, T., Wang, L., Chen, Y., Zhao, C., Li, K., and Chan, P. (2009). Changes of functional connectivity of the motor network in the resting state in Parkinson's disease. *Neurosci. Lett.* 460, 6–10. doi: 10.1016/j.neulet.2009.05.046

Yamamoto, Y., Struzik, Z. R., Soma, R., Ohashi, K., and Kwak, S. (2005). Noisy vestibular stimulation improves autonomic and motor responsiveness in central neurodegenerative disorders. *Ann. Neurol.* 58, 175–181. doi: 10.1002/ana.20574

Conflict of Interest Statement: The authors declare that the research was conducted in the absence of any commercial or financial relationships that could be construed as a potential conflict of interest.

frontiers in Human Neuroscience

PERSPECTIVE
published: 08 April 2019
doi: 10.3389/fnhum.2019.00111

Fast Intracortical Sensory-Motor Integration: A Window Into the Pathophysiology of Parkinson's Disease

Raffaele Dubbioso[1]*, *Fiore Manganelli*[1], *Hartwig Roman Siebner*[2,3,4†‡] *and Vincenzo Di Lazzaro*[5†‡]

[1]*Department of Neurosciences, Reproductive Sciences and Odontostomatology, University Federico II of Naples, Naples, Italy,* [2]*Danish Research Centre for Magnetic Resonance, Centre for Functional and Diagnostic Imaging and Research, Copenhagen University Hospital Hvidovre, Hvidovre, Denmark,* [3]*Department of Neurology, Copenhagen University Hospital Bispebjerg, Copenhagen, Denmark,* [4]*Institute for Clinical Medicine, Faculty of Health and Medical Sciences, University of Copenhagen, Copenhagen, Denmark,* [5]*Unit of Neurology, Neurophysiology, Neurobiology, Department of Medicine, University Campus Bio-Medico, Rome, Italy*

OPEN ACCESS

Edited by:
Matt J. N. Brown, California State University, Sacramento, United States

Reviewed by:
Aimee J. Nelson, McMaster University, Canada
Sean Kevin Meehan, University of Waterloo, Canada

***Correspondence:**
Raffaele Dubbioso
rafdubbioso@gmail.com

†These authors have contributed equally to this work

‡Co-senior authors

Received: *29 January 2019*
Accepted: *13 March 2019*
Published: *08 April 2019*

Citation:
Dubbioso R, Manganelli F, Siebner HR and Di Lazzaro V (2019) Fast Intracortical Sensory-Motor Integration: A Window Into the Pathophysiology of Parkinson's Disease. Front. Hum. Neurosci. 13:111. doi: 10.3389/fnhum.2019.00111

Parkinson's Disease (PD) is a prototypical basal ganglia disorder. Nigrostriatal dopaminergic denervation leads to progressive dysfunction of the cortico-basal ganglia-thalamo-cortical sensorimotor loops, causing the classical motor symptoms. Although the basal ganglia do not receive direct sensory input, they are important for sensorimotor integration. Therefore, the basal ganglia dysfunction in PD may profoundly affect sensory-motor interaction in the cortex. Cortical sensorimotor integration can be probed with transcranial magnetic stimulation (TMS) using a well-established conditioning-test paradigm, called short-latency afferent inhibition (SAI). SAI probes the fast-inhibitory effect of a conditioning peripheral electrical stimulus on the motor response evoked by a TMS test pulse given to the contralateral primary motor cortex (M1). Since SAI occurs at latencies that match the peaks of early cortical somatosensory potentials, the cortical circuitry generating SAI may play an important role in rapid online adjustments of cortical motor output to changes in somatosensory inputs. Here we review the existing studies that have used SAI to examine how PD affects fast cortical sensory-motor integration. Studies of SAI in PD have yielded variable results, showing reduced, normal or even enhanced levels of SAI. This variability may be attributed to the fact that the strength of SAI is influenced by several factors, such as differences in dopaminergic treatment or the clinical phenotype of PD. Inter-individual differences in the expression of SAI has been shown to scale with individual motor impairment as revealed by UPDRS motor score and thus, may reflect the magnitude of dopaminergic neurodegeneration. The magnitude of SAI has also been linked to cognitive dysfunction, and it has been suggested that SAI also reflects cholinergic denervation at the cortical level. Together, the results indicate that SAI is a useful marker of disease-related alterations in fast cortical sensory-motor integration driven by subcortical changes in the dopaminergic and cholinergic system.

Since a multitude of neurobiological factors contribute to the magnitude of inhibition, any mechanistic interpretation of SAI changes in PD needs to consider the group characteristics in terms of phenotypical spectrum, disease stage, and medication.

Keywords: short-latency afferent inhibition, cholinergic neuromodulation, cortical oscillations, dopaminergic dysfunction, Parkinson's disease, movement disorder, neurophysiological biomarker

INTRODUCTION

Parkinson's disease (PD) is a neurodegenerative disorder affecting multiple neuromodulatory transmitter systems (Barone, 2010). The cardinal motor symptoms of PD are due to the progressive loss of nigrostriatal dopaminergic neurons in the midbrain. Progressive nigrostriatal dopaminergic denervation causes a dysfunction in the cortex-basal ganglia sensorimotor loops, producing slowness of movements, rigidity, tremor, and difficulties with gait and balance (Dickson, 2012). Although the basal ganglia do not receive direct somatosensory input from the periphery, several lines of evidence support the idea that the basal ganglia are important for gating sensory input for motor control through cortico-basal ganglia-thalamo-cortical re-entry loops (Haber and Calzavara, 2009). Specifically, primary and secondary somatosensory cortices in the parietal lobe send inputs to the striatum of the basal ganglia, where sensory cortical projections are topographically mapped (Künzle, 1977; Di Martino et al., 2008). The notion that the basal ganglia are relevant to **sensorimotor integration** is rather old. Back in 1985, Lidsky introduced the notion that the basal ganglia serve as "sensory analyzer for motor systems" which "ultimately affect movement by gating sensory inputs into other motor areas" (Lidsky et al., 1985). Lesions of the basal ganglia mostly affect automatic movements that need sensory guidance, pointing towards a role of the basal ganglia in sensory-motor control of automatic or highly trained movements (Boecker et al., 1999).

KEY CONCEPT 1 | Sensorimotor integration

Sensorimotor integration is the process whereby somatosensory input is integrated by the central nervous system to shape motor program execution. Parkinson's disease (PD) is considered a pathological model of aberrant sensory-motor integration, where movement accuracy and speed are severely affected by the altered sensory feedback.

In addition, PD patients also exhibit impairment of selecting the appropriate response while simultaneously suppressing inappropriate response tendencies (Praamstra and Plat, 2001). Interestingly, patients with PD display difficulties in suppressing automatic response activation while proactive inhibitory control appears to be intact (Praamstra and Plat, 2001; Seiss and Praamstra, 2004; Wylie et al., 2009). Using transcranial magnetic stimulation (TMS), it was also shown that impaired inhibition also manifests itself within the corticomotor output system in PD (Kleine et al., 2001). The TMS-evoked excitation of the corticomotor projections produced an increased, prolonged and less synchronized excitation of the target muscle (Kleine et al., 2001). This converging evidence shows that anatomical and functional impairment of the cortico-basal ganglia-thalamo-cortical loop in PD profoundly affects sensory-motor integration in the cortex.

Sensorimotor integration at the cortical level can be probed non-invasively by pairing electrical stimulation of peripheral somatosensory afferents with focal TMS targeting the contralateral primary motor cortex (M1). In their seminal study, Tokimura et al. (2000) demonstrated that peripheral nerve stimulation at the contralateral wrist reduced the amplitude of motor evoked potentials (MEPs) when the TMS pulse was given to the primary motor hand area (M1-HAND) 2–8 ms after the arrival of the afferent volley in cortex. The term "**short-latency afferent inhibition**" (SAI) was coined for this conditioning-test paradigm, and SAI soon became a well-established neurophysiological technique to probe rapid intracortical sensorimotor integration in health and disease (Turco et al., 2018b). The inhibitory effect of the sensory input on the motor output provides a neurophysiological signature of fast sensory-motor integration. Three components constitute the SAI circuit that enables fast-integrative processing: the fast afferent-sensory pathway, the motor-efferent pathway and the integrative component in the sensorimotor cortex. The neuropharmacological profile of SAI is complex. The sensory input exerts its inhibitory effects on the corticospinal neurons through γ-Aminobutyric acid (GABA)-ergic intracortical circuits (Di Lazzaro et al., 2005c; Di Lazzaro and Ziemann, 2013), but its magnitude is also modulated by dopaminergic (Sailer et al., 2003) and cholinergic neuromodulatory circuits (Di Lazzaro et al., 2000). The fact that the magnitude of SAI is modulated by cholinergic drugs has provoked considerable interest in the use of SAI in patients with dementia. In patients with Alzheimer Disease (AD), a loss of SAI has been interpreted as an indicator of cortical cholinergic denervation and a normal SAI as a predictor of a positive effect of cholinergic medication on cognitive deficits (Di Lazzaro et al., 2000; Cantone et al., 2014).

KEY CONCEPT 2 | Short-latency afferent inhibition (SAI)

Fast component of sensorimotor integration can be studied *in vivo* by examining the effects of sensory input on the motor output at the cortical level. The amplitude of a motor evoked potential (MEP) induced by transcranial magnetic simulation (TMS) over the motor cortex is reduced by a peripheral nerve stimulation few milliseconds before the TMS pulse. The magnitude of this inhibition represents the neurophysiological correlate of sensorimotor integration efficiency.

The neurophysiological and neuropharmacological properties of SAI have motivated researchers to use SAI as a tool to examine whether and how PD is associated with an impairment of fast sensory-motor integration in the pericentral sensorimotor cortex. In the same vein, researchers have examined whether

the attenuation of SAI in individual patients scales with dopaminergic and cholinergic cortical neurodegeneration and is associated with particular clinical symptoms (Martin-Rodriguez and Mir, 2018). In this review, we first summarize some key features of SAI in the healthy human brain. We will then review the evidence for an alteration of SAI in PD and discuss, based on the published data, whether the individual reduction in SAI can be used as an electrophysiological biomarker of cholinergic or dopaminergic denervation of the sensorimotor cortex in PD. Finally, we will ask the question whether a reduction in SAI is associated with specific clinical manifestations of PD.

SHORT-LATENCY AFFERENT INHIBITION IN THE HEALTHY HUMAN BRAIN

Cortical Origin of SAI

Converging evidence supports the hypothesis that SAI is generated in the sensorimotor cortex, although the exact anatomic circuits generating SAI are still unknown. The most direct evidence that peripheral somatosensory input modulates the TMS-induced motor output at the cortical level comes from invasive recordings of corticospinal volleys in patients with implanted electrodes in the cervical epidural space (Tokimura et al., 2000). These studies showed that later I-waves (I2 and I3 waves) were reduced at an interval appropriate for SAI, whereas the early I-wave (I1 wave) remained unchanged. Based on these findings, it has been proposed that peripheral nerve stimulation activates glutamatergic thalamocortical projections onto intracortical $GABA_A$-ergic interneurons which in turn, suppress the intracortical inhibitory $GABA_A$-ergic circuits generating the late descending volleys (late I-waves) in the corticospinal tract (Di Lazzaro and Ziemann, 2013). A critical role of thalamocortical projections is substantiated by lesion studies, showing a marked reduction or loss of SAI in patients with unilateral (Oliviero et al., 2005) or bilateral (Nardone et al., 2010) paramedian thalamic stroke.

Which Factors Modulate the Expression of SAI?

The relative strength of SAI depends on the magnitude of the sensory afferent input evoked by peripheral stimulation. The greater the afferent volley evoked by peripheral stimulation, the stronger is the magnitude of SAI (Bailey et al., 2016). The expression of SAI also depends on the somatotopic relation between the sensory input and motor output. Electrical stimulation of digits close to the TMS-target muscle (i.e., homotopic stimulation) induces stronger inhibition than stimulation of digits distant to the TMS-target muscle (i.e., heterotopic stimulation; Classen et al., 2000). The somatotopic organization of SAI was studied in detail using a neuronavigated TMS mapping technique which adjusts the coil position and orientation to the individual shape of the central sulcus (Dubbioso et al., 2017c). Mapping the input-output relationship of SAI revealed a center-surround organization in the human M1-HAND. SAI was evoked by homotopic stimulation only, whereas the conditioning effect produced the opposite effect, namely short-latency afferent facilitation (SAF), in the case of heterotopic stimulation (Dubbioso et al., 2017c).

The expression of homotopic is highly state dependent. In healthy individuals, SAI is consistently expressed at rest, but attenuated during finger movements (Dubbioso et al., 2017c). In the active target muscle, SAI was reduced at movement initiation during both mixed and homotopic cutaneous nerve stimulation (Asmussen et al., 2013; Cho et al., 2016), whereas SAI was reduced during the maintenance phase of the movement (Asmussen et al., 2013) or found to be normal (Cho et al., 2016). Accordingly, SAI and SAF by homotopic or heterotopic stimulation were abolished during the tonic contraction of the target muscle (Dubbioso et al., 2017c). This state-dependent pattern of SAI modulation can be attributed to a sensorimotor gating mechanism, which attenuates the perceived intensity of stimuli generated by movements. Although SAI is closely modulated by movement, no relationship between SAI magnitude and manual dexterity has been found (Turco et al., 2018c).

The expression of SAI is not only modulated by the intrinsic sensorimotor state but also shaped by transcranial brain stimulation. Transcranial alternating current stimulation (TACS) at 20 Hz completely abolished SAI in the relaxed muscle (Guerra et al., 2016). The suppressive effect of 20 Hz TACS on SAI did not depend on the phase relationship between TACS and the timing of the TMS pulse probing SAI (Guerra et al., 2016). This finding suggests a link between SAI expression and the oscillatory state of the sensorimotor cortex, yet it remains to be shown that SAI is also suppressed by physiologically generated beta oscillations in sensorimotor cortex.

The magnitude of SAI can also be modulated by TMS interventions, for instance when electrical stimulation of the median nerve is consistently paired with TMS of the contralateral M1-HAND at an inter-stimulus interval (ISI) of 25 ms (Quartarone et al., 2006) or with TMS over the contralateral S1 at an ISI of N20-2.5 ms (Tsang et al., 2015). Sub-motor threshold 5 Hz repetitive paired associative stimulation produced a long-lasting increase in corticospinal excitability along with an attenuation of SAI (Quartarone et al., 2006; Tsang et al., 2015). Interventional TMS protocols which are thought to induce homosynaptic plasticity, such as continuous theta burst (cTBS) have also been sued to modify SAI. While cTBS over M1-HAND failed to modulate SAI, cTBS delivered over S1 reduced SAI along with an increase in cortico-spinal excitability (Tsang et al., 2014).

Cognitive processes, for instance attention and working memory, shape afferent sensory-motor integration involving distinct intracortical circuits as demonstrated by single monophasic TMS pulses that evoke different current directions in the brain (Mirdamadi et al., 2017; Suzuki and Meehan, 2018). Specifically, it has been demonstrated that SAI evoked using antero-posterior (AP), but not posterior-anterior (PA), current is reduced by a concurrent visual detection task with high attention demands. These results suggested that only AP-elicited intracortical circuits are sensitive to cross-modal attention task by altering sensory processing in premotor areas (Mirdamadi et al., 2017). Instead, a verbal working memory task modulated SAI, regardless of the TMS-induced current direction in the

brain (AP or PA), reflecting a generalized effect of this cognitive task across anatomically distinct circuits upon cortico-spinal neurons in the M1-HAND (Suzuki and Meehan, 2018).

The fact that intrinsically and extrinsically induced state changes in the sensorimotor system can dynamically tune the expression of SAI needs to be born in mind when SAI is considered as "biomarker" in PD.

Influence of Neurotransmitter Systems on SAI Magnitude

Pharmacological and clinical studies provided converging evidence that the expression of SAI is modulated by several neurotransmitters such as acetylcholine, dopamine, GABA and noradrenaline (Turco et al., 2018b). SAI is significantly reduced by scopolamine, a muscarinic cholinergic antagonist, in young healthy adults (Di Lazzaro et al., 2000) and can be improved with rivastigmine, an acetylcholinesterase inhibitor, in patients with abnormal reduction of SAI, such as AD (Di Lazzaro et al., 2002). Cholinergic inhibition of pyramidal neurons has been demonstrated directly in experimental studies (Gulledge and Stuart, 2005). Interestingly, this rivastigmine effect on SAI predicted the long term response to cholinesterase inhibitor in patients with AD (Di Lazzaro et al., 2005a). The effects of scopolamine and rivastigmine suggest that SAI may be useful to probe *in vivo* the functional integrity of central cholinergic circuits of the human brain. These studies indicate that SAI can trace the functional impairment of central cholinergic circuits, allowing to discriminate for example cholinergic from non-cholinergic form of dementia (Di Lazzaro et al., 2006; Manganelli et al., 2014; Dubbioso et al., 2017b).

Beyond cholinergic transmission, the dopaminergic system plays a relevant role in the modulation of SAI, in accordance with a strong synaptic interaction between dopamine an acetylcholine signaling in different brain areas (Di Cara et al., 2007; Millan et al., 2007). L-dopa treatment has been shown to normalize SAI in patients with restless legs syndrome (Rizzo et al., 2010) and AD (Martorana et al., 2009; Nardone et al., 2014). **Dopaminergic medication** also influences SAI in patients with PD (for more details see section on PD).

KEY CONCEPT 3 | Dopaminergic medication and sensory processing

Studies on PD patients consistently found reduced levels of SAI in the ON-medication state suggesting a role of dopamine replacement in driving this abnormality. Indeed, dopaminergic medication could lead to decreases in central processing or integration of sensory signals in PD patients. For instance, it has been shown that dopaminergic medication could worsen SAI and proprioception. The positive relationship between motor symptoms and SAI suppression in the ON-medication state suggests that the effect of medication may be more detrimental to SAI in patients that are less responsive to dopaminergic pharmacotherapy, for instance, patients with more prominent cholinergic involvement.

Regarding GABAergic system, in human cortical slices, it was observed that acetylcholine activated GABA neurons and triggered GABAergic postsynaptic currents (Alkondon et al., 2000). Thus, SAI may also be mediated through the interactions between cholinergic projections and specific GABAergic interneurons. This also explains the findings that the administration of positive $GABA_A$ but not $GABA_B$ receptor modulators influences SAI (Turco et al., 2018a). Zolpidem, a selective agonist of alpha1 subunit of $GABA_A$ receptor, and lorazepam, a positive allosteric modulator of $GABA_A$ receptor, significantly reduced SAI (Di Lazzaro et al., 2005b,c, 2007; Turco et al., 2018a), whereas diazepam, a non-selective agonist, induced a slight increase or no effect on SAI (Di Lazzaro et al., 2005c, 2007). This observation is presumably explained by a differential role of the different alpha subunits of $GABA_A$ receptor in the modulation of afferent inhibition with a suppression of cholinergic inhibition by alpha1 subunit activation.

Lastly, a recent study has also demonstrated that acute and chronic intake of reboxetine, a noradrenaline reuptake inhibitor, reduces SAI, likely through suppression of GABAergic neurotransmission (Kuo et al., 2017).

FAST SENSORY INPUT AND MOTOR OUTPUT PATHWAYS IN PD

As stated above the basal ganglia do not receive direct sensory input, yet patients with PD often report sensory symptoms (Pallis, 1971; Snider et al., 1976; Hillen and Sage, 1996). Objective somatosensory deficits are well documented in PD and have been mainly found in tasks that require the use of kinaesthetic sense such as conscious perception of limb position and motion in space proprioception and kinaesthesia (Schneider et al., 1987; Klockgether et al., 1995; Demirci et al., 1997; Jobst et al., 1997; Zia et al., 2000) or temporal or spatial discrimination (Conte et al., 2013).

The fast-afferent sensory volley eliciting SAI can be studied by recording the somatosensory evoked potentials (SSEPs) evoked by stimulation of the peripheral nerve. Most SSEP studies in PD have employed electrical stimulation of a mixed nerve that reflects activation of proprioceptive as well as cutaneous inputs. SSEP studies in patients with PD found a reduced amplitude of the late N30 component of the SSEP, while the early N20-P25 components were found to be normal (Rossini et al., 1989; Cheron et al., 1994; Ulivelli et al., 1999). SSEP studies following proprioceptive stimulation during passive flexion (Mima et al., 1996) or electric stimulation (Restuccia et al., 1999) of the proximal interphalangeal joint of the finger demonstrated that the origin of the N30 waveform is more complex than the early components, containing information from cutaneous afferents as well as from joint and tendinous inputs. Therefore, it has been hypothesized that the defective proprioception described in PD might be related to the depression of the N30 component.

The early cortical components of the SSEP, namely the dipole N20/P20 and P25 component, reflect early sensory processing in the pericentral cortex and are thought to give rise to fast sensory afferent inhibition. Since these early components are intact in PD patients, alterations of SAI in PD patients cannot be attributed to a dysfunction of the afferent sensory pathway. The same consideration applies to the fast cortico-motor output pathway which is unaffected in PD. Indeed, a TMS study, which recorded MEPs at increasing stimulus intensities, demonstrated

a normal gain function of corticospinal excitability in PD patients (Kojovic et al., 2012).

However, context-dependent modulation of early cortical sensory processing is impaired in PD. Normal movement-related attenuation of perceived stimuli, referred to as sensorimotor gating, is deficient in patients with PD while they are off dopaminergic treatment and can be restored by dopamine replacement therapy (Macerollo et al., 2016). In contrast to healthy controls, the early N20-P25 SSEP components were not modulated at all by movement in patients with PD. The authors speculated that abnormalities in sensory gating may contribute to the difficulties in movement initiation observed in PD (Macerollo et al., 2016). Another study on PD patients treated with deep brain stimulation (DBS) of the subthalamic nucleus or globus pallidum found that movement of the hand ipsilateral to median nerve stimulation gated the subcortical triphasic negative–positive–negative potentials—at latencies of 14–18–22.5 ms, similar to cortical gating observed with SSEP at N20, P20, and N30 (Insola et al., 2004). Converging evidence suggests that sensory gating preceding the onset of movement seems to be mediated by motor cortical areas that contribute to preparation and execution of movement (Cohen and Starr, 1987; Seki and Fetz, 2012; Macerollo et al., 2018).

CORTICAL SENSORIMOTOR INTEGRATION IN PD

Based on the work summarized in the previous sections, it can be concluded that SAI is a cortical process, albeit the exact circuit underlying this fast sensory-motor integration is still unknown. In addition, the lack of major impairment in the fast afferent sensory-to-cortical and efferent cortical-to-motor pathways in PD suggest that abnormalities of SAI in PD are caused by a dysfunction in fast intracortical sensorimotor integration.

Patients with electrodes implanted for DBS provide a unique opportunity to study the interplay between the subcortical target site and the cortex. Two electrophysiological studies showed that continuous high-frequency DBS of the STN modifies SAI in PD, confirming a close relationship between fast sensory-motor cortical integration and the basal ganglia. A first study examined medicated patients with the STN-DBS switched on or off (Sailer et al., 2007). SAI was reduced in the off-stimulation and was acutely restored after STN stimulation was resumed, suggesting that STN stimulation might normalize pathways that are adversely affected by dopaminergic medications (Sailer et al., 2007).

A second study focused on the long-term effect of STN-DBS on SAI and spatial proprioception (Wagle Shukla et al., 2013). SAI and proprioception were first normalized after 6 months, but not after 1 month of DBS. This study underscores the importance of chronic stimulation in the modulation of sensorimotor integration and proprioception.

The authors considered two possible mechanisms underlying SAI modulation by STN DBS. High-frequency DBS of the STN might normalize synchronization between basal ganglia structures, which might restore the ability of thalamocortical relay cells to respond to depolarizing inputs involved in sensorimotor integration (Brown et al., 2001; Rubin and Terman, 2004). Alternatively, STN DBS might have a direct effect on cortical structures through antidromic stimulation of the cortico-subthalamic pathway. In addition, the delayed effect of STN DBS on SAI may reflect long-term plastic changes in the sensorimotor cortex (Udupa et al., 2016). Whatever the underlying mechanisms may be, the modulatory effects of STN-DBS on SAI corroborate a sensorimotor integrative function of the STN as suggested by animal studies. Many STN neurons in the monkey (Wichmann et al., 1994) and patients with PD (Hutchison et al., 1998; Rodriguez-Oroz et al., 2001; Theodosopoulos et al., 2003) respond to cutaneous stimuli and passive movements. Alteration of sensory properties of the STN has been observed in animal models of PD. Peripheral sensory stimulation by hind paw pinch led to a greater increase in STN activity in dopamine-depleted rats than controls, suggesting altered STN sensitivity to afferent sensory inputs in the parkinsonian state (Magill et al., 2001).

IS SAI ABNORMAL IN PD?

To answer this question, we conducted a literature search on Pubmed[1] using the following search strings: "Short afferent inhibition" OR "SAI" AND "PD."

Exclusion criteria were as follows:

i. review articles or letter to the editors reporting no original data.
ii. studies about atypical parkinsonism [i.e., Progressive Supranuclear Palsy (PSP), Multisystemic Atrophy or Cortical Basal Syndrome], or dystonia not including PD population as control group.

This search resulted in 22 studies on the final search on November 2, 2018 (**Tables 1**, **2**). Fourteen studies reported a reduction of SAI in patients with PD. The average disease duration was 6.14 ± 4.39 years, mean ON UPDRS-III score was 24.03 ± 13.11, and the mean L-dopa equivalent dose 667.02 ± 314.51 mg across all positive studies (**Table 1**). In the remaining eight studies, six reported normal (Degardin et al., 2012; Zamir et al., 2012; Picillo et al., 2015; Dubbioso et al., 2017a; Ponzo et al., 2017; Nelson et al., 2018) and two found an enhanced SAI in PD patients (Di Lazzaro et al., 2004; Nardone et al., 2005). Mean disease duration was 5.63 ± 2.69 years, mean ON UPDRS-III score was 18.32 ± 8.52 and L-dopa equivalent dose was 633.94 ± 206.30 mg across all negative studies (**Table 2**).

Importantly, these studies found consistent reduction of SAI mainly in medicated PD patients, whereas the off state was not associated with SAI alterations. The idea that nigrostriatal dopaminergic denervation does not reduce SAI or might even enhance cortical inhibition is supported by two studies. The first one, a small study on three drug-free patients with pure hemiparkinsonism (Di Lazzaro et al., 2004) showed enhanced SAI on the affected side. The second one, performed on 10 PD patients in off-state confirmed the increased cortical inhibition respect to patients with PSP and healthy controls (Nardone et al.,

[1] https://www.ncbi.nlm.nih.gov/pubmed/

TABLE 1 | Studies showing short-latency afferent inhibition (SAI) alteration in Parkinson's Disease (PD) patients.

Reference	Participants (mean age ± SD, y)	ON/OFF medication (UPDRS III)	Disease duration (years) or (months)°	L-dopa equivalent dose (mg)	Cognitive decline	SAI ISI	Main findings	Interpretation
Versace et al. (2017)	15 PD borderline OERP (69.9 ± 5.4) 13 PD absent OERP (71.8 ± 5.4) 30 HC (67.4 ± 4.8)	PD-ON borderline OERP (16.1 ± 5.4) PD-ON absent OERP (16.9 ± 5.1)	PD-ON borderline OERP (7.7 ± 4.7) PD-ON absent OERP (8.0 ± 4.7)	PD-ON borderline OERP (516.7 ± 209.3) PD-ON absent OERP (530.8 ± 184.3)	MCI Level I in PD with absent OERP (92%) and in PD with borderline OERP (20%)*	N20+2 to +8 ms (1 ms Δ)	↓ SAI in PD with absent OERP	Altered SAI in PD patients with olfactory dysfunction and cognitive impairment
Oh et al. (2017)	28 PD hyposmia (63.04 ± 1.73) 26 PD anosmia (70.5 ± 1.88) 17 PD normosmia (67.35 ± 2.22) 20 HC (68.45 ± 1.61)	PD-ON hyposmia (18.96 ± 1.31) PD-ON anosmia (21.67 ± 2.27) PD-ON normosmia (14.94 ± 2.3)	PD-ON hyposmia (18.43 ± 1.56)° PD-ON anosmia (21.62 ± 1.68)° PD-ON normosmia (15.24 ± 1.78)°	PD-ON hyposmia (558.83 ± 47.02) PD-ON anosmia (544.7 ± 43.98) PD-ON normosmia (371.18 ± 43.8)	Normal MMSE	N20 to +4 ms (2 ms Δ)	↓ SAI in PD hyposmia and anosmia	Altered SAI in PD patients with olfactory dysfunction
Pelosin et al. (2016)	33 PD-fallers (7.6 ± 4.4) 17 elderly men-fallers (73.4 ± 4.2) 10 elderly men non-fallers (72.1 ± 4.9)	PD-ON (30.3 ± 9.13)	NA	775.5 ± 358.6	MCI Level I in PD-fallers*	N20-2 to +8 ms (2 ms Δ)	↓ SAI in PD-fallers and elderly men fallers	Altered cholinergic activity in patients with gait disturbances
Lee et al. (2015)	12 PD with dysphagia (73.33 ± 6.48) 17 PD without dysphagia (71.06 ± 6.98) 11 HC (62.4 ± 6.2)	PD-ON with dysphagia (24.17 ± 6.53) PD-ON without dysphagia (20.06 ± 4.07)	PD-ON with dysphagia (17.92 ± 9.16)° PD-ON without dysphagia (11.94 ± 4.98)°	PD-ON with dysphagia (589.58 ± 254.50) PD-ON without dysphagia (488.82 ± 181.86)	Normal MMSE	N20 to +4 ms (1 ms Δ)	↓ SAI in PD with dysphagia	Altered cholinergic activity in patients with dysphagia
Wagle Shukla et al. (2013)	11 PD with STN-DBS (58 ± 8.3) 10 HC (56 ± 7.1)	12 CONDITIONS	13.18 ± 4.21	1576.09 ± 1076.22	NA	N20	SAI is normalized 6 months after STN-DBS implant	Long-term STN-DBS improves sensorimotor integration and proprioception
Brusa et al. (2014)	10 PSP (59.3 ± 6.6) 10 PD (58 ± 6.4) 10 HC (57.2 ± 6.2)	PSP-ON (62.6 ± 9.4) PD-ON (36.2 ± 9)	PSP-ON (7 ± 1.2) PD-ON (6.3 ± 1.5)	PSP-ON (500 ± 150) PD-ON (750 ± 125)	Normal MMSE	N20-4 to +8 ms (4 ms Δ)	↓ SAI in PSP compared to PD, no effect induced by cerebellar iTBS	Cerebellar iTBS modulates cerebellar-cortical connectivity without affecting sensorimotor integration in PSP
Celebi et al. (2014)	11 MSA-P (58.7 ± 2.6) 8 MSA-C (58.9 ± 2.1) 10 PD (61.8 ± 1.8) 10 HC (65.8 ± 2.1)	PD-ON (8.8 ± 1.6)	3.2 ± 0.6	545 ± 57.6	MCI Level I in MSA type C and P*	N20+1 to +4 ms (1 ms Δ)	↓ SAI in MSA-C compared to PD and correlates with neuropsychological scores	Cholinergic dysfunction in MSA-C patients and cognitive impairment
Yarnall et al. (2013)	11 PD with MCI (73.3) 11 PD without MCI (66.9) 22 HC (67.9)	PD-ON with MCI (28.5) PD-ON without MCI (28.7)	PD-ON with MCI (20)° PD-ON without MCI (28.5)°	PD-ON with MCI (343.5) PD-ON without MCI (288.1)	MCI Level I in PD*	N20	↓ SAI in PD with MCI and correlates with MoCA score	Cholinergic dysfunction occurs early in PD with MCI
Nardone et al. (2013)	10 PD with RBD (65.9 ± 6.5) 13 PD without RBD (63.7 ± 6.4) 15 HC (66.4 ± 7)	PD-ON with RBD (17.5 ± 4.3) PD-ON without RBD (18.3 ± 4.3)	PD-ON with RBD (5 ± 2.3) PD-ON without RBD (6 ± 0.8)	PD-ON with RBD (578 ± 2.9) PD-ON without RBD (627 ± 341)	MCI in PD with RBD (90%) and without RBD (38%)#	N20+2 to +8 ms (1 ms Δ)	↓ SAI in PD with RBD and correlates with neuropsychological scores	Cholinergic dysfunction in PD with RBD and cognitive impairment

(Continued)

TABLE 1 | Continued

Reference	Participants (mean age ± SD, y)	ON/OFF medication (UPDRS III)	Disease duration (years) or (months)°	L-dopa equivalent dose (mg)	Cognitive decline	SAI ISI	Main findings	Interpretation
Rochester et al. (2012)	22 PD (70.18 ± 9.67) 22 HC (67.43 ± 8.43)	PD-ON (29.14 ± 9.54)	19.83 ± 8.6°	304.86 ± 130.91	MCI Level I in PD*	N20 to +4 ms (1 ms Δ)	↓ SAI in PD	Altered cholinergic activity in PD correlates with gait dysfunction
Celebi et al. (2012)	10 PD (72 ± 1.4) 10 PD with dementia (75 ± 2.2) 10 AD (76 ± 1.7) 10 HC (72.1 ± 2.3)	PD-ON (9.8 ± 1.6) PD-ON with dementia (22.9 ± 1.7)	PD-ON (2.3 ± 0.5) PD-ON with dementia (8.4 ± 1.6)	PD-ON (345.5 ± 77.7) PD-ON with dementia (943 ± 147.2)	Mild-moderate dementia	N20+1 to +8 ms (1 ms Δ)	↓ SAI in PD with dementia and AD	Cholinergic dysfunction in PD with dementia
Manganelli et al. (2009)	10 PD with VH (70.4 ± 5.3) 12 PD without VH (65.5 ± 10.1) 11 HC (62.4 ± 6.2)	PD-ON with VH (70.4 ± 5.3) PD-ON without VH (65.5 ± 10.1)	PD-ON with visual hallucination (8.7 ± 6.3) PD-ON without visual hallucination (9 ± 5.5)	PD-ON with visual hallucination (535.9 ± 307.8) PD-ON without visual hallucination (697.9 ± 271.5)	MCI in PD with VH (90%) and without VH (58%)§	N20+2 to +8 ms (2 ms Δ)	↓ SAI in PD with VH	Cholinergic dysfunction in PD patients with visual hallucinations and cognitive impairment
Sailer et al. (2007)	7 PD with STN-DBS (56.1 ± 3.6) 7 HC (56 ± 6.3)	PD-ON-STIM-OFF (10.86 ± 3.44) PD-ON-STIM-ON (7 ± 2.38) PD-OFF-STIM-OFF (6.17 ± 2.14) PD-OFF-STIM-ON (5.17 ± 2.23)	14 ± 4.51	723.14 ± 412.62	NA	N20+3	↓ SAI in PD-ON stimulator-OFF, SAI is restored by stimulator-ON	STN-DBS improves acutely sensorimotor integration
Sailer et al. (2003)	10 PD (58.2 ± 9.8) 10 HC (59.5 ± 10.7)	PD-ON (12.8 ± 6.3) PD-OFF (23.7 ± 11.1)	7.4 ± 5.7	835.25 ± 614.08	NA	N20 (MN) N23 (D3)	↓ SAI in PD-ON more affected side and normal in PD-OFF	SAI is altered by dopaminergic medication and may contribute to the side effects of dopaminergic drugs

*MN, median nerve stimulation; D3, digit 3 stimulation; iTBS, intermittent theta-burst-stimulation; NA, not applicable; PD, Parkinson's Disease; HC, healthy control; VH, visual hallucination; RBD, REM-sleep Behavior Disorders; MSA-P, multiple system atrophy parkinsonian type; MSA-C, multiple system atrophy cerebellar type; PSP, progressive supranuclear palsy; AD, Alzheimer disease; OERP, Olfactory Event-Related Potentials; STN-DBS, subthalamic nucleus deep brain stimulation; MMSE, mini mental state examination; MoCA, Montreal Cognitive Assessment; MCI, mild cognitive impairment; *MCI criteria according to the Level I of the MDS (Movement Disorder Society) commissioned Task Force (Litvan et al., 2012); #MCI criteria according to Petersen and Morris, 2005; §MCI criteria according to Caviness et al., 2007.*

TABLE 2 | Studies showing normal or enhanced SAI in PD patients.

Reference	Participants (mean age ± SD, y)	ON/OFF medication (UPDRS III)	Disease duration (years) or (months)°	L-dopa equivalent dose (mg)	Cognitive decline	SAI	Main findings	Interpretation
						ISI		
Nelson et al. (2018)	10 PD (61 ± 8) 11 HC (52.3 ± 10.4)	ON (12.2 ± 9.8) OFF (19.8 ± 7.9)	5.9 ± 3.42	614.2 ± 179	NA	N20+3	Normal SAI in ON and OFF in both side	PD demonstrates reduced activation of S1 (fMRI) and long sensorimotor integration (LAI)
Dubbioso et al. (2017a)	11 PD (62.3 ± 2.2) 8 LRRK2-PD (61.96 ± 3.9) 10 HC (59.4 ± 1.6)	PD-ON (23.4 ± 4.7) LRRK2-PD-ON (19.8 ± 7.9)	PD-ON (8.6 ± 1.2) LRRK2-PD-ON (8.4 ± 2.1)	PD-ON (838.1 ± 117.1) LRRK2-PD-ON (1015.9 ± 231.2)	NA	N20+2 to +8 ms (2 ms Δ)	Normal SAI	LRRK2-PD exhibits normal fast sensorimotor integration, but reduced motor cortex plasticity
Ponzo et al. (2017)	10 PD (65.7 ± 9,8) 8 LRRK2-PD (64.2 ± 8.3) 10 HC (63.5 ± 4.0)	PD-ON (9.5 ± 2.7) PD-OFF (24.2 ± 2.9) LRRK2-PD-ON (11.5 ± 4.2) LRRK2-PD-OFF (26.0 ± 9.3)	PD (7.4 ± 4.2) LRRK2-PD (8.5 ± 5)	PD (620 ± 87.1) LRRK2-PD (557.8 ± 53.4)	NA	N20-4 to +8 ms (4 ms Δ)	Normal SAI	LRRK2-PD exhibits normal fast sensorimotor integration, but increased motor cortex plasticity and disinhibition.
Picillo et al. (2015)	14 PD with FOG (63 ± 12) 10 PD without FOG (65 ± 10) 11 HC (62.4 ± 6.2)	PD-ON with FOG (17 ± 12) PD-ON without FOG (13.5 ± 8)	PD-ON with FOG (6.5 ± 4) PD-ON without FOG (5 ± 2)	PD-ON with FOG (1022.5 ± 771.2) PD-ON without FOG (560 ± 255)	MCI Level I in PD with FOG (71.4%) and without FOG (10%)*	N20+2 to +8 ms (2 ms Δ)	Normal SAI	Normal SAI in PD patients with FOG
Zamir et al. (2012)	12 PD (64.7 ± 10.3) 10 HC (63.1 ± 8.8)	PD-ON (13.6 ± 5.1) PD-OFF (23.1 ± 9.1)	7.3 ± 3.2	767.9 ± 484.3	Normal	N20+3	SAI is not modulated by iTBS	iTBS produces similar effects on cortical excitability for PD and controls
Degardin et al. (2012)	11 PD ON (61.5 ± 8.5) 8 PD OFF (61.3 ± 9.6) 10 PD *de novo* (60.6 ± 11.8) 11 PD ON-sham (61.5 ± 9.9)	PD-ON (17.4 ± 8.1) PD-OFF (29.3 ± 8.6) PD *de novo* (13.6 ± 4.5) PD-ON sham (19.5 ± 11.6)	PD-ON (6.8 ± 2.7) PD-OFF (6.2 ± 2.5) PD *de novo* (1.8 ± 1) PD-ON sham (8.2 ± 5.2)	PD-ON (785 ± 418) PD-OFF (646 ± 282) PD *de novo* (0) PD-ON sham (754 ± 485)	NA	N20	SAI is not modulated by iTBS	iTBS might improve both akinesia and sensory processing in patients with PD taking levodopa
Nardone et al. (2005)	8 PSP (68.2 ± 10.5) 10 PD (66.5 ± 11.8) 15 HC (NA)	PSP-OFF (36.4 ± 24.8) PD-OFF (39.7 ± 17.2)	8 PSP (22.4 ± 10.5)° 10 PD (19.1 ± 9.2)° 15 HC (NA)	8 PSP (68.2 ± 10.5) 10 PD (66.5 ± 11.8) 15 HC (NA)	Dementia in 60% of PD and in 50% of PSP (DSM-III criteria)	N20+2 to +8 ms (1 ms Δ)	↑ SAI in PD Normal SAI in PSP and HC	Different cholinergic dysfunction between PSP and PD
Di Lazzaro et al. (2004)	3 PD *de novo* (67.3 ± 9.1) 12 HC (73.1 ± 5.4)	PD-OFF affected side (8.7 ± 4.6)	NA	NA	NA	N20+2 to +8 ms (1 ms Δ)	↑ SAI more affected side compared to the less affected side and HC	SAI is enhanced in the more affected side in PD-OFF medication

*iTBS, intermittent theta-burst-stimulation; NA, not applicable; PD, Parkinson's Disease; HC, healthy control; FOG, freezing of gait; PSP, progressive supranuclear palsy; MMSE, mini mental state examination; MoCA, Montreal Cognitive Assessment; MCI, mild cognitive impairment; *MCI criteria according to the Level I of the MDS (Movement Disorder Society) commissioned Task Force (Litvan et al., 2012).*

2005). The enhancement of SAI in the affected side might be related to an increase of cholinergic muscarinic activity in the contralateral cerebral cortex. Altered muscarinic cortical activity in PD is also supported by several post-mortem studies that have shown an increase in the total number of muscarinic cholinergic receptors in the cerebral cortex (Ruberg et al., 1982; Sirviö et al., 1989; Lange et al., 1993).

An intriguing and alternative hypothesis might be that a reduced thalamo-cortical drive caused by nigrostriatal dopaminergic denervation may increase SAI, an effect which might be obscured by chronic dopamine replacing therapy.

In 2003, Sailer et al. (2003) systematically examined the effect of dopaminergic therapy in 10 PD patients on and off medication. Patients only showed a reduction in SAI when they were on medication, and the medication-induced reduction in SAI only emerged on the more affected side. The medication-related SAI reduction can be restored acutely with STN-DBS (Sailer et al., 2007). This finding was largely confirmed by a recent meta-analysis which only found a consistent reduction in SAI across studies for PD patients on medication, but the attenuating effect of medication on SAI in PD was retrieved in the meta-analysis regardless of the affected side (Martin-Rodriguez and Mir, 2018). Moreover, the meta-analysis revealed an association between SAI changes and disease severity as well as cognitive deficits. Specifically, SAI impairment scaled with cognitive deficits in the four major cognitive domains, although the strongest association was found for visuospatial and executive deficits.

Prompted by these findings, we pooled SAI data from our database and three previous studies (Manganelli et al., 2009; Picillo et al., 2015; Dubbioso et al., 2017a). The pooled data set included measurements from 81 PD patients (57 men) with a mean age of 64.37 ± 7.57 years, average disease duration of 8.41 ± 4.61 years, mean ON UPDRS-III score of 15.48 ± 10.89, and a daily L-dopa equivalent dose of 833.55 ± 470.70 mg. SAI was tested in all patient on the more affected side while they were taking their normal medication. SAI measurements covered five interstimulus intervals adjusted to the individual N20 wave latency (N20+0 ms, N20+2 ms, N20+4 ms, N20+6 ms, N20+8 ms). Patient's UPDRS III motor score in the ON medication state was the only variable that showed a positive linear correlation with SAI at an ISI of N20+4 ms ($\rho = 0.405$; $p < 0.01$) and with the mean SAI across all five interstimulus intervals ($\rho = 0.401$; $p < 0.01$, **Figures 1A,B**). Indeed, neither disease duration nor daily dopaminergic medication showed a significant relationship with SAI (all $p \geq 0.105$). Overall, the results suggest that the attenuating effect of medication state on SAI is more pronounced in patients in whom dopamine replacement therapy shows limited efficacy to normalize parkinsonian motor symptoms as indicated by high UPDRS scores in the on-medication state. It is conceivable that patients who show a less favorable

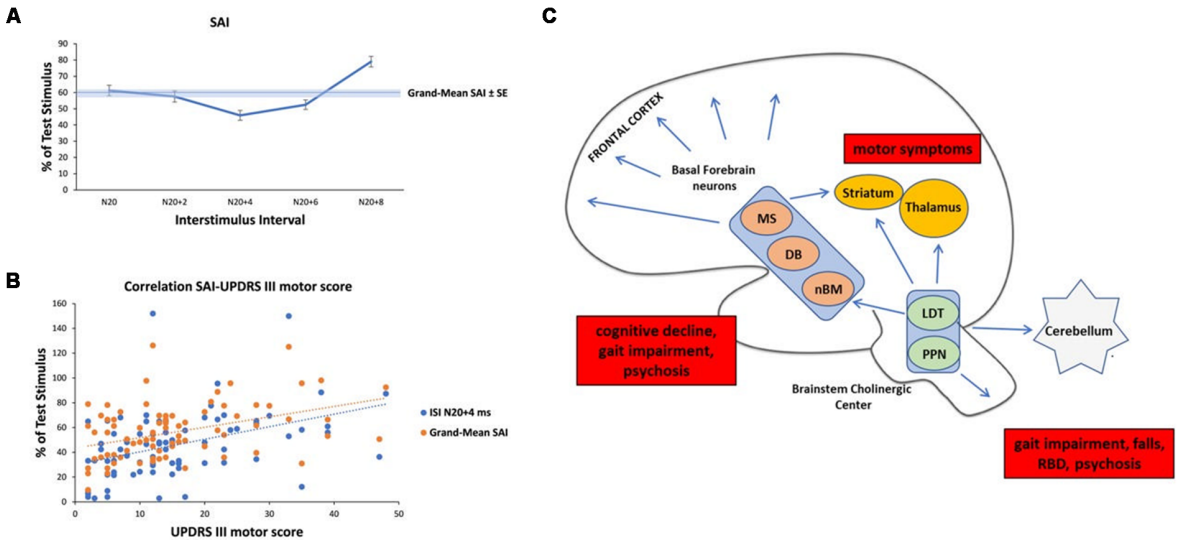

FIGURE 1 | Analysis of short-latency afferent inhibition (SAI) in our Parkinson's Disease (PD) cohort and schematic representation of cholinergic sources in the human brain with their clinical correlates in PD. **(A)** Temporal evolution of SAI in our cohort of PD patients. The horizontal axis shows inter-stimulus interval (ISI) values (the time between the peripheral stimulation and cortical stimulation). ISIs were determined by adding 0, 2, 4, 6, and 8 ms to the latency of the N20 component. The vertical axis shows the percentage of test motor evoked potential (MEP) at each ISI. **(B)** Linear positive correlation between SAI at ISI N20+4 ms, Grand-Mean SAI and UPDRS III motor score in medicated patients. **(C)** Schematic representation of the three major sources of cholinergic projections in the brain and main clinical correlates in PD (red boxes). Basal forebrain neurons, including the nucleus basalis of Meynert (nbM), medial septal nucleus (MS) and diagonal band of Broca (DB) provide the cholinergic projections to the cerebral cortex and are responsible for cognitive impairment, gait impairment and psychosis. The pedunculopontine nucleus-laterodorsal tegmental complex [referred to as the pedunculopontine tegmental nucleus (PPN) and LDT], a brainstem center, provides cholinergic inputs primarily to the thalamus, but also has connections to the cerebellum, several brainstem nuclei, some striatal fibers, and the spinal cord. This system is mainly involved in walking disturbances, rem-sleep behavior disorders (RBDs) and psychosis. In addition, small populations of intrinsic cholinergic neurons are present in the hippocampus, striatum (cholinergic interneurons), parts of the reticular formation, and cerebellum. The cholinergic interneurons might be the main cause of motor symptoms in PD.

response to dopamine replacement therapy may also have more cholinergic deficits and hence the reduction in SAI may, at least in part, resulting from a co-existing cholinergic deficit at the cortical level. Interestingly, patients with atypical parkinsonism (i.e., Progressive Supranuclear Palsy or Multisystemic Atrophy) that usually respond insufficiently to dopaminergic medication, might exhibit reduced levels of SAI (Brusa et al., 2014; Celebi et al., 2014).

DOES SAI IN PD SCALE WITH GAIT PROBLEMS AND NON-MOTOR SYMPTOMS?

PD causes a wide range of non-motor symptoms which may even precede the manifestation of the classic motor symptoms (Riedel et al., 2010). Non-motor symptoms include cognitive dysfunctions and decline, apathy, psychiatric disturbances (depression, psychosis, impulse control), autonomic failure (gastrointestinal, cardiovascular, urinary, sexual ability, thermoregulation), sleep disorders, and pain syndrome (Chaudhuri and Schapira, 2009). In recent years, SAI has been increasingly used in PD to identify whether specific **motor and non-motor symptoms** scale with abnormalities in SAI, presumably due to cholinergic and dopaminergic cortical dysfunction.

KEY CONCEPT 4 | Motor and non-motor symptoms

Sources of considerable burden in people with PD are the typical motor symptoms, such as resting tremor, rigidity, bradykinesia, postural instability and non-motor symptoms, namely cognitive declines, psychiatric disturbances, autonomic failures, sleep difficulties, and pain syndrome. These symptoms are variously associated with dopaminergic/cholinergic neurodegeneration and SAI alteration at the cortical level.

Among motor disturbances, gait abnormalities and falls have attracted attention for their association with cognitive decline and cholinergic dysfunction in PD (Newman et al., 2012; Perez-Lloret and Barrantes, 2016). Indeed, reduced SAI has been proven to be an independent predictor of slower gait speed (Rochester et al., 2012) and associated with a higher falls risk in PD (Pelosin et al., 2016). However, in a recent study performed on PD with freezing of gait (FOG; Picillo et al., 2015) the authors failed to prove alteration of SAI in this subtype of patients. Since gait disturbances in PD are heterogeneous and may be underpinned by different neurotransmitters and circuits, it is to be expected that the relation between SAI and gait deficits may be complex and the modulatory role of medication state also needs to be factored in when addressing this issue.

Regarding non-motor symptoms, SAI abnormalities have been found associated with dementia and Mild Cognitive Impairment (MCI; Celebi et al., 2012; Yarnall et al., 2013), confirming the role of cholinergic dysfunction in the development of cognitive impairment in PD. Indeed, SAI has been found to be reduced in PD patients with those symptoms associated with a higher risk of cognitive decline, such as visual hallucinations (VH; Manganelli et al., 2009), dysphagia (Lee et al., 2015), olfactory dysfunction (Oh et al., 2017; Versace et al., 2017) and REM-sleep Behavior Disorders (RBDs; Nardone et al., 2013). These studies are in agreement with the idea that the cholinergic dysfunction makes a major contribution to non-motor symptoms and associated cognitive deficits in PD (Marra et al., 2012; Newman et al., 2012).

A recent review summarized central cholinergic sources of the healthy human brain in two main tracks (Newman et al., 2012). On the one hand, brainstem nuclei, including the pedunculopontine tegmental nucleus (PPN) and the laterodorsal pontine tegmentum, send cholinergic projections to the thalamus, basal ganglia, basal forebrain and to a much lesser extent, the cerebral cortex. On the other hand, the magnocellular basal forebrain-cholinergic systems, including the nucleus basalis magnocellularis and nucleus basalis of Meinert (NBM) send major projections to neocortex, entorhinal cortex, limbic cortices, cingulate cortex, and hippocampus. In addition, small populations of intrinsic cholinergic neurons are present in the hippocampus, striatum (cholinergic interneurons), parts of the reticular formation, and cerebellum (Bohnen and Albin, 2011; Manganelli et al., 2013; Dubbioso et al., 2015). These cholinergic nuclei and their projections have selectively degenerated in PD (Bohnen and Albin, 2011; Perez-Lloret and Barrantes, 2016). Thus, we speculate that SAI in PD may mainly reflect a cortical cholinergic deficit due to cholinergic neurodegeneration. The cortical cholinergic imbalance may derive from many sources that are variably impaired according to disease severity and symptoms. For example, degeneration of cholinergic striatal tone is responsible for motor symptoms, alteration of the NBM and/or PPN nuclei for gait impairment and falls, cognitive decline, RBD, psychosis (Perez-Lloret and Barrantes, 2016), see **Figure 1C**.

CONCLUSION AND OUTLOOK

In this review, we have discussed the possible contributions of the fast-afferent somatosensory pathway, the intracortical integrative component and the fast-efferent corticomotor pathway to alterations of SAI in PD. We concluded that PD-related changes in SAI are most likely caused at the cortical level, where sensory input is rapidly integrated into a motor output. This makes SAI a useful tool to probe how PD impacts on the sensorimotor integration processing at the cortical level.

Studies performed on PD patients have shown variable results, ranging from reduced to normal or even enhanced SAI findings. Several factors may be responsible for these heterogenous results such as between-group differences in disease severity, disease duration, dopamine replacement therapy and cognitive status. While patients with PD show normal levels of SAI in the off-medication state, SAI is reduced in the on-medication state, suggesting a role of dopamine replacement in driving this abnormality. Interestingly, previous research has suggested that dopaminergic medication could lead to decreases in central processing or integration of sensory signals in PD patients. For instance, it has been shown that dopaminergic medication could worsen SAI and proprioception (distal and spatial errors) and were normalized by chronic STN-DBS, likely through

long-term plastic changes in the basal ganglia thalamocortical circuit (Wagle Shukla et al., 2013). Yet, pharmacological studies which systematically study dose-dependent effects of dopamine replacement therapy on SAI magnitude in PD are still lacking. The positive relationship between residual parkinsonian motor symptoms and SAI suppression in the on-medication state suggests that the effect of dopamine replacement may be more detrimental to SAI in patients that are less responsive to dopaminergic pharmacotherapy, for instance, patients with more prominent cholinergic involvement. This would also explain why non-motor symptoms have been associated with a reduction of SAI in PD.

Some important aspects of SAI still remain to be explored in PD. For instance, by systematically varying the intensity of peripheral stimulation one may derive a stimulus-response curve of SAI that may be more sensitive to intrinsic disease-related but also therapy-related changes in SAI. Furthermore, the application of homotopic or heterotopic somatosensory stimulation may reveal interesting insights into the altered center-surround organization of fast sensorimotor integration at the cortical level (Dubbioso et al., 2017c).

Future research on SAI in PD should focus on validating SAI as a biomarker of central cholinergic activity through a multimodal approach by combining neurophysiological results with neuroimaging. For example, correlation analysis with structural data (i.e., analysis of gray matter volume, diffusion tensor imaging) of the main cholinergic system nuclei, would reveal a structure-function relationship between SAI changes and structural cholinergic denervation. The introduction of new PET radioligands, such as (18 F) fluoroethoxybenzoyesamicol [(18 F) FEOBV], a ligand which shows a high affinity for the vesicular acetylcholine transporter, will enable the researcher to simultaneously examine functional changes of the cholinergic system *in vivo*. This line of research will help to clarify the role of impaired cholinergic neurotransmission in the development of motor and non-motor symptoms in PD.

AUTHOR CONTRIBUTIONS

All authors prepared the manuscript draft and approved the final manuscript.

FUNDING

HS received support from Lundbeck Fonden (Grant of Excellence: Mapping, Modulation and Modelling the Control of Actions; Grant no. 59-A5399) and Novo Nordisk Fonden (Synergy grant "Biophysically Adjusted State-Informed Cortex Stimulation," NNF14OC0011413). HS holds a 5-year professorship in precision medicine at the Faculty of Health Sciences and Medicine, University of Copenhagen which is sponsored by the Lundbeck Foundation (R186-2015-2138). HS has received honoraria as speaker from Sanofi Genzyme, Denmark and Novartis, Denmark, as consultant from Sanofi Genzyme, Denmark and as senior editor (NeuroImage) from Elsevier Publishers, Amsterdam, Netherlands. He has received royalties as book editor from Springer Publishers, Stuttgart, Germany. The funders had no role in study design, data collection and analysis, decision to publish, or preparation of the manuscript.

REFERENCES

Alkondon, M., Pereira, E. F., Eisenberg, H. M., and Albuquerque, E. X. (2000). Nicotinic receptor activation in human cerebral cortical interneurons: a mechanism for inhibition and disinhibition of neuronal networks. *J. Neurosci.* 20, 66–75. doi: 10.1523/jneurosci.20-01-00066.2000

Asmussen, M. J., Jacobs, M. F., Lee, K. G. H., Zapallow, C. M., and Nelson, A. J. (2013). Short-latency afferent inhibition modulation during finger movement. *PLoS One* 8:e60496. doi: 10.1371/journal.pone.0060496

Bailey, A. Z., Asmussen, M. J., and Nelson, A. J. (2016). Short-latency afferent inhibition determined by the sensory afferent volley. *J. Neurophysiol.* 116, 637–644. doi: 10.1152/jn.00276.2016

Barone, P. (2010). Neurotransmission in Parkinson's disease: beyond dopamine. *Eur. J. Neurol.* 17, 364–376. doi: 10.1111/j.1468-1331.2009.02900.x

Boecker, H., Ceballos-Baumann, A., Bartenstein, P., Weindl, A., Siebner, H. R., Fassbender, T., et al. (1999). Sensory processing in Parkinson's and Huntington's disease: investigations with 3D H215O-PET. *Brain* 122, 1651–1665. doi: 10.1093/brain/122.9.1651

Bohnen, N. I., and Albin, R. L. (2011). The cholinergic system and Parkinson's Disease. *Behav. Brain Res.* 221, 564–573. doi: 10.1016/j.bbr.2009.12.048

Brown, P., Oliviero, A., Mazzone, P., Insola, A., Tonali, P., and Di Lazzaro, V. (2001). Dopamine dependency of oscillations between subthalamic nucleus and pallidum in Parkinson's disease. *J. Neurosci.* 21, 1033–1038. doi: 10.1523/jneurosci.21-03-01033.2001

Brusa, L., Ponzo, V., Mastropasqua, C., Picazio, S., Bonnì, S., Di Lorenzo, F., et al. (2014). Theta burst stimulation modulates Cerebellar-cortical connectivity in patients with progressive supranuclear palsy. *Brain Stimul.* 7, 29–35. doi: 10.1016/j.brs.2013.07.003

Cantone, M., Di Pino, G., Capone, F., Piombo, M., Chiarello, D., Cheeran, B., et al. (2014). The contribution of transcranial magnetic stimulation in the diagnosis and in the management of dementia. *Clin. Neurophysiol.* 125, 1509–1532. doi: 10.1016/j.clinph.2014.04.010

Caviness, J. N., Driver-Dunckley, E., Connor, D. J., Sabbagh, M. N., Hentz, J. G., Noble, B., et al. (2007). Defining mild cognitive impairment in Parkinson's disease. *Mov. Disord.* 22, 1272–1277. doi: 10.1002/mds.21453

Celebi, O., Temuçin, C. M., Elibol, B., and Saka, E. (2012). Short latency afferent inhibition in Parkinson's disease patients with dementia. *Mov. Disord.* 27, 1052–1055. doi: 10.1002/mds.25040

Celebi, O., Temuçin, Ç. M., Elibol, B., and Saka, E. (2014). Cognitive profiling in relation to short latency afferent inhibition of frontal cortex in multiple system atrophy. *Parkinsonism Relat. Disord.* 20, 632–636. doi: 10.1016/j.parkreldis.2014.03.012

Chaudhuri, K. R., and Schapira, A. H. (2009). Non-motor symptoms of Parkinson's disease: dopaminergic pathophysiology and treatment. *Lancet Neurol.* 8, 464–474. doi: 10.1016/S1474-4422(09)70068-7

Cheron, G., Piette, T., Thiriaux, A., Jacquy, J., and Godaux, E. (1994). Somatosensory evoked potentials at rest and during movement in Parkinson's disease: evidence for a specific apomorphine effect on the frontal N30 wave. *Electroencephalogr. Clin. Neurophysiol.* 92, 491–501. doi: 10.1016/0168-5597(94)90133-3

Cho, H. J., Panyakaew, P., Thirugnanasambandam, N., Wu, T., and Hallett, M. (2016). Dynamic modulation of corticospinal excitability and short-latency afferent inhibition during onset and maintenance phase of selective finger movement. *Clin. Neurophysiol.* 127, 2343–2349. doi: 10.1016/j.clinph.2016.02.020

Classen, J., Steinfelder, B., Liepert, J., Stefan, K., Celnik, P., Cohen, L. G., et al. (2000). Cutaneomotor integration in humans is somatotopically organized at various levels of the nervous system and is task dependent. *Exp. Brain Res.* 130, 48–59. doi: 10.1007/s002210050005

Cohen, L. G., and Starr, A. (1987). Localization, timing and specificity of gating of somatosensory evoked potentials during active movement in man. *Brain* 110, 451–467. doi: 10.1093/brain/110.2.451

Conte, A., Khan, N., Defazio, G., Rothwell, J. C., and Berardelli, A. (2013). Pathophysiology of somatosensory abnormalities in Parkinson's Disease. *Nat. Rev. Neurol.* 9, 687–697. doi: 10.1038/nrneurol.2013.224

Degardin, A., Devos, D., Defebvre, L., Destée, A., Plomhause, L., Derambure, P., et al. (2012). Effect of intermittent theta-burst stimulation on akinesia and sensorimotor integration in patients with Parkinson's disease. *Eur. J. Neurosci.* 36, 2669–2678. doi: 10.1111/j.1460-9568.2012.08158.x

Demirci, M., Grill, S., McShane, L., and Hallett, M. (1997). A mismatch between kinesthetic and visual perception in Parkinson's disease. *Ann. Neurol.* 41, 781–788. doi: 10.1002/ana.410410614

Di Cara, B., Panayi, F., Gobert, A., Dekeyne, A., Sicard, D., De Groote, L., et al. (2007). Activation of dopamine D1 receptors enhances cholinergic transmission and social cognition: a parallel dialysis and behavioural study in rats. *Int. J. Neuropsychopharmacol.* 10, 383–399. doi: 10.1017/s1461145706007103

Di Lazzaro, V., Oliviero, A., Pilato, F., Saturno, E., Dileone, M., Marra, C., et al. (2005a). Neurophysiological predictors of long term response to AChE inhibitors in AD patients. *J. Neurol. Neurosurg. Psychiatry* 76, 1064–1069. doi: 10.1136/jnnp.2004.051334

Di Lazzaro, V., Oliviero, A., Saturno, E., Dileone, M., Pilato, F., Nardone, R., et al. (2005b). Effects of lorazepam on short latency afferent inhibition and short latency intracortical inhibition in humans. *J. Physiol.* 564, 661–668. doi: 10.1113/jphysiol.2004.061747

Di Lazzaro, V., Pilato, F., Dileone, M., Tonali, P. A., and Ziemann, U. (2005c). Dissociated effects of diazepam and lorazepam on short-latency afferent inhibition. *J. Physiol.* 569, 315–323. doi: 10.1113/jphysiol.2005.092155

Di Lazzaro, V., Oliviero, A., Tonali, P. A., Marra, C., Daniele, A., Profice, P., et al. (2002). Noninvasive *in vivo* assessment of cholinergic cortical circuits in AD using transcranial magnetic stimulation. *Neurology* 59, 392–397. doi: 10.1212/wnl.59.3.392

Di Lazzaro, V., Oliviero, A., Pilato, F., Saturno, E., Dileone, M., Bentivoglio, A. R., et al. (2004). Normal or enhanced short-latency afferent inhibition in Parkinson's disease? *Brain* 127:E8; author reply E9. doi: 10.1093/brain/awh089

Di Lazzaro, V., Oliviero, A., Profice, P., Pennisi, M. A., Di Giovanni, S., Zito, G., et al. (2000). Muscarinic receptor blockade has differential effects on the excitability of intracortical circuits in the human motor cortex. *Exp. Brain Res.* 135, 455–461. doi: 10.1007/s002210000543

Di Lazzaro, V., Pilato, F., Dileone, M., Profice, P., Ranieri, F., Ricci, V., et al. (2007). Segregating two inhibitory circuits in human motor cortex at the level of GABAA receptor subtypes: a TMS study. *Clin. Neurophysiol.* 118, 2207–2214. doi: 10.1016/j.clinph.2007.07.005

Di Lazzaro, V., Pilato, F., Dileone, M., Saturno, E., Oliviero, A., Marra, C., et al. (2006). *In vivo* cholinergic circuit evaluation in frontotemporal and Alzheimer dementias. *Neurology* 66, 1111–1113. doi: 10.1212/01.wnl.0000204183.26231.23

Di Lazzaro, V., and Ziemann, U. (2013). The contribution of transcranial magnetic stimulation in the functional evaluation of microcircuits in human motor cortex. *Front. Neural Circuits* 7:18. doi: 10.3389/fncir.2013.00018

Di Martino, A., Scheres, A., Margulies, D. S., Kelly, A. M. C., Uddin, L. Q., Shehzad, Z., et al. (2008). Functional connectivity of human striatum: a resting state fMRI study. *Cereb. Cortex* 18, 2735–2747. doi: 10.1093/cercor/bhn041

Dickson, D. W. (2012). Parkinson' s disease and Parkinsonism: neuropathology. *Cold Spring Harb. Perspect. Med.* 2:a009258. doi: 10.1101/cshperspect.a009258

Dubbioso, R., de Rosa, A., Esposito, M., Peluso, S., Iodice, R., de Michele, G., et al. (2017a). Does motor cortex plasticity depend on the type of mutation in the leucine-rich repeat kinase 2 gene? *Mov. Disord.* 32, 947–948. doi: 10.1002/mds.27012

Dubbioso, R., Esposito, M., Peluso, S., Iodice, R., De Michele, G., Santoro, L., et al. (2017b). Disruption of $GABA_A$-mediated intracortical inhibition in patients with chorea-acanthocytosis. *Neurosci. Lett.* 654, 107–110. doi: 10.1016/j.neulet.2017.06.032

Dubbioso, R., Raffin, E., Karabanov, A., Thielscher, A., and Siebner, H. R. (2017c). Centre-surround organization of fast sensorimotor integration in human motor hand area. *Neuroimage* 158, 37–47. doi: 10.1016/j.neuroimage.2017.06.063

Dubbioso, R., Pellegrino, G., Antenora, A., De Michele, G., Filla, A., Santoro, L., et al. (2015). The effect of cerebellar degeneration on human sensori-motor plasticity. *Brain Stimul.* 8, 1144–1150. doi: 10.1016/j.brs.2015.05.012

Guerra, A., Pogosyan, A., Nowak, M., Tan, H., Ferreri, F., Di Lazzaro, V., et al. (2016). Phase dependency of the human primary motor cortex and cholinergic inhibition cancelation during β tACS. *Cereb. Cortex* 26, 3977–3990. doi: 10.1093/cercor/bhw245

Gulledge, A. T., and Stuart, G. J. (2005). Cholinergic inhibition of neocortical pyramidal neurons. *J. Neurosci.* 25, 10308–10320. doi: 10.1523/jneurosci.2697-05.2005

Haber, S. N., and Calzavara, R. (2009). The cortico-basal ganglia integrative network: the role of the thalamus. *Brain Res. Bull.* 78, 69–74. doi: 10.1016/j.brainresbull.2008.09.013

Hillen, M. E., and Sage, J. I. (1996). Nonmotor fluctuations in patients with Parkinson's disease. *Neurology* 47, 1180–1183. doi: 10.1212/WNL.47.5.1180

Hutchison, W. D., Allan, R. J., Opitz, H., Levy, R., Dostrovsky, J. O., Lang, A. E., et al. (1998). Neurophysiological identification of the subthalamic nucleus in surgery for Parkinson's disease. *Ann. Neurol.* 44, 622–628. doi: 10.1002/ana.410440407

Insola, A., Le Pera, D., Restuccia, D., Mazzone, P., and Valeriani, M. (2004). Reduction in amplitude of the subcortical low- and high-frequency somatosensory evoked potentials during voluntary movement: an intracerebral recording study. *Clin. Neurophysiol.* 115, 104–111. doi: 10.1016/j.clinph.2003.08.003

Jobst, E. E., Melnick, M. E., Byl, N. N., Dowling, G. A., and Aminoff, M. J. (1997). Sensory perception in Parkinson's Disease. *Arch. Neurol.* 54, 450–454. doi: 10.1001/archneur.1997.00550160080020

Kleine, B. U., Praamstra, P., Stegeman, D. F., and Zwarts, M. J. (2001). Impaired motor cortical inhibition in Parkinson's disease: motor unit responses to transcranial magnetic stimulation. *Exp. Brain Res.* 138, 477–483. doi: 10.1007/s002210100731

Klockgether, T., Borutta, M., Rapp, H., Spieker, S., and Dichgans, J. (1995). A defect of kinesthesia in Parkinson's disease. *Mov. Disord.* 10, 460–465. doi: 10.1002/mds.870100410

Kojovic, M., Bologna, M., Kassavetis, P., Murase, N., Palomar, F. J., Berardelli, A., et al. (2012). Functional reorganization of sensorimotor cortex in early Parkinson's Disease. *Neurology* 78, 1441–1448. doi: 10.1212/wnl.0b013e318253d5dd

Künzle, H. (1977). Projections from the primary somatosensory cortex to basal ganglia and thalamus in the monkey. *Exp. Brain Res.* 30, 481–492. doi: 10.1007/bf00237639

Kuo, H. I., Paulus, W., Batsikadze, G., Jamil, A., Kuo, M. F., and Nitsche, M. A. (2017). Acute and chronic noradrenergic effects on cortical excitability in healthy humans. *Int. J. Neuropsychopharmacol.* 20, 634–643. doi: 10.1093/ijnp/pyx026

Lange, K. W., Wells, F. R., Jenner, P., and Marsden, C. D. (1993). Altered muscarinic and nicotinic receptor densities in cortical and subcortical brain regions in Parkinson's disease. *J. Neurochem.* 60, 197–203. doi: 10.1111/j.1471-4159.1993.tb05838.x

Lee, K. D., Koo, J. H., Song, S. H., Jo, K. D., Lee, M. K., and Jang, W. (2015). Central cholinergic dysfunction could be associated with oropharyngeal dysphagia in early Parkinson's disease. *J. Neural Transm.* 122, 1553–1561. doi: 10.1007/s00702-015-1427-z

Lidsky, T. I., Manetto, C., and Schneider, J. S. (1985). A consideration of sensory factors involved in motor functions of the basal ganglia. *Brain Res. Rev.* 9, 133–146. doi: 10.1016/0165-0173(85)90010-4

Litvan, I., Goldman, J. G., Tröster, A. I., Schmand, B. A., Weintraub, D., Petersen, R. C., et al. (2012). Diagnostic criteria for mild cognitive impairment in Parkinson's disease: Movement Disorder Society Task Force guidelines. *Mov. Disord.* 27, 349–356. doi: 10.1002/mds.24893

Macerollo, A., Brown, M. J. N., Kilner, J. M., and Chen, R. (2018). Neurophysiological changes measured using somatosensory evoked potentials. *Trends Neurosci.* 41, 294–310. doi: 10.1016/j.tins.2018.02.007

Macerollo, A., Chen, J. C., Korlipara, P., Foltynie, T., Rothwell, J., Edwards, M. J., et al. (2016). Dopaminergic treatment modulates sensory attenuation at the onset of the movement in Parkinson's disease: a test of a new

framework for bradykinesia. *Mov. Disord.* 31, 143–146. doi: 10.1002/mds.26493

Magill, P. J., Bolam, J. P., and Bevan, M. D. (2001). Dopamine regulates the impact of the cerebral cortex on the subthalamic nucleus-globus pallidus network. *Neuroscience* 106, 313–330. doi: 10.1016/s0306-4522(01)00281-0

Manganelli, F., Dubbioso, R., Iodice, R., Topa, A., Dardis, A., Russo, C. V., et al. (2014). Central cholinergic dysfunction in the adult form of Niemann Pick disease type C: a further link with Alzheimer's disease? *J. Neurol.* 261, 804–808. doi: 10.1007/s00415-014-7282-2

Manganelli, F., Dubbioso, R., Pisciotta, C., Antenora, A., Nolano, M., De Michele, G., et al. (2013). Somatosensory temporal discrimination threshold is increased in patients with cerebellar atrophy. *Cerebellum* 12, 456–459. doi: 10.1007/s12311-012-0435-x

Manganelli, F., Vitale, C., Santangelo, G., Pisciotta, C., Iodice, R., Cozzolino, A., et al. (2009). Functional involvement of central cholinergic circuits and visual hallucinations in Parkinsons disease. *Brain* 132, 2350–2355. doi: 10.1093/brain/awp166

Marra, C., Quaranta, D., Profice, P., Pilato, F., Capone, F., Iodice, F., et al. (2012). Central cholinergic dysfunction measured "*in vivo*" correlates with different behavioral disorders in Alzheimer's disease and dementia with Lewy body. *Brain Stimul.* 5, 533–538. doi: 10.1016/j.brs.2011.08.009

Martin-Rodriguez, J. F., and Mir, P. (2018). Short-afferent inhibition and cognitive impairment in Parkinson's disease: a quantitative review and challenges. *Neurosci. Lett.* doi: 10.1016/j.neulet.2018.06.048 [Epub ahead of print].

Martorana, A., Mori, F., Esposito, Z., Kusayanagi, H., Monteleone, F., Codecà, C., et al. (2009). Dopamine modulates cholinergic cortical excitability in Alzheimer's disease patients. *Neuropsychopharmacology* 34, 2323–2328. doi: 10.1038/npp.2009.60

Millan, M. J., Di Cara, B., Dekeyne, A., Panayi, F., De Groote, L., Sicard, D., et al. (2007). Selective blockade of dopamine D3 versus D2 receptors enhances frontocortical cholinergic transmission and social memory in rats: a parallel neurochemical and behavioural analysis. *J. Neurochem.* 100, 1047–1061. doi: 10.1111/j.1471-4159.2006.04262.x

Mima, T., Terada, K., Maekawa, M., Nagamine, T., Ikeda, A., and Shibasaki, H. (1996). Somatosensory evoked potentials following proprioceptive stimulation of finger in man. *Exp. Brain Res.* 111, 233–245. doi: 10.1007/bf00227300

Mirdamadi, J. L., Suzuki, L. Y., and Meehan, S. K. (2017). Attention modulates specific motor cortical circuits recruited by transcranial magnetic stimulation. *Neuroscience* 359, 151–158. doi: 10.1016/j.neuroscience.2017.07.028

Nardone, R., Bergmann, J., Brigo, F., Christova, M., Kunz, A., Seidl, M., et al. (2013). Functional evaluation of central cholinergic circuits in patients with Parkinson's disease and REM sleep behavior disorder: a TMS study. *J. Neural Transm.* 120, 413–422. doi: 10.1007/s00702-012-0888-6

Nardone, R., Bergmann, J., Kronbichler, M., De Blasi, P., Caleri, F., Tezzon, F., et al. (2010). Functional involvement of the cerebral cortex following paramedian bithalamic infarction. *Neurocase* 16, 286–292. doi: 10.1080/13554790903463593

Nardone, R., Florio, I., Lochner, P., and Tezzon, F. (2005). Cholinergic cortical circuits in Parkinson's disease and in progressive supranuclear palsy: a transcranial magnetic stimulation study. *Exp. Brain Res.* 163, 128–131. doi: 10.1007/s00221-005-2228-7

Nardone, R., Höller, Y., Thomschewski, A., Kunz, A. B., Lochner, P., Golaszewski, S., et al. (2014). Dopamine differently modulates central cholinergic circuits in patients with Alzheimer disease and CADASIL. *J. Neural Transm.* 121, 1313–1320. doi: 10.1007/s00702-014-1195-1

Nelson, A. J., Hoque, T., Gunraj, C., and Chen, R. (2018). Altered somatosensory processing in Parkinson's disease and modulation by dopaminergic medications. *Parkinsonism Relat. Disord.* 53, 76–81. doi: 10.1016/j.parkreldis.2018.05.002

Newman, E. L., Gupta, K., Climer, J. R., Monaghan, C. K., and Hasselmo, M. E. (2012). Cholinergic modulation of cognitive processing: insights drawn from computational models. *Front. Behav. Neurosci.* 6:24. doi: 10.3389/fnbeh.2012.00024

Oh, E., Park, J., Youn, J., Kim, J. S., Park, S., and Jang, W. (2017). Olfactory dysfunction in early Parkinson's disease is associated with short latency afferent inhibition reflecting central cholinergic dysfunction. *Clin. Neurophysiol.* 128, 1061–1068. doi: 10.1016/j.clinph.2017.03.011

Oliviero, A., León, A. M., Holler, I., Vila, J. F., Siebner, H. R., Della Marca, G., et al. (2005). Reduced sensorimotor inhibition in the ipsilesional motor cortex in a patient with chronic stroke of the paramedian thalamus. *Clin. Neurophysiol.* 116, 2592–2598. doi: 10.1016/j.clinph.2005.07.015

Pallis, C. A. (1971). Parkinsonism—natural history and clinical features. *Br. Med. J.* 3, 683–690. doi: 10.1136/bmj.3.5776.683

Pelosin, E., Ogliastro, C., Lagravinese, G., Bonassi, G., Mirelman, A., Hausdorff, J. M., et al. (2016). Attentional control of gait and falls: is cholinergic dysfunction a common substrate in the elderly and Parkinson's disease? *Front. Aging Neurosci.* 8:104. doi: 10.3389/fnagi.2016.00104

Petersen, R. C., and Morris, J. C. (2005). Mild Cognitive Impairment as a Clinical Entity and Treatment Target. *Arch. Neurol.* 62, 1160–1163. doi: 10.1001/archneur.62.7.1160

Perez-Lloret, S., and Barrantes, F. J. (2016). Deficits in cholinergic neurotransmission and their clinical correlates in Parkinson's disease. *NPJ Park. Dis.* 2:16001. doi: 10.1038/npjparkd.2016.1

Picillo, M., Dubbioso, R., Iodice, R., Iavarone, A., Pisciotta, C., Spina, E., et al. (2015). Short-latency afferent inhibition in patients with Parkinson's disease and freezing of gait. *J. Neural Transm.* 122, 1533–1540. doi: 10.1007/s00702-015-1428-y

Ponzo, V., Di Lorenzo, F., Brusa, L., Schirinzi, T., Battistini, S., Ricci, C., et al. (2017). Impaired intracortical transmission in G2019S leucine rich-repeat kinase Parkinson patients. *Mov. Disord.* 32, 750–756. doi: 10.1002/mds.26931

Praamstra, P., and Plat, F. M. (2001). Failed suppression of direct visuomotor activation in Parkinson's disease. *J. Cogn. Neurosci.* 13, 31–43. doi: 10.1162/089892901564153

Quartarone, A., Rizzo, V., Bagnato, S., Morgante, F., Sant'Angelo, A., Girlanda, P., et al. (2006). Rapid-rate paired associative stimulation of the median nerve and motor cortex can produce long-lasting changes in motor cortical excitability in humans. *J. Physiol.* 575, 657–670. doi: 10.1113/jphysiol.2006.114025

Restuccia, D., Valeriani, M., Barba, C., Le Pera, D., Tonali, P., and Mauguière, F. (1999). Different contribution of joint and cutaneous inputs to early scalp somatosensory evoked potentials. *Muscle Nerve* 22, 910–919. doi: 10.1002/(sici)1097-4598(199907)22:7<910::aid-mus15>3.0.co;2-v

Riedel, O., Klotsche, J., Spottke, A., Deuschl, G., Förstl, H., Henn, F., et al. (2010). Frequency of dementia, depression and other neuropsychiatric symptoms in 1,449 outpatients with Parkinson's disease. *J. Neurol.* 257, 1073–1082. doi: 10.1007/s00415-010-5465-z

Rizzo, V., Aricò, I., Liotta, G., Ricciardi, L., Mastroeni, C., Morgante, F., et al. (2010). Impairment of sensory-motor integration in patients affected by RLS. *J. Neurol.* 257, 1979–1985. doi: 10.1007/s00415-010-5644-y

Rochester, L., Yarnall, A. J., Baker, M. R., David, R. V., Lord, S., Galna, B., et al. (2012). Cholinergic dysfunction contributes to gait disturbance in early Parkinson's disease. *Brain* 135, 2779–2788. doi: 10.1093/brain/aws207

Rodriguez-Oroz, M. C., Rodriguez, M., Guridi, J., Mewes, K., Chockkman, V., Vitek, J., et al. (2001). The subthalamic nucleus in Parkinson's disease: somatotopic organization and physiological characteristics. *Brain* 124, 1777–1790. doi: 10.1055/b-0034-89968

Rossini, P. M., Babiloni, F., Bernardi, G., Cecchi, L., Johnson, P. B., Malentacca, A., et al. (1989). Abnormalities of short-latency somatosensory evoked potentials in parkinsonian patients. *Electroencephalogr. Clin. Neurophysiol.* 74, 277–289. doi: 10.1016/0168-5597(89)90058-0

Ruberg, M., Ploska, A., Javoy-Agid, F., and Agid, Y. (1982). Muscarinic binding and choline acetyltransferase activity in Parkinsonian subjects with reference to dementia. *Brain Res.* 232, 129–139. doi: 10.1016/0006-8993(82)90615-1

Rubin, J. E., and Terman, D. (2004). High frequency stimulation of the subthalamic nucleus eliminates pathological thalamic rhythmicity in a computational model. *J. Comput. Neurosci.* 16, 211–235. doi: 10.1023/b:jcns.0000025686.47117.67

Sailer, A., Cunic, D. I., Paradiso, G. O., Gunraj, C. A., Wagle-Shukla, A., Moro, E., et al. (2007). Subthalamic nucleus stimulation modulates afferent inhibition in Parkinson's Disease. *Neurology* 68, 356–363. doi: 10.1212/01.wnl.0000252812.95774.aa

Sailer, A., Molnar, G. F., Paradiso, G., Gunraj, C. A., Lang, A. E., and Chen, R. (2003). Short and long latency afferent inhibition in Parkinson's disease. *Brain* 126, 1883–1894. doi: 10.1093/brain/awg183

Schneider, J. S., Diamond, S. G., and Markham, C. H. (1987). Parkinson's disease: sensory and motor problems in arms and hands. *Neurology* 37, 951–956. doi: 10.1212/wnl.37.6.951

Seiss, E., and Praamstra, P. (2004). The basal ganglia and inhibitory mechanisms in response selection: evidence from subliminal priming of motor responses in Parkinson's disease. *Brain* 127, 330–339. doi: 10.1093/brain/awh043

Seki, K., and Fetz, E. E. (2012). Gating of sensory input at spinal and cortical levels during preparation and execution of voluntary movement. *J. Neurosci.* 32, 890–902. doi: 10.1523/JNEUROSCI.4958-11.2012

Sirviö, J., Rinne, J. O., Valjakka, A., Rinne, U. K., Riekkinen, P. J., and Paljärvi, L. (1989). Different forms of brain acetylcholinesterase and muscarinic binding in Parkinson's disease. *J. Neurol. Sci.* 90, 23–32. doi: 10.1016/0022-510x(89)90042-7

Snider, S. R., Fahn, S., Isgreen, W. P., and Cote, L. J. (1976). Primary sensory symptoms in parkinsonism. *Neurology* 26, 423–429. doi: 10.1212/wnl.26.5.423

Suzuki, L. Y., and Meehan, S. K. (2018). Verbal working memory modulates afferent circuits in motor cortex. *Eur. J. Neurosci.* 48, 3117–3125. doi: 10.1111/ejn.14154

Theodosopoulos, P. V., Marks, W. J. Jr., Christine, C., and Starr, P. A. (2003). Locations of movement-related cells in the human subthalamic nucleus in Parkinson's disease. *Mov. Disord.* 18, 791–798. doi: 10.1002/mds.10446

Tokimura, H., Di Lazzaro, V., Tokimura, Y., Oliviero, A., Profice, P., Insola, A., et al. (2000). Short latency inhibition of human hand motor cortex by somatosensory input from the hand. *J. Physiol.* 523, 503–513. doi: 10.1111/j.1469-7793.2000.t01-1-00503.x

Tsang, P., Bailey, A. Z., and Nelson, A. J. (2015). Rapid-rate paired associative stimulation over the primary somatosensory cortex. *PLoS One* 10:e0120731. doi: 10.1371/journal.pone.0120731

Tsang, P., Jacobs, M. F., Lee, K. G. H., Asmussen, M. J., Zapallow, C. M., and Nelson, A. J. (2014). Continuous theta-burst stimulation over primary somatosensory cortex modulates short-latency afferent inhibition. *Clin. Neurophysiol.* 125, 2253–2259. doi: 10.1016/j.clinph.2014.02.026

Turco, C. V., El-Sayes, J., Locke, M. B., Chen, R., Baker, S., and Nelson, A. J. (2018a). Effects of lorazepam and baclofen on short- and long-latency afferent inhibition. *J. Physiol.* 596, 5267–5280. doi: 10.1113/jp276710

Turco, C. V., El-Sayes, J., Savoie, M. J., Fassett, H. J., Locke, M. B., and Nelson, A. J. (2018b). Short- and long-latency afferent inhibition; uses, mechanisms and influencing factors. *Brain Stimul.* 11, 59–74. doi: 10.1016/j.brs.2017.09.009

Turco, C. V., Locke, M. B., El-Sayes, J., Tommerdahl, M., and Nelson, A. J. (2018c). Exploring behavioral correlates of afferent inhibition. *Brain Sci.* 8:E64. doi: 10.3390/brainsci8040064

Udupa, K., Bahl, N., Ni, Z., Gunraj, C., Mazzella, F., Moro, E., et al. (2016). Cortical plasticity induction by pairing subthalamic nucleus deep-brain stimulation and primary motor cortical transcranial magnetic stimulation in Parkinson's disease. *J. Neurosci.* 36, 396–404. doi: 10.1523/JNEUROSCI.2499-15.2016

Ulivelli, M., Rossi, S., Pasqualetti, P., Rossini, P. M., Ghiglieri, O., Passero, S., et al. (1999). Time course of frontal somatosensory evoked potentials: relation to L-dopa plasma levels and motor performance in PD. *Neurology* 53, 1451–1457. doi: 10.1212/wnl.53.7.1451

Versace, V., Langthaler, P. B., Sebastianelli, L., Höller, Y., Brigo, F., Orioli, A., et al. (2017). Impaired cholinergic transmission in patients with Parkinson's disease and olfactory dysfunction. *J. Neurol. Sci.* 377, 55–61. doi: 10.1016/j.jns.2017.03.049

Wagle Shukla, A., Moro, E., Gunraj, C., Lozano, A., Hodaie, M., Lang, A., et al. (2013). Long-term subthalamic nucleus stimulation improves sensorimotor integration and proprioception. *J. Neurol. Neurosurg. Psychiatry* 84, 1020–1028. doi: 10.1136/jnnp-2012-304102

Wichmann, T., Bergman, H., and DeLong, M. R. (1994). The primate subthalamic nucleus. I. Functional properties in intact animals. *J. Neurophysiol.* 72, 494–506. doi: 10.1152/jn.1994.72.2.494

Wylie, S. A., van den Wildenberg, W. P. M., Ridderinkhof, K. R., Bashore, T. R., Powell, V. D., Manning, C. A., et al. (2009). The effect of Parkinson's disease on interference control during action selection. *Neuropsychologia* 47, 145–157. doi: 10.1016/j.neuropsychologia.2008.08.001

Yarnall, A. J., Rochester, L., Baker, M. R., David, R., Khoo, T. K., Duncan, G. W., et al. (2013). Short latency afferent inhibition: a biomarker for mild cognitive impairment in Parkinson's disease? *Mov. Disord.* 28, 1285–1288. doi: 10.1002/mds.25360

Zamir, O., Gunraj, C., Ni, Z., Mazzella, F., and Chen, R. (2012). Clinical neurophysiology effects of theta burst stimulation on motor cortex excitability in Parkinson's disease. *Clin. Neurophysiol.* 123, 815–821. doi: 10.1016/j.clinph.2011.07.051

Zia, S., Cody, F., and O'Boyle, D. (2000). Joint position sense is impaired by Parkinson's disease. *Ann. Neurol.* 47, 218–228. doi: 10.1002/1531-8249(200002)47:2<218::aid-ana12>3.0.co;2-#

Conflict of Interest Statement: HS has received honoraria as speaker from Sanofi Genzyme, Denmark and Novartis, Denmark, as consultant from Sanofi Genzyme, Denmark and as senior editor (NeuroImage) from Elsevier Publishers, Amsterdam, Netherlands. He has received royalties as book editor from Springer Publishers, Stuttgart, Germany.

The remaining authors declare that the research was conducted in the absence of any commercial or financial relationships that could be construed as a potential conflict of interest.

frontiers in Human Neuroscience

ORIGINAL RESEARCH
published: 17 April 2019
doi: 10.3389/fnhum.2019.00126

Sensory Re-weighting for Postural Control in Parkinson's Disease

Kelly J. Feller[1,2], *Robert J. Peterka*[2,3] *and Fay B. Horak*[1,2,3]*

[1]Department of Biomedical Engineering, Oregon Health & Science University, Portland, OR, United States, [2]Department of Neurology, Oregon Health & Science University, Portland, OR, United States, [3]Veterans Adminstration Portland Health Care System, Portland, OR, United States

Postural instability in Parkinson's disease (PD) is characterized by impaired postural responses to transient perturbations, increased postural sway in stance and difficulty transitioning between tasks. In addition, some studies suggest that loss of dopamine in the basal ganglia due to PD results in difficulty in using proprioceptive information for motor control. Here, we quantify the ability of subjects with PD and age-matched control subjects to use and re-weight sensory information for postural control during steady-state conditions of continuous rotations of the stance surface or visual surround. We measure the postural sway of subjects in response to a pseudorandom, surface-tilt stimulus with eyes closed, and in response to a pseudorandom, visual-tilt stimulus. We use a feedback control model of the postural control system to interpret our results, focusing on sensory weighting as a function of stimulus amplitude. We find that subjects with PD can re-weight their dependence upon sensory information in response to changes in surface- or visual-stimulus amplitude. Specifically, subjects with PD behaved like age-matched control subjects by decreasing proprioceptive contribution to stance control with increasing surface-tilt amplitude and decreasing visual contribution with increasing visual-tilt amplitude. However, subjects with PD do not decrease their reliance on proprioception as much as age-matched controls for small increases in surface-stimulus amplitudes. Levodopa medication did not affect sensory re-weighting behaviors for postural control. The impairment in PD subject's ability to respond differently to small changes in surface rotation amplitudes is consistent with an increased threshold for perceiving proprioceptive signals, which may result from decreased signal-to-noise in the dopaminergic pathways associated with sensory processing and/or sensory integration.

Keywords: basal ganglia, sensory integration, feedback, computational model, balance, Parkinson's disease

OPEN ACCESS

Edited by:
Matt J. N. Brown,
California State University, Sacramento, United States

Reviewed by:
Rahul Goel,
Baylor College of Medicine, United States
Arata Horii,
Niigata University, Japan

***Correspondence:**
Fay B. Horak
horakf@ohsu.edu

Received: *18 November 2018*
Accepted: *27 March 2019*
Published: *17 April 2019*

Citation:
Feller KJ, Peterka RJ and Horak FB (2019) Sensory Re-weighting for Postural Control in Parkinson's Disease. Front. Hum. Neurosci. 13:126. doi: 10.3389/fnhum.2019.00126

Abbreviations: CoM, center of mass; CoP, center of pressure; FRF, frequency response function; J, body moment of inertia about ankle joints; K_d, neural control damping constant; K_p, neural control stiffness constant; K_T, torque feedback gain; mgh, body mass times gravity constant times height of CoM above ankle joint; PD, Parkinson's disease; PD_{Off}, Parkinson's disease subjects off medication; PD_{On}, Parkinson's disease subjects on medication; PIGD, postural instability and gait disorders; RMS, root-mean-square; τ_d, neural control time delay; τ_T, torque feedback time-constant; UPDRS, Unified Parkinson's Disease Rating Scale; W_{prop}, proprioceptive weight; W_{vest}, vestibular weight; W_{vis}, visual weight.

INTRODUCTION

Evidence suggests that the basal ganglia are involved in processing and integrating sensory information (Abbruzzese and Berardelli, 2003; Nagy et al., 2006). There is increasing evidence that basal ganglia-related diseases, such as Parkinson's disease (PD), are associated with kinesthetic deficits, including reduced tactile discrimination, poor joint kinesthesia, asymmetrical spatial pointing, and over-estimating of reaching and stepping when vision is not available (Maschke et al., 2003; Jacobs and Horak, 2006; Tagliabue et al., 2009; Wright et al., 2010). PD also results in motor signs of postural instability, rigidity, tremor and bradykinesia (Horak et al., 1992; Bloem et al., 2001), due to loss of dopaminergic and other neurons throughout the central nervous system, with the severity of motor symptoms related to the amount of nigral-striatal dopamine (Agid, 1991). Although rigidity, tremor and bradykinesia are improved with dopamine replacement therapy, postural control and risk of falls does not improve and may even worsen with levodopa (Horak et al., 1992, 1996).

People with PD fall five times more than age-matched controls (Fasano et al., 2017). Evidence for abnormal postural control in patients with PD comes from studies of unperturbed, quiet stance and studies where balance was perturbed by various sensory stimuli. For quiet stance studies, the effect of PD on postural sway, as quantified by center of pressure (CoP) or center of mass (CoM) displacement, is controversial and may depend upon the sensory conditions and on how CoP or CoM displacement is quantified (Mancini et al., 2011; Curtze et al., 2015; Ozinga et al., 2017; Cruz et al., 2018). Sway area in subjects with PD, when standing with eyes open or closed, can be similar to sway in age-matched controls (Bronstein et al., 1990; Chong et al., 1999a; Bronte-Stewart et al., 2002), especially during early stages of PD (Frenklach et al., 2009). However, sway velocity and jerk have been shown to be increased, even in early PD without medication (Mancini and Horak, 2010; Mancini et al., 2011). In addition, CoP displacement is increased in patients with PD off medication as compared to controls, especially in the mediolateral direction, and levodopa replacement increases CoP displacement (Rocchi et al., 2002). As PD progresses, postural sway area tends to be correlated with the severity of PD (Frenklach et al., 2009).

Studies using perturbed stance have also shown conflicting results. Subjects with PD can generate appropriate sway, even while experiencing a sinusoidal surface displacement (De Nunzio et al., 2007). However, approximately 50% of subjects with PD sway more than age-matched controls with eyes closed on a sway-referenced surface (Bronte-Stewart et al., 2002). Increased sway in subjects with PD under this condition could indicate vestibular dysfunction, because stance with eyes closed on a sway-referenced surface requires increased reliance upon vestibular information. However, peripheral vestibular function is thought to be normal in subjects with PD (Pastor et al., 1993; Bronstein et al., 1996), and a recent study suggests that subjects with PD rely more on vestibular information than control subjects to control postural sway during stance, irrespective of treatment with medication or stimulation of the subthalamic nucleus (Maurer, 2009).

Alternatively, increased sway during sway-referenced conditions with eyes closed could be related to an impaired ability to quickly reorganize the sensory contributions to balance control. To maintain postural stability under suddenly changing sensory conditions, individuals must quickly alter how much they depend upon vision, proprioception, and vestibular information (Peterka and Loughlin, 2004; Jeka et al., 2008; Assländer and Peterka, 2016). It is well known that subjects with PD have a reduced ability to quickly change postural set when sensory or cognitive conditions suddenly change (Chong et al., 2000). For example, subjects with PD take longer than controls to achieve steady-state postural responses following eyes closed to eyes open transitions during sinusoidal surface displacements (Brown et al., 2006; De Nunzio et al., 2007). Furthermore, subjects with PD do not decrease sway with repeated exposure to lateral displacement of visual stimuli (Bronstein et al., 1990). However, many of the studies that manipulate the availability of orientation cues from different sensory systems use short-duration tests. As a result, the observed behavioral differences between subjects with PD and controls may be due to the reduced ability of subjects with PD to quickly adjust when sensory conditions are altered rather than a fundamental inability of subjects with PD to appropriately use sensory information if they are given enough time to adjust.

Our primary goal was to test the fundamental abilities of subjects with PD to adjust to sensory conditions and to regulate sensory integration for postural control in steady-state conditions. We quantified subjects' relative reliance on visual, vestibular, and proprioceptive information for postural orientation in response to sensory stimuli. Young, healthy subjects typically rely primarily on proprioceptive cues during eyes closed stance but shift toward decreased reliance on proprioception and increased reliance on vestibular cues when the stance is perturbed by support surface rotations of increasing amplitude (Peterka, 2002). Similarly, when visual cues are perturbed by visual surround rotations of increasing amplitude, subjects decrease their reliance on visual orientation cues (Peterka, 2002).

The quantitative assessment of reliance on a particular sensory modality is made by estimating sensory weighting parameters (Peterka, 2002). The sensory weights are parameters in a linear feedback control system model of the postural control system. Specifically, in our postural control model (**Figure 1**), the relative reliance on each sensory modality (i.e., vision, proprioceptive, vestibular) is represented as a weighting parameter. Sensory weighting is constrained by $W_{vis} + W_{vest} + W_{prop} = 1$, where W_{vis} is the visual weight, W_{vest} is the vestibular weight, and W_{prop} is the proprioceptive weight. Therefore, the sensory weight for each of the three weighting parameters can range from 0 to 1. When a subject's eyes are closed, $W_{vis} = 0$ and the sensory weighting constraint is reduced to $W_{vest} + W_{prop} = 1$. Additional parameters of the model include a position- and a velocity-dependent neural control parameter, a neural time delay, and torque feedback

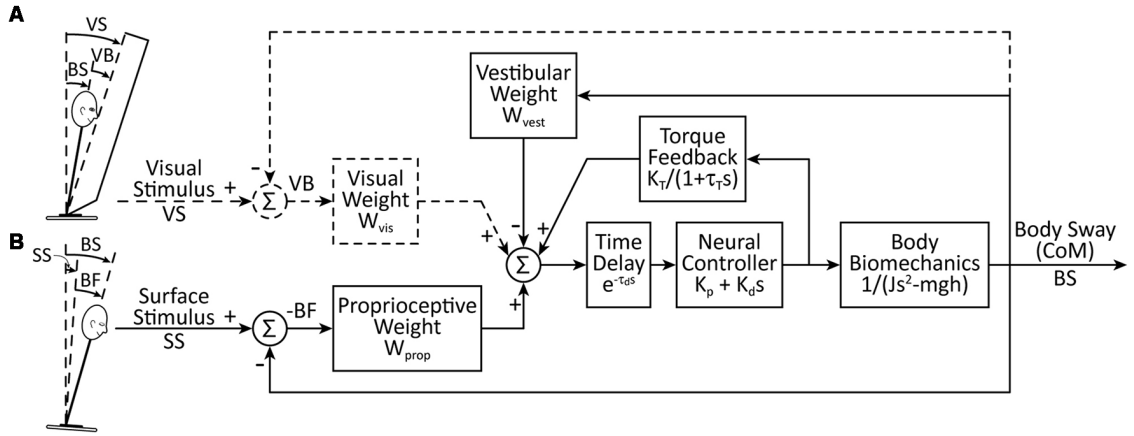

FIGURE 1 | A simplified feedback control model of postural control, including sensory weighting and torque feedback. For the data and analysis we present here, we considered **(A)** a visual-stimulus with a stationary surface and **(B)** a surface-stimulus with eyes closed. The model for the surface-stimulus condition (W_{vis} = 0) is indicated by the solid lines in the schematic. For the visual-stimulus condition, the dashed lines are added to the model and there is no surface stimulus. For the sensory integration component of the model, we constrained $W_{prop} + W_{vest} + W_{vis} = 1$. The body biomechanics are modeled as an inverted pendulum. The biomechanics, neural controller, torque feedback, and time delay blocks include Laplace transform representations of the differential equations of these model components where s is the Laplace variable.

implemented as a low-pass filter with a gain and time constant (**Figure 1**). Previous results showed that young adult subjects with normal sensory function very precisely regulate sensory weights with little variation across subjects and systematically alter these weights as the amplitude of the perturbations change (Peterka, 2002).

Our secondary goal was to determine whether levodopa influences sensory integration. Although dopamine replacement with levodopa medication improves many motor symptoms of PD, its effects on postural control are complex. For example, levodopa improves rigidity, bradykinesia, and tremor, but automatic postural responses (Horak et al., 1996) and postural sway during stance (Nardone and Schieppati, 2006; Rocchi et al., 2006a) worsen with levodopa. Previously, we reported that levodopa does not reduce excessive axial postural tone during stance, despite the reduction of limb rigidity (Wright et al., 2007). However, some components of postural control may improve with levodopa, such as the magnitude of anticipatory postural adjustments prior to movement (Burleigh-Jacobs et al., 1997). There is also evidence that dopaminergic medication further impairs kinesthesia (O'Suilleabhain et al., 2001; Mongeon et al., 2009), although studies have not reported how dopamine replacement affects sensory re-weighting for postural control.

Given that subjects with PD are reported to have various limitations and deficits regarding sensory processing, we hypothesized that sensory re-weighting for postural control would be impaired in subjects with PD. To test this hypothesis, we measured the postural sway of PD and age-matched control subjects while standing in response to pseudorandom surface- and visual-rotations and then used our postural control model to estimate postural control parameters. In this study, we focused primarily on the change of sensory weighting parameters when sensory conditions change. We also tested the additional hypothesis that levodopa medication would improve sensory weighting for postural control.

MATERIALS AND METHODS

Subjects

The Institutional Review Board at Oregon Health and Science University (OHSU) approved the protocol for this experiment, and all subjects gave informed consent prior to participating. Eight subjects with PD (three female) and eight healthy, age-matched controls (two female) were recruited from the Balance Disorders Laboratory database and the Parkinson's Center of Oregon Clinic at OHSU.

Subjects with PD were selected based on the following inclusion criteria: (1) a diagnosis of idiopathic PD; (2) levodopa responsive, as demonstrated by a lower score on the Unified PD Rating Scale (UPDRS) motor examination when on anti-Parkinsonian medication compared to off medication; and (3) the ability to stand unsupported for 5 min both on and off medication. Subjects with PD were excluded if they had other neurological, sensory, or muscular disorders (e.g., diabetes, peripheral neuropathies, uncorrected visual problems, arthritis, stroke, or seizure).

Control subjects were selected so that no significant differences existed between subjects with PD and controls in age (p = 0.79), height (p = 0.96), or weight (p = 0.71). Additional selection criteria for control subjects were: (1) no known neurological, sensory, or muscular problems; and (2) the ability to stand unsupported for 5 min. **Table 1** describes the anthropometric and clinical characteristics of the subjects with PD and the mean anthropometric characteristics of the control subjects. All subjects with PD in the off medication state (PD_{Off}), except Subject 1, either had a Hoehn and Yahr score of three or greater or showed impaired balance control in response to a

TABLE 1 | Characteristics of Parkinson's disease (PD) and control subjects.

Subjects[a]	Sex	Age (years)	Height (cm)	Weight (kg)	DOPA Equiv[b].	Years Since Diag.	Most affected side	Hoehn & Yahr (Off/On)	Unified Parkinson's Disease Rating Scale					
									Total Motor (Off/On)	PIGD (Off/On)	Tremor (Off/On)	Bradykinesia (Off/On)	Rigidity (Off/On)	Dyskinesia (Off/On)
PD1	F	59	164	83	825	3	R	1/1	[c]/2.5	[c]/1	[c]/0	[c]/1	[c]/0	[c]/0
PD2	M	62	180	105	[d]	5	L	2/1	20.5/4.5	8/4	0/0	2/0.5	2/0	0/0
PD3	M	72	171	71	500	8	R	2.5/2.5	25/16	5/5	9/3	2/2	3/1	0/0
PD4	F	63	163	66	900	13	L	2/1.5	28/11	11/1	1/2	2/0	5/6	0/8
PD5	M	67	174	97	1,180	8	L	3/2	39/21	5/4	6/3	1/1	12/5	0/0
PD6	M	50	182	76	1,000	11	R	3.5/3	49/24	8/5	6/5	3/0	10/3	0/10
PD7	M	70	177	85	1,250	9	L	4/2	59/30	12/6	2/3	3/1	16/6	0/5
PD8	F	69	150	47	1,300	34	R	4/3	63/46	17/11	9/6	4/2	9/8	0/9
Mean PD		64	170	79	994	11		2.8/2	40.5/19.4	9.4/4.6	4.7/2.8	2.4/0.9	8.1/3.6	0/4
Mean Control		64	170	76										

*[a]Subjects with PD and controls were matched for age, height, and weight. Biomechanical parameters used in the modeling included J: moment of inertia about the ankle joints and mgh: the product of body mass (not including the feet), the gravity constant, and height of the center of mass (CoM). The mean values for controls and subjects with PD, respectively were J: 76.6 and 79.7 kg m^2 and mgh: 692 and 717 kg m^2 s^{-2}. Subjects with PD are listed in the order of increasing disease severity, based on the total Unified Parkinson's Disease Rating Scale (UPDRS) motor score when off medication. [b]Dopaminergic medications were converted to levodopa equivalents using: DOPA Equiv. (in mg) = levodopa + 0.75*controlled-release levodopa + 100*pramipexole + 16.67*ropinirole + 1.5*amantadine + E_{LDE}, where E_{LDE} = 0.25*[levodopa + 0.75*(controlled-release levodopa)] is included if carbidopa/levodopa was coadministered with entacapone and each medication is given in mg of drug administered daily (Nutt et al., 2003). [c]The UPDRS was not performed for PD1 in the off condition. [d]A medications list for PD2 was not collected.*

backwards pull on the shoulders [part of the postural instability and gait (PIGD) sub-score of the UPDRS].

We also included data from four younger controls (mean age = 37 years.) that were part of a previously published study (Peterka, 2002).

Experimental Apparatus

We used a custom-built, balance-testing device for the experiments (Peterka, 2002). The device is comprised of a motor-driven support surface and a motor-driven visual surround. The subject stood on the support surface and faced the visual surround. The support surface can rotate in a toe-up/toe-down direction about the subject's ankle joints and uses force sensors (Transducer Techniques, Temecula, CA, USA) to measure the subject's CoP. The visual surround is a half-cylinder, imprinted with a random, complex checkerboard pattern, which can rotate in the anteroposterior direction about the subject's ankle joint. The balance-testing device measures anterior-posterior body sway by recording the displacement of two sway rods; each sway rod is comprised of a potentiometer (Midori Precisions Co, LTD—Tokyo, Japan) connected to a light metal rod. One sway rod rests in a hook at the subject's hip height, and the second sway rod rests in a hook at the subject's shoulder height (see Peterka et al., 2018 for details).

Experimental Design

Each experiment consisted of six blocks of trials: (1) a calibration trial, (2) surface-stimulus trials, (3) a sway-referenced trial, (4) visual-stimulus trials, (5) a quiet-stance trial, and (6) surface-stimulus trials (repeat). **Table 2** lists the blocks of trials and the number of trials comprising each block. The surface-stimulus trials (blocks 2 and 6) and the visual-stimulus trials (block 4) were the focus of the experiment; these blocks tested whether subjects could re-weight sensory information in response to changing sensory stimuli. The sway-referenced trial (block 3) and quiet-stance trial (block 5) tested whether the behavioral characteristics of our subjects with PD were comparable to previously published results.

Control subjects performed the experiment once, and subjects with PD performed the experiment twice: once on and once off medication. For off-medication testing, subjects were tested at least 12 h after their last dose of anti-Parkinsonian medication. Five subjects (PD1, PD2, PD3, PD7, and PD8) were tested off medication the first day and on medication the second day. Two subjects were tested on medication the first day and off medication the second day (PD4 and PD6). One subject (PD5) was tested off and then on medication on the same day.

During all testing, except during calibration, subjects wore headphones and listened to an audio book to minimize conscious control of their posture. To prevent injury in the event of losing balance, subjects wore a harness attached to the ceiling of the room, and a researcher spotted them at all times. Subjects rested between trials to minimize fatigue. If a subject fell on a trial, the trial was repeated. If the second attempt also resulted in a fall, a third trial was attempted. All subjects successfully completed all trial types in three attempts, except for the sway-referenced trial. If a subject did not successfully complete a full sway-referenced

TABLE 2 | Description of trial blocks, conditions, and data analyses.

	Blocks of trials	Trial #	Description of trial conditions			Data analyses
			Subject's vision	Support surface	Visual surround	
Block 1:	Calibration	1	Eyes Open	Stationary	Stationary	Linear Model
Block 2:	Surface-stimulus trials	2	Eyes Closed	2° PRTS	Stationary	RMS, FRF, Feedback Model
		3	Eyes Closed	1° PRTS	Stationary	
		4	Eyes Closed	4° PRTS	Stationary	
Block 3:	Sway-referenced trial	5	Eyes Closed	Sway-Referenced	Stationary	Peak-to-Peak CoM Sway
Block 4:	Visual-stimulus trials	6	Eyes Open	Stationary	2° PRTS	RMS, FRF, Feedback Model
		7	Eyes Open	Stationary	1° PRTS	
		8	Eyes Open	Stationary	4° PRTS	
Block 5:	Quiet-standing trial	9	Eyes Closed	Stationary	Stationary	RMS
Block 6:	Surface-stimulus trials	10	Eyes Closed	2° PRTS	Stationary	RMS, FRF, Feedback Model
	(Reprise of Block 2)	11	Eyes Closed	1° PRTS	Stationary	
		12	Eyes Closed	4° PRTS	Stationary	

trial within three attempts, we proceeded to the next block of trials.

Calibration Trial

The calibration trial (block 1) defined the relationship between the displacement of the sway rods and the displacement of a subject's CoM (Peterka, 2002; Peterka et al., 2018). During the 120 s trial, subjects were vocally cued to lean slowly forward and backward through a range of hip and/or ankle angles while they stood with eyes opened on a stationary support surface.

Surface-Stimulus Trials

The purpose of the surface-stimulus trials (blocks 2 and 6) was to determine the dynamic characteristics of responses to surface perturbations and to identify how subjects alter their use of proprioceptive orientation cues as a function of stimulus amplitude.

Each surface-stimulus trial was performed with eyes closed. Following 10 s of standing on a stationary surface, the surface rotated according to a stimulus derived from a pseudorandom ternary sequence (PRTS; Davies, 1970). The PRTS was chosen because it has properties similar to white noise (i.e., flat velocity power spectrum over a wide bandwidth), and it appears unpredictable to subjects (see Peterka, 2002 for details). Each trial consisted of four sequential cycles of the PRTS, with each cycle lasting 43.72 s.

In each surface-stimulus block (blocks 2 and 6), subjects performed three surface-stimulus trials with peak-to-peak amplitudes of 2°, 1°, and 4° for the first, second, and third trials, respectively. Subjects rested between trials to prevent fatigue. The surface-stimulus trials of block 6 were a repetition of the surface-stimulus trials of block 2, to determine any learning effect on the subject's ability to maintain balance.

Visual-Stimulus Trials

The purpose of the visual-stimulus trials (block 4) was to determine the dynamic characteristics of responses to visual perturbations and to identify how subjects alter their use of visual cues for spatial orientation as a function of stimulus amplitude.

On each visual-stimulus trial, subjects stood with eyes opened on a stationary support surface looking forward into the visual surround, but not staring at a single point in the pattern. After 10 s, the visual surround rotated according to a PRTS stimulus while the support surface remained stationary. Each trial consisted of four sequential cycles of the PRTS, with each cycle lasting 60.5 s. Subjects performed three visual-stimulus trials with peak-to-peak amplitudes of 2°, 1°, and 4° on the first, second, and third trials, respectively. The subjects rested between trials to prevent fatigue.

A lower bandwidth PRTS was used for the visual stimulus trials than the surface-stimulus trials, because the motor controlling the visual surround had a lower bandwidth than the motor controlling the support surface. Therefore, the PRTS for the visual-stimulus trials contained lower frequencies than the PRTS for the surface-stimulus trials. Consequently, the length of a single cycle of the PRTS was longer for the visual-stimulus trials (60.5 s) than the surface-stimulus trials (43.72 s).

Quiet-Standing Trial

The purpose of the quiet-standing trial (block 5) was to quantify the magnitude of the subject's unperturbed body sway. For the quiet-standing trial, the subject stood upright with eyes closed on the stationary support surface for 120 s.

Sway-Referenced Trial With Eyes Closed

The sway-referenced trial (block 3) determined whether subjects could change their reliance on sensory information to maintain their balance when vision was absent and relevant proprioceptive cues were suddenly eliminated. In this trial, subjects were required to rely on vestibular information to maintain balance. During the sway-referenced trial, the subjects stood upright on a stationary support surface with their eyes closed. After 60 s, the angular displacement of the lower body, measured using the hip sway rod, was used to control the angular position of the support surface for 60 s; the surface rotated in direct proportion to the subject's lower body angle with a proportionality constant of 1 (Peterka and Loughlin, 2004). The trial ended with the subject standing quietly on the stationary support surface for another 60 s. These sway-referenced trials are comparable to condition five of the clinical Sensory Organization Test (Horak, 1987; Black et al., 1988).

Data Analysis

Linear Model for Calibration Trial

Using sway data from each subject's calibration trial, a linear model was used to relate sway rod displacement to CoM displacement, $CoM = A_1S_S + A_2S_H + OFF$, where S_S and S_H are body displacements measured using the sway rods at shoulder level and hip level, respectively. The coefficients A_1 and A_2 are multipliers for the shoulder and hip displacement, respectively, and OFF is an offset. Based on the assumption that, for slow movements, CoP displacement approximates CoM displacement (Brenière, 1996; Winter et al., 1998), the A_1, A_2, and OFF coefficients were determined by minimizing the mean squared error of measured CoP minus the estimated CoM using the fmincon function in MATLAB R2008b (The MathWorks, Inc., Natick, MA, USA). For subsequent trials, the calculated A_1, A_2, and OFF coefficients from each subject were used in the linear model, described above, to calculate the CoM displacement from the sway rod measured displacements. A recent publication provides a detailed explanation of this method and includes a Matlab program for the calibration analysis (Supplementary Materials in Peterka et al., 2018).

CoM measurement using this method accounted for the combined motions of the upper and lower body segments and thus provided valid CoM measures whether subjects use ankle or hip strategies. Previous studies have shown that subjects with PD tend to use an inverted pendulum ankle strategy to control standing posture while a mixed hip-ankle strategy is used in control subjects (Baston et al., 2016; Matsuda et al., 2016).

Root Mean Square (RMS)

We calculated the root mean square (RMS) for: (1) the CoM displacement for surface- and visual-stimulus trials; (2) the PRTS stimulus displacement for the surface- and visual-stimulus trials; (3) the CoM displacement for successful sway-referenced trials; and (4) the CoP displacement for quiet-standing trials. The signals were zero-meaned prior to calculating their RMS values.

For surface- and visual-stimulus trials, CoM sway data for each subject were first averaged across all available cycles and then an RMS value of the average waveform was calculated. A comparison of the RMS of CoM sway between blocks 2 and 6 indicated that there was no significant learning between blocks in response to surface-stimuli. Therefore, all six cycles from these two blocks were averaged before calculating the RMS, which increased the signal-to-noise ratio of our data. Three cycles of CoM sway data were used for the RMS calculation of responses to visual stimuli for each subject.

Analysis for PRTS Trials

Analysis of the surface- and visual-stimulus trials in the time and frequency domains has been previously described (Peterka, 2002). In brief, we considered the subject's response to the first cycle of the PRTS stimulus to be a transitional cycle during which the subject's response did not yet reach a steady-state. Therefore, only the second, third, and fourth cycles of a given trial were included in the analysis. For all time domain analyses, we calculated a subject's average response to each stimulus by averaging the response (CoM displacement) across the three steady-state cycles (cycles 2, 3 and 4). For the frequency domain analysis, we used spectral analyses of each cycle of the stimulus and response in a given trial. The various spectra were averaged across cycles, and further averaged across adjacent frequencies, to yield frequency response function (FRF) and coherence function values at frequency points that were approximately linearly spaced on a logarithmic frequency scale for each stimulus type and for each subject (see Peterka, 2002 for details). FRFs are expressed as gain and phase values that represent the amplitude and timing, respectively, of CoM sway relative to the stimulus across frequency. We computed the mean FRF across subjects and calculated the mean gain and phase curves from the mean FRF.

Feedback Control Model

Model Choice and Optimization

We implemented a model-based interpretation of responses to surface- and visual-stimuli by applying a feedback model of the postural control system, which has been described previously (Peterka, 2003; Cenciarini and Peterka, 2006). Briefly, our model included components for sensory weighting (W_{prop}, W_{vis}, and W_{vest}), neural stiffness (K_p), neural damping (K_d), neural time delay (τ_d), and torque feedback (K_T) with a low-pass filter time-constant (τ_T).

Model parameters were estimated using optimized fits to the FRF data. For both the surface- and visual-stimulus trials, fits were made to the three FRFs from each block simultaneously. For the surface-stimulus trials, optimal fits were performed for each subject individually allowing W_{prop} and τ_d to vary across the three stimulus amplitudes, but allowing only single values of K_p, K_d, τ_T, and K_T. These constraints on the optimization fits provided parsimonious descriptions of the experimental FRFs while limiting the total number of free parameters. We also calculated the mean FRF across all subjects and the optimal parameters that fit the mean data.

For the visual-stimulus trials, optimal fits were made only to the mean FRFs for each stimulus amplitude, because the responses to visual-stimulus trials were noisier, and the FRFs fits to individual subjects were not insightful. The visual-stimulus trials were optimized allowing W_{vis} to vary across the three stimulus amplitudes, but allowing only single values of τ_d, K_p, K_d, τ_T, and K_T.

Statistical Analyses

For all statistical analyses, we considered: (1) the effect of PD; and/or (2) the effect of anti-Parkinsonian medication on postural control mechanisms. To determine the effect of PD, we quantified the effect of PD on postural control mechanisms by comparing the behavior of control subjects (C) to PD_{Off}. To determine the effect of medication, we quantified the effect of medication on steady-state postural control mechanisms by comparing the behavior of PD_{Off} to subjects with PD on medication (PD_{On}). The threshold for significance was $p < 0.05$ for all statistical tests. All statistical analyses were computed in R (The R Project for Statistical Computing; www.r-project.org).

Individual Comparisons

Due to the size of our groups, we could not reasonably test whether our data were normally distributed. Therefore, we used the more conservative non-parametric tests to determine significance of individual comparisons. For individual comparisons, the effect of disease (i.e., C compared to PD_{Off}) was assessed with the two-sample Wilcoxon rank-sum test, and the effect of medication (i.e., PD_{Off} compared to PD_{On}) was assessed with the paired Wilcoxon signed-rank test. For statistical testing of the clinical measures of the UPDRS, and sub-scores of the UPDRS, we used a single-sided distribution, because we were testing whether there was an improvement in the UPDRS score on vs. off medication. All other individual comparison tests were calculated with a two-sided distribution.

Repeated-Measures ANOVAs

We used repeated-measures ANOVAs (i.e., using aov in R) to test the hypotheses that PD influences: (1) CoM displacement in response to surface-stimuli, (2) W_{prop} in response to surface-stimuli, and (3) the time-delay parameter in our feedback control model. In the above three ANOVAs, RMS of CoM displacement, W_{prop}, and τ_d were the dependent variables, respectively. We included factors for group (i.e., Controls vs. PD_{Off}), stimulus amplitude (i.e., 1°, 2°, and 4°), and an interaction effect (i.e., group × stimulus amplitude). We also included a random factor for subject, accounting for the fact that each subject performed the experiment for all three stimulus amplitudes.

Similarly, we used a repeated-measures ANOVA to test the hypothesis that levodopa influenced W_{prop} in response to surface-stimuli. This ANOVA included factors for medication conditions (i.e., ON vs. OFF), stimulus amplitude, and an interaction effect. This ANOVA also included a random factor for subject, accounting for the fact that each subject performed the experiment for all three stimulus amplitudes and two medication conditions.

RESULTS

Clinical Balance and Quiet Stance Measures

Quiet stance measures of sway and clinical signs on and off levodopa were similar to those reported in previous studies. During quiet stance with eyes open, RMS of CoP displacement was not significantly different between PD_{Off} and control subjects in the anteroposterior direction (**Figure 2A**; $p = 0.38$) or in the mediolateral direction ($p = 0.083$). Levodopa increased the RMS of CoP displacement from PD_{Off} to PD_{On} in the mediolateral ($p = 0.023$), but not in the anteroposterior direction ($p = 0.20$), as shown previously (Mitchell et al., 1995; Rocchi et al., 2002; Curtze et al., 2015).

The peak-to-peak CoM sway of the PD_{On} and elderly control subjects, who did not fall on the sway-referenced trial, were consistent with previously published results (Chong et al., 1999a). Two of the eight controls, three of the eight PD_{On} subjects, and four of the eight PD_{Off} subjects fell on all three attempts of standing on a sway-referenced surface with eyes closed. This result is consistent with previous results (Bronte-Stewart et al., 2002; Frenklach et al., 2009) showing that a subset of patients with PD fall on all sway-referenced attempts, regardless of disease severity.

As expected, levodopa improved the UPDRS III Motor score ($p = 0.011$). Levodopa also improved the PIGD sub-score of the

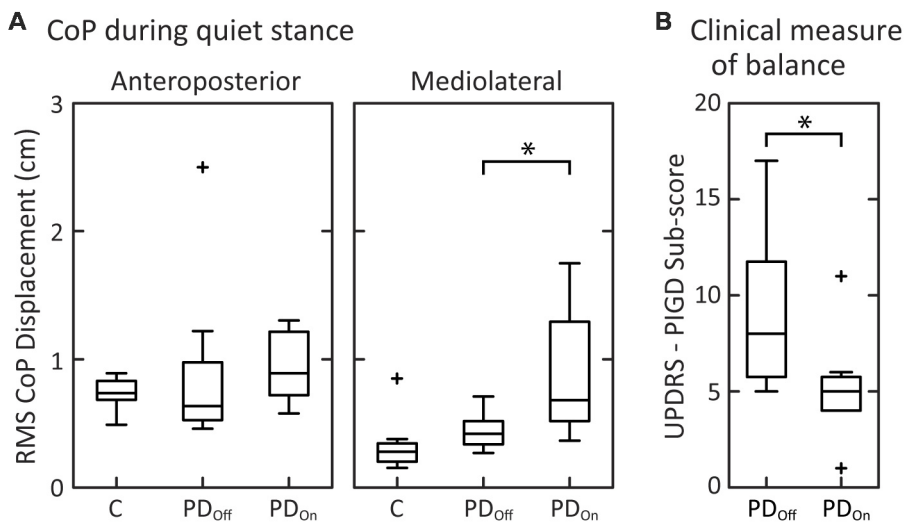

FIGURE 2 | Clinical measures of balance and center of pressure (CoP) measurements. **(A)** Box and whisker plots of the CoP during quiet stance for the anteroposterior and mediolateral directions. **(B)** Box and whisker plots of the postural instability and gait disorders components (PIGD) of the Unified Parkinson's Disease Rating Scale (UPDRS; $N = 7$; PD1 is not included due to incomplete data for the UPDRS off medication). For each subject group, the center line is the median, the bottom of the box is the 25th percentile (Q1), and the top of the box is the 75th percentile (Q3). The whiskers extend to include all data points that are within the range defined by Q1−1.5(Q3 - Q1) and Q3 + 1.5(Q3 - Q1). Data points that extend beyond the whiskers are defined as outliers and denoted with a "+." Brackets with "*" indicate significant differences between mean values.

UPDRS (Items 26–30; **Figure 2B**; $p = 0.018$) as well as rigidity (Item 22; **Table 1**; $p = 0.021$), and bradykinesia (Item 31; **Table 1**; $p = 0.027$).

Stimulus-Evoked Sway

For all stimulus amplitudes, control subjects and subjects with PD on and off medication tended to orient the angular displacement of their body CoM to either the moving support surface (**Figure 3A**) or visual surround (**Figure 3B**). At the lowest stimulus amplitudes, CoM sway was larger than the surface-stimulus amplitude (**Figure 3A**, row 1). CoM sway increased with increasing surface-stimulus amplitude. However, control subjects did not sway as much as subjects with PD at the largest surface-stimulus amplitude (**Figure 3A**, row 3). Control subjects swayed less than the surface-stimulus amplitude, and PDs swayed approximately the same as the surface-stimulus amplitude in response to the 4° surface-stimulus. CoM sway was similar between PD_{Off} and PD_{On} for all surface-stimulus amplitudes (**Figure 3A**, two rightmost columns). The variability across subjects of the CoM sway was larger in PD_{Off} and PD_{On} than control subjects (**Figure 3A**, gray shaded regions).

As with surface stimuli, all subjects tended to orient their CoM sway to the visual stimulus (**Figure 3B**). Overall, responses to visual stimuli were smaller in magnitude than responses

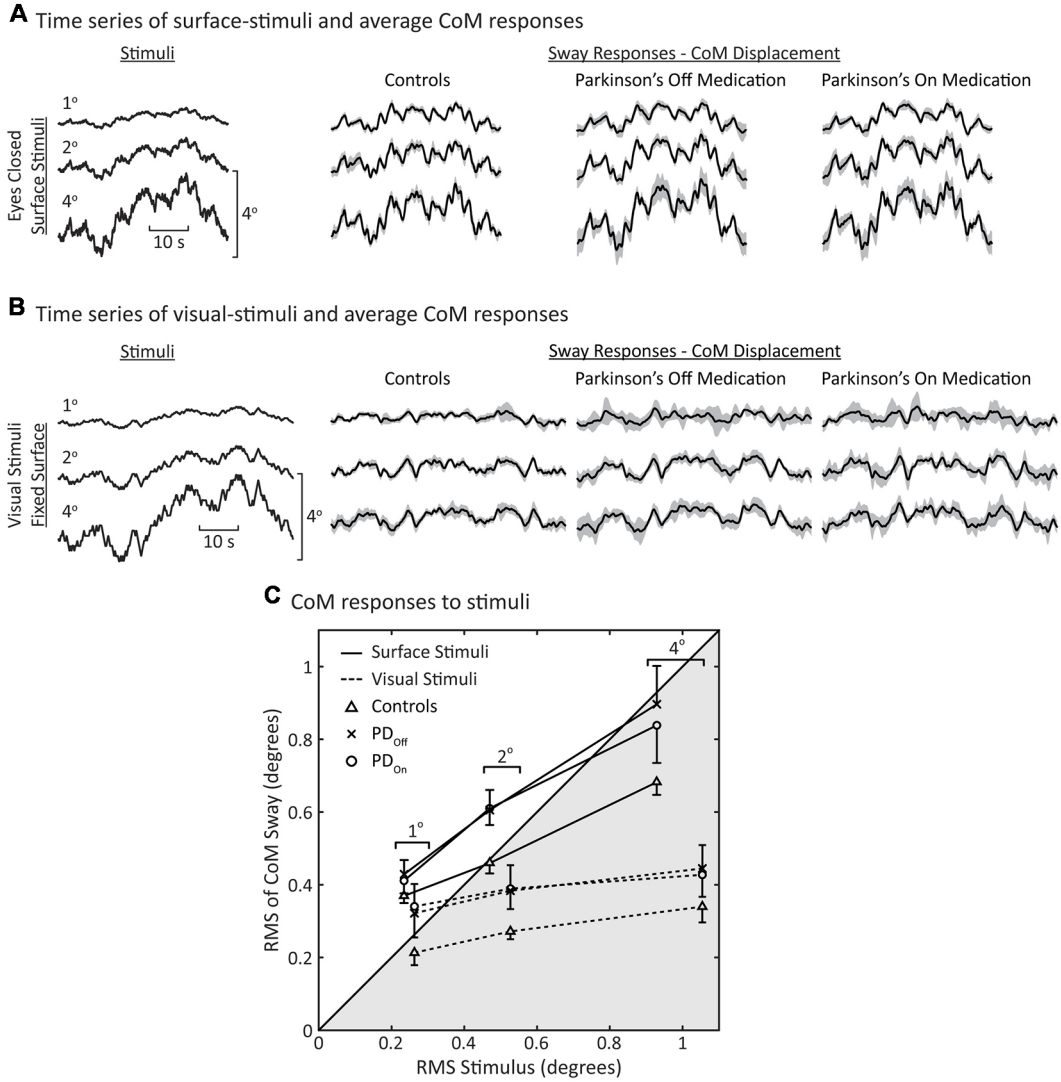

FIGURE 3 | Sway during surface and visual stimuli. Time series of average center of mass (CoM) responses to **(A)** surface stimuli and **(B)** visual stimuli. The shaded gray regions represent the 95% confidence intervals of the mean response across subjects. **(C)** Root mean square (RMS) of the CoM sway vs. RMS of the stimulus. Each data point represents the average behavior across subjects ($N = 8$ for each group). Data in the unshaded half of the figure represents CoM responses that are larger than the stimulus (ratio >1); the shaded portion of the plot represents responses that are smaller than the stimulus (ratio <1). Note that the surface and visual stimuli were different pseudorandom ternary sequences (PRTSs; see Stimuli columns in **(A,B)** and see "Materials and Methods" section), consequently the RMS of the stimuli are slightly different for the same peak-to-peak stimulus amplitude. The error bars denote standard errors for the surface-stimulus data. For clarity, only single-sided error bars are shown.

to surface stimuli (**Figures 3A,B**). There were no obvious differences in the average sway of PD_{Off}, PD_{On}, and control subjects in response to visual-stimuli. However, the variability across subjects was greater for subjects with PD than controls in response to visual stimuli (**Figure 3B**, gray shaded regions).

To quantify the degree by which subjects increased body sway in response to increased surface-stimulus amplitudes, we calculated the RMS of the CoM sway and stimulus (**Figure 3C**). There was an increase in the RMS of CoM sway with increasing surface-stimulus amplitude for PD_{Off}, PD_{On}, and control subjects. This increase in the RMS of CoM sway was smaller than the increase in the RMS of the stimulus. PD_{Off}, PD_{On} and control subjects had similar sway in response to 1° surface stimuli, and all subject groups swayed more than the stimulus amplitude in response to the 1° surface stimulus (**Figure 3C**, 1° data in white region).

For larger surface-stimulus amplitudes, subjects with PD showed greater RMS sway than controls (**Figure 3C**, solid lines). Statistical analysis based on a repeated-measures ANOVA showed a significant main effect of stimulus amplitude ($p < 0.001$) on the RMS of CoM sway. The main effect of disease on the RMS of CoM sway was not significant ($p = 0.059$), nor was the interaction between disease and stimulus amplitude ($p = 0.11$).

For visual stimuli, the RMS sway was similar for PD_{Off} and PD_{On} with controls having lower RMS sway than subjects with PD at all stimulus amplitudes (**Figure 3C**, dashed lines). For subjects with PD and controls, RMS sway levels showed moderate increases with increasing visual stimulus amplitude and these sway levels were smaller than for surface stimuli.

Postural Dynamics

Individual Responses to Surface-Stimuli

We used a frequency domain analysis to characterize each subjects' postural sway over a range of perturbation frequencies. **Figure 4** shows examples of experimental FRFs and model fits for an individual PD_{Off} subject's response to three surface-stimulus amplitudes. The main feature of the FRF is a decreasing gain with increasing stimulus amplitude (**Figure 4**, top). The phase is similar across stimulus amplitude for most frequencies, except at higher frequencies where there is a slightly larger phase lag for the 1° than for 2° and 4° stimulus amplitudes (**Figure 4**, middle). The coherence of the experimental data decreases with increasing frequency (**Figure 4**, bottom). **Figure 4** also shows the model fits to the experimental data (see **Figure 1** for model). The model fits replicate the main features of the experimental data, with decreasing dependence on proprioception (smaller W_{prop}) accounting for the gain decrease as stimulus amplitude increases and decreasing time delay (τ_d) accounting for phase changes at higher frequencies.

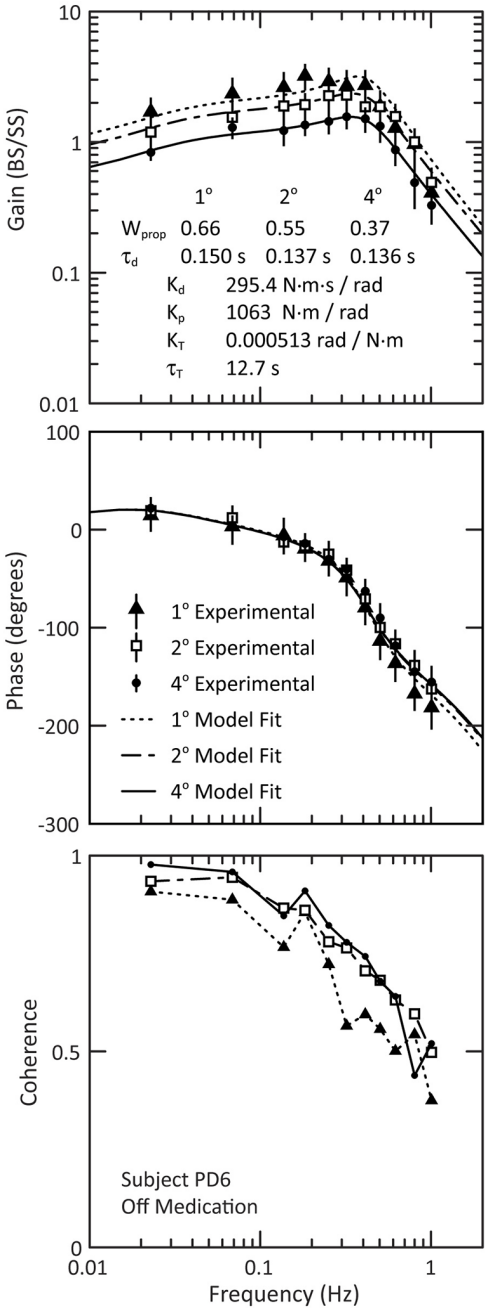

FIGURE 4 | Example of experimental frequency response functions and model fits for PD subject PD6 off medication. The experimental data are shown for the gain (top figure) and phase (middle figure), and the 95% confidence intervals of the mean are indicated by the vertical lines through each data point of the gain and phase curves. The bottom figure shows the coherence of the experimental data. Note that the lines in the coherence plot (bottom figure) are for visualization of the experimental data; these lines are not related to the model fits.

Group Responses to Surface-Stimuli

The results observed for the individual PD_{Off} subject (**Figure 4**) were representative not only of the mean behavior across all PD_{Off} subjects but also of the mean behavior for the control and PD_{On} subjects. The mean behavior of each subject group included a decrease in the gain with increasing stimulus amplitude, and small phase changes at higher stimulus frequencies (**Figure 5**). There were no qualitative differences between PD_{Off}, PD_{On}, and control subjects in the gain, phase or coherence curves for any stimulus amplitude. Consequently, the

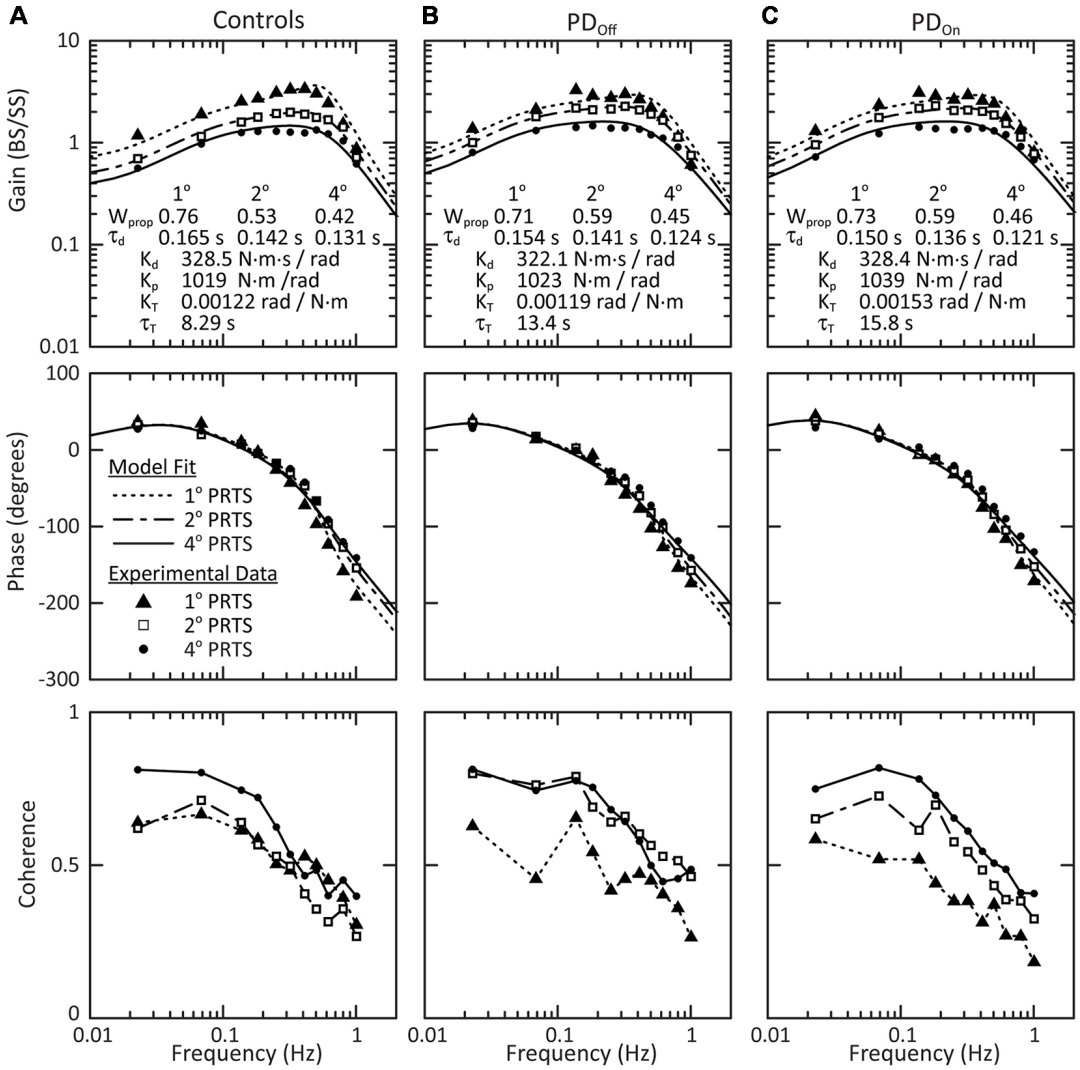

FIGURE 5 | Mean behavior across subjects in response to surface stimuli with eyes closed. Gain, phase and coherence curves for **(A)** control subjects, **(B)** subjects with PD off medication, and **(C)** subjects with PD on medication. The data points denote experimental data for the mean behavior across subjects and the curves on the gain and phase plots are the model fits to this mean behavior. The parameters of the model fits are listed in the gain plots. Data for all three stimulus amplitudes were fit simultaneously, with a W_{prop} and τ_d for each stimulus amplitude, and a single K_d, K_p, K_T, and τ_T across all stimulus amplitudes. The lines connecting data points in the coherence plots (bottom row) are for visualization and are not related to model fits.

parameters of the model fits to the mean group data were similar for PD_{Off}, PD_{On}, and control subjects.

Model-Based Interpretation for Surface Stimuli

There were no significant effects of disease (controls vs. PD_{Off}) on sensory-to-motor characteristics of posture control: K_p (p = 0.88), K_d (p = 0.80), τ_d (p = 0.74), K_T (p = 0.64), or τ_T (p = 0.083). Medication (PD_{Off} vs. PD_{On}) also did not significantly affect K_p ($p > 0.99$), K_d (p = 0.38), τ_d (p = 0.82), K_T (p = 0.20), or τ_T (p = 0.25). All subject groups showed a significant decrease in proprioceptive weighting (W_{prop}) with increasing surface-stimulus amplitude (**Figure 6A**; $p < 0.001$). Although the mean W_{prop} was larger for controls than for subjects with PD at 1° and smaller for controls than for subjects with PD at 2° and 4°, there was no significant main effect of disease (controls vs. PD_{Off}) on W_{prop} (**Figure 6A**; p = 0.84), and there was no interaction effect between group and stimulus amplitude (p = 0.28). In addition, there was no main effect of medication on W_{prop} (p = 0.92) and no interaction between medication and stimulus amplitude (p = 0.82).

Viewing the changing W_{prop} values of individual subjects across stimulus amplitude revealed some qualitative differences between subjects with PD and age-matched control subjects (**Figure 6C**). There was more inter-subject variability in W_{prop} in subjects with PD than in control subjects in response to the 4° surface-stimulus amplitude (**Figure 6C**). This inter-subject variability in the PD groups was due, in part, to the large proprioceptive weights for a single PD_{Off} subject (PD8) and

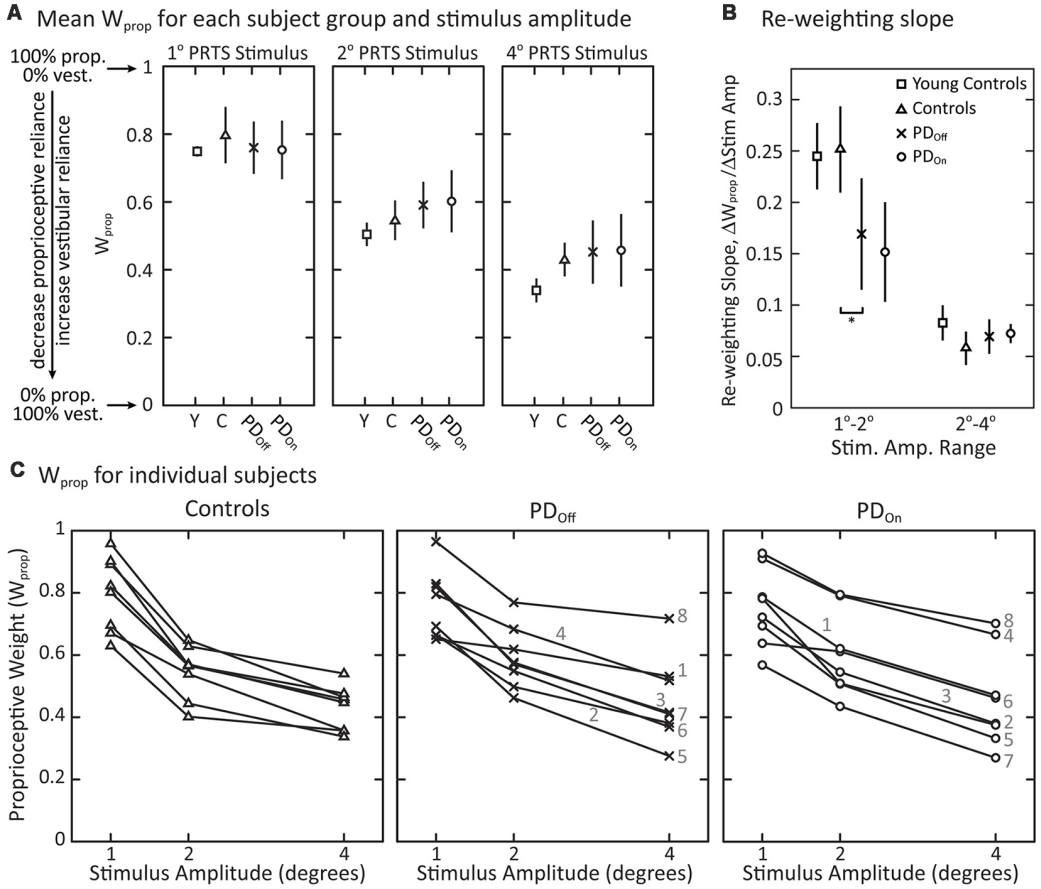

FIGURE 6 | Proprioceptive weighting in response to surface-stimuli with eyes closed. **(A)** Sensory weighting across subject groups and stimulus amplitudes. Data are shown for young controls (Y: $N = 4$; age range 28–47 years), older controls (C: $N = 8$; age range 57–77 years), and subjects with PD off (PD_{Off}: $N = 8$) and on (PD_{On}: $N = 8$) medication. A proprioceptive weight of 1 indicates 100% reliance on proprioceptive information, while a weight of 0 indicates 100% reliance on vestibular information. The symbols represent mean behavior for each group, and the error bars denote the 95% confidence interval of the mean. **(B)** Slope factor representing the normalized change in proprioceptive weights between 1° and 2° surface-stimuli and between 2° and 4° surface-stimuli for each subject group. All changes in W_{prop} are positive, indicating a decrease in W_{prop} for increasing stimulus amplitude. The error bars denote the 95% confidence intervals of the mean and "*" indicates a significant difference between subjects with PD off medication and age-matched controls. Young controls were not included in statistical tests. **(C)** Sensory weighting in individual subjects in response to surface stimuli for controls, and subjects with PD off medication and on medication. Each data point represents a single subject at the given stimulus amplitude. Lines connect the data points for an individual subject across stimulus amplitudes. For subjects with PD, the numbers 1–8 correspond to the subject identifiers in **Table 1** (e.g., PD1 denoted as 1). All subject groups showed significant decreases in W_{prop} with increasing stimulus amplitude.

two PD_{On} subjects (PD4, PD8) across all stimulus amplitudes. In fact, when off medication, PD8 weighted proprioception more than any control subject for the 2° and 4° surface-stimulus amplitudes. In the on medication condition, PD4 and PD8 had a larger W_{prop} than any controls for the 2° and 4° surface-stimuli. Medication noticeably changed W_{prop} in two of the eight subjects with PD (**Figure 6C**); W_{prop} increased in PD4 and decreased in PD7 across all stimulus amplitudes when on vs. off medication. Thus, large changes in W_{prop} occurred with medication in some individual subjects, but the direction of change was not systematic. In addition, three (PD1, PD4, PD8) of the four PD_{Off} subjects who fell on all attempts at sway-referenced trials had larger W_{prop} in the 2° and 4° surface-stimulus trials than the PD_{Off} subjects that did not fall. One of the three PD_{On} subjects (PD8) who fell on all attempts at sway-referenced trials also had larger proprioceptive weights for all surface-stimulus trials than PD_{On} subjects who did not fall.

Additional differences between control and individual subjects with PD were related to how well they changed proprioceptive weighting between surface-stimulus amplitudes (**Figure 6C**). To quantify this difference in W_{prop} between control and subjects with PD, we computed the slope of the proprioceptive weights between successive surface-stimulus amplitudes. PD_{Off} subjects' slope of proprioceptive weighting was less than controls between 1° and 2° surface-stimulus amplitudes (**Figure 6B**; $p = 0.038$). However, there was no difference between PD_{Off} and control subjects in the slope of proprioceptive weighting between 2° and 4° surface-stimulus amplitudes ($p = 0.51$).

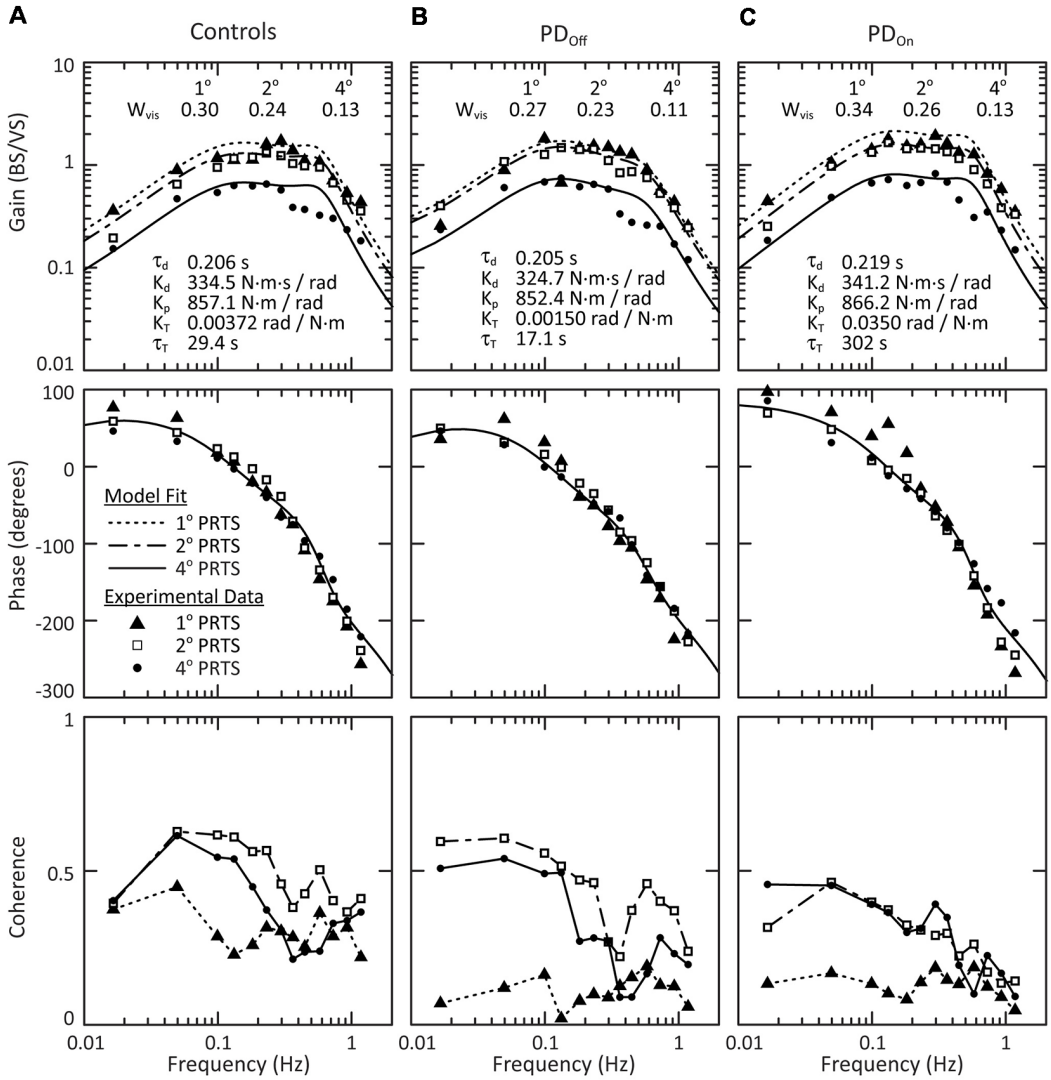

FIGURE 7 | Mean behavior across subjects in response to visual stimuli. Gain, phase and coherence plots for **(A)** control subjects, **(B)** subjects with PD off medication, and **(C)** subjects with PD on medication. The data points denote experimental data for the mean behavior across subject and the curves on the gain and phase plots are the model fits to this mean behavior. The parameters of the model fits are listed on the gain plots. Data for all three stimulus amplitudes were fit simultaneously, with a W_{vis} for each stimulus amplitude and a single τ_d, K_d, K_p, K_T, and τ_T across all stimulus amplitudes. The lines connecting data points on the coherence plots (bottom row) are for visualization and are not related to the model fits.

Group Response to Visual-Stimuli

In response to visual-stimuli, both PD and age-matched control subjects had decreasing FRF gains with increasing stimulus amplitude (**Figure 7**, top row). For a given stimulus amplitude, the gain in response to a visual stimulus was lower than the gain in response to a surface stimulus (compare **Figures 5**, **7**). In contrast to responses to surface stimuli, the phase curves in response to visual stimuli were similar across stimulus amplitude for all frequencies (**Figure 7**, middle row). Individual subject's responses to visual stimuli were small and variable. Consistent with this low gain and high variability, the coherence of the experimental data was consistently low for individual subjects (not shown) and the mean coherence across subjects (**Figure 7**, bottom row). Therefore, we did not consider statistics for individual subject responses to visual stimuli, and conclusions were based on a qualitative assessment of the average response across subjects.

All groups showed a mean tendency to decrease reliance on visual information with increasing visual-stimulus amplitude, as indicated by a monotonic decrease in W_{vis} with increasing visual-stimulus amplitude (**Figure 8**). Neither PD nor levodopa influenced visual weighting in response to visual stimuli (**Figure 8**).

Effect of Aging on Sensory Weighting

There was a tendency for our age-matched control subjects to have larger mean proprioceptive weights than younger controls (data from Peterka, 2002) in response to each surface

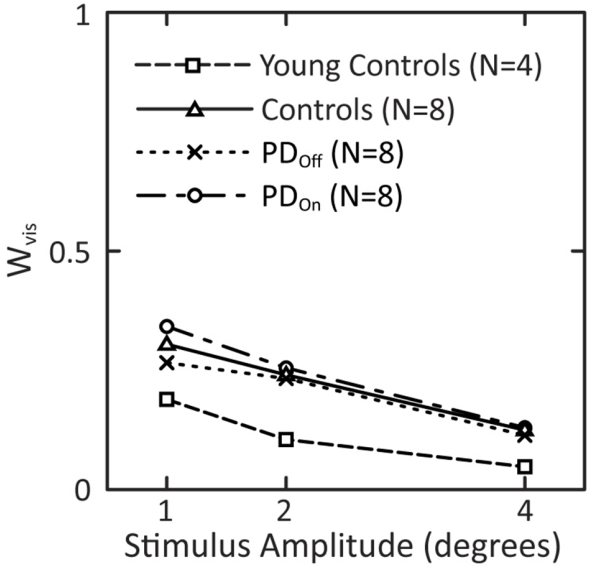

FIGURE 8 | Visual weights in response to visual-stimuli of different stimulus amplitudes. Data for subjects with PD and age-matched controls are taken from the model fits to the mean FRF data in **Figure 7.** Visual weights from fits to mean FRF data from four young controls are added to this plot.

stimulus (**Figure 6A**). On average across surface-stimulus amplitudes, W_{prop} for older controls was 1.1 times the W_{prop} for younger controls. The difference in the mean W_{prop} between older and younger control subjects was greatest for the 4° surface-stimulus amplitude. In addition, subjects with PD had larger proprioceptive weights than younger subjects for the 2° and 4° stimulus amplitudes (**Figure 6A**). The difference in proprioceptive weighting between 1° and 2° surface stimuli were similar for age-matched and younger control subjects, and both control groups had noticeably larger slopes than subjects with PD (**Figure 6B**).

The mean visual weight, W_{vis}, at each individual amplitude was smaller for young control subjects than either PD or age-matched control subjects (**Figure 8**). W_{vis} for older controls was on average 2.2 times larger than the W_{vis} for the younger controls. In addition, W_{vis} for PD_{On} and PD_{Off} subjects was on average 2.0 and 2.3 times, respectively, larger than W_{vis} for younger controls.

DISCUSSION

Despite profound balance and motor control deficits, our results demonstrate that subjects with PD can re-weight proprioceptive, visual, and vestibular information for postural control when sensory conditions change. Each PD and age-matched control subject decreased reliance on proprioceptive information as the surface-stimulus amplitude increased (**Figures 6A,C**). However, subjects with PD did not change proprioceptive weights as much as control subjects between the smallest surface-stimulus amplitudes (**Figure 6B**).

To appreciate the functional significance of the relatively small differences in sensory weighting between subjects with PD and controls, comparisons can be made to sensory weight changes associated with other neurological deficits. Specifically, sensory weights have been measured in subjects with bilateral (Figure 10 in Peterka, 2002) and unilateral vestibular loss (Figure 4 in Peterka et al., 2011) using similar methods. Bilateral vestibular loss subjects are 100% reliant on proprioception (W_{prop} = 1) and are unable to change weight when amplitudes of surface stimuli change on tests performed with eyes closed. Bilateral vestibular loss subjects were also unable to change visual weights with changing visual stimulus amplitude. Unilateral vestibular loss subjects were able to decrease W_{prop} with increasing surface amplitude, but their W_{prop} values were larger than age-matched controls by an average value of 0.28. Additionally, there was very little overlap in the distributons of W_{prop} values from unilateral loss and control subjects. These results in vestibular deficient subjects are in contrast to the substantial overlap of W_{prop} values in subjects with PD and controls at all stimulus amplitudes (**Figure 6C**) and emphasize the minimal effect of PD on sensory weighting and re-weighting.

The subjects in our study would be considered at increased risk for falls compared to age-matched controls given that they had moderate to severe PD (UPDRS Motor score 20–63), were diagnosed from 3 to 36 years ago, were dependent upon levodopa, and seven out of eight showed clinically apparent balance and gait problems. The moderately-to-severely affected patients in our study showed larger spontaneous sway in the mediolateral (ML) direction, especially when taking their levodopa medication, consistent with previous studies (Rocchi et al., 2002) and possibly related to dyskinesia (Chung et al., 2010; Curtze et al., 2015). In addition, fewer of our subjects with PD than age-matched controls were able to stand unsupported on a sway-referenced surface with eyes closed, especially when off levodopa, which is similar to other studies (Bronte-Stewart et al., 2002).

Other studies have shown that subjects with PD as severe as those in our study, have significant impairments in automatic postural responses, postural instability during gait, and in anticipatory postural adjustments (Horak et al., 1996; Rocchi et al., 2006b; Tagliabue et al., 2009). Despite including subjects with PD with a range of disease severity, we did not see any significant correlations between disease severity and impairments in sensory weighting. However, there was some indication that disease severity may be related to sensory weighting in that the two subjects with PD (PD4 and PD8) who had the disease the longest and had among the worst clinical PIGD scores in the UPDRS (**Table 1**) also relied more on proprioception than the other subjects with PD when on or off medication (**Figure 6C**). Future studies with larger sample sizes would be necessary to investigate this possible relatationship of severity and sensory weighting with other relevant outcome measures such as incidence of falls.

Sensory Integration and Sensory Transitions

Our results demonstrate that subjects with PD are capable of re-weighting sensory information for postural control. This is consistent with a previous study concluding that subjects with

PD can integrate sensory information to successfully perform a turning task before and after walking on a circular treadmill (Earhart et al., 2007). However, previous findings from our laboratory show that subjects with PD take more trials than control subjects to switch postural synergies when sensory conditions change (Horak et al., 1992; Chong et al., 1999b,c, 2000). For example, subjects with PD do not immediately inhibit ankle muscles when holding a handle or sitting on a stool during surface perturbations (Schieppati and Nardone, 1991; Horak et al., 1992, 1996). In addition, on the first trial of each of the sensory organization tests, subjects with PD fall more often than controls (Chong et al., 1999a). However, subjects with PD improve with repeated exposure to each sensory condition, such that by the third trial of a particular sensory condition, subjects with PD reach near control levels (Chong et al., 1999a). The third trial of each sensory condition is most similar to the steady-state conditions of our experiment. Therefore, this previous result is consistent with the mostly appropriate steady-state performance of our subjects with PD when compared to age-matched controls.

In response to changing surface-stimulus amplitudes in the absence of vision, our subjects with PD demonstrated an ability to re-weight proprioceptive information in a similar manner as age-matched controls. This result indicates that vision is not required for subjects with PD to generate appropriate steady-state postural responses. On the contrary, previous studies suggest that subjects with PD are more visually-dependent than age-matched controls, especially when visual information is misleading (Bronstein et al., 1990). For example, subjects with PD consistently undershoot voluntary arm movements and involuntary postural stepping responses when they cannot see their limbs (Jacobs and Horak, 2006; Tagliabue et al., 2009). It has also been shown that body sway is more driven by sinusoidally moving visual surrounds in subjects with PD than age-matched controls (Maurer et al., 2003). Although our subjects with PD showed slightly greater sway than our age-matched controls (**Figure 3C**), both groups showed sway increases with increasing visual-stimulus amplitude. These results differ qualitatively from the Maurer study in that their control subjects showed essentially no increase in sway with increasing visual-stimulus amplitude and showed significantly less sway than their subjects with PD. The difference between our results and the Maurer study may be due to the unusually young ages of their subjects with PD and hence the ages of their age-matched controls (48 years mean age of both groups). Consistent with age accounting for increased sensitivity to visual stimuli are the results in **Figure 8** showing that W_{vis} measures for young controls are about half the value of W_{vis} for our age-matched controls. That is, normal aging may result in a shift toward increased reliance on vision for balance; early onset PD may accelerate the shift, but older subjects show a similar reliance on vision independent of disease state.

Furthermore, some of our subjects with PD performed poorly on sway-referenced surface trials with eyes closed. In these trials, subjects must rely on vestibular information, as vision is absent and the sway-referenced surface minimizes proprioceptive cues. However, vestibular function has been shown to be normal in PD (Pastor et al., 1993). In fact, it has been shown that subjects with PD with deep brain stimulation weight proprioceptive information less and over-weight vestibular sense for postural control compared to age-matched controls (Maurer, 2009). Thus, it is unlikely that either vestibular dysfunction or an inability to use vestibular information for postural control account for the poor performance in subjects with PD on eyes closed sway-referenced trials. Consistent with our sensory re-weighting results, we suggest that most subjects with PD have normal vestibular function and are able to utilize it if given enough time to adjust to altered sensory conditions. The cause of poor performance on surface sway-referencing is likely a reduced ability of subjects with PD to quickly re-weight toward increased reliance on vestibular cues at the start of each test. Poor performance on eyes-closed sway-referenced trials is also observed in older subjects without PD and with normal vestibular function (Peterka and Black, 1990).

Re-weighting Sensitivity

Although subjects with PD were able to re-weight away from proprioception as surface-stimulus amplitude increased (**Figures 6A,C**), the difference in proprioceptive weights between the two smallest amplitudes of surface-stimuli was smaller in subjects with PD than age-matched controls but was the same for the two largest amplitudes (**Figure 6B**). This result is consistent with previous studies showing that subjects with PD have a higher threshold for perceiving the amplitude of proprioceptive stimuli (i.e., kinesthesia) than age-matched controls (Konczak et al., 2009), including an impaired ability to consciously perceive limb position (Maschke et al., 2003) or axial position (Wright et al., 2010). In addition, previous studies have demonstrated an increased neural synchrony in the basal ganglia circuitry with PD (Levy et al., 2000; Raz et al., 2001; Goldberg et al., 2004), suggesting a decrease in the signal-to-noise ratio of neural activity in the basal ganglia as dopamine levels decrease (Bergman et al., 1998; Bevan et al., 2002; Bar-Gad et al., 2003; Hammond et al., 2007). The higher threshold for detecting changes between the smallest proprioceptive stimuli that we observed in our study could be related to a decreased signal-to-noise ratio in the processing of sensory signals by dopaminergic circuitry.

Stiffness in PD

The parameter K_p, identified in model curve fits to FRF data (**Figures 5**, **7**), characterizes the amount of corrective torque generated per unit of body sway and, thus, can be considered to quantify the stiffness of the postural control system (Latash and Zatsiorsky, 1993). That is, if one were to apply a perturbing torque of a given amplitude to subjects of equal body dimensions, a subject with a larger K_p would have a smaller sway amplitude than a subject with a smaller K_p. Because rigidity is considered to be a hallmark of PD it may appear unexpected that K_p did not differ between subjects with PD and controls, and medication had no effect on K_p in subjects with PD.

However, in interpreting the meaning of stiffness and rigidity it is important to consider the context of the task that the subject is asked to perform, because the motor actions required for

some tasks are highly constrained while motor actions for other tasks are not constrained. For example, when arm rigidity is tested, as in a UPDRS measurement of rigidity, control subjects allow free movement of their arms and low rigidity is observed, while subjects with PD resist movement of their arm, and high rigidity is observed. Similarly, tests show that subjects with PD off levodopa medication have increased axial rigidity when compared to controls, and levodopa does not significantly reduce axial rigidity (Wright et al., 2007). In both arm movement and trunk twisting tasks there are no functionally detrimental consequences if subjects allow arm or axial trunk movements in response to a perturbing force. That is, these tasks are not fundamentally constrained. Control subjects are apparently able to recognize the context of these situations and naturally allow free movement whereas subjects with PD are unable to adjust to the context.

In contrast, the task of maintaining upright stance places constraints on motor control. Both subjects with PD and controls must maintain a minimal K_p in order to resist the destabilizing torque due to gravity. Therefore, control subjects do not have an option of choosing a postural stiffness that is much less than that of subjects with PD. The upper limit of K_p is also constrained because large K_p values also produce instability (Masani et al., 2008). Therefore, only limited differences in K_p between subjects with PD and controls are possible. Furthermore, the very close correspondence between K_p values in subjects with PD and controls suggests that subjects with PD were able to regulate stiffness under steady-state conditions as well as control subjects to achieve dynamic control of upright stance (Peterka and Loughlin, 2004).

Aging and Sensory Weighting

In response to a surface and visual stimuli, subjects with PD and age-matched controls show greater use of proprioceptive (**Figure 6A**) and visual (**Figure 8**) information (corresponding to larger W_{prop} and W_{vis} measures, respectively) compared to younger control subjects from a previous study (Peterka, 2002). For surface stimuli, greater sensitivity has been confirmed in more recent studies comparing younger and older adults with normal balance function (Cenciarini et al., 2010; Wiesmeier et al., 2015). These results indicate that subject age, not PD, determined the extent to which subjects utilized visual and proprioceptive information for postural control.

Effects of Dopamine Replacement

Levodopa improved clinical indicators of balance and gait, as well as rigidity, bradykinesia and tremor, as measured by the UPDRS. However, consistent with the literature, we demonstrated that levodopa increases CoP displacement in the mediolateral direction during quiet stance, consistent with increased risk for falling (Mitchell et al., 1995; Rocchi et al., 2002). Previously, we showed that automatic postural responses to transient perturbations were further reduced by levodopa medication (Horak et al., 1996). Our current results indicate that levodopa neither improves nor impairs sensory weighting in PD patients in conditions where sufficient time is allotted to achieve steady-state behavior.

Clinical Implications

Despite larger than normal postural sway during quiet stance and during larger sensory stimuli, our results show that subjects with PD do have the ability to change reliance on sensory information for postural control, given enough time to switch between tasks. This result does not conflict with our previous results showing that subjects with PD have difficulty switching quickly between different task demands (Horak et al., 1992; Chong et al., 1999b,c, 2000). Rather, it may be necessary for subjects with PD to transition slowly between tasks to avoid falls in the transition periods. In other words, postural instability in subjects with PD may be specific to the transition period. Consistent with this notion, we recently demonstrated that postural instability during walking in subjects with PD was specific to the transition period during heel-strike (Fino et al., 2018). If subjects with PD can ease through transition periods, they may be able to participate in activities that appear to challenge their postural stability (e.g., walking on a sandy beach). Conversely, if subjects with PD are required to produce a postural response during their transition period, they will likely demonstrate impaired postural responses that potentially increase the risk of falling. In addition, tasks requiring central processing of relatively small changes in sensory signals, such as walking from a firm to a more compliant surface, may be more affected by the loss of dopamine neurons, due to a decreased signal-to-noise ratio in the neural processing of sensory information and/or sensory integration signals. Consequently, patients may have trouble with tasks involving smaller changes in sensory conditions, but be successful at tasks in which there are larger changes in sensory conditions.

ETHICS STATEMENT

The Institutional Review Board at Oregon Health and Science University (OHSU) approved the protocol for this experiment, and all subjects gave written informed consent prior to participating.

AUTHOR CONTRIBUTIONS

KF contributed to the analysis, interpretation of the results, and preparation of the manuscript. RP and FH both contributed to the research funding and resources, conception, experimental design, data collection, analysis and interpretation of the results, and editing of the manuscript.

FUNDING

This research was supported by NIH grants R37-AG006457 and T32-NS045553.

ACKNOWLEDGMENTS

We thank the Parkinson's Center of Oregon for referring subjects to participate in this study. We also thank K. Statler and T. Nagel for collecting data, P. Carlson-Kuhta and J. Jacobs for administering the UPDRS, and S. Oster for editorial assistance.

REFERENCES

Abbruzzese, G., and Berardelli, A. (2003). Sensorimotor integration in movement disorders. *Mov. Disord.* 18, 231–240. doi: 10.1002/mds.10327

Agid, Y. (1991). Parkinson's disease: pathophysiology. *Lancet* 337, 1321–1324. doi: 10.1016/0140-6736(91)92989-F

Assländer, L., and Peterka, R. J. (2016). Sensory reweighting dynamics following removal and addition of visual and proprioceptive cues. *J. Neurophysiol.* 116, 272–285. doi: 10.1152/jn.01145.2015

Bar-Gad, I., Morris, G., and Bergman, H. (2003). Information processing, dimensionality reduction and reinforcement learning in the basal ganglia. *Prog. Neurobiol.* 71, 439–473. doi: 10.1016/j.pneurobio.2003.12.001

Baston, C., Mancini, M., Rocchi, L., and Horak, F. (2016). Effects of levodopa on postural strategies in Parkinson's disease. *Gait Posture* 46, 26–29. doi: 10.1016/j.gaitpost.2016.02.009

Bergman, H., Feingold, A., Nini, A., Raz, A., Slovin, H., Abeles, M., et al. (1998). Physiological aspects of information processing in the basal ganglia of normal and parkinsonian primates. *Trends Neurosci.* 21, 32–38. doi: 10.1016/s0166-2236(97)01151-x

Bevan, M. D., Magill, P. J., Terman, D., Bolam, J. P., and Wilson, C. J. (2002). Move to the rhythm: oscillations in the subthalamic nucleus-external globus pallidus network. *Trends Neurosci.* 25, 525–531. doi: 10.1016/s0166-2236(02)02235-x

Black, F. O., Shupert, C. L., Horak, F. B., and Nashner, L. M. (1988). Abnormal postural control associated with peripheral vestibular disorders. *Prog. Brain Res.* 76, 263–275. doi: 10.1016/s0079-6123(08)64513-6

Bloem, B. R., van Vugt, J. P., and Beckley, D. J. (2001). Postural instability and falls in Parkinson's disease. *Adv. Neurol.* 87, 209–223.

Brenière, Y. (1996). Why we walk the way we do. *J. Mot. Behav.* 28, 291–298. doi: 10.1080/00222895.1996.10544598

Bronstein, A. M., Hood, J. D., Gresty, M. A., and Panagi, C. (1990). Visual control of balance in cerebellar and parkinsonian syndromes. *Brain* 113, 767–779. doi: 10.1093/brain/113.3.767

Bronstein, A. M., Yardley, L., Moore, A. P., and Cleeves, L. (1996). Visually and posturally mediated tilt illusion in Parkinson's disease and in labyrinthine defective subjects. *Neurology* 47, 651–656. doi: 10.1212/wnl.47.3.651

Bronte-Stewart, H. M., Minn, A. Y., Rodrigues, K., Buckley, E. L., and Nashner, L. M. (2002). Postural instability in idiopathic Parkinson's disease: the role of medication and unilateral pallidotomy. *Brain* 125, 2100–2114. doi: 10.1093/brain/awf207

Brown, L. A., Cooper, S. A., Doan, J. B., Dickin, D. C., Whishaw, I. Q., Pellis, S. M., et al. (2006). Parkinsonian deficits in sensory integration for postural control: temporal response to changes in visual input. *Parkinsonism Relat. Disord.* 12, 376–381. doi: 10.1016/j.parkreldis.2006.03.004

Burleigh-Jacobs, A., Horak, F. B., Nutt, J. G., and Obeso, J. A. (1997). Step initiation in Parkinson's disease: influence of levodopa and external sensory triggers. *Mov. Disord.* 12, 206–215. doi: 10.1002/mds.870120211

Cenciarini, M., Loughlin, P. J., Sparto, P. J., and Redfern, M. S. (2010). Stiffness and damping in postural control increase with age. *IEEE Trans. Biomed. Eng.* 57, 267–275. doi: 10.1109/tbme.2009.2031874

Cenciarini, M., and Peterka, R. J. (2006). Stimulus-dependent changes in the vestibular contribution to human postural control. *J. Neurophysiol.* 95, 2733–2750. doi: 10.1152/jn.00856.2004

Chong, R. K., Horak, F. B., Frank, J., and Kaye, J. (1999a). Sensory organization for balance: specific deficits in Alzheimer's but not in Parkinson's disease. *J. Gerontol. A Biol. Sci. Med. Sci.* 54, M122–M128. doi: 10.1093/gerona/54.3.m122

Chong, R. K., Horak, F. B., and Woollacott, M. H. (1999b). Time-dependent influence of sensorimotor set on automatic responses in perturbed stance. *Exp. Brain Res.* 124, 513–519. doi: 10.1007/s002210050647

Chong, R. K., Jones, C. L., and Horak, F. B. (1999c). Postural set for balance control is normal in Alzheimer's but not in Parkinson's disease. *J. Gerontol. A Biol. Sci. Med. Sci.* 54, M129–M135. doi: 10.1093/gerona/54.3.m129

Chong, R. K., Horak, F. B., and Woollacott, M. H. (2000). Parkinson's disease impairs the ability to change set quickly. *J. Neurol. Sci.* 175, 57–70. doi: 10.1016/s0022-510x(00)00277-x

Chung, K. A., Lobb, B. M., Nutt, J. G., McNames, J., and Horak, F. (2010). Objective measurement of dyskinesia in Parkinson's disease using a force plate. *Mov. Disord.* 25, 602–608. doi: 10.1002/mds.22856

Cruz, C. F., Peionte, M. E. P., Okai-Nobrega, L. A., Okamoto, E., Fortaleza, A. C. S., Mancini, M., et al. (2018). Parkinson's disease does not alter automatic visual-motor coupling in postural control. *Neurosci. Lett.* 686, 47–52. doi: 10.1016/j.neulet.2018.08.050

Curtze, C., Nutt, J. G., Carlson-Kuhta, P., Mancini, M., and Horak, F. B. (2015). Levodopa is a double-edged sword for balance and gain in people with Parkinson's disease. *Mov. Disord.* 30, 1361–1370. doi: 10.1002/mds.26269

Davies, W. D. T. (1970). *System Identification for Self-Adaptive Control.* London, UK: Wiley-Interscience.

De Nunzio, A. M., Nardone, A., and Schieppati, M. (2007). The control of equilibrium in Parkinson's disease patients: delayed adaptation of balancing strategy to shifts in sensory set during a dynamic task. *Brain Res. Bull.* 74, 258–270. doi: 10.1016/j.brainresbull.2007.06.020

Earhart, G. M., Stevens, E. S., Perlmutter, J. S., and Hong, M. (2007). Perception of active and passive turning in Parkinson disease. *Neurorehabil. Neural Repair* 21, 116–122. doi: 10.1177/1545968306290674

Fasano, A., Canning, C. G., Hausdorff, J. M., Lord, S., and Rochester, L. (2017). Falls in Parkinson's disease: a complex and evolving picture. *Mov. Disord.* 32, 1524–1536. doi: 10.1002/mds.27195

Fino, P. C., Mancini, M., Curtze, C., Nutt, J. G., and Horak, F. B. (2018). Gait stability has phase-dependent dual-task costs in Parkinson's disease. *Front. Neurol.* 9:373. doi: 10.3389/fneur.2018.00373

Frenklach, A., Louie, S., Koop, M. M., and Bronte-Stewart, H. (2009). Excessive postural sway and the risk of falls at different stages of Parkinson's disease. *Mov. Disord.* 24, 377–385. doi: 10.1002/mds.22358

Goldberg, J. A., Rokni, U., Boraud, T., Vaadia, E., and Bergman, H. (2004). Spike synchronization in the cortex/basal-ganglia networks of Parkinsonian primates reflects global dynamics of the local field potentials. *J. Neurosci.* 24, 6003–6010. doi: 10.1523/JNEUROSCI.4848-03.2004

Hammond, C., Bergman, H., and Brown, P. (2007). Pathological synchronization in Parkinson's disease: networks, models and treatments. *Trends Neurosci.* 30, 357–364. doi: 10.1016/j.tins.2007.05.004

Horak, F. B. (1987). Clinical measurement of postural control in adults. *Phys. Ther.* 67, 1881–1885. doi: 10.1093/ptj/67.12.1881

Horak, F. B., Frank, J., and Nutt, J. (1996). Effects of dopamine on postural control in parkinsonian subjects: scaling, set, and tone. *J. Neurophysiol.* 75, 2380–2396. doi: 10.1152/jn.1996.75.6.2380

Horak, F. B., Nutt, J. G., and Nashner, L. M. (1992). Postural inflexibility in parkinsonian subjects. *J. Neurol. Sci.* 111, 46–58. doi: 10.1016/0022-510x(92)90111-w

Jacobs, J. V., and Horak, F. B. (2006). Abnormal proprioceptive-motor integration contributes to hypometric postural responses of subjects with Parkinson's disease. *Neuroscience* 141, 999–1009. doi: 10.1016/j.neuroscience.2006.04.014

Jeka, J. J., Oie, K. S., and Kiemel, T. (2008). Asymmetric adaptation with functional advantage in human sensorimotor control. *Exp. Brain Res.* 191, 453–463. doi: 10.1007/s00221-008-1539-x

Konczak, J., Corcos, D. M., Horak, F., Poizner, H., Shapiro, M., Tuite, P., et al. (2009). Proprioception and motor control in Parkinson's disease. *J. Mot. Behav.* 41, 543–552. doi: 10.3200/35-09-002

Latash, M. L., and Zatsiorsky, V. M. (1993). Joint stiffness: myth or reality? *Hum. Mov. Sci.* 12, 653–692. doi: 10.1016/0167-9457(93)90010-m

Levy, R., Hutchison, W. D., Lozano, A. M., and Dostrovsky, J. O. (2000). High-frequency synchronization of neuronal activity in the subthalamic nucleus of parkinsonian patients with limb tremor. *J. Neurosci.* 20, 7766–7775. doi: 10.1523/jneurosci.20-20-07766.2000

Mancini, M., and Horak, F. B. (2010). The relevance of clinical balance assessment tools to differentiate balance deficits. *Eur. J. Phys. Rehabil. Med.* 46, 239–248.

Mancini, M., Horak, F. B., Zampieri, C., Carlson-Kuhta, P., Nutt, J., and Chiari, L. (2011). Trunk accelerometry reveals postural instability in untreated Parkinson's disease. *Parkinsonism Relat. Disord.* 17, 557–562. doi: 10.1016/j.parkreldis.2011.05.010

Masani, K., Vette, A. H., Kawashima, N., and Popovic, M. R. (2008). Neuromusculoskeletal torque-generation process has a large destabilizing effect on the control mechanism of quiet standing. *J. Neurophysiol.* 100, 1465–1475. doi: 10.1152/jn.00801.2007

Maschke, M., Gomez, C. M., Tuite, P. J., and Konczak, J. (2003). Dysfunction of the basal ganglia, but not the cerebellum, impairs kinaesthesia. *Brain* 126, 2312–2322. doi: 10.1093/brain/awg230

Matsuda, K., Suzuki, Y., Yoshikawa, N., Yamamoto, T., Kiyono, K., Tanahashi, T., et al. (2016). Postural flexibility during quiet standing in healthy elderly and patients with Parkinson's disease. *Conf. Proc. IEEE Eng. Med. Biol. Soc.* 2016, 29–32. doi: 10.1109/embc.2016.7590632

Maurer, C. (2009). Postural deficits in Parkinson's disease are caused by insufficient feedback motor error correction and by deficits in sensory reweighting. *Clin. Neurophysiol.* 120:e82. doi: 10.1016/j.clinph.2008.07.198

Maurer, C., Mergner, T., Xie, J., Faist, M., Pollak, P., and Lücking, C. H. (2003). Effect of chronic bilateral subthalamic nucleus (STN) stimulation on postural control in Parkinson's disease. *Brain* 126, 1146–1163. doi: 10.1093/brain/awg100

Mitchell, S. L., Collins, J. J., DeLuca, C. J., Burrows, A., and Lipsitz, L. A. (1995). Open-loop and closed-loop postural control mechanisms in Parkinson's disease: increased mediolateral activity during quiet standing. *Neuosci. Lett.* 197, 133–136. doi: 10.1016/0304-3940(95)11924-l

Mongeon, D., Blanchet, P., and Messier, J. (2009). Impact of Parkinson's disease and dopaminergic medication on proprioceptive processing. *Neuroscience* 158, 426–440. doi: 10.1016/j.neuroscience.2008.10.013

Nagy, A., Eördegh, G., Parüczy, Z., Márkus, Z., and Benedek, G. (2006). Multisensory integration in the basal ganglia. *Eur. J. Neurosci.* 24, 917–924. doi: 10.1111/j.1460-9568.2006.04942.x

Nardone, A., and Schieppati, M. (2006). Balance in Parkinson's disease under static and dynamic conditions. *Mov. Disord.* 21, 1515–1520. doi: 10.1002/mds.21015

Nutt, J. G., Burchiel, K. J., Comella, C. L., Jankovic, J., Lang, A. E., Laws, E. R., et al. (2003). Randomized, double-blind trial of glial cell line-derived neurotrophic factor (GDNF) in PD. *Neurology* 60, 69–73. doi: 10.1212/wnl.60.1.69

O'Suilleabhain, P., Bullard, J., and Dewey, R. B. (2001). Proprioception in Parkinson's disease is acutely depressed by dopaminergic medications. *J. Neurol. Neurosurg. Psychiatry* 71, 607–610. doi: 10.1136/jnnp.71.5.607

Ozinga, S. J., Koop, M. M., Linder, S. M., Machado, A. G., Dey, T., and Alberts, J. L. (2017). Three-dimensional evaluation of postural stability in Parkinson's disease with mobile technology. *NeuroRehabilitation* 41, 211–218. doi: 10.3233/nre-171473

Pastor, M. A., Day, B. L., and Marsden, C. D. (1993). Vestibular induced postural responses in Parkinson's disease. *Brain* 116, 1177–1190. doi: 10.1093/brain/116.5.1177

Peterka, R. J. (2002). Sensorimotor integration in human postural control. *J. Neurophysiol.* 88, 1097–1118. doi: 10.1152/jn.2002.88.3.1097

Peterka, R. J. (2003). Simplifying the complexities of maintaining balance. *IEEE Eng. Med. Biol. Mag.* 22, 63–68. doi: 10.1109/memb.2003.1195698

Peterka, R. J., and Black, F. O. (1990). Age-related changes in human postural control: sensory organization tests. *J. Vestib. Res.* 1, 73–85.

Peterka, R. J., and Loughlin, P. J. (2004). Dynamic regulation of sensorimotor integration in human postural control. *J. Neurophysiol.* 91, 410–423. doi: 10.1152/jn.00516.2003

Peterka, R. J., Murchison, C. F., Parrington, L., Fino, P. C., and King, L. A. (2018). Implementation of a central sensorimotor integration test for characterizaion of human balance control during stance. *Front. Neurol.* 9:1045. doi: 10.3389/fneur.2018.01045

Peterka, R. J., Statler, K. D., Wrisley, D. M., and Horak, F. B. (2011). Postural compensation for unilateral vestibular loss. *Front. Neurol.* 2:57. doi: 10.3389/fneur.2011.00057

Raz, A., Frechter-Mazar, V., Feingold, A., Abeles, M., Vaadia, E., and Bergman, H. (2001). Activity of pallidal and striatal tonically active neurons is correlated in mptp-treated monkeys but not in normal monkeys. *J. Neurosci.* 21:RC128. doi: 10.1523/JNEUROSCI.21-03-j0006.2001

Rocchi, L., Chiari, L., Cappello, A., and Horak, F. B. (2006a). Identification of distinct characteristics of postural sway in Parkinson's disease: a feature selection procedure based on principal component analysis. *Neurosci. Lett.* 394, 140–145. doi: 10.1016/j.neulet.2005.10.020

Rocchi, L., Chiari, L., Mancini, M., Carlson-Kuhta, P., Gross, A., and Horak, F. B. (2006b). Step initiation in Parkinson's disease: influence of initial stance conditions. *Neurosci. Lett.* 406, 128–132. doi: 10.1016/j.neulet.2006.07.027

Rocchi, L., Chiari, L., and Horak, F. B. (2002). Effects of deep brain stimulation and levodopa on postural sway in Parkinson's disease. *J. Neurol. Neurosurg. Psychiatry* 73, 267–274. doi: 10.1136/jnnp.73.3.267

Schieppati, M., and Nardone, A. (1991). Free and supported stance in Parkinson's disease. The effect of posture and 'postural set' on leg muscle responses to perturbation, and its relation to the severity of the disease. *Brain* 114, 1227–1244. doi: 10.1093/brain/114.3.1227

Tagliabue, M., Ferrigno, G., and Horak, F. (2009). Effects of Parkinson's disease on proprioceptive control of posture and reaching while standing. *Neuroscience* 158, 1206–1214. doi: 10.1016/j.neuroscience.2008.12.007

Wiesmeier, I. K., Dalin, D., and Maurer, C. (2015). Elderly use proprioception rather than visual or vestibular cues for postural motor control. *Front. Aging Neurosci.* 7:97. doi: 10.3389/fnagi.2015.00097

Winter, D. A., Patla, A. E., Prince, F., Ishac, M., and Gielo-Perczak, K. (1998). Stiffness control of balance in quiet standing. *J. Neurophysiol.* 80, 1211–1221. doi: 10.1152/jn.1998.80.3.1211

Wright, W. G., Gurfinkel, V. S., King, L. A., Nutt, J. G., Cordo, P. J., and Horak, F. B. (2010). Axial kinesthesia is impaired in Parkinson's disease: effects of levodopa. *Exp. Neurol.* 225, 202–209. doi: 10.1016/j.expneurol.2010.06.016

Wright, W. G., Gurfinkel, V. S., Nutt, J., Horak, F. B., and Cordo, P. J. (2007). Axial hypertonicity in Parkinson's disease: direct measurements of trunk and hip torque. *Exp. Neurol.* 208, 38–46. doi: 10.1016/j.expneurol.2007.07.002

Conflict of Interest Statement: The authors declare that the research was conducted in the absence of any commercial or financial relationships that could be construed as a potential conflict of interest.

frontiers in Neurology

ORIGINAL RESEARCH
published: 26 April 2019
doi: 10.3389/fneur.2019.00385

Motor Timing in Tourette Syndrome: The Effect of Movement Lateralization and Bimanual Coordination

Davide Martino[1], *Andreas Hartmann*[2,3,4], *Elisa Pelosin*[5,6], *Giovanna Lagravinese*[5], *Cecile Delorme*[2,3,4], *Yulia Worbe*[2,7] *and Laura Avanzino*[6,8]*

[1] Department of Clinical Neurosciences, University of Calgary and Hotchkiss Brain Institute, Calgary, AB, Canada, [2] Sorbonne Université, UMR S 1127, CNRS UMR 7225, ICM, Paris, France, [3] Department of Neurology, Groupe Hospitalier Pitié-Salpêtrière, Assistance Publique-Hôpitaux de Paris, 47-83 boulevard de l'Hôpital, Paris, France, [4] French National Reference Centre for Gilles de la Tourette Syndrome, Groupe Hospitalier Pitié-Salpêtrière, Paris, France, [5] Department of Neuroscience, Rehabilitation, Ophthalmology, Genetics and Maternal Child Health, Genoa, Italy, [6] Ospedale Policlinico San Martino-IRCCS, Genoa, Italy, [7] Department of Physiology, Saint-Antoine Hospital, Paris, France, [8] Section of Human Physiology, Department of Experimental Medicine, University of Genoa, Genoa, Italy

OPEN ACCESS

Edited by:
Matt J. N. Brown, California State University, Sacramento, United States

Reviewed by:
Christos Ganos, Charité Medical University of Berlin, Germany
Pedro Ribeiro, Federal University of Rio de Janeiro, Brazil

***Correspondence:**
Laura Avanzino
lavanzino76@gmail.com

Specialty section:
This article was submitted to Movement Disorders, a section of the journal Frontiers in Neurology

Received: *14 December 2018*
Accepted: *29 March 2019*
Published: *26 April 2019*

Citation:
Martino D, Hartmann A, Pelosin E, Lagravinese G, Delorme C, Worbe Y and Avanzino L (2019) Motor Timing in Tourette Syndrome: The Effect of Movement Lateralization and Bimanual Coordination. Front. Neurol. 10:385. doi: 10.3389/fneur.2019.00385

The study of motor timing informs on how temporal information integrates with motor acts. Cortico-basal ganglia and cortico-cerebellar circuits control this integration, whereas transcallosal interhemispheric connectivity modulates finely timed lateralized or bimanual actions. Motor timing abilities are under-explored in Tourette syndrome (TS). We adopted a synchronization-continuation task to investigate motor timing in sequential movements in TS patients. We studied 14 adult TS patients and 19 age-matched healthy volunteers. They were asked to tap in synchrony with a metronome cue (SYNC) and then, when the tone stopped, to keep tapping, maintaining the same rhythm (CONT). We tested both a sub-second and a supra-second inter-stimulus interval between the cues. Subjects randomly performed a single-hand task with the right hand and a bimanual task using both hands simultaneously wearing sensor-engineered gloves. We measured the temporal error and the interval reproduction accuracy index. We also performed MRI-based diffusion tensor imaging and probabilistic tractography of inter-hemispheric corpus callosum (CC) connections between supplementary motor areas (SMA) and the left SMA-putamen fiber tract. TS patients were less accurate than healthy individuals only on the single-hand version of the CONT task when asked to reproduce supra-second time interval. Supra-second time processing improved in TS patients in the bimanual task, with the performance of the right hand on the bimanual version of the CONT task being more accurate than that of the right hand on the single-hand version of the task. We detected a significantly higher fractional anisotropy (FA) in both SMA-SMA callosal and left-sided SMA-putamen fiber tracts in TS patients. In TS patients only, the structural organization of transcallosal connections between the SMAs and of the left SMA-putamen tract was higher when the motor timing accuracy of the right hand on the bimanual version of the task was lower. Abnormal timing performance for supra-second time processing is suggestive of a defective network inter-connecting the

striatum, the dorsolateral prefrontal cortex and the SMA. An increase in accuracy on the bimanual version of the CONT task may be the result of compensatory processes linked to self-regulation of motor control, as witnessed by plastic rearrangement of inter-hemispheric and cortical-subcortical fiber tracts.

Keywords: Tourette syndrome, timing, supplementary motor area, motor control, MRI, bimanual

INTRODUCTION

The study of motor timing explores the processing of information on temporal durations during the preparation and execution of motor actions (1–4). Motor timing is a key functional domain influencing the efficiency and the appropriateness to the context of any motor output. Both cortico-basal ganglia and cerebellar networks are involved in this neural computation (5–9), and represent also the pivotal circuitries in the generation of abnormal movements. Furthermore, inter-hemispheric connectivity, primarily supported by callosal fibers, integrates temporal information for finely timed lateralized or bimanual acts (10, 11). Despite the relevance of time processing to the organization of motor control and the overlap between neural networks of motor timing and the neural substrate of tic generation, data on motor timing abilities in patients with Tourette syndrome (TS) are scarce (12). Similar to other uncontrollable, abnormal movements like chorea and dystonia, the temporal pattern of tic expression appears to have a random, albeit repetitive, character, which is clearly different from the appropriately contextualized timing of voluntary, goal-directed movements. Unlike other abnormal movements, on the other hand, tics are characterized by the subject's ability to inhibit them on demand, albeit with variable efficiency. This ability implies a time-sensitive motor control that aims to interrupt the chronological succession of premonitory urge and tic; the timing aspect of this inhibitory effort is relevant to the proficient application of strategies to diminish tics used in behavioral treatment approaches, e.g., habit reversal therapy or exposure response prevention. Moreover, anecdotal and science literature (13) reports an association of TS patients with altered sense and perception of time, including speed of motor actions. Therefore, motor timing performance in patients with tics represents a topic deserving greater attention and investigation.

Motor timing can be directly evaluated by performing explicit timing tasks, in which subjects make explicit use of temporal information (e.g., estimates of the duration of stimuli or intervals between stimuli) to represent precise temporal durations through a motor action (4). One of the most commonly adopted explicit timing tasks is the synchronization-continuation paradigm, which involves the time-controlled execution of sequential movements. This paradigm consists in: (i) a synchronization –or externally triggered- phase, in which subjects are asked to tap in synchrony with a train of tones separated by a constant inter-stimulus interval (ISI), and (ii) a continuation –or internally triggered- phase, in which subjects are requested to continue tapping at the previous rate in the absence of the auditory cue. The difference in external/internal drive between these two phases is consistent with differences in their neural substrate, with the continuation phase being selectively associated with the activation of a network connecting the supplementary motor area, the left caudal putamen and the left ventrolateral thalamus (14).

In this study, we apply the synchronization-continuation paradigm to adults with TS and age-matched healthy volunteers, and explore the relationship between performance on this task and structural connectivity of putatively relevant neural networks. Furthermore, since performance on the synchronization-continuation test is largely dependent on the duration of the inter-stimulus interval (ISI), we tested both a sub-second (metronome rate: 2 Hz, ISI: 500 ms) and a supra-second (metronome rate: 0.5 Hz, ISI: 2,000 ms) inter-stimulus interval between the cues. Importantly, processing of different interval durations in explicit timing tasks may also have a neural correlate, as cerebellar networks appear to be specifically involved in the processing of sub-second intervals when synchronization to an external rhythm is required. Finally, in the version of the synchronization-continuation paradigm adopted herein, subjects performed both a single-hand task with the right hand and a bimanual task using both hands simultaneously. This distinction is also relevant to TS, as we have previously shown in the same sample, that adult TS patients exhibit an abnormal ability to lateralize finger movements in sequential tasks, with increased accuracy when the task is performed bimanually (15). In this previous study, we also documented the loss of a physiological association between lateralization ability and transcallosal connectivity of motor cortical regions. However, the timing aspect of this motor lateralization pattern has never been investigated.

The first aim of our study was to explore the presence of differences in performance on this explicit timing paradigm between TS patients and healthy subjects, and whether these differences are specific for sub-second or supra-second time processing, as well as for the externally triggered (SYNC) mode or the internally triggered (CONT) mode on the single hand task. Given the established relationship between tic generation and the sensorimotor loop of the cortico-basal ganglia circuitry, we anticipate that TS patients with tics persisting in adulthood will manifest decreased accuracy on the explicit timing task explored herein. In particular, given the hypothesized specific role of the sensorimotor loop of the cortico-basal ganglia in sustaining explicit timing activities related to previously learned time durations (16), we anticipate: (i) a greater loss of accuracy in TS patients on the continuation phase for longer duration intervals; (ii) a negative correlation between timing accuracy and tic severity; (iii) a positive correlation between the structural organization of the fiber tracts connecting supplementary motor area and putamen of

the left hemisphere and timing accuracy of the right hand in TS patients.

The second aim of our study was to evaluate whether single hand vs. bimanual mode of execution of the task influences explicit motor timing accuracy. In line with our previous findings showing abnormal ability to lateralize finger movements (15), we anticipate decreased accuracy on the explicit timing task when this is performed with a single hand compared to bimanual mode. Moreover, based on our previous work, we hypothesize a lack of association between the ability to lateralize motor performance and the structural organization of the callosal tracts interconnecting the supplementary motor area of the two hemispheres.

MATERIALS AND METHODS

Participants

Patients were recruited from the National Reference Center for Gilles de la Tourette syndrome at the Pitié-Salpêtrière Hospital in Paris, France. Fourteen patients with TS (8 males; mean age 32.9 ± 9.9 SD years) participated in the study. The sample of TS patients recruited in the present study is the same explored in our previous work (15). Inclusion criteria for patients were: (i) age >18 years; (ii) having a confirmed diagnosis of TS according to the Diagnostic and Statistical Manual of Mental Disorders-5 (DSM-5) criteria (17). We applied the following exclusion criteria: (i) co-occurrence of Axis I psychiatric disorders, established by the Mini International Neuropsychiatry Inventory (18), with the exception of obsessive-compulsive disorder; co-occurrence of autistic spectrum disorder, substance abuse aside from nicotine, current major depressive episode, current or past diagnosis of psychotic disorder; patients with a current or past diagnosis of ADHD, as per DSM-5 criteria, were also excluded; (ii) any neurologic disorder other than tics; (iii) visual or hearing impairment; (iv) severe orthopedic problems of the upper limb. We recruited 19 age- and sex-matched healthy subjects (HC, 10 males; mean age 31.8 ± 5.1 years) as control subjects from hospital staff or patients' spouses or friends. Exclusion criteria were the same as for TS patients, plus (i) a personal history of tics, and (ii) any concomitant treatment except for oral contraceptives. All participants were right-handed; we confirmed right hand dominance using the Edinburgh Handedness Inventory (19).

Table 1 reports demographic and clinical information for TS patients. Three TS patients were on treatment with antipsychotic drugs (aripiprazole, risperidone, pimozide), one with citalopram, and one with clonazepam; in each of these patients, the medication dose had been stable for at least 4 weeks. Tic severity was assessed using the Yale Global Tic Severity Scale (YGTSS), 0–50 total tic severity score (20). The local ethics committee (Pitie -Salpêtrière Hospital) approved the study and every participant gave informed written consent for participation. The Ethics committee project' number is INSERM C11-34, CPP 97/12.

Motor Studies

All subjects performed the motor task. Subjects sat in a comfortable chair in a quiet and darkened room. They wore a sensor-engineered glove (eTT, Genova, Italy) on both their hands. We acquired data at 1 KHz. We chose an eyes closed paradigm to avoid possible confounding effects due to the integration of acoustic and visual information. Subjects were demonstrated the finger sequence task (opposition of thumb to index, medium, ring, and little fingers) only once; subsequently, they were asked to perform the task keeping their eyes closed. The task consisted of performing the finger tapping sequential task in synchrony with a metronome cue (SYNC), and subsequently, when the tone stopped, to continue the same task trying to maintain the same rhythm as accurately as possible (CONT). Each phase (SYNC and CONT) lasted 45 s. Subjects performed two blocks in random order with a different metronome pace (2 Hz, i.e., time interval between two successive metronome cues: 500 ms; 0.5 Hz, i.e., time interval: 2,000 ms). The metronome pace values were chosen in order to have one sub-second time interval (500 ms) and one supra-second time interval (2,000 ms) between two successive auditory stimuli to be reproduced in the CONT task. Subjects randomly performed a single-hand task with the right hand and a bimanual task using both hands simultaneously. **Figure 1** summarizes the experimental protocol.

We processed data using a customized software (GAS, eTT, Genoa, Italy) that extracts the duration of the time interval between two successive finger contacts (in ms). In the CONT task, this interval corresponded to the time interval reproduced by the subjects. Performance on the tasks was analyzed by measuring the temporal error and the interval reproduction accuracy index (1). The temporal error corresponds to the duration of the time interval reproduced by the subject minus the duration of the time interval set by the metronome and provides a direct measure of the magnitude of the error in reproducing the corresponding time interval (in ms). The interval reproduction accuracy index is the ratio between the time interval reproduced by the subject and the time interval set by the metronome, and allows a comparison of performance at each time interval, independent of duration. This index provides also the directionality of the tapping performance, being >1 if the participant is behind the beat and <1 if the participant is ahead of the beat. The temporal error and the interval reproduction accuracy index were analyzed to explore: (1) performance on the single-hand task with the right hand, (2) movement lateralization (comparison of right hand performance on single-hand and bimanual tasks), (3) bimanual coordination (comparison of right- and left-hand performance during the bimanual task).

Statistical Analysis of Motor Performance

Single-Hand Task With the Right Hand

Temporal error and interval reproduction accuracy index were analyzed by means of a repeated measures analysis of variance (RM-ANOVA) with GROUP (TS patients, healthy subjects) as between-subjects factor and MODE (SYNC and CONT) and TIME INTERVAL (500 and 2,000 ms) as within-subjects factors.

Movement Lateralization

Temporal error and interval reproduction accuracy index were analyzed by means of a repeated measures analysis of variance (RM-ANOVA) with GROUP (TS patients, healthy subjects)

TABLE 1 | Main demographic and clinical data of patients with Tourette syndrome.

Patient	Age (years)	Sex	Age at onset (years)	Yale global tic severity scale (severity subscore/50)	Yale global tic severity scale (total score/100)	Presence of obsessive-compulsive symptoms	Current pharmacological treatment
1	42	F	6	10	20	OCBs	Clonazepam
2	29	F	6	12	12	No	Aripiprazole
3	38	M	7	18	38	OCD	Citalopram
4	24	M	6	14	14	No	None
5	30	M	8	12	32	OCBs	None
6	33	M	6	8	8	No	None
7	22	M	10	14	24	No	Risperidone
8	24	F	6	22	32	No	None
9	30	F	7	19	29	No	None
10	33	M	6	27	47	No	Pimozide
11	40	F	8	22	32	No	None
12	60	F	5	15	35	No	None
13	24	M	6	14	24	No	None
14	32	M	9	29	37	No	None

OCBs, obsessive-compulsive behavior; OCD, obsessive-compulsive disorder.

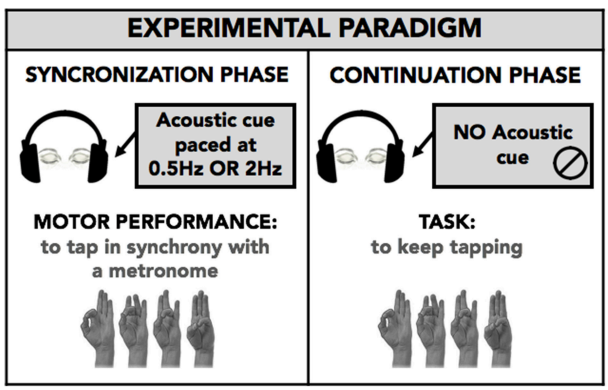

FIGURE 1 | Experimental paradigm. Subject performed with eyes closed a finger opposition movement sequence (opposition of thumb to index, medium, ring, and little fingers) in a synchronization-continuation task. Subjects were requested to tap in synchrony with a metronome cue (SYNC) and then, when the tone stopped, to tap the fingers in a sequential order, trying to maintain the same rhythm as accurately as possible (CONT-EXE). The acoustic cue was set at 0.5 and 2 Hz, to explore timing performance within a supra-second (0.5 Hz, 2,000 ms) and sub-second (2 Hz, 500 ms) time interval. The task was executed with right hand only (single hand task; RH-S) or both the right (RH-B) and left (LH-B) hands simultaneously (bimanual task). The analysis was planned to study for movement lateralization and bimanual coordination.

as between-subjects factor and MODE (SYNC and CONT), TASK (single-hand, bimanual), and TIME INTERVAL (500 and 2,000 ms) as within-subjects factors.

Bimanual Coordination

Temporal error and interval reproduction accuracy index were analyzed by means of a repeated measures analysis of variance (RM-ANOVA) with GROUP (TS patients, healthy subjects) as between-subjects factor and MODE (SYNC and CONT), SIDE (right, left), and TIME INTERVAL (500 and 2,000 ms) as within-subjects factors.

We performed *post hoc* analyses of significant interactions using *t*-tests applying the Bonferroni correction for multiple comparisons where necessary. We considered p values lower than 0.05 as threshold for statistical significance. We performed statistical analysis with SPSS 13.0.

Magnetic Resonance Imaging (MRI) Tractography Studies

Image Acquisition

Thirteen TS patients and 13 of the 19 healthy subjects underwent MRI-based diffusion tensor imaging and probabilistic tractography of inter-hemispheric corpus callosum (CC) connections between supplementary motor areas (SMA) and probabilistic tractography of the SMA-putamen connection of the left hemisphere.

Images were acquired on a 3T Siemens Trio MRI scanner (body coil excitation, 12-channel receive phased-array head coil). Anatomical scans were acquired using sagittal 3D T1-weighted magnetization prepared rapid acquisition gradient echo. The characteristics of diffusion weighted scans were as follow: echo time (TE): 87 ms; repetition time (TR): 12 s; 65 slices; matrix: 128 × 128; voxel size: 2 × 2 × 2 mm^3; partial Fourier factor: 6/8; grappa factor: 2; read bandwidth: 1,502 Hz/pixel; flip angle: 9°. Diffusion weighting was performed along 50 directions with a b-value of 1,000 $s{\cdot}mm^{-2}$. We also obtained a reference image with no diffusion weighting. We asked TS patients to suppress their tics during the acquisition in order to avoid movement artifacts.

Image Processing

We performed image pre-processing using the FSL toolbox from the FMRIB Software Library. We corrected diffusion

images for eddy current artifacts, and generated fractional anisotropy (FA) maps using FDT (FMRIB's Diffusion Toolbox). We applied the analytical Q-ball model to estimate the local underlying orientation distribution function (ODF) using a spherical harmonics order 6 and a regularization factor equal to 0.006 (21). We realigned the high-resolution 3D T1 volume to the diffusion data. We calculated the probabilistic distributions of the fiber orientations at each voxel using a constrained spherical deconvolution (CSD) model with the MRtrix software (22).

Probabilistic tractography was performed by the probtrackx toolbox of FSL software, using the left SMA a seed region of interest (ROI), and the left posterior putamen as waypoint and termination ROI. An exclusion mask was added on the midsagittal plane in order to avoid erratic fibers from the corpus callosum. ROI masks were created in each participant's diffusion space. The supplementary motor area (SMA) was anatomically defined as the medial cortex caudal to the VCA line of Talairach (line drawn through the anterior commissure perpendicular to the anterior commissure-posterior commissure line) (23). The posterior putamen was defined as the segment of the putamen caudal to the VCA line (24). The following parameters were used: 5,000 samples, curvature threshold 0.2. The tract mask from the probabilistic tractography map of each subject was used to compute the mean of FA weighted by track probability. We reconstructed tracts between the two SMA (SMA-SMA tract) regions and between the SMA and putamen for the left hemisphere. FA was extracted from each tract of interest in every subject.

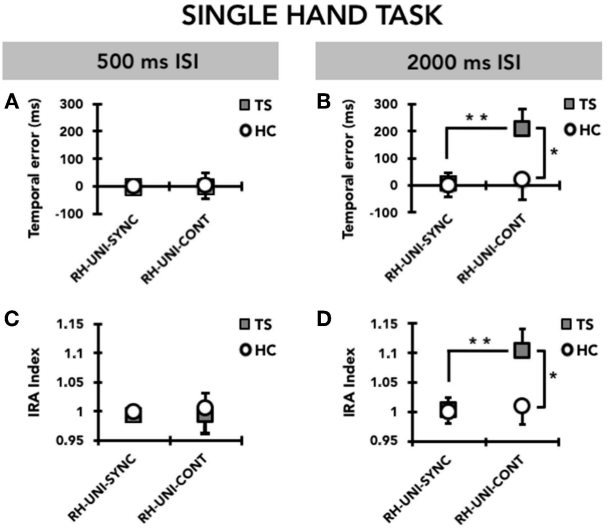

FIGURE 2 | Timing performance on the single-hand task (UNI) performed with the right hand (RH). Data of both patients with Tourette syndrome (TS) and healthy control subjects (HC) are shown. The results of the synchronization (SYNC) and continuation (CONT) tasks with a supra-second (0.5 Hz, 2,000 ms ISI) and sub-second (2 Hz, 500 ms ISI) time interval are shown. On the x-axis, we show the type of task. On the y-axis, we show the duration of the temporal error in ms **(A,B)** and the IRA expressed as a ratio between the time interval reproduced by the subject and the time interval set by the metronome **(C,D)**. Asterisks indicate when statistical analysis showed a significant difference (*$p < 0.05$, **$p < 0.01$). Mean data + standard error mean (SEM) are shown.

Statistical Analysis: Neuroimaging Data

Mean FA measures from SMA-SMA and from left-sided SMA-putamen fiber tracts were compared between the two groups using univariate ANOVA (separately for each tract) with age as a covariate of non-interest.

We also performed correlation analyses between FA values of SMA-SMA and left-sided SMA-putamen fiber tracts and severity of tics measured by YGTSS severity sub-score and relevant outcome measures of the motor task using Pearson's correlation test. These correlation analyses were performed separately for the TS patients and HC groups. All statistical analyses were performed with SPSS 22.0.

RESULTS

Single-Hand Task

Temporal Error

RM-ANOVA showed a significant effect of the TIME INTERVAL*GROUP*MODE interaction term ($F_{(1,31)} = 4.20$; $p = 0.049$). *Post hoc* analyses revealed that the temporal error for the supra-second time interval (2,000 ms, 0.5 Hz) was significantly larger in TS patients than in HC only in the CONT mode ($p = 0.045$), but not in the SYNC mode ($p = 0.47$ (**Figure 2**). Moreover, for the supra-second time interval, the temporal error was significantly larger in the CONT mode compared to the SYNC mode ($p = 0.008$) only in TS patients, but not in HC ($p = 0.77$). Finally, in TS patients only, temporal error in the CONT mode was significantly larger for the supra-second time interval compared to the sub-second time interval (TS, $p = 0.005$; HC, $p = 0.98$). *Post hoc* analyses revealed no difference in temporal error between TS patients and HC subjects for the sub-second time interval, either in the CONT or in the SYNC modes (all $p > 0.05$).

Interval Reproduction Accuracy Index

Like for temporal error, RM-ANOVA showed a significant effect of the TIME INTERVAL*GROUP*MODE interaction ($F_{(1,31)} = 4.42$; $p = 0.044$) also for the interval reproduction accuracy index. *Post hoc* analyses revealed that the accuracy in reproducing the supra-second time interval (2,000 ms, 0.5 Hz) was reduced in patients with TS compared to HC only in the CONT mode ($p = 0.045$), but not in the SYNC mode ($p = 0.48$) (**Figure 2**). Whereas the interval reproduction accuracy for the supra-second time interval was similar between CONT and SYNC in HC ($p = 0.77$), this parameter was significantly larger (i.e., performance was less accurate) in CONT with respect to SYNC ($p = 0.008$) in TS patients, but not in HC ($p = 0.78$). This indicates that TS patients manifest a significant tendency to remain "behind the beat" when asked to reproduce the supra-second time interval without the metronome cueing. Finally, only in the CONT mode and only in TS patients, the reproduction accuracy for the supra-second time interval was lower than for the sub-second time interval (TS, $p = 0.007$; HC, $p = 0.71$). We did not find any difference in the reproduction accuracy

for the sub-second time interval between TS patients and HC (all $p > 0.05$).

Movement Lateralization

Temporal Error

When we compared the timing ability of the right hand between the single-hand and the bimanual versions of the task, we observed that TS patients had greater timing ability on bimanual compared to single-hand (**Figure 3**). RM-ANOVA showed a significant effect of the TASK*MODE*TIME INTERVAL* GROUP interaction term ($F_{(1,31)} = 7.97$; $p = 0.008$). *Post hoc* analyses revealed that the temporal error was significantly larger in TS patients than in HC only for the supra-second time interval (2,000 ms, 0.5 Hz), on the single-hand version of the task and in the CONT mode ($p = 0.048$), but not on the bimanual version of the task or in the SYNC mode (all $p > 0.05$). Moreover, the temporal error of the right hand was significantly larger when reproducing a supra-second time interval compared to a sub-second time interval only in the single-hand version of the task, only in the CONT mode, and only in TS patients ($p = 0.005$). There was no statistically significant difference when comparing temporal error for supra-second and sub-second intervals in HC (all $p > 0.05$). Finally, for the supra-second time interval measured in the CONT mode, the temporal error of the right hand was significantly larger on the single-hand version of the task than on the bimanual version of the task in TS subjects ($p = 0.03$), but not in HC subjects ($p = 0.34$).

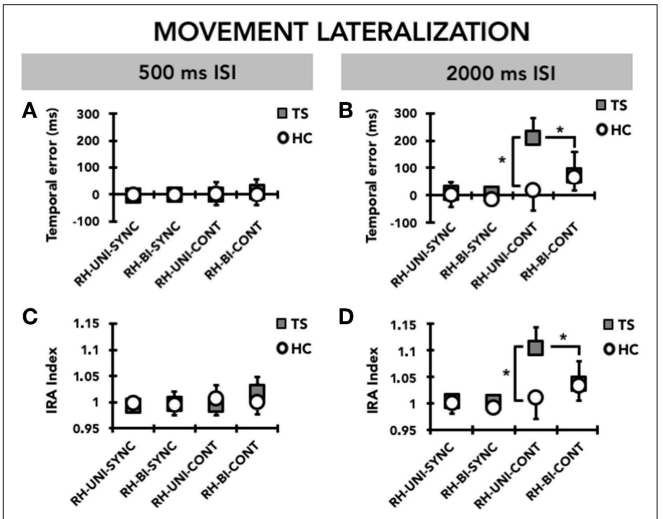

FIGURE 3 | Movement lateralization: timing performance of the right hand (RH) on the single-hand task (UNI) and on the bimanual task (BI). Data of both patients with Tourette syndrome (TS) and healthy control subjects (HC) are shown. The results of the synchronization (SYNC) and continuation (CONT) tasks with a supra-second (0.5 Hz, 2,000 ms ISI) and sub-second (2 Hz, 500 ms ISI) time interval are shown. On the x-axis, we show the type of task. On the y-axis, we show the duration of the temporal error in ms **(A,B)** and the IRA expressed as a ratio between the time interval reproduced by the subject and the time interval set by the metronome **(C,D)**. Asterisks indicate when statistical analysis showed a significant difference (*$p < 0.05$). Mean data + standard error mean (SEM) are shown.

Interval Reproduction Accuracy Index

RM-ANOVA showed a significant interaction TASK*MODE* TIME INTERVAL* GROUP ($F(1,31) = 10.34$; $p = 0.002$) (**Figure 3**). *Post hoc* analyses revealed that reproduction accuracy for the supra-second time interval (2,000 ms, 0.5 Hz) was smaller in TS patients than in HC only on the single-hand version of the task and in the CONT mode ($p = 0.045$), but not on the bimanual version of the task and in the SYNC mode (all $p > 0.05$). Moreover, TS patients were less accurate when reproducing a supra-second time interval compared to a sub-second time interval with the right hand only in the single-hand version of the task and in the CONT mode ($p = 0.007$), whereas no difference emerged when comparing supra-second and sub-second timing performance in HC (all $p > 0.05$). Finally, reproduction accuracy for the supra-second time interval was smaller on the single-hand version of the task than on the bimanual version of the task only in TS subjects and in the CONT mode ($p = 0.03$), but not in the SYNC mode and in HC subjects ($p = 0.34$).

Bimanual Coordination

Temporal Error

When we compared the timing ability of the right and left hand on the bimanual version of the task, we did not observe any difference either in the TS group or in the HC group (**Figure 4**). Accordingly, RM-ANOVA showed a significant effect only of MODE ($F_{(1,31)} = 4.42$; $p = 0.044$); *post hoc* analysis showed a larger temporal error in the CONT compared to the SYNC mode ($p = 0.044$). We did not detect any other significant effect for any of the other factors, or interaction terms between GROUP and any of the within-subjects factors.

Interval Reproduction Accuracy Index

Similar to the temporal error, RM-ANOVA for interval reproduction accuracy showed a significant effect of MODE ($F(1,31) = 5.36$; $p = 0.027$), whereby performance in the CONT mode was less accurate than that recorded in the SYNC mode ($p = 0.027$). Again, we did neither observe a significant effect for any other main factor, nor a significant interaction between GROUP and any of the within-subjects factors, indicating that there was no difference between TS and HC (**Figure 4**).

Tractographic Analysis

Compared to HC, TS patients yielded a significantly higher FA in both the SMA-SMA transcallosal tract ($F_{(1,26)} = 6.375$, $p = 0.018$; mean ± SD FA: 0.551 ± 0.109 in TS patients and 0.499 ± 0.018 in HC) and the left SMA-putamen tracts ($F_{(1,26)} = 4.47$, $p = 0.04$; mean ± SD FA: 0.478 ± 0.11 in TS patients and 0.415 ± 0.01 in HC). Importantly, there was no difference in the ROI mask size between groups in either hemisphere (all $p > 0.5$).

Correlation Analysis

We did not observe any significant correlation between FA values and severity of tics measured by YGTSS total severity score ($p > 0.5$).

We conducted correlation analyses in HC and TS patients separately between FA values and two selected motor outcome

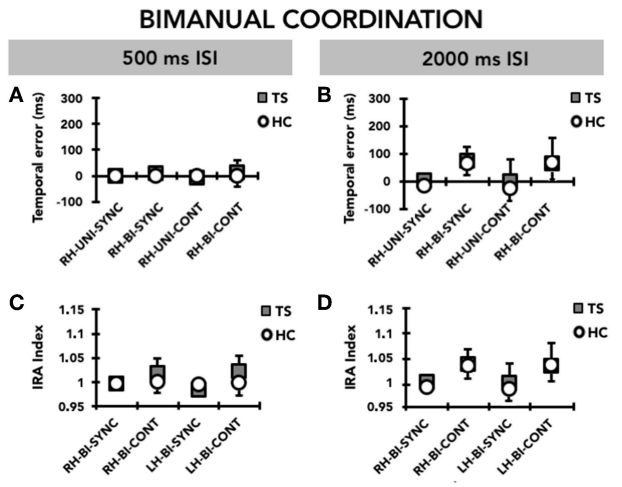

FIGURE 4 | Bimanual coordination: timing performance of the right hand (RH) and the left hand (LH) on the bimanual task (BI). Data of both patients with Tourette syndrome (TS) and healthy control subjects (HC) are shown. The results of the synchronization (SYNC) and continuation (CONT) tasks with a supra-second (0.5 Hz, 2,000 ms ISI) and sub-second (2 Hz, 500 ms ISI) time interval are shown. On the x-axis, we show the type of task. On the y-axis, we show the duration of the temporal error in ms **(A,B)** and the IRA expressed as a ratio between the time interval reproduced by the subject and the time interval set by the metronome **(C,D)**. Mean data + standard error mean (SEM) are shown.

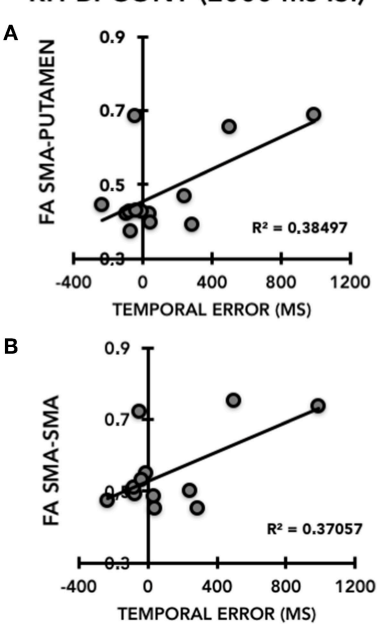

FIGURE 5 | Correlation between the temporal error of the right hand (RH) on the bimanual task (BI), continuation task (CONT) in the supra-second time interval task (2,000 ms, 0.5 Hz) (X-axis) and the FA of the left SMA-putamen (Y-axis) **(A)** and the FA SMA-SMA tracts (Y-axis) **(B)** in patients with Gilles de la Tourette syndrome (TS).

measures: (i) right hand temporal error for supra-second intervals in the CONT mode on the single-hand version of the task, selected because significantly different between TS patients and HC; (ii) right hand temporal error for supra-second intervals in the CONT mode on the bimanual version of the task, selected as a measure of movement lateralization. We chose not to conduct correlation analyses on interval reproduction accuracy because it yielded very similar between-group differences to temporal error and due to our limited sample size. There was no significant correlation in either the TS group or the HC group between FA values of the left SMA-putamen or of the SMA-SMA transcallosal tracts and right hand timing performance on the single-hand version of the motor timing task (all $p > 0.5$). Conversely, in TS patients we detected a positive correlation between the temporal error of the right hand on the bimanual version of the task in the CONT mode and for the supra-second time interval (2,000 ms, 0.5 Hz), and the FA value of the SMA-SMA tract ($r = 0.60$), which was just above the Bonferroni-corrected 0.025 (=0.05/2) threshold of significance ($p = 0.027$ (**Figure 5**). The same motor outcome measure yielded a significant positive correlation with the FA value of the left SMA-putamen tract ($r = 0.62$, $p = 0.024$) of TS patients. The same correlation analysis was not significant for HC (all $p > 0.05$ (**Figure 5**). Hence, in our TS patients we observed that the worse the timing performance of the right hand for the supra-second time interval on the bimanual version of the task (CONT mode only), the higher the FA value in the SMA-SMA and left SMA-putamen tracts.

DISCUSSION

In the present study, we adopted a synchronization-continuation task to investigate motor timing abilities in adult patients with TS and age-matched healthy volunteers. Further, we compared the performance of the right hand between a single-hand and a bimanual version of the same motor timing task to assess movement lateralization. Finally, we compared the performance of the two hands on the bimanual version of the task to assess bimanual coordination. Our task is an explicit motor timing task, in which the goal is to provide an accurate estimate of time intervals (4). During the metronome-cued phase (SYNC mode), subjects stored temporal information related to an auditory stimulus presented at regular inter-stimulus intervals (ISI) whilst reproducing the same ISI synchronously with the cue. During the non-cued phase (CONT mode), subjects used the temporal information acquired during the previous phase to continue reproducing through a motor sequence the same ISI, but in the absence of the auditory pacing cue.

In line with our hypotheses, we observed that adults with TS exhibit a specific deficit of motor timing accuracy with the right (dominant) hand, in which they consistently remain "behind the beat" when asked to reproduce a supra-second interval of 2,000 ms in the absence of metronome cueing (CONT mode). The reproduction accuracy is similar to healthy volunteers when patients reproduce the same interval synchronously with the metronome, or when they reproduce a sub-second interval of 500 ms.

The present findings add to a very scarce body of evidence of general and motor timing abilities in TS. Earlier studies (25, 26) failed to detect abnormalities of time estimation and reproduction in TS adults, but their recording methodology (a manual stopwatch) was inaccurate. Subsequently, using computerized timing tasks (27), our group showed that a pediatric TS population was more accurate than age-matched youth in the reproduction of supra-second time intervals using a motor action (tapping a keyboard key) to signal the end of the interval. In that study, timing accuracy correlated negatively with tic severity, which led to speculate a link between enhanced ability in time processing and adaptive changes within prefronto-basal ganglia circuits related to inhibitory control over tics. In a subsequent work, we reported that dopaminergic modulation with dopamine receptor blockers could improve the variability on a temporal discrimination task in TS children (28).

While these previous studies explored only the perceptual aspects of timing, the present study is the first in TS to address timing accuracy in the context of a fine motor task. The neural substrate of the motor performance exhibited during the synchronization-continuation task spans across the sensorimotor loop of the cortico-basal ganglia circuitry (interconnecting the dorsolateral striatum, the ventral thalamus, and primary motor and somatosensory, premotor and supplementary motor cortical regions) and cortico-cerebellar circuits. In particular, the striatal dopaminergic tone is believed to modulate a hypothetical "internal clock" beating the rhythm during internally generated movements. A recent conceptualization of temporal processing (16) suggests a unified timing mechanism across both sub- and supra-second intervals. According to this model, different regions within the deeply interconnected network involving both cortico-basal ganglia and cerebellar output pathways may specialize in different phases of time processing, albeit working in conjunction and across the whole spectrum of temporal durations. A body of evidence supports a prominent involvement of cerebellar output pathways in the initiation and adjustment of timing when facing a novel timing task (29–31), whereas the cortico-striato-thalamo-cortical circuits are more involved in the continuation phase or in the initiation of previously learned temporal durations (16, 32, 33). Following this conceptualization of timing, the synchronization-continuation task appears to be an ideal paradigm to inform on the neural substrate underlying selective deficits in motor timing abilities, such as that manifested by TS patients in this study. Along these lines, the specific decrease in motor timing accuracy in the continuation mode and for a supra-second interval is suggestive of a partial deficiency to sustain the accuracy of explicit motor timing, a functional domain likely to be subserved by the cortico-striato-thalamo-cortical circuit (34), in particular by its sensorimotor loop. In keeping with this, paced finger tapping tasks at supra-second intervals were found to be executed at a lower degree of accuracy in patients with different basal ganglia disorders, and this was associated with reduced activation within primary sensorimotor and supplementary motor cortical regions on functional imaging (4, 35–37). The lack of correlation between the timing inaccuracy on the single hand version of our task and tic severity does not confirm our a priori hypothesis, and suggests that explicit motor timing deficiencies do not directly reflect neural mechanisms underlying tic generation, but more likely represent a "trait" marker of dysfunction in this putative explicit timing network.

The second part of our findings indicates, in keeping with our a priori hypothesis, that the selective motor timing abnormality expressed, on a group basis, by the right hand of TS patients on the single-hand version of the task is no longer manifest when the same task is simultaneously performed by both hands. This suggests that the implementation of a bimanual set-up of a novel, moderately skilful manual task activates adaptive mechanisms that counteract this timing inaccuracy and/or that bimanual execution facilitates motor timing performance.

Previous studies from our group (15, 38) have demonstrated that TS patients of different age groups are more accurate in executing bimanually than single-handedly a fine manual task like the finger opposition task used herein. In our previous work on the same sample of TS adult patients, we observed that the gain in accuracy observed on the bimanual task compared to the single-hand one was larger when tics were less severe, suggesting this is likely an epiphenomenon of compensatory mechanisms (15). Furthermore, when we explored the neural substrate of the lateralization performed expressed as percentage of spatially correct sequences (15), we found that TS patients (i) exhibit higher structural organization of transcallosal connections between the primary motor and supplementary motor area and that (ii) they had lost the physiological association between the ability to lateralize motor performance and the transcallosal connectivity of these motor cortical regions. We therefore concluded that the abnormality to lateralize finger movements in the sequential tasks in TS could be the effect of neural compensation involving the transcallosal pathway with the aim to self-regulate motor control.

Whereas, these previous studies measured task accuracy as the percentage of correct movements, thus focusing on spatial structural aspects of the motor sequence, the present study explores the degree of lateralization of explicit motor timing abilities. In the present study, the same TS sample of adult patients used for the previous study exhibited higher structural organization of transcallosal connections between the supplementary motor regions and of the left SMA-putamen, confirming findings from our previous work (15). Furthermore, when the motor timing accuracy of the right hand on the bimanual version of the task was lower (i.e., larger temporal error), the structural organization of transcallosal and subcortical connections of left SMA was higher. Although based only on cross-sectional observation, this increase of the ipsi- and contralateral connectivity of a key nodal region in the cortico-striato-thalamo-cortical circuitry like the SMA can be interpreted as the consequence of an attempt to compensate for a functionally broader (i.e., both single hand and bimanual) deficit in motor timing accuracy. Consistently, Buse et al. (39) reported that the callosal sub-region 3, which includes the fiber tracts examined in our study, exhibits progressive growth over time during development in TS patients, probably underlying an attempt to accelerate interhemispheric transfer as a compensatory process. However, in the present study we did not observe any significant correlation between neither timing performance in the

single-hand nor in the bimanual version of the task and severity of tics. A possible explanation relies on the nature of the task that, by exploring motor timing abilities, is more dependent on a larger cortico-subcortical (involving also the prefrontal cortex) network than a pure motor task reliant only on accuracy of finger movements. Thus, even if there is not a direct link between motor timing ability and tic expression (differently from accuracy in motor performance).

Overall we interpret our cumulative evidence as an abnormality to lateralize finger movements in sequential tasks occurring in TS as a consequence of compensatory mechanisms in neural organization.

In conclusion, our study demonstrates that TS patients manifest "trait" abnormalities in the timing of sequential motor tasks, which are in keeping with the continuation phase of time processing, likely controlled by the sensorimotor loop of the cortico-basal ganglia network. We also show that the abnormal lateralization of fine motor control, previously reported in the context of the structural sequencing of fine motor tasks, extends also to motor timing accuracy. Finally, we highlight SMA connectivity as a potentially pivotal neural substrate of adaptive compensation of motor timing deficits in fine manual tasks in TS. We acknowledge that our results are based on a relatively small sample size. Another potential limitation is the lack of assessment for sub-diagnostic threshold ADHD symptomatology, although none of our TS patients had any history of current or past ADHD diagnosis. In this respect, future studies on larger samples should explore the presence of compensatory activation patterns using functional MRI, and correlate the level of this compensatory activation to the pattern of lateralization of motor timing abilities in TS patients. As for many other aspects of this complex neurodevelopmental disorder, longitudinal studies of multivariate datasets combining brain structure, brain performance and brain activation would have the potential to reveal the temporal trajectory of compensatory mechanisms that underlie phenotypic heterogeneity.

ETHICS STATEMENT

The local ethics committee (Pitie -Salpêtrière Hospital) approved the study and every participant gave informed written consent for participation. The Ethics committee project' number is INSERM C11-34, CPP 97/12.

AUTHOR CONTRIBUTIONS

LA, DM, YW, and AH conceived and designed the experiments and interpreted the data and critically revised the article for important intellectual content. LA, EP, CD, and DM performed the experiments. EP, GL, CD, and YW analyzed the data. LA, DM, EP, GL, CD, YW, and AH wrote the paper. LA, DM, and EP drafted the article.

FUNDING

This research was partly funded by the COST scientific programme, COST Action BM0905.

REFERENCES

1. Avanzino L, Pelosin E, Martino D, Abbruzzese G. Motor timing deficits in sequential movements in parkinson disease are related to action planning: a motor imagery study. *PLoS ONE.* (2013) 8:e75454. doi: 10.1371/journal.pone.0075454
2. Avanzino L, Martino D, Martino I, Pelosin E, Vicario CM, Bove M, et al. Temporal expectation in focal hand dystonia. *Brain.* (2013) 136:444–54. doi: 10.1093/brain/aws328
3. Martino D, Lagravinese G, Pelosin E, Chaudhuri RK, Vicario CM, Abbruzzese G, et al. Temporal processing of perceived body movement in cervical dystonia. *Mov Disord.* (2015) 30:1005–7. doi: 10.1002/mds.26225
4. Coull J, Nobre A. Dissociating explicit timing from temporal expectation with fMRI. *Curr Opin Neurobiol.* (2008) 18:137–44. doi: 10.1016/j.conb.2008.07.011
5. Witt ST, Laird AR, Meyerand ME. Functional neuroimaging correlates of finger-tapping task variations: an ALE meta-analysis. *Neuroimage.* (2008) 42:343–56. doi: 10.1016/j.neuroimage.2008.04.025
6. Ivry RB, Keele SW, Diener HC. Dissociation of the lateral and medial cerebellum in movement timing and movement execution. *Exp Brain Res.* (1988) 73:167–80.
7. Penhune VB, Zattore RJ, Evans AC. Cerebellar contributions to motor timing: a PET study of auditory and visual rhythm reproduction. *J Cogn Neurosci.* (1998) 10:752–65.
8. Jäncke L, Loose R, Lutz K, Specht K, Shah NJ. Cortical activations during paced finger-tapping applying visual and auditory pacing stimuli. *Cogn Brain Res.* (2000) 10:51–66. doi: 10.1016/S0926-6410(00)00022-7
9. Avanzino L, Bove M, Pelosin E, Ogliastro C, Lagravinese G, Martino D. The cerebellum predicts the temporal consequences of observed motor acts. *PLoS ONE.* (2015) 10:e0116607. doi: 10.1371/journal.pone.0116607
10. Sisti HM, Geurts M, Gooijers J, Heitger MH, Caeyenberghs K, Beets IA, et al. Microstructural organization of corpus callosum projections to prefrontal cortex predicts bimanual motor learning. *Learn Mem.* (2012) 19:351–7. doi: 10.1101/lm.026534.112
11. Gooijers J, Caeyenberghs K, Sisti HM, Geurts M, Heitger MH, Leemans A, et al. Diffusion tensor imaging metrics of the corpus callosum in relation to bimanual coordination: effect of task complexity and sensory feedback. *Hum Brain Mapp.* (2013) 34:241–52. doi: 10.1002/hbm.21429
12. Avanzino L, Pelosin E, Vicario CM, Lagravinese G, Abbruzzese G, Martino D. Time processing and motor control in movement disorders. *Front. Hum. Neurosci.* (2016) 10:631. doi: 10.3389/fnhum.2016.00631
13. Sacks O. FACT; a neurologist's notebook. *The New Yorker*. The Conde Nast Publications, Inc. (2004, August 23). p. 60.
14. Rao SM, Harrington DL, Haaland KY, Bobholz JA, Cox RW, Binder JR. Distributed neural systems underlying the timing of movements. *J Neurosci.* (1997) 17:5528–35.
15. Martino D, Delorme C, Pelosin E, Hartmann A, Worbe Y, Avanzino L. Abnormal lateralization of fine motor actions in tourette syndrome persists into adulthood. *PLoS ONE.* (2017) 12:e0180812. doi: 10.1371/journal.pone.0180812
16. Petter EA, Lusk NA, Hesslow G, Meck WH. Interactive roles of the cerebellum and striatum in sub-second and supra-second timing: support for an initiation, continuation, adjustment, and termination (ICAT) model of temporal processing. *Neurosci Biobehav Rev.* (2016) 71:739–55. doi: 10.1016/j.neubiorev.2016.10.015
17. American Psychiatric Association. *Diagnostic and Statistical Manual of Mental Disorders, DSM-5.* 5th ed. Arlington, VA (2013).

18. Sheehan DV, Lecrubier Y, Sheehan KH, Amorim P, Janavs J, Weiller E, et al. The mini-international neuropsychiatric interview (M.I.N.I.): the development and validation of a structured diagnostic psychiatric interview for DSM-IV and ICD-(2016) 10. *J Clin Psychiatry.* (1998) 59(Suppl 20):22–33;quiz 34–57.
19. Oldfield RC. The assessment and analysis of handedness: the edinburgh inventory. *Neuropsychologia.* (1971) 9:97–113.
20. Leckman JF, Riddle MA, Hardin MT, Ort SI, Swartz KL, Stevenson J, et al. The Yale global tic severity scale: initial testing of a clinician-rated scale of tic severity. *J Am Acad Child Adolesc Psychiatry.* (1989) 28:566–73.
21. Descoteaux M, Angelino E, Fitzgibbons S, Deriche R. Regularized, fast, and robust analytical Q-ball imaging. *Magn Reson Med.* (2007) 58:497–510. doi: 10.1002/mrm.21277
22. Tournier JD, Calamante F, Connelly A. Robust determination of the fibre orientation distribution in diffusion MRI: non-negativity constrained super-resolved spherical deconvolution. *Neuroimage.* (2007) 35:1459–72. doi: 10.1016/j.neuroimage.2007.02.016
23. Mayka MA, Corcos DM, Leurgans SE, Vaillancourt DE. Three-dimensional locations and boundaries of motor and premotor cortices as defined by functional brain imaging: a meta-analysis. *Neuroimage.* (2006) 31:1453–74. doi: 10.1016/j.neuroimage.2006.02.004
24. Lehéricy S, Ducros M, Krainik A, Francois C, Van de Moortele PF, Ugurbil K, et al. 3-D diffusion tensor axonal tracking shows distinct SMA and pre-SMA projections to the human striatum. *Cereb Cortex.* (2004) 14:1302–9. doi: 10.1093/cercor/bhh091
25. Goldstone S, Lhamon WT. The effects of haloperidol upon temporal information processing by patients with tourette's syndrome. *Psychopharmacology.* (1976) 50:7–10.
26. Goudriaan AE, Oosterlaan J, de Beurs E, van den Brink W. Neurocognitive functions in pathological gambling: a comparison with alcohol dependence, tourette syndrome and normal controls. *Addiction.* (2006) 101:534–47. doi: 10.1111/j.1360-0443.2006.01380.x
27. Vicario CM, Martino D, Spata F, Defazio G, Giacchè R, Martino V, et al. Time processing in children with Tourette's syndrome. *Brain Cogn.* (2010) 73:28–34. doi: 10.1016/j.bandc.2010.01.008
28. Vicario CM, Gulisano M, Martino D, Rizzo R. Timing recalibration in childhood Tourette syndrome associated with persistent pimozide treatment. *J Neuropsychol.* (2016) 10:211–22. doi: 10.1111/jnp.12064
29. Gooch CM, Wiener M, Wencil EB, Coslett HB. Interval timing disruptions in subjects with cerebellar lesions. *Neuropsychologia.* (2010) 48:1022–31. doi: 10.1016/j.neuropsychologia.2009.11.028
30. Ohmae S, Uematsu A, Tanaka M. Temporally specific sensory signals for the detection of stimulus omission in the primate deep cerebellar nuclei. *J Neurosci.* (2013) 33:15432–41. doi: 10.1523/JNEUROSCI.1698-13.2013
31. Teki S, Grube M, Kumar S, Griffiths TD. Distinct neural substrates of duration-based and beat-based auditory timing. *J Neurosci.* (2011) 31:3805–12. doi: 10.1523/JNEUROSCI.5561-10.2011
32. Bartolo R, Prado L, Merchant H. Information processing in the primate basal ganglia during sensory-guided and internally driven rhythmic tapping. *J Neurosci.* (2014) 34:3910–23. doi: 10.1523/JNEUROSCI.2679-13.2014
33. Jahanshahi M, Obeso I, Rothwell JC, Obeso JA. A Fronto-Striato-subthalamic-pallidal network for goal-directed and habitual inhibition. *Nat Rev Neurosci.* (2015) 16:719–32. doi: 10.1038/nrn4038
34. Merchant H, Harrington DL, Meck WH. Neural basis of the perception and estimation of time. *Annu Rev Neurosci.* (2013) 36:313–36. doi: 10.1146/annurev-neuro-062012-170349
35. Elsinger CL, Rao SM, Zimbelman JL, Reynolds NC, Blindauer KA, Hoffmann RG. Neural basis for impaired time reproduction in parkinson's disease: an fMRI study. *J Int Neuropsychol Soc.* (2003) 9:1088–98. doi: 10.1017/S1355617703970123
36. Jahanshahi M, Jones CR, Dirnberger G, Frith CD. The substantia Nigra pars compacta and temporal processing. *J Neurosci.* (2006) 26:12266–73. doi: 10.1523/JNEUROSCI.2540-06.2006
37. Jahanshahi M, Jones CR, Zijlmans J, Katzenschlager R, Lee L, Quinn N, et al. Dopaminergic modulation of striato-frontal connectivity during motor timing in Parkinson's disease. *Brain.* (2010) 133 (Pt 3):727–45. doi: 10.1093/brain/awq012
38. Avanzino L, Martino D, Bove M, De Grandis E, Tacchino A, Pelosin E, et al. Movement lateralization and bimanual coordination in children with Tourette syndrome. *Mov Disord.* (2011) 26:2114–8. doi: 10.1002/mds.23839
39. Buse J, August J, Bock N, Dörfel D, Rothenberger A, Roessner V. Fine motor skills and interhemispheric transfer in treatment-naive male children with Tourette syndrome. *Dev Med Child Neurol.* (2012) 54:629–35. doi: 10.1111/j.1469-8749.2012.04273.x

Conflict of Interest Statement: The authors declare that the research was conducted in the absence of any commercial or financial relationships that could be construed as a potential conflict of interest.

frontiers in Systems Neuroscience

ORIGINAL RESEARCH
published: 30 April 2019
doi: 10.3389/fnsys.2019.00015

Modulations in Oscillatory Activity of Globus Pallidus Internus Neurons During a Directed Hand Movement Task—A Primary Mechanism for Motor Planning

Shreya Saxena[1], Sridevi V. Sarma[2], Shaun R. Patel[3], Sabato Santaniello[4], Emad N. Eskandar[5†] and John T. Gale[6†]*

[1] Zuckerman Mind Brain Behavior Institute, Columbia University, New York, NY, United States, [2] Neuromedical Control Systems Laboratory, Department of Biomedical Engineering, Institute for Computational Medicine, Johns Hopkins University, Baltimore, MD, United States, [3] Genetics and Aging Research Unit, Department of Neurology, McCance Center for Brain Health, Harvard Medical School, Massachusetts General Hospital, Boston, MA, United States, [4] Biomedical Engineering Department, CT Institute for the Brain and Cognitive Sciences, University of Connecticut, Storrs, CT, United States, [5] Leo M. Davidoff Department of Neurological Surgery, Albert Einstein College of Medicine, The Bronx, NY, United States, [6] Department of Neurosurgery, Emory University, Atlanta, GA, United States

OPEN ACCESS

Edited by:
Martijn Beudel, University Medical Center Amsterdam, Netherlands

Reviewed by:
Constance Hammond, Institut National de la Santé et de la Recherche Médicale (INSERM), France
Joshua A. Goldberg, Hebrew University of Jerusalem, Israel
Carola Sales-Carbonell, Researcher at B&A Therapeutics, France, in collaboration with reviewer CH

***Correspondence:**
Shreya Saxena
ss5513@columbia.edu

† These authors have contributed equally to this work and share senior authorship

Received: *23 November 2018*
Accepted: *02 April 2019*
Published: *30 April 2019*

Citation:
Saxena S, Sarma SV, Patel SR, Santaniello S, Eskandar EN and Gale JT (2019) Modulations in Oscillatory Activity of Globus Pallidus Internus Neurons During a Directed Hand Movement Task—A Primary Mechanism for Motor Planning. Front. Syst. Neurosci. 13:15. doi: 10.3389/fnsys.2019.00015

Globus pallidus internus (GPi) neurons in the basal ganglia are traditionally thought to play a significant role in the promotion and suppression of movement via a change in firing rates. Here, we hypothesize that a primary mechanism of movement control by GPi neurons is through specific modulations in their oscillatory patterns. We analyzed neuronal spiking activity of 83 GPi neurons recorded from two healthy nonhuman primates executing a radial center-out motor task. We found that, in directionally tuned neurons, the power in the gamma band is significantly ($p < 0.05$) greater than that in the beta band (a "cross-over" effect), during the planning stages of movements in their preferred direction. This cross-over effect is not observed in the non-directionally tuned neurons. These data suggest that, during movement planning, information encoding by GPi neurons may be governed by a sudden emergence and suppression of oscillatory activities, rather than simply by a change in average firing rates.

Keywords: basal ganglia, globus pallidus internus (GPi), beta-band, motor control, movement planning

INTRODUCTION

A central question in motor neuroscience is how the best action is selected at any given moment while carrying out a voluntary movement. The basal ganglia (BG) neurons are thought to play a significant role in movement selection, wherein the globus pallidus internus (GPi) neurons form a major structure (Kandel et al., 2000). A widely accepted theory suggests that for any given state, there is a range of possible and competing actions, and the BG participate in the process of selecting the most desirable or profitable action given the current context and prior learning in a "center-surround" model (Nambu, 2004). Specifically, the theory suggests that modulations in the firing rate of task-related GPi/substantia niagra neurons signal the promotion of desired movements and the suppression of unwanted movements (Albin et al., 1989; DeLong, 1990; Mink, 1996; Nambu, 2004). In this study, however, we hypothesize that movement control occurs via modulations

in *oscillatory activity* in the BG neurons, more specifically in the "beta" (15–30 Hz) and "gamma" (35–90 Hz) bands.

Several experiments have demonstrated the modulation of GPi neurons' firing rates to direction-specific movements as well as reward information (Bromberg-Martin et al., 2010; Shin and Sommer, 2010; Tachibana and Hikosaka, 2012; Howell et al., 2016). Moreover, numerous studies have focused on the potential role of beta oscillatory activity in the basal ganglia, in both single unit and local field activities, in the pathophysiology of PD (Miller and DeLong, 1987; Filion and Tremblay, 1991; Levy et al., 2000, 2002; Brown et al., 2001). However, few studies have examined the role of beta oscillatory activity of basal ganglia in normal function (Courtemanche et al., 2003; Feingold et al., 2015). To this end, we examined single-unit activity of 83 GPi neurons in two naive non-human primates engaged in a radial center-out motor task. We set out to ascertain the functional relationship between movement and oscillatory activity in beta and gamma bands in the healthy condition. Here, we refer to "oscillatory activity" as modulations in the power spectrum of individually recorded neurons in a specific frequency band.

In the directionally tuned, i.e., task-related neurons, our results show a significant increase in gamma power as compared to beta power ($p < 0.05$), specifically during the planning of movement. This trend is not observed in the non-directionally tuned neurons. This suggests that the GPi neurons involved in the planning of movement communicate information through a "cross-over" effect, i.e., an emergence in gamma oscillatory activity with a concurrent suppression in beta oscillatory activity. A cross-over effect has previously been observed in other parts of the motor circuit, specifically the motor and premotor cortex (Schoffelen et al., 2005; Donner et al., 2009), as well as in a preliminary analysis of a subset of the data used in the present study (Saxena et al., 2011).

The data in this study are the first to demonstrate that beta and gamma modulation in the GPi is direction specific and that movements are encoded in the temporal domain at the level of single-unit activities. Hence, the interaction between beta and gamma oscillatory activity may serve to encode additional orders of information, not encoded in the firing rate domain, as originally hypothesized.

MATERIALS AND METHODS

Experimental Methods

Two healthy adult male Rhesus monkeys (*macaca mulatta*) were trained to perform a radial "center-out" motor task; more details below. "Center-out" tasks were originally developed by (Georgopoulos et al., 1988), but have used extensively in subsequent studies (Georgopoulos et al., 1988; Truccolo et al., 2008). Both animals were independently housed in a climate and light controlled environment. Target structures were localized using magnetic resonance imaging (MRI) and recording chambers were placed stereotactically, under isoflourine using sterile technique, such that the electrode trajectory avoided sinus and ventricle space. One chamber was centered at A13, L15, aligned vertically to allow a dorsal approach to the GP. The other chamber was centered at A11, with an approach of approximately 40 degrees relative to vertical (roughly normal to the skull). An MRI image (MPRAGE; TR 11.1; TE 4.3/1; TA 13:37) was obtained after the recording chamber had been implanted, using mineral-oil filled capillary tubes placed at known grid positions as fiducial markers. For the angled chamber, penetrations were advanced until the GP was encountered. For the vertical chamber, separate penetrations were made medial to the putaminal sites to positively identify the GP. GP units were clearly identified from putaminal units by their much higher spontaneous firing rates (DeLong, 1971). In addition to the chamber placement, scleral search coil (Judge et al., 1980) were implanted to allow for accurate measure of eye position (Crist Instruments, Bethesda MD). All animal procedures were performed in accordance with the National Institutes of Health guidelines and the Institutional Animal Care and Use Committee approved study protocol.

Each day, the animals sat in a chair that was placed into a sound-attenuating enclosure facing an LCD computer monitor. A sipper-tube was positioned at the tip of their mouth for reward delivery and a joystick was fixed to the chair for the animal to manipulate during the task. In addition, a shielding plate was positioned next to the joystick such that the animal was only able to manipulate the joystick using the hand contralateral to the recording chamber. The animals were then trained 5–6 days a week on a visual-motor task.

To initiate a trial, the animals were required to fixate ("F") and position the cursor on a central fixation point for a period of 200–300 ms. At this point, eight gray objects appeared in a radial arrangement equidistant from the center of the screen, signifying stimulus on ("S"). While maintaining gaze on the fixation point for a period of another 200–300 ms, a random gray target was replaced by a stimulus cue ("Cue 1"). The stimulus cue was either a green or red circle, which instructed the animal to choose that target (for the green circle) or the diametrically opposing target (for the red circle). As an additional setting, dual-cued trials were also added to the task. In these trials, the first cue would be replaced by a second cue ("Cue 2") that instructed the animal to change the target selection. The second cue would appear 100–900 ms after the first cue. Trials with only one cue are denoted as *single-cue* trials and trials with two cues are denoted as *dual-cue* trials (**Figure 1**).

The start of movement is denoted by "M." The trial was concluded when the primate selected a target. In the *dual-cue* trial type, the trial was concluded without a liquid reward if the primate started movement before the target light changed in color. If at any point the animal broke fixation, prematurely moved the joystick or failed to select the correct target (in the required time), the trial was aborted and the animal was not rewarded. The animals were water-deprived, and the trials that were completed correctly were followed by a liquid reward (water). The animal's arm was not immobilized while moving the joystick. Target positions and movement types were randomized such that many movements toward each of the eight positions could be analyzed over the course of a single recording session. An average of 53% (55%) of the successful trials in any session were single-cue trials for Monkey 1 (Monkey 2).

Once the animal had been fully trained on the behavioral task, extracellular microelectrode recordings were made from the

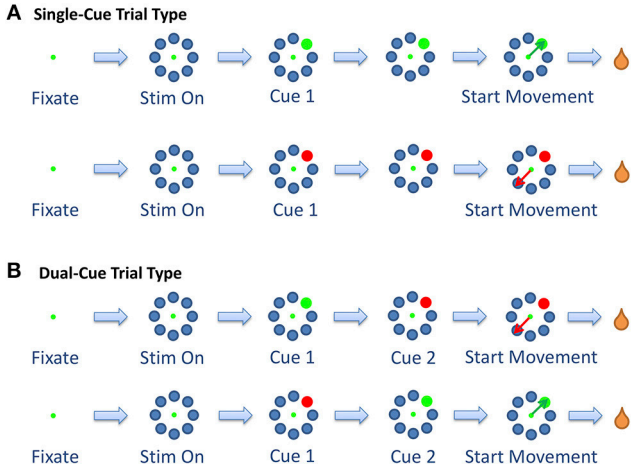

FIGURE 1 | The two trial types. **(A)** The single-cue trial type consists of trials in which the stimulus did not change throughout the trial. **(B)** The dual-cue trial type consists of the trials in which the stimulus changed colors. Figure adapted from Saxena et al. (2011).

GPi while the primates performed the behavioral task. Electrodes (300–500 KOhm metal micro-electrodes; FHC, Bowden, ME) were introduced into the brain through a 1 mm spaced grid (Crist Instruments, Bethesda, MD). Neurons were not preselected for task-specific modulation, assuring random sampling of GPi neurons. Instead, the electrode was advanced until the activity of one or more neurons was well-isolated. The localization of the GPi was based both on MRI positioning information (as detailed above) and neurophysiological characteristic, such as high irregular firing rate and lack of pause-burst spiking patterns (which are characteristic of globus pallidus externus). In any given session, the activity of up to three neurons was recorded from a single electrode. Single electrode recordings were repeated on a semi-daily basis for the duration of the study.

Neurophysiological activity was digitized and high-pass filtered at 0.2–6.5 KHz through the head-stage and continuously stored, along with behavioral events, by a PowerLinc 1401 acquisition system (Cambridge Electronic Design, Cambridge UK) at 20 kHz. Offline, the continuous data was parsed into single neuron records using an offline sorting algorithm (Spike2, Cambridge Electronic Design, Cambridge UK). To do this, data was thresholded to identify spike events from noise and clustered using the first and second principal components of the waveform signal. Data was disregarded if the recording was unstable or if individual single unit activity was indiscernible from noise or multi-unit activity.

Data Analysis

We considered the two trial types, *single-cue* and *dual-cue*, separately. We first built point process models (PPMs) for the activity of each neuron as the primate was reaching in the 8 directions. We then used specific parameters of these PPMs to determine directional tuning of the neuron for each trial type. Finally, we computed the population-averaged power in the beta and the gamma frequency bands in overlapping windows throughout the entire trial for both directionally tuned neurons and the non-directionally tuned neurons. The details are provided in the following sections.

Determining Directional Tuning

Point process methods have been used to analyze the spike train activity for a broad range of neural systems (Sarma et al., 2010, 2012; Saxena et al., 2010, 2012; Santaniello et al., 2012; Sumsky et al., 2017; Sumsky and Santaniello, 2018). A neural spike train can be treated as a stochastic series of random binary events (i.e., the spike times) continuously occurring in time, otherwise known as a point process (Truccolo et al., 2005; Coleman and Sarma, 2010; Sarma et al., 2010).

The spike train can be discretized into bins of length Δ, and if Δ is small enough, we are left with a discrete time series of 1 and 0 s. In this case, the 1 s are individual spike times and the 0 s are the times at which no spikes occur. To define a point process model (PPM) of neural spiking activity, an observation interval (0,T] is considered to be the length of the spike train, and N(t) is allotted to be the number of spikes counted in interval (0,t] for $t \in (0,T]$. A PPM of a neural spike train is completely characterized on a given observation interval (0,T] by defining the conditional intensity function (CIF) (Snyder and Miller, 2012). The timings between spike events can be described as a stochastic point process and its probability distribution is characterized by a rate function, $\lambda(t|\cdot)$, formally known as the CIF, defined as:

$$\lambda(t|H_t) \triangleq \lim_{\Delta \to 0} \frac{\Pr(N(t+\Delta) - N(t) = 1|H_t)}{\Delta},$$

where H_t is a vector comprising the relevant covariates in the past and up to including time t, and Pr the probability. PPMs have been extensively used to extract temporal patterns and non-stationarities in spiking data (Sarma et al., 2010, 2012; Saxena et al., 2011, 2012; Santaniello et al., 2012). In these studies, the CIF is modeled as an explicit function of extrinsic and intrinsic factors, and can be estimated directly, via maximum likelihood estimation (Truccolo et al., 2005; Coleman and Sarma, 2010; Sarma et al., 2010) from extracellular *in-vivo* recordings. Estimating $\lambda(t|H_t)$ is equivalent to estimating of the entire probability distribution of the spiking activity, and is thus more powerful than the traditional calculations of first- and second-order statistics of the spike train.

In this study, we calculated the probability of spiking of each neuron as a function of the stimulus information and the neuron's own spiking history. Specifically, at each time window, the CIF was expressed as

$$\lambda(t|H_t, \Theta) = \lambda^s(t|\Theta) \cdot \lambda^H(t|H_t, \Theta)$$

Where $\lambda^S(t|\Theta)$ describes the effect of the movement direction stimulus on the neural response and $\lambda^H(t|H_t,\Theta)$ describes the effect of spiking history on the neural response. Θ is a parameter vector to be estimated from data, using maximum likelihood methods.

The following structure for λ^S was used to model the history-independent component, i.e., the stimulus component, in each window.

$$\log \lambda^S \left(\mathrm{t}|\alpha, \mathrm{d}\right) = \alpha_d,\ d \in 1, \ldots, 8,$$

where movement direction $\mathrm{d} = 1, 2, \ldots 8$, corresponds to 0, 45, 90, …315 degrees clockwise from the "Up" direction, respectively, and α_d is a scalar.

The history-dependent component was modeled in the following manner in each time window.

$$\begin{aligned}\log \lambda^H (\mathrm{t}|\varphi,\gamma,\beta) = &\sum_{j=0}^{9} \varphi_j\, n\left(t-j : t-\left(j+1\right)\right) \\ &+\sum_{k=0}^{8} \gamma_k\, n\left(t-\left(2k+12\right) : t-\left(2k+14\right)\right) \\ &+\sum_{l=0}^{8} \beta_l\, n\left(t-\left(5l+30\right) : t-\left(5l+35\right)\right),\end{aligned}$$

where $n\left(a:b\right)$ is the number of spikes observed in the time interval $[a, b)$ during the epoch. The $\left\{\varphi_j\right\}_{j=0}^{9}$parameters measure the effects of spiking history in the previous 10 ms and therefore can capture refractoriness and / or bursting on the spiking probability in the given time window (Sarma et al., 2010, 2012; Santaniello et al., 2012). The $\{\gamma_k\}_{k=0}^{8}$and the $\{\beta_l\}_{l=0}^{8}$ parameters capture longer-term history effects such as oscillatory activity between 10 and 100 Hz. We estimated the following parameter vector using maximum likelihood methods.

$$\Theta = \left[\left\{\alpha_d\right\}_{d=1}^{8}, \left\{\varphi_j\right\}_{j=0}^{9}, \left\{\gamma_k\right\}_{k=0}^{8}, \left\{\beta_l\right\}_{l=0}^{8}\right]$$

Each PPM was estimated during 80% of the trials, and the goodness-of-fit was assessed on the remaining 20% of the trials (cross-validation) with the Kolmogorov Smirnov (KS) plot after time rescaling of the spike trains (Brown et al., 2002). Only neurons with PPMs whose KS plots were within the 95% confidence bounds were included in this study; the summary statistics are provided in **Table 1**. For more details on fitting PPMs, see (Brown et al., 2002; Sarma et al., 2010, 2012; Santaniello et al., 2012).

To establish direction tuning, we inquired whether, given the same spiking history, the spiking activity of a neuron was significantly different when the primate was moving in one of the eight target directions. If the history-independent parameter in one direction was found to be significantly different from at least four other directions at a 95% confidence level, the neuron was determined directionally tuned. Thus, we examined the history-independent parameters α_d. rresponding to each direction of movement of the primate.

Specifically, for each direction $d' = 1, \ldots, 8$, $p_{d'd} = \Pr\left(e^{\alpha_{d'}} > e^{\alpha_d}\right) = \Pr\left(\alpha_{d'} > \alpha_d\right)$ was computed for $d \neq d'$. $p_{d'd'}$ was defined as 0. The Gaussian approximation was used, which is one of the asymptotic properties of maximum likelihood estimates to compute $p_{d'd}$ (Brown et al., 2003). Let N_d be the number of $d' \in 1, \ldots, 8$ for which $p_{d'd} > 0.975$. If $N_d \geq 4$ for any $d \in 1, \ldots, 8$, then the neuron was determined directionally tuned in this direction, now termed d^*. If more than one direction was tuned in the neuron, then the following formula was used.

$$d^* = \underset{d}{\operatorname{argmax}} \left|\alpha_d - \frac{\sum_{i=1}^{8} \alpha_i}{8}\right|,\ d \in 1, \ldots, 8$$

We first computed the percentage of directionally tuned neurons in each time window studied for each of the four movement types presented in the task (cf. **Figure 1**). We identified the epoch e* for which each movement type had the maximum percentage of directionally tuned neurons (**Supplementary Figure 1**). In the subsequent analysis, a neuron was classified as directionally tuned in a trial type (i.e., *single-cue* or *dual-cue*) if it was directionally tuned for either movement type in this epoch e*. Only the neurons which were recorded during both movement types in a trial type were kept in the analysis.

TABLE 1 | Time taken for movement planning and completion of movement for Monkey 1.

Category	Single-cue trials	Dual-cue trials
Median time taken from last cue to start of movement (ms)	839 (894)	537 (505)
Median time taken from start of movement to reward (ms)	299 (423)	289 (413)

Values in parentheses for Monkey 2.

Determining the Presence of a Cross-Over Effect Using Traditional Spectral Analysis

The analyses were performed separately for directionally tuned neurons and for non-directionally tuned neurons, for each trial type: *single-cue* and *dual-cue*. Oscillatory characteristics of the neurons in the beta (15–30 Hz) and gamma (35–90 Hz) frequency band were assessed by using the power spectrum density (PSD) with the Welch method (Welch, 1967). Given a neuron and a task type (i.e., *single-cue* or *dual-cue* tasks), for each task-related marker m (*single-cue* tasks: $m = \{F, S, Cue_1, M\}$; *dual-cue* tasks: $m = \{F, S, Cue_1, Cue_2, M\}$, **Figure 1**), the spike trains around m were divided into 9 overlapping segments (length: 512 ms; step size: 50 ms) centered from $m - 144$ to $m + 256$ ms and each segment was multiplied by a Hanning window of equal length. The PSD of the neuron in each time window was computed as the average periodogram across the number of trains available in that window (Welch, 1967). Finally, the signal-to-noise ratio (SNR) in that window was computed at each frequency f according to the formula (Gale et al., 2009):

$$SNR\left(f\right) \triangleq \frac{PSD\left(f\right) - \mu}{\sigma}, \tag{1}$$

where $PSD\left(f\right)$ is the PSD at frequency f and μ (σ) is the mean (standard deviation) of the PSD across all the frequencies. Only frequencies for which SNR is $\geq$1.5 were considered significant

and included in this study. For each time window, the average power of the neuron in the beta (gamma) frequency band was estimated as the average value of $SNR(f)$ in the interval [15, 30] Hz ([35, 90] Hz). If the neuron was directionally tuned, only trains recorded during tasks involving the tuned direction were considered, otherwise all the recorded spike trains of the neuron were considered.

Determining the Presence of a Cross-Over Effect Using PPMs

For the analysis of prominent oscillatory activity, different PPMs were constructed for directionally tuned and non-directionally tuned neurons.

If the neuron was determined to be directionally tuned, a *Direction-Specific* model was constructed for that neuron using *only* the data from the trials where the primate was reaching in direction d^*, where d^* is the tuned direction as determined above. The model structure for the history-independent term was defined as $\log \lambda^S(t|\alpha) = \alpha$. The model structure for the history-dependent term λ^H remained the same as above.

If the neuron was not tuned in any direction, model structures remained the same as above, and the *Multi-Direction* PPM was used to determine the presence of oscillatory activity.

We first determined the presence of beta and gamma oscillatory activity for each neuron. The parameters $\{\gamma_k\}_{k=0}^{8}$, corresponding to the history bins -12 to -30 ms from right to left measure the effects of spiking history in the previous 12–30 ms, and therefore can capture the presence of oscillatory activity in the frequency range of 33–83 Hz. This corresponds to the gamma frequency band, and the presence of gamma oscillatory activity was determined if any one of the parameters representing oscillatory activity in this frequency range was significantly higher than 1, that is, for at least one $k \in 0, \ldots 8$, $LB_k^{\gamma} > 1, LB_k^{\gamma} \leq e^{\gamma_k}$. LB_k^{γ} is the 95% lower confidence bound for parameter γ_k.

Similarly, we analyzed parameters $\{\beta_l\}_{l=0}^{8}$, capturing recurrent patterns with period -30 to -75 ms, corresponding to the beta frequency band. The presence of beta oscillatory activity was determined if any one of the parameters representing oscillatory activity in this frequency range was significantly higher than 1, that is, for at least one $l \in 0, \ldots 8$, $LB_l^{\beta} > 1, LB_l^{\beta} \leq e^{\beta_l}$. LB_l^{β} is the 95% lower confidence bound for parameter β_l.

Next, we determined whether the neuron has a higher tendency to display gamma oscillatory activity or beta oscillatory activity. If a neuron has no parameters significantly higher than 1 in the beta band, but does in the gamma band, it automatically has a higher tendency to display gamma oscillatory activity than beta. However, if a neuron had significant parameters in both bands, we compared the lower bounds of the highest parameters in both bands to determine whether it had a higher tendency to oscillate in the beta band or the gamma band, i.e., if $\max_k \left(LB_k^{\gamma}\right) > \max_l \left(LB_l^{\beta}\right)$ for $k, l \in 0, \ldots 8$, then the neuron has a higher tendency to oscillate in the gamma band.

Finally, we separately calculated the percentage of directionally tuned and non-directionally tuned neurons that had a higher tendency to have gamma oscillatory activity than beta oscillatory activity. We calculated this percentage for each overlapping window as described in the previous section. Thus, we could infer the suppression and increase of oscillatory activity in the gamma and beta bands across the trial. For comparison, we also calculated the percentage of directionally tuned and non-directionally tuned neurons in each time window that had a higher tendency to have beta oscillatory activity than gamma oscillatory activity.

The same statistic was also computed for randomized spike trains, built by randomly shuffling the inter spike intervals of the original spike trains for each trial of each neuron a total of 100 times. We calculated the 5 and 95% bounds of the percentage of neurons falling in each bin from these randomized spike trains.

RESULTS

A total of 83 neurons were isolated from the GPi from two non-human primates (Monkey 1, $n = 27$; Monkey 2, $n = 56$) as the animals performed the task. Monkey 1 (2) performed a total of 18,978 (28,303) trials, out of which 14,370 (21,183) were successful across both trial types over 31 (50) days. Monkey 1 (2) had an average success rate of 77 ± 7% (75.2 ± 6%) trials per recorded day. On average each animal performed 16.39 ±6.53 successful trials per day, per direction of movement. These successful trials are analyzed in this study. Some further behavioral statistics for each animal are provided in **Table 1**.

For each neuron, the directional tuning for each trial type was calculated. We identified the epoch e* for which each movement type had the maximum percentage of directionally tuned neurons (**Supplementary Figure 1**). **Figure 2** shows the PPM of two example neurons in one trial type. In the top row of **Figures 2A,B**, parameters e^{α_d}, $d = 1, \ldots 8$, account for the history-independent, non-oscillatory component of the discharge rate of a single neuron when the primate is reaching in direction d. In **Figure 2A**, the history-independent parameter in direction d_3 is significantly different from those in 6 other directions. Thus, this neuron is determined tuned in the direction d_3. Note that directionally tuned neurons may have a significantly *lower* or *higher* parameter e^{α_d}. In **Figure 2B**, none of the history-independent parameters are significantly different from those in any other direction; this neuron is thus not directionally tuned. **Supplementary Figure 2** shows the percentage of neurons displaying tuning in each direction. **Supplementary Figure 3** shows an example raster plot of a directionally tuned neuron, where we also see an inhibition in the firing activity of the neuron in the tuned direction within the relevant epoch.

Table 2 shows the number of neurons that fell in each category. We accepted a neuron as significantly tuned for a trial type if it demonstrated directional tuning during either movement cue.

In **Figure 3**, we note that the SNR is high throughout the trial in the *single-cue* as well as *dual-cue* directionally tuned neurons. However, before movement we see a sharp drop in SNR across all frequencies. The opposite trend is seen in the non-directionally tuned neurons, with an increase in power across all frequencies.

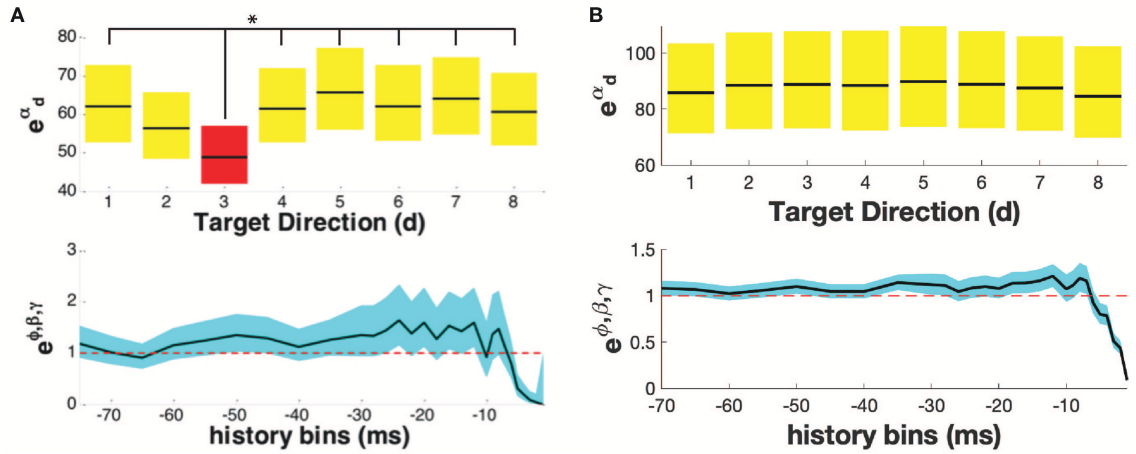

FIGURE 2 | Point process model for **(A)** a directionally tuned neuron, **(B)** a non-directionally tuned neuron. Both **(A,B)** show the propensity of the neuron to fire at time t, given the movement direction (top row), and the neuron's own history (bottom row). The parameters of the PPM are given in black, while the 95% confidence bounds are given in yellow/ red/ blue. In **(A)**, the neuron is tuned in the direction with an asterisk, highlighted in red, i.e., direction d_3. In **(B)**, the neuron is not tuned in any direction.

TABLE 2 | Number of neurons displaying directional tuning in one or both movement cues (i.e., while the subject is moving toward the green target or away from the red target), for each trial type.

Category	Single-cue trials	Dual-cue trials
Directionally tuned for both movement cues	35 (47)	31 (37)
Directionally tuned for only one movement cue	26 (31)	24 (29)
Non Directionally tuned for both movement cues	19 (23)	25 (30)
Not enough data to successfully cross-validate PPM	3 (4)	3 (4)
Total	83 (100)	83 (100)

Values in parenthesis represent percent of neurons.

When considering the difference between average power in the gamma and beta frequency bands (**Figure 4**), we see that the average power in the gamma band is not significantly above that in the beta band until the first cue is observed. After the presence of the first cue in both the single-cue and the dual-cue trial types, we see that the average power in the gamma band is significantly above that in the beta band, till before movement onset. In the case of the dual-cue trials, this "cross-over" effect, i.e., the significantly higher levels of gamma band as compared to the beta band, holds from the onset of the first cue till after the onset of the final cue. Note that no significant differences between the average power in the gamma and beta frequency bands is observed for the non-directionally tuned neurons, see **Figures 4C, D**. **Supplementary Figure 4** shows an example neuron's raster plot during the relevant epochs, as well as the average beta and gamma band power during these epochs. We see that the frequency information is not directly apparent using the rasters alone, but we see the emergence of gamma band and non-emergence or suppression of beta-band power during the relevant epoch.

In order to further examine the relationship between the beta and gamma bands after onset of cue, we conducted a series of hypothesis tests to test the exact onset of the cross-over. For each trial-type, we built a separate PPM for each neuron, and calculated the percentage of neurons in each trial type for which the tendency to oscillate in the gamma band is higher than the tendency to oscillate in the beta band, as grouped by directional tuning. This is shown for the *single-cue* and *dual-cue* trial types in **Figure 5**.

We see that throughout the trials in both trials types, the percentages in the non-directionally tuned neurons do not cross the 5 and 95% bounds computed from the randomized spike trains in a consistent manner. On the other hand, in the directionally tuned neurons, we see that the 95% bounds are crossed by the percentage of neuron model displaying a higher tendency to oscillate in the gamma frequency band as compared to the beta frequency band. This cross-over effect, i.e., the emergence of gamma band and suppression of beta band, holds from the onset of the final cue to 200 ms after the onset of the cue.

Note that this effect is not observed in the directionally tuned neurons after the first cue in the *dual-cue* trials, since these neurons are not tuned in the direction of movement that the first cue suggests. Rather, the cross-over effect in dual-cue trials is seen only after the final cue is presented and lasts until about 200 ms before movement onset.

We also computed the percentage of neuron models displaying a higher tendency to oscillate in the beta frequency band as compared to the gamma frequency band (**Supplementary Figure 5**). We see that the percentages in both the directionally tuned and the non-directionally tuned neurons do not cross the 5 and 95% bounds computed from the randomized spike trains in a consistent manner.

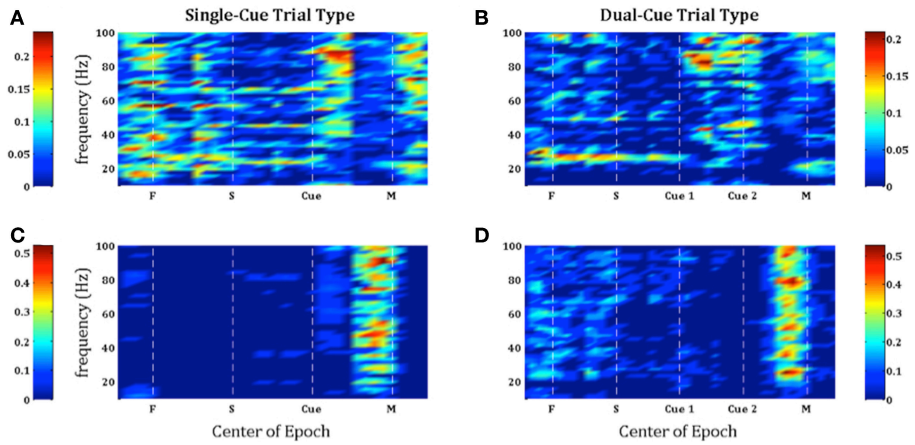

FIGURE 3 | Population-averaged SNR on consecutive windows for directionally tuned neurons **(A,B)** and non directionally tuned neurons **(C,D)** during single-cue tasks **(A,C)** and dual-cue tasks **(B,D)**. For each neuron, only significant frequencies were considered. F, fixation; S, stimulus ON; Cue 1, first cue; Cue 2, second cue; M, movement onset.

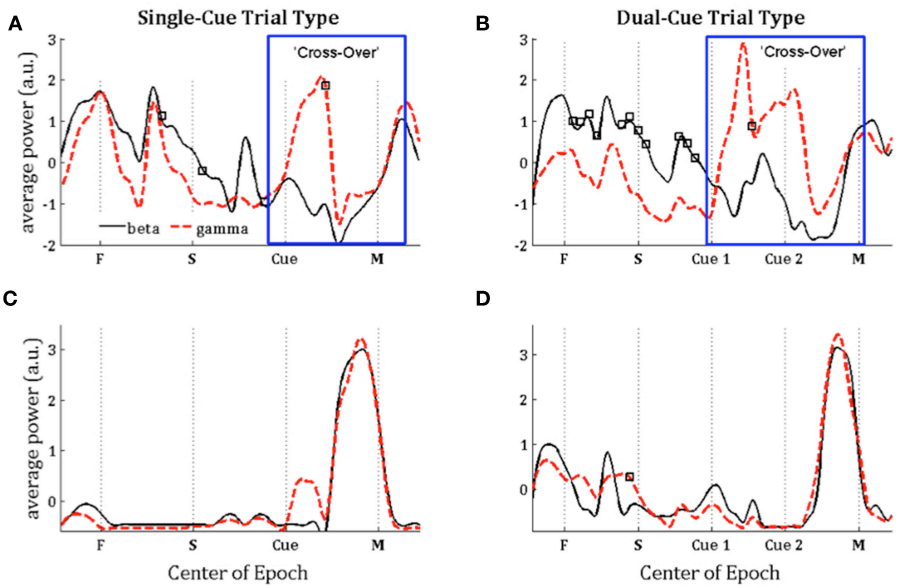

FIGURE 4 | Population-averaged power in the beta (15–30 Hz, black lines) and gamma (35–90 Hz, red lines) frequency band on consecutive windows for directionally tuned neurons **(A,B)** and non-directionally tuned neurons **(C,D)** during single-cue tasks **(A,C)** and dual-cue tasks **(B,D)**. F, fixation; S, stimulus ON; Cue 1, first cue; Cue 2, second cue; M, movement onset. For each window, a black square indicates a significant difference between the power in beta and gamma band in that window (Wilcoxon rank-sum test, $p < 0.05$). Each curve in **(A–D)** is normalized by subtracting the mean value and dividing by the standard deviation.

In **Figure 6**, directly after the first cue, we see an emergence of high frequency firing as compared to low frequency firing in the directionally tuned neuron ($p < 0.05$ two-sided Wilcoxon rank sum test of gamma band power as compared to beta band power), supporting the results seen in **Figures 4**, **5**. We do not see these modulations in spiking activity in the non-directionally tuned neuron.

DISCUSSION

The findings in this study suggest that one mechanism for movement planning in GPi is a specific modulation in the beta-gamma power in the spiking activity of individual neurons. The current theory (Turner and Anderson, 1997; Nambu, 2004) suggests a relationship between movement correlates

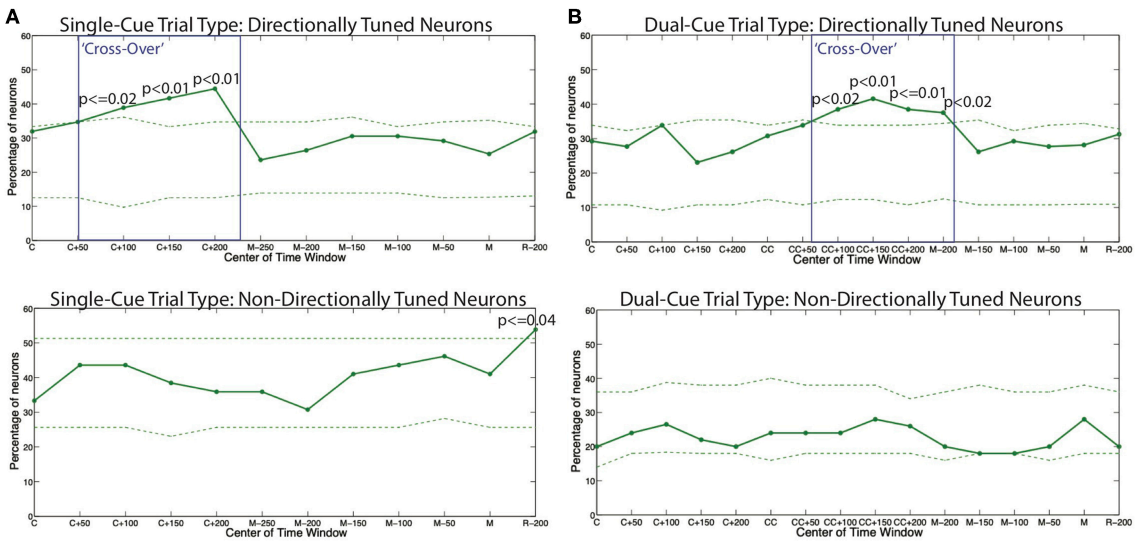

FIGURE 5 | The percentage of all models displaying a higher tendency to oscillate in the gamma frequency band as compared to the beta frequency band for **(A)** the single-cue trial type and **(B)** the dual-cue trial type. The dashed lines show 5 and 95% confidence bounds built by randomly shuffling the inter spike intervals of the original spike trains for each trial of each neuron a total of 100 times. The boxes indicate the areas of cross-over. C, first cue; CC, second cue; M, start of movement; R, administration of reward.

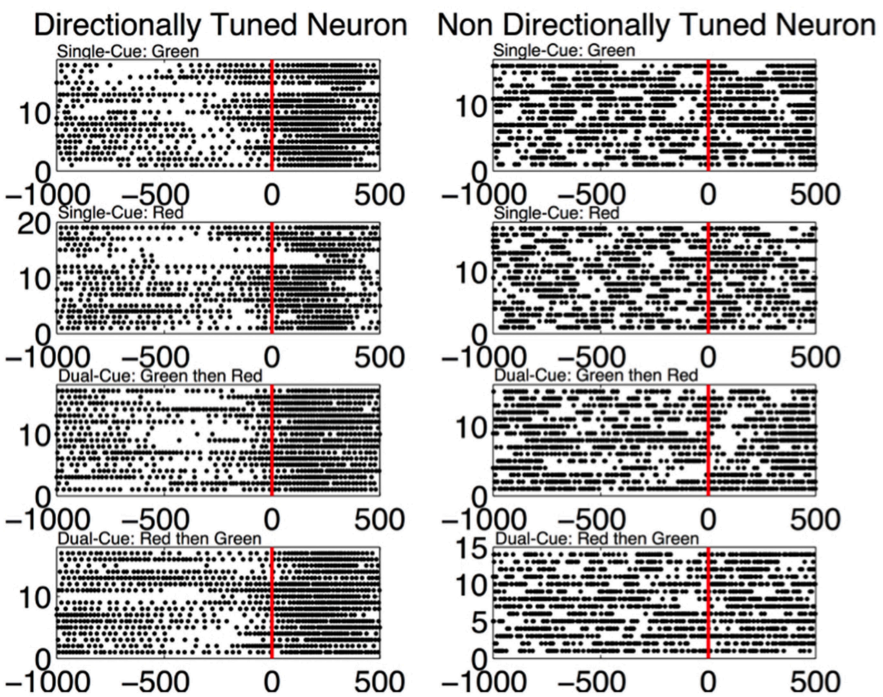

FIGURE 6 | (Left) The spiking activity of a directionally tuned neuron 1,000 ms before and 500 ms after the first cue (data aligned at first cue = 0 ms). Only the trials where the monkey is moving in the tuned direction are shown. Each dot corresponds to a spike in the corresponding time bin. **(Right)** The trials from a non-directionally tuned neuron while the monkey is moving in the same direction as the directionally tuned neuron.

and the firing rate of neurons, and it is unclear whether the findings in the current study are a causative or a correlative effect of a modulation in the firing rate. Turner & Anderson themselves have performed an extensive study of GPi firing during movements, and found that around 95% of the GPi neurons are tuned to a direction (Turner and Anderson, 1997). Through our directional tuning analysis, we classify 89% of the neurons (71 out of the 80 neurons with cross-validated

PPMs) as tuned for at least one movement cue in either of the single-cue or dual-cue trial types. Since we model the complete spiking statistics of a GPi neuron's activity and then test the direction-dependent term for differences in activity, we have a more nuanced measure of directional tuning, and principled comparisons between the two can be performed in a future study.

More specifically, our results show the existence of a "cross-over" effect in the GPi neurons, i.e., a simultaneous increase in gamma band power and decrease in beta band power during movement planning by the task related neurons. It was shown in the results section that the average beta power was significantly higher than the average gamma power before a cue was presented ($p < 0.05$), which then switched to the average gamma band power being significantly higher the average beta band power *after* a cue was presented ($p < 0.05$). Moreover, the existence of beta band oscillatory activity in the task related GPi neurons before the target cue indicates the integral role of this oscillatory activity in achieving accurate directed movements, in contrast with studies involving LFP suggesting that beta band oscillations are inherently pathological (Filion and Tremblay, 1991; Bergman et al., 1994; Raz et al., 2000). In contrast, the non-directionally tuned neurons do not display modulations in the beta or gamma band oscillatory activity until immediately before the onset of movement. During movement, the average power increases concurrently in the beta and gamma bands, with no apparent cross-over effect. Thus, the modulations in oscillatory activity of the task-related or directionally tuned neurons are sharply distinct from those of the non-directionally tuned neurons.

The BG has long been known to participate in movement planning, and the GPi neurons have been shown to consist of directionally tuned and non-directionally tuned neurons (Albin et al., 1989; DeLong, 1990; Mink, 1996; Nambu, 2004; Bromberg-Martin et al., 2010; Shin and Sommer, 2010; Tachibana and Hikosaka, 2012; Howell et al., 2016). Here, we propose that the "directionally-tuned" neurons happen to encode the appropriate course of action, and "non-directionally tuned" neurons represent alternative possible actions. The former are modulated by the ongoing task and the latter are not selectively activated, since those alternative actions are neither appropriate nor tuned for the current context, and are not performed. Moreover, we propose that expression of gamma band activity during motor planning in directionally-tuned neurons amounts to facilitation of the desired or appropriate action given the current state, whereas the expression of beta band activity in non-directionally tuned neurons amounts to suppression of competing but inappropriate or unprofitable actions in the current state and context. This interpretation incorporates the classical 'center-surround' hypothesis as well as previously reported beta-band suppression into a coherent theory.

The results of this analysis depend on the use of PPMs to separate the directionally tuned from the non-directionally tuned neurons. PPMs effectively capture the entire spiking activity of each neuron, separating out the relative contribution of history effects and movement direction on the probability that the neuron will spike at any given time, thus making it an effective paradigm to compute directional tuning (Barbieri et al., 2001; Brown et al., 2003; Truccolo et al., 2005, 2008; Sarma et al., 2010; Kahn et al., 2015). Assessing directional tuning using the history-independent covariates of the PPMs is different from simply choosing task-related neurons using firing rates alone, as the PPM separates the contribution of the stimulus and the intrinsic temporal patterns on firing rate (Sarma et al., 2010; Kahn et al., 2015). In fact, traditional means to compute directional tuning rely on first-order statistics of the point process. The PPM parameters instead take into account the probability distributions of the α_d (not just the mean values), and directional tuning is determined from these distributions.

The modulation in the frequency domain of GPi neurons in healthy animals has not yet been fully investigated in single-neuron studies during movement, to the best of the knowledge of the authors. However, beta and gamma LFP activity and their modulations are long known to have an effect on motor areas, as evidenced by data recorded in various structures during healthy motor control. In one study, it was demonstrated that neural activity in the striatum of awake, behaving macaques is characterized by the presence of widespread synchronous oscillatory activity in the beta band (10–25 Hz) frequency range (Courtemanche et al., 2003). However, as the monkeys performed a visuomotor task in this study, it was found that focal sites could disengage from the beta band oscillations (observed in LFPs) during the time in which neurons at the sites show increased spike activity related to the task. This "pop-out" phenomenon suggests that in the behaving monkey, the temporal structure of ensemble oscillatory activity in the striatum interfaces with a modular spatial organization of task-related activity patterns (Courtemanche et al., 2003). In the human putamen, a similar decrease in beta band power was noted in LFPs with self-paced hand movements (Sochurkova and Rektor, 2003). In addition, numerous EEG studies have demonstrated decrements in beta power and/or increase in gamma power with movements from various regions of the cortex including the primary sensorimotor (Pfurtscheller and Neuper, 1992; Sanes and Donoghue, 1993; Toro et al., 1994; Murthy and Fetz, 1996; Leocani et al., 1997; Donoghue et al., 1998; Alegre et al., 2002; Schoffelen et al., 2005; Donner et al., 2009) and supplementary motor cortex (Leocani et al., 1997; Ohara et al., 2000; Alegre et al., 2002).

The authors propose that the study of oscillatory activity in single neurons in the globus pallidus may provide a novel avenue of analysis for investigating frequency modulations. Although LFP is very useful for studying network oscillations, the recordings integrate signals from multiple neurons (Mitzdorf, 1985; Juergens et al., 1999; Kreiman et al., 2006). It has been suggested in the "funneling" hypothesis by Bergman et al. (1998) that convergence of information takes place from the cortex to the GPi, and a consequent divergence from the GPi back to the cortex, leading to more localized groups of neurons in the GPi that are synchronized in a specific frequency band during a given movement. According to this hypothesis, although LFP recordings from the cortex should show frequency modulation in the relevant bands during movement, especially

due to the somatotopic organization of information (Penfield and Rasmussen, 1950; Amirikian and Georgopoulos, 2003), this same effect would not be seen in the GPi neurons since the information at this level should be more locally clustered. Thus, examining the frequency modulation in a group of directionally tuned neurons, that is neurons that modulate their activity in a given movement, is the approach that we implemented in this study.

Our results also concur with studies performed regarding PD conditions in primates. Increased beta band activity in the BG was seen in both the PD human and the monkey treated with the 1-methyl-4-phenyl-1, 2, 3, 6-tetrahydropyridine (MPTP) animal model of Parkinsonism (Filion and Tremblay, 1991; Nini et al., 1995; Levy et al., 2000; Brown et al., 2001; Kuhn et al., 2006; Weinberger et al., 2006). We propose that the reason for impaired motor control in PD may be the inability to perform a cross-over between beta and gamma band oscillations due to pathologically high levels of beta band power present in the basal ganglia. Administering therapies such as Levodopa or deep brain stimulation decreases beta band oscillations in the BG (Priori et al., 2004; Foffani et al., 2005; Wingeier et al., 2006), which may restore the ability to perform a cross-over between beta and gamma band oscillations during the planning of movement, thus restoring healthy motor control.

In conclusion, our results suggest that the parameters of beta-band and gamma-band generation, maintenance and modulation may be pivotal to understanding the mechanism(s) that underlie normal basal ganglia function and may provide insight into the mechanism(s) that underlie pathophysiology of the basal ganglia during PD.

ETHICS STATEMENT

All animal procedures were performed in accordance with the National Institutes of Health guidelines and the Institutional Animal Care and Use Committee approved study protocol.

AUTHOR CONTRIBUTIONS

ShS, SrS, EE, and JG contributed to generating ideas, coming up with the hypothesis, and writing the manuscript. JG and EE contributed to experimental procedures. ShS, SP, and SaS contributed to data analysis.

ACKNOWLEDGMENTS

This work is supported by the Swiss National Science Foundation (Research Award P2SKP2_178197) to ShS, and the Burroughs Wellcome Fund CASI Award 1007274, the National Science Foundation CAREER Award 1055560, and NIH R01NS073118-02 to SrS. The data and accompanying code will be made available on reasonable request to the corresponding author.

SUPPLEMENTARY MATERIAL

The Supplementary Material for this article can be found online at: https://www.frontiersin.org/articles/10.3389/fnsys.2019.00015/full#supplementary-material

REFERENCES

Albin, R. L., Young, A. B., and Penney, J. B. (1989). The functional anatomy of basal ganglia disorders. *Trends Neurosci.* 12, 366–375. doi: 10.1016/0166-2236(89)90074-X

Alegre, M., Labarga, A., Gurtubay, I. G., Iriarte, J., Malanda, A., and Artieda, J. (2002). Beta electroencephalograph changes during passive movements: sensory afferences contribute to beta event-related desynchronization in humans. *Neurosci. Lett.* 331, 29–32. doi: 10.1016/S0304-3940(02)00825-X

Amirikian, B., and Georgopoulos, A. P. (2003). Modular organization of directionally tuned cells in the motor cortex: is there a short-range order? *Proc. Natl. Acad. Sci. U.S.A.* 100, 12474–12479. doi: 10.1073/pnas.2037719100

Barbieri, R., Quirk, M. C., Frank, L. M., Wilson, M. A., and Brown, E. N. (2001). Construction and analysis of non-Poisson stimulus-response models of neural spiking activity. *J. Neurosci. Methods* 105, 25–37.

Bergman, H., Feingold, A., Nini, A., Raz, A., Slovin, H., Abeles, M., et al. (1998). Physiological aspects of information processing in the basal ganglia of normal and parkinsonian primates. *Trends Neurosci.* 21, 32–38. doi: 10.1016/S0166-2236(97)01151-X

Bergman, H., Wichmann, T., Karmon, B., and DeLong, M. R. (1994). The primate subthalamic nucleus. II. Neuronal activity in the MPTP model of parkinsonism. *J. Neurophysiol.* 72, 507–520. doi: 10.1152/jn.1994.72.2.507

Bromberg-Martin, E. S., Matsumoto, M., Hong, S., and Hikosaka, O. (2010). A pallidus-habenula-dopamine pathway signals inferred stimulus values. *Am. J. Physiol. Heart Circul. Physiol.* 104, 1068–1076. doi: 10.1152/jn.00158.2010

Brown, E. N., Barbieri, R., Eden, U. T., and Frank, L. M. (2003). Likelihood methods for neural spike train data analysis. *Computat. Neurosci. A Comprehen. Approach* 253–286. doi: 10.1201/9780203494462.ch9

Brown, E. N., Barbieri, R., Ventura, V., Kass, R. E., and Frank, L. M. (2002). The time-rescaling theorem and its application to neural spike train data analysis. *Neural. Comput.* 14, 325–346. doi: 10.1162/08997660252741149

Brown, P., Oliviero, A., Mazzone, P., Insola, A., Tonali, P., and Di Lazzaro, V. (2001). Dopamine dependency of oscillations between subthalamic nucleus and pallidum in Parkinson's disease. *J. Neurosci.* 21, 1033–1038. doi: 10.1523/JNEUROSCI.21-03-01033.2001

Coleman, T. P., and Sarma, S. S. (2010). A computationally efficient method for nonparametric modeling of neural spiking activity with point processes. *Neural. Comput.* 22, 2002–2030. doi: 10.1162/NECO_a_00001-Coleman

Courtemanche, R., Fujii, N., and Graybiel, A. M. (2003). Synchronous, focally modulated beta-band oscillations characterize local field potential activity in the striatum of awake behaving monkeys. *J. Neurosci.* 23, 11741–11752. doi: 10.1523/JNEUROSCI.23-37-11741.2003

DeLong, M. R. (1971). Activity of pallidal neurons during movement. *J. Neurophysiol.* 34, 414–427. doi: 10.1152/jn.1971.34.3.414

DeLong, M. R. (1990). Primate models of movement disorders of basal ganglia origin. *Trends Neurosci.* 13, 281–285. doi: 10.1016/0166-2236(90)90110-V

Donner, T. H., Siegel, M., Fries, P., and Engel, A. K. (2009). Buildup of choice-predictive activity in human motor cortex during perceptual decision making. *Curr. Biol.* 19, 1581–1585. doi: 10.1016/j.cub.2009.07.066

Donoghue, J. P., Sanes, J. N., Hatsopoulos, N. G., and Gaál, G. (1998). Neural discharge and local field potential oscillations in primate motor cortex during voluntary movements. *J. Neurophysiol.* 79, 159–173.

Feingold, J., Gibson, D. J., DePasquale, B., and Graybiel, A. M. (2015). Bursts of beta oscillation differentiate postperformance activity in the striatum and motor cortex of monkeys performing movement tasks. *Proc. Natl. Acad. Sci. U.S.A.* 112, 13687–13692. doi: 10.1073/pnas.1517629112

Filion, M., and Tremblay, L. (1991). Abnormal spontaneous activity of globus pallidus neurons in monkeys with MPTP-induced parkinsonism. *Brain Res.* 547, 140–144. doi: 10.1016/0006-8993(91)90585-J

Foffani, G., Bianchi, A. M., Baselli, G., and Priori, A. (2005). Movement-related frequency modulation of beta oscillatory activity in the human subthalamic nucleus. *J. Physiol.* 568, 699–711. doi: 10.1113/jphysiol.2005.089722

Gale, J. T., Shields, D. C., Jain, F. A., Amirnovin, R., and Eskandar, E. N. (2009). Subthalamic nucleus discharge patterns during movement in the normal monkey and Parkinsonian patient. *Brain Res.* 1260, 15–23. doi: 10.1016/j.brainres.2008.12.062

Georgopoulos, A. P., Kettner, R. E., and Schwartz, A. B. (1988). Primate motor cortex and free arm movements to visual targets in three-dimensional space. II. Coding of the direction of movement by a neuronal population. *J. Neurosci.* 8, 2928–2937. doi: 10.1523/JNEUROSCI.08-08-02928.1988

Howell, N. A., Prescott, I. A., Lozano, A. M., Hodaie, M., Voon, V., and Hutchison, W. D. (2016). Preliminary evidence for human globus pallidus pars interna neurons signaling reward and sensory stimuli. *Neuroscience* 328, 30–39. doi: 10.1016/j.neuroscience.2016.04.020

Judge, S. J., Richmond, B. J., and Chu, F. C. (1980). Implantation of magnetic search coils for measurement of eye position: an improved method. *Vision Res.* 20, 535–538. doi: 10.1016/0042-6989(80)90128-5

Juergens, E., Guettler, A., and Eckhorn, R. (1999). Visual stimulation elicits locked and induced gamma oscillations in monkey intracortical-and EEG-potentials, but not in human EEG. *Exp. Brain Res.* 129, 247–259. doi: 10.1007/s002210050895

Kahn, K., Saxena, S., Eskandar, E., Thakor, N., Schieber, M., Gale, J. T., et al. (2015). A systematic approach to selecting task relevant neurons. *J. Neurosci. Methods* 245, 156–168. doi: 10.1016/j.jneumeth.2015.02.020

Kandel, E. R., Schwartz, J. H., and Jessell, T. M. (eds.) (2000). *Principles of Neural Science, Volume. 4, 1227–1246*. New York, NY: McGraw-hill.

Kreiman, G., Hung, C. P., Kraskov, A., Quiroga, R. Q., Poggio, T., and DiCarlo, J. J. (2006). Object selectivity of local field potentials and spikes in the macaque inferior temporal cortex. *Neuron* 49, 433–445. doi: 10.1016/j.neuron.2005.12.019

Kuhn, A. A., Kupsch, A., Schneider, G. H., and Brown, P. (2006). Reduction in subthalamic 8-35 Hz oscillatory activity correlates with clinical improvement in Parkinson's disease. *Eur. J. Neurosci.* 23, 1956–1960. doi: 10.1111/j.1460-9568.2006.04717.x

Leocani, L., Toro, C., Manganotti, P., Zhuang, P., and Hallett, M. (1997). Event-related coherence and event-related desynchronization/synchronization in the 10 Hz and 20 Hz EEG during self-paced movements. *Electroencephalogr. Clin. Neurophysiol.* 104, 199–206. doi: 10.1016/S0168-5597(96)96051-7

Levy, R., Hutchison, W. D., Lozano, A. M., and Dostrovsky, J. O. (2000). High-frequency synchronization of neuronal activity in the subthalamic nucleus of parkinsonian patients with limb tremor. *J. Neurosci.* 20, 7766–7775. doi: 10.1523/JNEUROSCI.20-20-07766.2000

Levy, R., Hutchison, W. D., Lozano, A. M., and Dostrovsky, J. O. (2002). Synchronized neuronal discharge in the basal ganglia of parkinsonian patients is limited to oscillatory activity. *J. Neurosci.* 22, 2855–2861. doi: 10.1523/JNEUROSCI.22-07-02855.2002

Miller, W. C., and DeLong, M. R. (1987). "Altered tonic activity of neurons in the globus pallidus and subthalamic nucleus in the primate MPTP model of parkinsonism," in *The Basal Ganglia II*. eds M. B. Carpenter and A. Jayaraman (Boston, MA: Springer), 415–427.

Mink, J. W. (1996). The basal ganglia: focused selection and inhibition of competing motor programs. *Progr. Neurobiol.* 50, 381–425. doi: 10.1016/S0301-0082(96)00042-1

Mitzdorf, U. (1985). Current source-density method and application in cat cerebral cortex: investigation of evoked potentials and EEG phenomena. *Physiol. Rev.* 65, 37–100. doi: 10.1152/physrev.1985.65.1.37

Murthy, V. N., and Fetz, E. E. (1996). Oscillatory activity in sensorimotor cortex of awake monkeys: synchronization of local field potentials and relation to behavior. *J. Neurophysiol.* 76, 3949–3967.

Nambu, A. (2004). "A new dynamic model of the cortico-basal ganglia loop," in *Progress in Brain Research, Vol. 143*, eds S. Mori, D. Stuart, and M. Weisendanger (New York, NY: Elsevier), 461–466.

Nini, A., Feingold, A., Slovin, H., and Bergman, H. (1995). Neurons in the globus pallidus do not show correlated activity in the normal monkey, but phase-locked oscillations appear in the MPTP model of parkinsonism. *J. Neurophysiol.* 74, 1800–1805. doi: 10.1152/jn.1995.74.4.1800

Ohara, S., Ikeda, A., Kunieda, T., Yazawa, S., Baba, K., Nagamine, T., et al. (2000). Movement-related change of electrocorticographic activity in human supplementary motor area proper. *Brain* 123(Pt 6), 1203–1215. doi: 10.1093/brain/123.6.1203

Penfield, W., and Rasmussen, T. (1950). *The Cerebral Cortex of Man; A Clinical Study of Localization of Function*. Oxford: Macmillan.

Pfurtscheller, G., and Neuper, C. (1992). Simultaneous EEG 10 Hz desynchronization and 40 Hz synchronization during finger movements. *Neuroreport* 3, 1057–1060. doi: 10.1097/00001756-199212000-00006

Priori, A., Foffani, G., Pesenti, A., Tamma, F., Bianchi, A. M., Pellegrini, M., et al. (2004). Rhythm-specific pharmacological modulation of subthalamic activity in Parkinson's disease. *Exp. Neurol.* 189, 369–379. doi: 10.1016/j.expneurol.2004.06.001

Raz, A., Vaadia, E., and Bergman, H. (2000). Firing patterns and correlations of spontaneous discharge of pallidal neurons in the normal and the tremulous 1-methyl-4-phenyl-1, 2, 3, 6-tetrahydropyridine vervet model of parkinsonism. *J. Neurosci.* 20, 8559–8571. doi: 10.1523/JNEUROSCI.20-22-08559.2000

Sanes, J. N., and Donoghue, J. P. (1993). Oscillations in local field potentials of the primate motor cortex during voluntary movement. *Proc. Natl. Acad. Sci. U.S.A.* 90, 4470–4474.

Santaniello, S., Montgomery Jr., E. B., Gale, J. T., and Sarma, S. V. (2012). Non-stationary discharge patterns in motor cortex under subthalamic nucleus deep brain stimulation. *Front. Integr. Neurosci.* 6:35. doi: 10.3389/fnint.2012.00035

Sarma, S. V., Cheng, M. L., Eden, U. T., Williams, Z., Brown, E. N., and Eskandar, E. (2012). The effects of cues on neurons in the basal ganglia in Parkinson's disease. *Front. Integr. Neurosci.* 6:40. doi: 10.3389/fnint.2012.00040

Sarma, S. V., Eden, U. T., Cheng, M. L., Williams, Z. M., Hu, R., Eskandar, E., et al. (2010). Using point process models to compare neural spiking activity in the subthalamic nucleus of Parkinson's patients and a healthy primate. *IEEE Transac. Biomed. Eng.* 57, 1297–1305. doi: 10.1109/TBME.2009.2039213

Saxena, S., Gale, J. T., Eskandar, E. N., and Sarma, S. V. (2011). "Modulations in the oscillatory activity of the globus pallidus internus neurons during a behavioral task-a point process analysis," in *2011 Annual International Conference of the IEEE Engineering in Medicine and Biology Society* (Boston, MA), 4179–4182.

Saxena, S., Santaniello, S., Montgomery, E. B., Gale, J. T., and Sarma, S. V. (2010). "Point process models show temporal dependencies of basal ganglia nuclei under deep brain stimulation," in *2010 Annual International Conference of the IEEE Engineering in Medicine and Biology* (Buenos Aires: IEEE), 4152–4155.

Saxena, S., Schieber, M. H., Thakor, N. V., and Sarma, S. V. (2012). Aggregate input-output models of neuronal populations. *IEEE Transac. Biomed. Eng.* 59, 2030–2039. doi: 10.1109/TBME.2012.2196699

Schoffelen, J. M., Oostenveld, R., and Fries, P. (2005). Neuronal coherence as a mechanism of effective corticospinal interaction. *Science* 308, 111–113. doi: 10.1126/science.1107027

Shin, S., and Sommer, M. A. (2010). Activity of neurons in monkey globus pallidus during oculomotor behavior in comparison with substantia nigra pars reticulata. *J. Neurophysiol.* 103, 1874–1887. doi: 10.1152/jn.00101.2009

Snyder, D. L., and Miller, M. I. (2012). *Random Point Processes in Time and Space*. New York, NY: Springer Science & Business Media.

Sochurkova, D., and Rektor, I. (2003). Event-related desynchronization/synchronization in the putamen. An SEEG case study. *Exp. Brain Res.* 149, 401–404. doi: 10.1007/s00221-003-1371-2

Sumsky, S. L., and Santaniello, S. (2018). Temporal pattern of ripple events in temporal lobe epilepsy: towards a pattern-based localization of the seizure onset zone. *Conf. Proc. IEEE Eng. Med. Biol. Soc.* 2018:2288–2291. doi: 10.1109/EMBC.2018.8512742

Sumsky, S. L., Schieber, M. H., Thakor, N. V., Sarma, S. V., and Santaniello, S. (2017). Decoding kinematics using task-independent movement-phase-specific encoding models. *IEEE Trans. Neural Syst. Rehabil. Eng.* 25:2122–2132. doi: 10.1109/TNSRE.2017.2709756

Tachibana, Y., and Hikosaka, O. (2012). The primate ventral pallidum encodes expected reward value and regulates motor action. *Neuron* 76, 826–837. doi: 10.1016/j.neuron.2012.09.030

Toro, C., Deuschl, G., Thatcher, R., Sato, S., Kufta, C., and Hallett, M. (1994). Event-related desynchronization and movement-related cortical potentials on the ECoG and EEG. *Electroencephalogr. Clin. Neurophysiol.* 93, 380–389. doi: 10.1016/0168-5597(94)90126-0

Truccolo, W., Eden, U. T., Fellows, M. R., Donoghue, J. P., and Brown, E. N. (2005). A point process framework for relating neural spiking activity to spiking

history, neural ensemble and extrinsic covariate effects. *J. Neurophysiol.* 93, 1074–1089. doi: 10.1152/jn.00697.2004

Truccolo, W., Friehs, G. M., Donoghue, J. P., and Hochberg, L. R. (2008). Primary motor cortex tuning to intended movement kinematics in humans with tetraplegia. *J. Neurosci.* 28, 1163–1178. doi: 10.1523/JNEUROSCI.4415-07.2008

Turner, R. S., and Anderson, M. E. (1997). Pallidal discharge related to the kinematics of reaching movements in two dimensions. *J. Neurophysiol.* 77, 1051–1074. doi: 10.1152/jn.1997.77.3.1051

Weinberger, M., Mahant, N., Hutchison, W. D., Lozano, A. M., Moro, E., Hodaie, M., et al. (2006). Beta oscillatory activity in the subthalamic nucleus and its relation to dopaminergic response in Parkinson's disease. *J. Neurophysiol.* 96, 3248–3256. doi: 10.1152/jn.00697.2006

Welch, P. (1967). The use of fast Fourier transform for the estimation of power spectra: a method based on time averaging over short, modified periodograms. *IEEE Transac. Audio Electroacoust.* 15, 70–73. doi: 10.1109/TAU.1967.1161901

Wingeier, B., Tcheng, T., Koop, M. M., Hill, B. C., Heit, G., and Bronte-Stewart, H. M. (2006). Intra-operative STN DBS attenuates the prominent beta rhythm in the STN in Parkinson's disease. *Exp. Neurol.* 197, 244–251. doi: 10.1016/j.expneurol.2005.09.016

Conflict of Interest Statement: The authors declare that the research was conducted in the absence of any commercial or financial relationships that could be construed as a potential conflict of interest.

frontiers in Neurology

PERSPECTIVE
published: 10 May 2019
doi: 10.3389/fneur.2019.00462

Linking Pathological Oscillations With Altered Temporal Processing in Parkinsons Disease: Neurophysiological Mechanisms and Implications for Neuromodulation

Martijn Beudel[1,2]*, *Anna Sadnicka*[3,4], *Mark Edwards*[4] *and Bauke M. de Jong*[2]

[1] Department of Neurology, Amsterdam Neuroscience Institute, Amsterdam University Medical Center, Amsterdam, Netherlands, [2] Department of Neurology, University Medical Center Groningen, University of Groningen, Groningen, Netherlands, [3] Faculty of Brain Sciences, Institute of Neurology, University College London, London, United Kingdom, [4] Department of Neurology, St. George's University of London, London, United Kingdom

OPEN ACCESS

Edited by:
Tim Anderson,
University of Otago, Christchurch, New Zealand

Reviewed by:
Antonella Conte,
Sapienza University of Rome, Italy
Rick Helmich,
Radboud University Nijmegen Medical Centre, Netherlands

***Correspondence:**
Martijn Beudel
m.beudel@amc.uva.nl

Specialty section:
This article was submitted to Movement Disorders, a section of the journal Frontiers in Neurology

Received: 29 January 2019
Accepted: 16 April 2019
Published: 10 May 2019

Citation:
Beudel M, Sadnicka A, Edwards M and de Jong BM (2019) Linking Pathological Oscillations With Altered Temporal Processing in Parkinsons Disease: Neurophysiological Mechanisms and Implications for Neuromodulation. Front. Neurol. 10:462. doi: 10.3389/fneur.2019.00462

Emerging evidence suggests that Parkinson's disease (PD) results from disrupted oscillatory activity in cortico-basal ganglia-thalamo-cortical (CBGTC) and cerebellar networks which can be partially corrected by applying deep brain stimulation (DBS). The inherent dynamic nature of such oscillatory activity might implicate that is represents temporal aspects of motor control. While the timing of muscle activities in CBGTC networks constitute the temporal dimensions of distinct motor acts, these very networks are also involved in somatosensory processing. In this respect, a temporal aspect of somatosensory processing in motor control concerns matching predicted (feedforward) and actual (feedback) sensory consequences of movement which implies a distinct contribution to demarcating the temporal order of events. Emerging evidence shows that such somatosensory processing is altered in movement disorders. This raises the question how disrupted oscillatory activity is related to impaired temporal processing and how/whether DBS can functionally restore this. In this perspective article, the neural underpinnings of temporal processing will be reviewed and translated to the specific alternated oscillatory neural activity specifically found in Parkinson's disease. These findings will be integrated in a neurophysiological framework linking somatosensory and motor processing. Finally, future implications for neuromodulation will be discussed with potential implications for strategy across a range of movement disorders.

Keywords: Parkinson's disease, deep brain stimulation, oscillations, timing, movement disorders

TIME AND THE BRAIN

Purposeful motor behavior requires adequate spatio-temporal co-ordination of limbs and axial body parts. E.g., in catching a ball, joint movements, are arranged in such a way that the hand reaches the target's location at the correct time. These spatial and temporal characteristics of movement are also distinctively represented in the organization underlying cerebral motor control, embedded in both segregated and integrated neuronal circuitries (1, 2). Regarding motor timing, at least two interrelated levels of organization may be discerned:

(i) planning "to be" at the right time at the right place and

(ii) planning the serial order of required muscle contractions in order "to move" effectively. The first highlights engagement with a dynamic environment and underscores the relation between motor and perceptual timing. Given the relative slow cerebral processing time, such environmental engagement requires anticipation on near-future events. With regard to the temporal orchestration of muscle contractions, proprioception makes an additional sensory contribution to motor control, both in feedforward and feedback modes (3).

The dynamics of an environment, i.e., the succession of events, is perceived as a sequence of spatial changes. Segregated analysis of the various features of (visual) stimuli, such as shape, color, and visual motion, along parallel processing streams with varying synaptic delays, implies that the initial stimulus time is dispersed within the brain, thus losing an absolute (external) measure of time (4, 5). Moreover, a consequence of such necessary cerebral processing time is that the flow of external change is fractionated, demarcating intervals between distinct spatial frames. This is consistent with daily-life experience that at certain speed, a moving dot will appear as a line. Apparently, intervals of minimal change define the threshold at which a moving dot is either perceived as a dot or changes into a line. Based on functional imaging results the cerebellum is particularly implicated in assessing differences between past and future spatial frames enabling anticipation on coming events (6, 7), while the striatum plays a specific role in monitoring minimal intervals of successive spatial change, providing an internal measure of non-contextual time, i.e., an internal clock (5, 8, 9). For the latter, parallel streams of cortical processing steps, with the intrinsic consequence of introducing temporal dispersion, efferent copies might be emitted to the striatum and provide sequential regularity at system level (**Figure 1**). This is consistent with the model of cortical networks that enable "timing" as a result of time-dependent network changes (10). Closely related to this concept, the basal ganglia have been proposed to play a role in the synchronization of multiple cortical oscillators (11, 12).

The concept of minimal intervals of spatial change finds particularly support from a variant of the "flash-lag illusion," i.e., a "flash-lead" illusion. This phenomenon implies that a moving object is perceived to be behind a spatially concurrent stationary flash before the two disappear (13). Disappearance of the moving dot interrupts building the final "frame," leaving perception of the preceding frame registering its foregoing location. Assuming that the delay reflects processing time required to construct a "single spatial frame," it was speculated that this temporal measure is in the magnitude of 100 ms. In the classical "flash-lag" illusion, which implied that the moving object did not disappear but proceeded its trajectory, the moving object is perceived to be ahead of the spatially concurrent stationary flash (14, 15). Here, it is proposed that the percept ("spatial frame") attributed to the time of the flash is a function of events that happen in the ∼100 ms after the flash, i.e., the processing time to construct such frame, with interpolation of the past concerning the moving object (16, 17). In Parkinson's disease (PD), this illusion is disrupted (18). In the present paper, we will discuss the specific alterations of temporal processing in PD and its implications for applying neuromodulation, in particular deep brain stimulation (DBS).

TEMPORAL PROCESSING IN PARKINSON'S DISEASE

One of the most remarkable features of disturbed temporal processing in PD is noticed when assessing the defining feature of PD; bradykinesia. When asked to make regular finger, hand and arm movements, PD patients show specific difficulty in maintaining sufficient velocity and regularity/rhythm. Furthermore, there is a vast amount of experimental evidence that shows that temporal processing in the perceptual domain is abnormal in PD (19–21). This not only holds for the temporal discrimination threshold (TDT)–the minimum inter-stimulus time between two sensory stimuli which a subject can reliably detect that there are two stimuli rather than one (22) but also for the perception of inter-stimulus intervals (23) and rhythm processing (24). As a consequence, perceptual illusions, such as the rubber hand (25) and flash-lag illusion (18), are perceived differently in PD patients compared to controls. After the application of dopaminergic drugs, several studies have shown a reduction of the TDT more toward healthy controls (22), similar observations are noticed after the application of DBS whereafter the discrimination of auditory inter-stimulus intervals improves (26). As temporal processing improves, recent evidence shows that also perceptual illusions like the rubber hand illusion improve after the application of DBS (27). In several studies the degree of the disturbance in temporal processing is correlated with the severity of Parkinsonian motor symptoms (18, 22, 28). These correlations link the disturbed velocity of movements with temporal processing capacities; the slower a patient moves the slower he / or she can perceive temporal changes.

The pathophysiological mechanism of the disrupted temporal processing in PD are not yet fully elucidated. The fact that there is a dopaminergic depletion in PD and that dopaminergic drugs (and DBS) restore alterations in temporal-processing made initial hypothesis about the its origin go to a "dopaminergic clock" (29). This is further supported by animal-experiments showing that drugs with an opposite effect, neuroleptics, show a decrease of the velocity of the dopaminergic clock and that this is dependent on de D2 affinity of the neuroleptic (30). Further evidence for such dopaminergic clock comes from PET imaging in which TDT values were correlated with the severity of the striatal dopaminergic deficit (31) and fMRI studies in healthy volunteers in which striatal activation occurred during temporal processing (5, 8). Although this correlation provides further evidence for a dopaminergic role. It does not yet elucidate the mechanism at a more explicit neural network level. For this reason, data with a higher temporal resolution; neurophysiological signals, can provide such evidence.

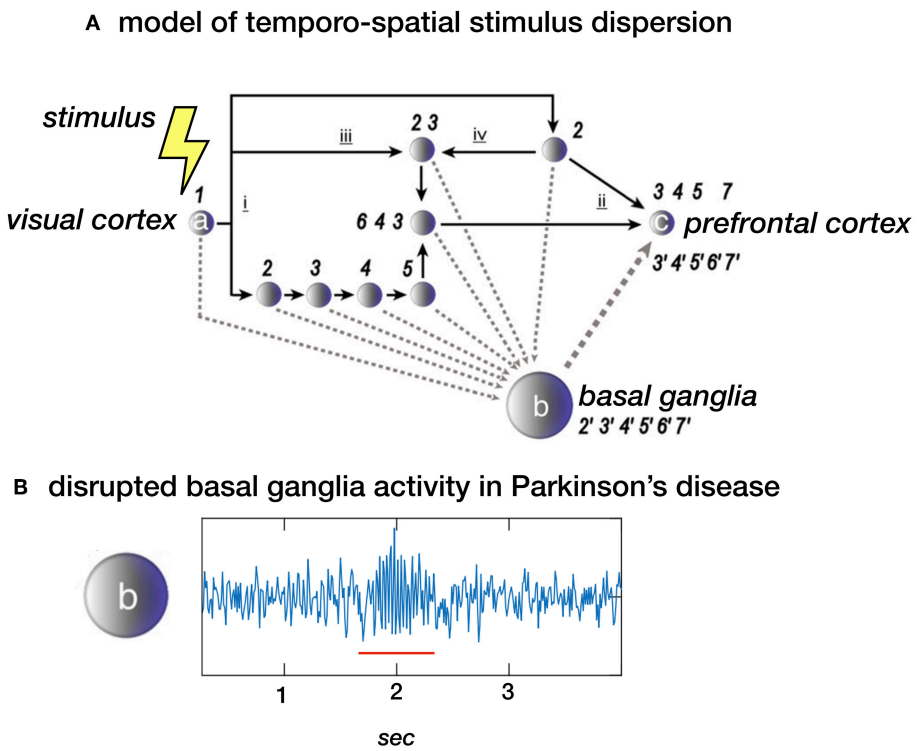

FIGURE 1 | (A) Stimulus dispersion in space and time. Scheme of a simplified neuronal network to illustrate dispersion in space and time following the initial stimulus-induced activation (1) of e.g., the visual cortex (locus a). Successive processing steps (indicated by the numbers 2–7) take place according to principles of functional segregation (i) and integration (ii), as well as bottom-up (iii) and top-down (iv) mechanisms. Differences in synaptic delay along parallel processing streams, due to different number of processing nodes along each pathway, may introduce sequence irregularity. At system-level, however, sequential regularity is maintained by the integration of efferent copies sent to the basal ganglia (locus b). The latter may act as an oscillator, providing a measure of "processing-based" time at network locus c (e.g., the prefrontal cortex). **(B)** Local field potential (LFP) showing neural activity in the subthalamic nucleus (STN) in a healthy subject of a patient with Parkinsons disease. The "burst" with increased and more synchronized activity in the beta (13–30 Hz) domain (underscored with a red line) is typical for Parkinsons disease. In theory, the proposed model depicted in *a*. could be disturbed by this pathological activity. **(A)** Derived from (5), NeuroImage **(B)** unpublished data.

NEUROPHYSIOLOGICAL ALTERATIONS IN PARKINSON'S DISEASE

Stereotactic and functional neurosurgery for movement disorders have provided a unique opportunity to directly record neural activity in the basal ganglia and cortex from either the single neuron, using micro-electrode recordings (MER), or from populations of neurons, using local field potentials (LFP). Furthermore, with advanced signal processing techniques it is currently also possible to extract EEG characteristics, that are specific for movement disorders.

In PD, an excessive domination of beta (13–30 Hz) oscillations is found throughout the motor system. Up to now, the origin of these oscillation in patients is not yet established but recent animal studies have shown that dopaminergic depletion leads to increased firing of striatal spinal projection neurons of the indirect pathway which in turn become prone to being recruited for exaggerated beta oscillations (32) These beta-oscillations decrease after the application of dopaminergic medication (33) and DBS (34). One of the limitations of these findings is that no reference values are present from healthy controls, which makes disease-specificity difficult to prove. However, the amount of beta oscillations correlates with contralateral akinesia-rigidity scores (35) and are more pronounced in PD as in dystonia in a recent meta-analysis (36). Furthermore, not only, the power of local beta oscillations but also the coherence in the beta range between cortex and STN is altered (37) and can be restored by applying DBS (38). One recent, finding is that the presence of increased beta activity changes over time and transient increases of beta activation occurs in so called "bursts" (39, 40). The longer the average burst duration is, the more severe PD symptoms are. Further evidence for a relation between symptom severity with the stability of beta oscillations over time comes from a study in which the *variability* of beta-power inversely correlated with symptom severity in PD (41). This is consistent with the implication that longer beta bursts reflect reduced beta power variability. In other words, excessive enhanced synchronization of activity in the beta band is present in PD and is correlated with the severity of motor symptoms.

LINKING NEUROPHYSIOLOGICAL ALTERATIONS WITH TEMPORAL PROCESSING

So far, no experimental evidence is available that directly links disturbed (beta) oscillatory activity to disturbed temporal processing in PD. However, beta oscillations have been involved in many other processes beyond movement. Transient beta oscillations play an important role in the successful stopping of actions (42, 43). Furthermore, beta oscillations play a role in "status quo maintenance" (44) and "top-down" based attention (45). Next to this, the *volatility* of beta oscillations (beta modulation) is involved in the sequencing of complex sensorimotor processes including repetitive movements (46) as well as passive listening to isochronous sounds (47). Based on these findings and the arguments presented in the previous sections one may infer that the correlation of PD symptom severity with (i) the amount of beta oscillations as well as (ii) altered perceptual time processing, provides an indirect arguments for the context that exaggerated oscillatory activity in the motor system [e.g., (38)] represents a neuronal mechanisms causing altered temporal processing in general. In other words, one may ask whether it is possible that exaggerated synchronized activity discards temporally sensitive information (efferent copies) as a noise filter (**Figure 2**) And consequently, is the magnitude of established change in perceptual illusions determined based on exaggerated beta oscillations? These hypotheses can be tested by combining psychophysical paradigms with time-locked neurophysiological recordings [e.g., (48)].

IMPLICATIONS FOR NEUROMODULATION

Although DBS is an established treatment for refractory movement disorders, it has its limitations in terms of efficacy and side-effects. One of the reasons for this is that not only pathological but also physiological neural activity is suppressed. Given the natural fluctuation of the severity of Parkinsonian symptoms, e.g., due to dopaminergic medication and fatigue, DBS might, in PD, only be effective when pathological neural activity is present, and symptoms are present [e.g., (49)]. This implies that DBS should indeed not be provided continuously but in an intermittent and adaptive way, adaptive DBS (aDBS) (50). Up to now, all the experimental evidence for aDBS comes from paradigms in which high frequency stimulation ($\pm$130 Hz) is either switched ON or OFF or modulated in amplitude based on the amount of pathological beta oscillations (**Figure 3**). On the other hand, beta oscillations also fulfill a physiological, anti-kinetic role in terminating actions (43). When applying DBS in such a way that it is only switched on when disruptive beta oscillations are present, DBS might provide a more profound effect while stimulation induced side effects would be reduced (51).

Although the approach described before adapts stimulation on the amount of pathological oscillations, it is still independent of sensorimotor processing. Another approach to time neuromodulation is to apply stimulation based on the presence of *events* when pathological activation occurs. Such approach has been clinically applied for almost a decade in epilepsy patients [e.g., (52)] and recently also a patient with Tourette syndrome (53). In these two disorders DBS was triggered by the presence of epileptic activity and presence of neural activity associated with tics, respectively. In theory, DBS could also be triggered by other potentials that are, for example, related to movement initiation. This approach has recently been trialed a in a stroke recovery model (54). In this study, electrical stimulation time-locked to transient LFO's, which occur during skilled upper limb tasks, significantly improved upper limb function. Such form of precision medicine highlights the importance of the accurate timing of neuromodulation. Further support for such a phase-specific role of neuromodulation comes from tremor studies in which DBS (55) or transcranial direct current stimulation [TDCS, (49)] aligned to tremor phase, resulted in significant tremor suppression with minimally delivered energy. Although, such an "event-based" form of stimulation has not been trialed in PD, a recent paper (56) showed the temporal course of STN activation during inhibitory, motor, and cognitive tasks, which might form the basis for such stimulation algorithms. By applying these event based analyses of LFP's the effects of different forms of stimulation can be tested and a the role between physiological oscillatory activity [e.g., (48)] and disturbed oscillatory activity could be better elucidated (**Figure 3**). In line with this, by filtering disturbed oscillatory activity, but leaving physiological neuronal activity unaffected, sensorimotor processing, including temporal processing might be return to physiological conditions. Evidence for this comes from recent studies showing that conventional (continuous) DBS shows both a more constant suppression of subcortical (39) and cortical beta activity (57), which might lack the essential volatility to show peri-stimulus beta modulation to process essential temporal information. Of course this needs to be proven by empirical findings and we hope to test these hypotheses in the nearby future.

PARALLELS WITHIN OTHER MOVEMENT DISORDERS

Dystonia is another movement disorder in which temporal processing has been extensively tested. Temporal discrimination thresholds have been found to be elevated across both the visual and somatosensory domains (58). Interestingly in cervical dystonia, abnormalities in temporal discrimination in relatives has led to the hypothesis that abnormalities in TDT are a marker of non-manifesting gene carriage [acting as an endophenotype, (59)]. In contrast to PD, TDT abnormalities persist despite the efficacy of GPi-DBS, suggesting that DBS does not appear to improve dystonic motor activity by correcting abnormalities in sensory processing, at least as measured by the TDT (60). A distributed network is likely to be involved in the processing of TDT, however, notably much of the variability of TDT values across subjects has been linked to neural markers of inhibition in the primary

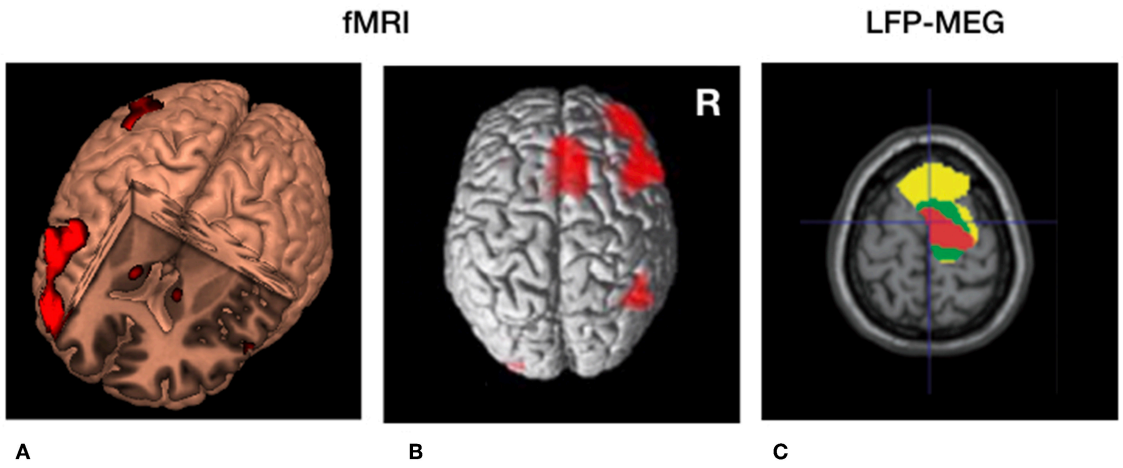

FIGURE 2 | Cerebral circuitry involved in temporal processing and cerebral circuitry selectively modulated by deep brain stimulation (DBS) in Parkinson's disease. **(A)** 3D fMRI activation pattern in healthy volunteers during a temporal estimation task showing increased bilateral basal ganglia activity and right frontal activation. **(B)** Similar rendered contrast showing additional activation of the supplementary motor area (SMA). **(C)** Beta (13–30 Hz) coherence between local field potentials (LFP's) of the subthalamic nucleus (STN) and frontal regions recorded with magnetoencephalography (MEG). Yellow, low beta (13–21 Hz); Green, high beta (21–30 Hz) coherence. Red = decreased cortical beta coherence after the application of DBS. **(A,B)** Derived with permission from (5), NeuroImage **(C)** derived with permission from (38), Brain.

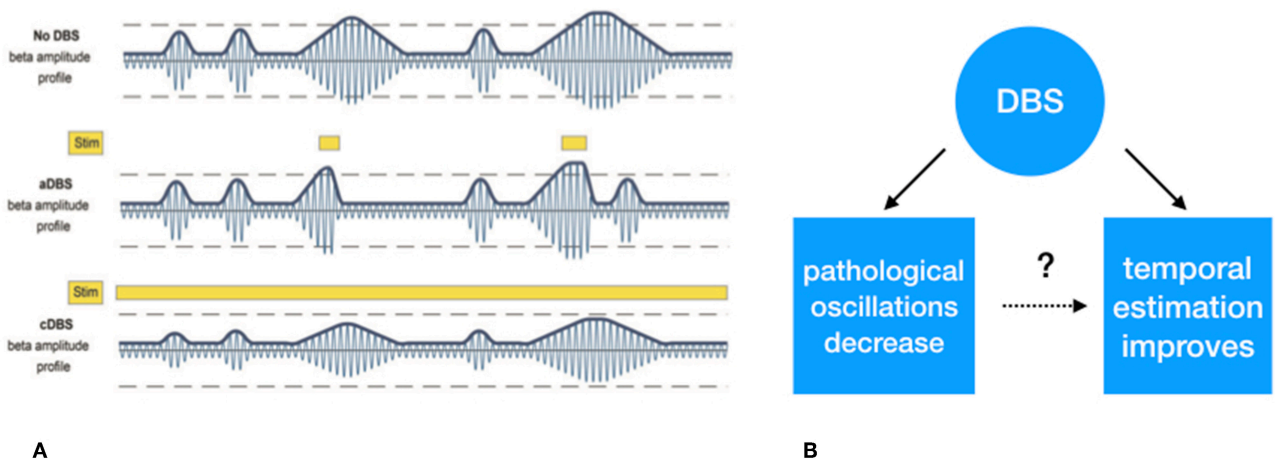

FIGURE 3 | (A) Schematic representation of exaggerated beta (13–30 Hz) "burst" activity derived from the subthalamic nucleus. The first row depicts the similar periodically enhanced beta activity as depicted in **Figure 1**. The second row depicts the effect of selective suppression of beta burst activity of a certain magnitude and duration. This leads to selective, i.e., adaptive, stimulation. In the third row, the non-selective effect of continuous stimulation, conventional DBS, is depicted which leads to an overall suppression of beta activity, irrespective its magnitude, and duration. **(B)** Whether the suppression of exaggerated leads to improved temporal estimation is to be tested. **(A)** Derived with permission from (39), Brain.

somatosensory cortex [S1, (61)]. Furthermore, high frequency repetitive stimulation over the S1 increases neurophysiological makers of inhibition and sensory function and such changes correlate with improvements in TDT (62). Thus, similar to PD, such findings hint that neural correlates of TDT abnormalities could be used to provide a richer input environment to inform adaptive DBS strategies. This is particularly relevant in dystonia as clinical response often lags many months behind changes or the initiation of DBS offering the operator little real time feedback by which to optimize stimulation parameters.

Compared to cerebellar ataxia, as seen in cerebellar degeneration, PD patients show a selective disturbance in rhythmic temporal prediction, and not in single interval prediction (19, 21). These findings are in line with the role of the basal ganglia in monitoring minimal intervals of successive spatial change, providing an internal measure of non-contextual time (See section Time and the Brain).

FUTURE WORK

In order to further elucidate the true nature of disturbed temporal processing and its potential therapeutic consequences in PD, several new avenues are currently being explored. Testing temporal processing draws on psychophysics, and there are some drawbacks of the different psychophysical paradigms which have been previously applied. Since most of these paradigms rely on self-report, they can be subject to bias. Standard staircase methodology in which the separation between two stimuli is slowly increased or decreased in a predictable manner allows the obtained thresholds to be readily biased by a decision strategy unrelated to temporal discrimination ability (63). For example, if stimuli are gradually changed in the direction of threshold over several trials experimentally it has been shown that some observers develop a habit of repeating the same response and thus continuing to make the response after the threshold point has been reached. This "error of habituation" affects the data by falsely increasing thresholds (64). Within some paradigms catch trials (single stimuli trials) are also introduced which attempts to mitigate these errors and encourages participants to evaluate the sensory information arriving on each trial. However, such biases are best mitigated by randomizing the order of presentation (64).

The analysis of psychophysical paradigms has also progressed hugely since the methods of limits were established and their limitations acknowledged in the 1960s. By using reaction time data as well as well as accuracy of response inferences can also be made about the decision making components integral to the TDT. Such factors have begun to be explored in PD. For example, computational modeling has revealed that timing deficits in PD cannot be solely attributed to perceptual temporal distortions, but are also associated with impulsive decision strategies that bias patients toward premature responses (65). Similarly, drift diffusion decision modeling in a large group of subjects with cervical dystonia points to a more conservative decision strategy in cervical dystonia over and above a temporal discrimination deficit (63). Such finding are highly feasible as the subtle neuropsychiatric profile of many movement disorders are increasingly appreciated.

Although such studies increase the complexity of interpretation of simple TDT threshold embracing such techniques and analysis may prove its utility in the future. We are still far from having disease specific psychophysical markers for temporal processing. By better estimation of the true psychophysical deficit psychophysical deficits unique to particular disease states may be found. This yields greater power to researchers to discover the corresponding neural correlate which could be used for aDBS. This especially involves the experiments in which state of art neuromodulation, neurophysiology and psychophysics are simultaneously applied.

CONCLUSION

Temporal processing is disturbed in PD while the severity of the movement disorder is sometimes correlated with the magnitude of changes in perceptual temporal processing. It is not yet established whether there is a causative link but pathological neural oscillatory activity might play a role. Furthermore, DBS improves motor performance and perceptual temporal processing and reduces pathological neural oscillatory activity. These observations provide indirect evidence that temporal processing is similarly affected by the same pathological neural oscillatory activity. As we move toward an era of more effective adaptive DBS finding neural correlates of temporal processing abnormalities may allow DBS to be dynamically titrated in response to a wider range of pathophysiological parameters. By bringing together neuromodulation, advanced neurophysiology and psychophysics, these hypotheses can be tested.

AUTHOR CONTRIBUTIONS

BdJ and AS respectively wrote the 1st and 6th + 7th sections of the manuscript. MB wrote the first draft of the manuscript. MB. BdJ, AS, and ME revised the manuscript.

REFERENCES

1. Medendorp WP. Spatial constancy mechanisms in motor control. *Philosoph Trans R Soc B Biol Sci.* (2011) 366:476–91. doi: 10.1098/rstb.2010.0089
2. Ciullo V, Vecchio D, Gili T, Spalletta G, Piras F. Segregation of brain structural networks supports spatio-temporal predictive processing. *Front Hum Neurosci.* (2018) 12:212. doi: 10.3389/fnhum.2018.00212
3. Gritsenko V, Yakovenko S, Kalaska JF. Integration of predictive feedforward and sensory feedback signals for online control of visually guided movement. *J Neurophysiol.* (2009) 102:914–30. doi: 10.1152/jn.91324.2008
4. Bartels A, Zeki S. The chronoarchitecture of the human brain–natural viewing conditions reveal a time-based anatomy of the brain. *Neuroimage.* (2004) 22:419–33. doi: 10.1016/j.neuroimage.2004.01.007
5. Beudel M, Renken R, Leenders KL, de Jong BM. Cerebral representations of space and time. *Neuroimage.* (2009) 44:1032–40. doi: 10.1016/j.neuroimage.2008.09.028
6. Spencer RMC, Zelaznik HN, Diedrichsen J, Ivry RB. Disrupted timing of discontinuous but not continuous movements by cerebellar lesions. *Science.* (2003) 300:1437–9. doi: 10.1126/science.1083661
7. Schlerf JE, Spencer RMC, Zelaznik HN, Ivry RB. Timing of rhythmic movements in patients with cerebellar degeneration. *Cerebellum.* (2007) 6:221–31. doi: 10.1080/14734220701370643
8. Meck WH, Malapani C. Neuroimaging of interval timing. *Brain Res Cogn Brain Res.* (2004) 21:133–7. doi: 10.1016/j.cogbrainres.2004.07.010
9. Shen B, Wang Z-R, Wang X-P. The fast spiking subpopulation of striatal neurons coding for temporal cognition of movements. *Front Cell Neurosci.* (2017) 11:406. doi: 10.3389/fncel.2017.00406
10. Karmarkar UR, Buonomano DV. Timing in the absence of clocks: encoding time in neural network states. *Neuron.* (2007) 53:427–38. doi: 10.1016/j.neuron.2007.01.006
11. Matell MS, Meck WH, Nicolelis MAL. Interval timing and the encoding of signal duration by ensembles of cortical and striatal neurons. *Behav Neurosci.* (2003) 117:760–73. doi: 10.1037/0735-7044.117.4.760
12. Buhusi C, Meck W. What makes us tick? Functional and neural mechanisms of interval timing. *Nat Rev Neurosci.* (2005) 6:755–65. doi: 10.1038/nrn1764
13. Roulston BW, Self MW, Zeki S. Perceptual compression of space through position integration. *Proc Biol Sci.* (2006) 273:2507–12. doi: 10.1098/rspb.2006.3616

14. Nijhawan R. Motion extrapolation in catching. *Nature.* (1994) 370:256–7. doi: 10.1038/370256b0
15. Eagleman DM, Sejnowski TJ. Motion integration and postdiction in visual awareness. *Science.* (2000) 287:2036–8. doi: 10.1126/science.287.5460.2036
16. Schneider KA. The flash-lag, fröhlich and related motion illusions are natural consequences of discrete sampling in the visual system. *Front Psychol.* (2018) 9:1227. doi: 10.3389/fpsyg.2018.01227
17. Beudel M, de Geus CM, Leenders KL, de Jong BM. Acceleration bias in visually perceived velocity change and effects of Parkinson's bradykinesia. *Neuro Rep.* (2013) 24:773–8. doi: 10.1097/WNR.0b013e328363f739
18. Beudel M, Roosma E, Martinez Manzanera OE, van Laar T, Maurits NM, de Jong BM. Parkinson bradykinesia correlates with EEG background frequency and perceptual forward projection. *Parkinsonism Relat Disord.* (2015) 21:783–8. doi: 10.1016/j.parkreldis.2015.05.004
19. Beudel M, Galama S, Leenders KL, de Jong BM. Time estimation in Parkinson's disease and degenerative cerebellar disease. *Neuroreport.* (2008) 19:1055–8. doi: 10.1097/WNR.0b013e328303b7b9
20. Conte A, Khan N, Defazio G, Rothwell JC, Berardelli A. Pathophysiology of somatosensory abnormalities in Parkinson disease. *Nat Publ Group.* (2013) 9:687–97. doi: 10.1038/nrneurol.2013.224
21. Breska A, Ivry RB. Double dissociation of single-interval and rhythmic temporal prediction in cerebellar degeneration and Parkinson's disease. *Proc Natl Acad Sci USA.* (2018) 115:12283–8. doi: 10.1073/pnas.1810596115
22. Artieda J, Pastor MA, Lacruz F, Obeso JA. Temporal discrimination is abnormal in Parkinson's disease. *Brain.* (1992) 115:199–210. doi: 10.1093/brain/115.1.199
23. O'Boyle DJ, Freeman JS, Cody FW. The accuracy and precision of timing of self-paced, repetitive movements in subjects with Parkinson's disease. *Brain.* (1996) 119(Pt 1):51–70. doi: 10.1093/brain/119.1.51
24. Grahn JA, Brett M. Impairment of beat-based rhythm discrimination in Parkinson's disease. *Cortex.* (2009) 45:54–61. doi: 10.1016/j.cortex.2008.01.005
25. Ding C, Palmer CJ, Hohwy J, Youssef GJ, Paton B, Tsuchiya N, et al. Parkinson's disease alters multisensory perception: Insights from the Rubber Hand Illusion. *Neuropsychologia.* (2017) 97:38–45. doi: 10.1016/j.neuropsychologia.2017.01.031
26. Koch G, Brusa L, Caltagirone C, Oliveri M, Peppe A, Tiraboschi P, et al. Subthalamic deep brain stimulation improves time perception in Parkinson's disease. *Neuro Rep.* (2004) 15:1071–3. doi: 10.1097/00001756-200404290-00028
27. Ding C, Palmer CJ, Hohwy J, Youssef GJ, Paton B, Tsuchiya N, et al. Deep Brain Stimulation for Parkinson's disease changes perception in the Rubber Hand Illusion. *Sci Rep.* (2018) 8:13842. doi: 10.1038/s41598-018-31867-8
28. Conte A, Leodori G, Ferrazzano G, De Bartolo MI, Manzo N, Fabbrini G, et al. Somatosensory temporal discrimination threshold in Parkinson's disease parallels disease severity and duration. *Clin Neurophysiol.* (2016) 127:2985–9. doi: 10.1016/j.clinph.2016.06.026
29. Meck WH, Benson AM. Dissecting the brain's internal clock: how frontal-striatal circuitry keeps time and shifts attention. *Brain Cogn.* (2002) 48:195–211. doi: 10.1006/brcg.2001.1313
30. Meck WH. Affinity for the dopamine D2 receptor predicts neuroleptic potency in decreasing the speed of an internal clock. *Pharmacol Biochem Behav.* (1986) 25:1185–9. doi: 10.1016/0091-3057(86)90109-7
31. Lyoo CH, Ryu YH, Lee MJ, Lee MS. Striatal dopamine loss and discriminative sensory dysfunction in Parkinson's disease. *Acta Neurol Scand.* (2012) 126:344–9. doi: 10.1111/j.1600-0404.2012.01657.x
32. Sharott A, Vinciati F, Nakamura KC, Magill PJ. A population of indirect pathway striatal projection neurons is selectively entrained to parkinsonian beta oscillations. *J Neurosci.* (2017) 37:9977–98. doi: 10.1523/JNEUROSCI.0658-17.2017
33. Kühn AA, Kupsch A, Schneider G-H, Brown P. Reduction in subthalamic 8-35 Hz oscillatory activity correlates with clinical improvement in Parkinson's disease. *Eur J Neurosci.* (2006) 23:1956–60. doi: 10.1111/j.1460-9568.2006.04717.x
34. Eusebio A, Thevathasan W, Doyle Gaynor L, Pogosyan A, Bye E, Foltynie T, et al. Deep brain stimulation can suppress pathological synchronisation in parkinsonian patients. *J Neurol Neurosurg Psychiatr.* (2011) 82:569–73. doi: 10.1136/jnnp.2010.217489
35. Beudel M, Oswal A, Jha A, Foltynie T, Zrinzo L, Hariz M, et al. Oscillatory beta power correlates with akinesia-rigidity in the Parkinsonian subthalamic nucleus. *Mov Disord.* (2017) 32:174–5. doi: 10.1002/mds.26860
36. Pi-a-Fuentes D, van Dijk JMC, Drost G, van Zijl JC, van Laar T, Tijssen MAJ, et al. Direct Comparison of oscillatory activity in the motor system of Parkinson's disease and dystonia: a review of the literature and meta-analysis. *Clin Neurophysiol.* (2019) 130:917–24. doi: 10.1016/j.clinph.2019.02.015
37. Litvak V, Jha A, Eusebio A, Oostenveld R, Foltynie T, Limousin P, et al. Resting oscillatory cortico-subthalamic connectivity in patients with Parkinson's disease. *Brain.* (2011) 134:359–74. doi: 10.1093/brain/awq332
38. Oswal A, Beudel M, Zrinzo L, Limousin P, Hariz M, Foltynie T, et al. Deep brain stimulation modulates synchrony within spatially and spectrally distinct resting state networks in Parkinson's disease. *Brain.* (2016) 139:1482–96. doi: 10.1093/brain/aww048
39. Tinkhauser G, Pogosyan A, Little S, Beudel M, Herz DM, Tan H, et al. The modulatory effect of adaptive deep brain stimulation on beta bursts in Parkinson's disease. *Brain.* (2017) 140:1053–67. doi: 10.1093/brain/awx010
40. Anidi C, O'Day JJ, Anderson RW, Afzal MF, Syrkin-Nikolau J, Velisar A, et al. Neuromodulation targets pathological not physiological beta bursts during gait in Parkinson's disease. *Neurobiol Dis.* (2018) 120:107–17. doi: 10.1016/j.nbd.2018.09.004
41. Little S, Pogosyan A, Kühn AA, Brown P. β band stability over time correlates with Parkinsonian rigidity and bradykinesia. *Exp Neurol.* (2012) 236:383–8. doi: 10.1016/j.expneurol.2012.04.024
42. Jha A, Nachev P, Barnes G, Husain M, Brown P, Litvak V. The frontal control of stopping. *Cereb Cortex.* (2015) 25:4392–406. doi: 10.1093/cercor/bhv027
43. Wessel JR, Ghahremani A, Udupa K, Saha U, Kalia SK, Hodaie M, et al. Stop-related subthalamic beta activity indexes global motor suppression in Parkinson's disease. *Mov Disord.* (2016) 31:1846–53. doi: 10.1002/mds.26732
44. Engel AK, Fries P. Beta-band oscillations–signalling the status quo? *Curr Opin Neurobiol.* (2010) 20:156–65. doi: 10.1016/j.conb.2010.02.015
45. Buschman TJ, Miller EK. Top-down versus bottom-up control of attention in the prefrontal and posterior parietal cortices. *Science.* (2007) 315:1860–2. doi: 10.1126/science.1138071
46. Joundi RA, Brittain J-S, Green AL, Aziz TZ, Brown P, Jenkinson N. Persistent suppression of subthalamic beta-band activity during rhythmic finger tapping in Parkinson's disease. *Clin Neurophysiol.* (2013) 124:565–73. doi: 10.1016/j.clinph.2012.07.029
47. Fujioka T, Trainor LJ, Large EW, Ross B. Internalized timing of isochronous sounds is represented in neuromagnetic beta oscillations. *J Neurosci.* (2012) 32:1791–802. doi: 10.1523/JNEUROSCI.4107-11.2012
48. Hall TM, Nazarpour K, Jackson A. Real-time estimation and biofeedback of single-neuron firing rates using local field potentials. *Nat Commun.* (2014) 5:5462. doi: 10.1038/ncomms6462
49. Brittain J-S, Sharott A, Brown P. The highs and lows of beta activity in cortico-basal ganglia loops. *Eur J Neurosci.* (2014) 39:1951–9. doi: 10.1111/ejn.12574
50. Little S, Brown P. What brain signals are suitable for feedback control of deep brain stimulation in Parkinson's disease? *Ann N Y Acad Sci.* (2012) 1265:9–24. doi: 10.1111/j.1749-6632.2012.06650.x
51. Little S, Tripoliti E, Beudel M, Pogosyan A, Cagnan H, Herz D, et al. Adaptive deep brain stimulation for Parkinson's disease demonstrates reduced speech side effects compared to conventional stimulation in the acute setting. *J Neurol Neurosurg Psychiatr.* (2016) 87:1388–9. doi: 10.1136/jnnp-2016-313518
52. Geller EB, Skarpaas TL, Gross RE, Goodman RR, Barkley GL, Bazil CW, et al. Brain-responsive neurostimulation in patients with medically intractable mesial temporal lobe epilepsy. *Epilepsia.* (2017) 58:994–1004. doi: 10.1111/epi.13740
53. Molina R, Okun MS, Shute JB, Opri E, Rossi PJ, Martinez-Ramirez D, et al. Report of a patient undergoing chronic responsive deep brain stimulation for Tourette syndrome: proof of concept. *J Neurosurg.* (2017) 129:277–565. doi: 10.3171/2017.6.JNS17626
54. Ramanathan DS, Guo L, Gulati T, Davidson G, Hishinuma AK, Won S-J, et al. Low-frequency cortical activity is a neuromodulatory target that tracks recovery after stroke. *Nat Med.* (2018) 24:1257–67. doi: 10.1038/s41591-018-0058-y
55. Cagnan H, Pedrosa D, Little S, Pogosyan A, Cheeran B, Aziz T, et al. Stimulating at the right time: phase-specific deep brain stimulation. *Brain.* (2017) 140:132–45. doi: 10.1093/brain/aww286

56. Neumann W-J, Schroll H, de Almeida Marcelino AL, Horn A, Ewert S, Irmen F, et al. Functional segregation of basal ganglia pathways in Parkinson's disease. *Brain.* (2018) 12:366–316. doi: 10.1093/brain/awy206
57. Gulberti A, Moll CKE, Hamel W, Buhmann C, Koeppen JA, Boelmans K, et al. Predictive timing functions of cortical beta oscillations are impaired in Parkinson's disease and influenced by L-DOPA and deep brain stimulation of the subthalamic nucleus. *NeuroImage Clin.* (2015) 9:436–49. doi: 10.1016/j.nicl.2015.09.013
58. Tinazzi M, Frasson E, Bertolasi L, Fiaschi A, Aglioti S. Temporal discrimination of somesthetic stimuli is impaired in dystonic patients. *Neuro Rep.* (1999) 10:1547–50. doi: 10.1097/00001756-199905140-00028
59. Conte A, McGovern EM, Narasimham S, Beck R, Killian O, O'Riordan S, et al. Temporal discrimination: mechanisms and relevance to adult onset dystonia. *Front Neurol.* (2017) 8:625. doi: 10.3389/fneur.2017.00625
60. Sadnicka A, Kimmich O, Pisarek C, Ruge D, Galea J, Kassavetis P, et al. Pallidal stimulation for cervical dystonia does not correct abnormal temporal discrimination. *Mov Disord.* (2013) 28:1874–7. doi: 10.1002/mds.25581
61. Rocchi L, Casula E, Tocco P, Berardelli A, Rothwell J. Somatosensory temporal discrimination threshold involves inhibitory mechanisms in the primary somatosensory area. *J Neurosci.* (2016) 36:325–35. doi: 10.1523/JNEUROSCI.2008-15.2016
62. Rocchi L, Erro R, Antelmi E, Berardelli A, Tinazzi M, Liguori R, et al. High frequency somatosensory stimulation increases sensori-motor inhibition and leads to perceptual improvement in healthy subjects. *Clin Neurophysiol.* (2017) 128:1015–25. doi: 10.1016/j.clinph.2017.03.046
63. Sadnicka A, Daum C, Cordivari C, Bhatia KP, Rothwell JC, Manohar S, et al. Mind the gap: temporal discrimination and dystonia. *Eur J Neurol.* (2017) 24:796–806. doi: 10.1111/ene.13293
64. Gescheider GA. *Psychophysics: The Fundamentals.* Abingdon, UK: Psychology Press (2013). doi: 10.4324/9780203774458
65. Zhang J, Nombela C, Wolpe N, Barker RA, Rowe JB. Time on timing: dissociating premature responding from interval sensitivity in Parkinson's disease. *Mov Dis.* (2016) 31:1163–72. doi: 10.1002/mds.26631

Conflict of Interest Statement: The authors declare that the research was conducted in the absence of any commercial or financial relationships that could be construed as a potential conflict of interest.

frontiers in Human Neuroscience

CASE REPORT
published: 28 May 2019
doi: 10.3389/fnhum.2019.00163

Cortico-subthalamic Coherence in a Patient With Dystonia Induced by Chorea-Acanthocytosis: A Case Report

Chunyan Cao[1], Peng Huang[1], Tao Wang[1], Shikun Zhan[1], Wei Liu[1], Yixin Pan[1], Yiwen Wu[2], Hongxia Li[2], Bomin Sun[1], Dianyou Li[1]† and Vladimir Litvak[3]†*

[1]Department of Functional Neurosurgery, Affiliated Ruijin Hospital, School of Medicine, Shanghai JiaoTong University, Shanghai, China, [2]Department of Neurology, Affiliated Ruijin Hospital, School of Medicine, Shanghai JiaoTong University, Shanghai, China, [3]Wellcome Centre for Human Neuroimaging, UCL Queen Square Institute of Neurology, London, United Kingdom

The subthalamic nucleus (STN) is a common target for deep brain stimulation (DBS) treatment in Parkinson's disease (PD) but much less frequently targeted for other disorders. Here we report the results of simultaneous local field potential (LFP) recordings and magnetoencephalography (MEG) in a single patient who was implanted bilaterally in the STN for the treatment of dystonia induced by chorea-acanthocytosis. Consistent with the previous results in PD, the dystonia patient showed significant subthalamo-cortical coherence in the high beta band (28–35 Hz) on both sides localized to the mesial sensorimotor areas. In addition, on the right side, significant coherence was found in the theta-alpha band (4–12 Hz) that localized to the medial prefrontal cortex with the peak in the anterior cingulate gyrus. Comparison of STN power spectra with a previously reported PD cohort showed increased power in the theta and alpha bands and decreased power in the low beta band in dystonia which is consistent with most of the previous studies. The present report extends the range of disorders for which cortico-subthalamic oscillatory connectivity has been characterized. Our results strengthen the evidence that at least some of the subthalamo-cortical oscillatory coherent networks are a feature of the healthy brain, although we do not rule out that coherence magnitude could be affected by disease.

Keywords: DBS, magnetoencephalography (MEG), human, movement disorder, oscillations

OPEN ACCESS

Edited by:
Seiki Konishi,
Juntendo University, Japan

Reviewed by:
Dan Piña-Fuentes,
University Medical Center Groningen, Netherlands
Antonella Macerollo,
University College London, United Kingdom
Kiyoshi Nakahara,
Kochi University of Technology, Japan

***Correspondence:**
Dianyou Li
ldy11483@rjh.com.cn

†*These authors have contributed equally to this work*

Received: *12 December 2018*
Accepted: *03 May 2019*
Published: *28 May 2019*

Citation:
Cao C, Huang P, Wang T, Zhan S, Liu W, Pan Y, Wu Y, Li H, Sun B, Li D and Litvak V (2019) Cortico-subthalamic Coherence in a Patient With Dystonia Induced by Chorea-Acanthocytosis: A Case Report. Front. Hum. Neurosci. 13:163. doi: 10.3389/fnhum.2019.00163

INTRODUCTION

Synchronized oscillations are a prevalent phenomenon in neural systems and are hypothesized to play an important role in communication between different neuronal populations (Friston et al., 2015). Cortical oscillatory connectivity in the human brain can be studied non-invasively with electroencephalography (EEG) and magnetoencephalography (MEG; Gross, 2014). However, activity from subcortical nuclei can only be recorded invasively. Deep brain stimulation (DBS) surgery provides a unique opportunity to study the subcortical activities by recording local field potentials (LFPs) from macroelectrodes which are stereotactically targeted with high precision to specific anatomical structures. DBS is a powerful treatment for Parkinson's disease (PD; Limousin et al., 1995), dystonia (Cao et al., 2013) and also for severe obsessive compulsive

disorder (OCD; Chabardès et al., 2013; Mulders et al., 2016). The subthalamic nucleus (STN) is the most common DBS target, primarily used for PD. The internal Globus Pallidus (GPi) is the primary target for dystonia but it is also used in PD. Thus, while electrophysiological markers of PD have been well characterized in both STN and GPi, those of dystonia are mostly known from GPi recordings. A view consolidated in recent years sees both PD and dystonia as oscillopathies (Nimmrich et al., 2015), disorders closely linked to abnormal oscillatory activity in the cortico-basal ganglia circuits. For dystonia the abnormal activity is in theta-alpha (4–12 Hz) range (Silberstein et al., 2003); whereas, for PD the abnormality is in the beta (13–30 Hz) range (Brown et al., 2001). Several previous studies directly comparing LFP power spectra between the two disorders reproduced the same pattern with increased alpha-theta power in dystonia relative to PD and increased beta power in PD (particularly after withdrawal of dopaminergic medication) relative to dystonia. This pattern was observed in both GPi (Silberstein et al., 2003; Wang et al., 2018; Piña-Fuentes et al., 2019) and STN (Neumann et al., 2012; Geng et al., 2017). One study (Wang et al., 2016) did not find clear differences in STN LFP spectra between the dystonia and PD groups. In the motor cortex, the differences between dystonia and PD are less pronounced with one study showing an increase of the peak frequency of alpha and beta oscillations in PD relative to dystonia (Crowell et al., 2012) and another study finding increased broadband high gamma activity in PD but no differences for alpha and beta (Miocinovic et al., 2015). For both dystonia and PD, the study of abnormal oscillations can have clinical implications for improvement of DBS targeting (Yoshida et al., 2010; Horn et al., 2017; Neumann et al., 2017) and development of brain activity driven closed-loop DBS methods (Little et al., 2013; Barow et al., 2014; Meidahl et al., 2017; Piña-Fuentes et al., 2019).

The mechanisms that generate pathological rhythms are not well understood. The modeling work to date has focused primarily on the pathological beta in PD where several competing models have been put forward (see Pavlides et al., 2015 for review). The main unresolved question in modeling work, which is equally likely to apply to theta-alpha in dystonia, is whether the pathological synchronization is generated locally in the basal ganglia or involves abnormal amplification of cortical inputs. Simultaneous recording of MEG and LFP could potentially make it possible to distinguish between these theories as it facilitates the characterization of the interaction between subcortical activity seen in the LFP and cortical areas whose activity can be recorded by MEG (Harmsen et al., 2018).

The two published studies of simultaneous MEG and STN LFP recordings in PD patients at rest (Hirschmann et al., 2011; Litvak et al., 2011a), both show that the STN is coherent with the mesial motor areas [likely, the supplementary motor area (SMA)] in the beta range and with the temporo-parietal areas and the brainstem in the alpha-theta range. A study applying similar methods to dystonia patients with GPi electrodes (Neumann et al., 2015) found beta coherence with the sensorimotor cortex, theta coherence with the inferior temporal cortex and alpha coherence with the cerebellum. The latter was correlated with the degree of clinical impairment.

To determine the relation between these oscillatory coherent networks and pathophysiology of disease it would be helpful to compare recordings from the same DBS target for different neurological disorders. To this end, here we report here an analysis of STN-cortical coherence in a patient with dystonia. This combination of methods, target and disease has not been reported before.

MATERIALS AND METHODS

Patient Details

The study was approved by the local ethics committee of Ruijin hospital, Shanghai JiaoTong University School of Medicine. The patient was informed about the aim and the scope of the study and gave written informed consent. The patient also consented to the publication of the present case report. A 34 years old male developed involuntary movements 4 years prior to the surgery and was diagnosed with chorea-acanthocytosis. Neuroacanthocytosis due to mutations in the VPS13A gene encoding chorein is an autosomal-recessive neurodegenerative disorder which is characterized by chorea and dystonia (Rampoldi et al., 2001). The patient presented with impairment of fine movements of the upper limbs and bradykinesia, mainly involving the right limb. In addition, the patient opened and closed his mouth involuntarily, snorted intermittently and gradually developed lower limb weakness. Two years before the surgery, the symptoms of the left limb gradually became more obvious and difficulty in swallowing and coughing from drinking water appeared. Blood tests showed red blood cell count of 5.25×10^{12}/L. Some red blood cells varied in size and had a spiked cell membrane consistent with the appearance of acanthocytes. Genetic testing revealed a mutation in the gene VPS13A. The structural magnetic resonance imaging (MRI) showed lateral ventricle enlargement and putamen and caudate nucleus atrophy. The patient was not pharmacologically treated prior to surgery.

Deep Brain Stimulation Operation and MEG-LFP Recording

Implantation of the quadripolar DBS electrodes (model 3387; Medtronic, Minneapolis, MN, USA) was performed under general anesthesia bilaterally using a MRI-guided targeting (3.0 T, General Electric), which was co-registered with a CT image (General Electric) with the Leksell stereotactic frame (Zhan et al., 2018). The electrode leads were externalized for a week and temporary externally applied stimulation during this period could partially control the patient's symptoms particularly the involuntary movement of the mouth, pronunciation, and hand movement impairment. We cannot report the results of long-term follow-up at this stage since the patient was operated less than a year ago. We also used the externalization period to record bilateral STN-LFP and whole head MEG simultaneously while the patient was awake. The MEG was recorded with a 306-channel MEG scanner (Elekta Oy, Helsinki, Finland) in a magnetically shielded chamber (Euroshield, Eura, Finland). The EEG system which is integrated with the MEG device was used for the LFP recording. The patient was instructed to rest with eyes

open, and the absence of voluntary movement was confirmed by continuous visual inspection. The raw data were band pass filtered in 0.03–330 Hz range and digitized at 1,000 Hz. The DBS electrode had four platinum-iridium cylindrical surfaces of diameter 1.27 mm, length 1.5 mm and center-to-center separation 1.5 mm. The contacts were numbered 0–3 from the ventral to dorsal.

Reconstruction of Electrode Locations in the STN

We used the Lead-DBS toolbox[1] (Horn and Kühn, 2015) to reconstruct the contact locations. Post-operative CT was co-registered to pre-operative T1 scan using a two-stage linear registration (rigid followed by affine) as implemented in Advanced Normalisation Tools (ANT[2]; Avants et al., 2008). The pre-operative T2 scan was linearly co-registered to pre-operative T1 using SPM12 (Friston et al., 2007). Pre- (and post-) operative acquisitions were spatially normalized into MNI_ICBM_2009b_NLIN_ASYM space (Fonov et al., 2011) using the SyN registration approach in ANT. DBS-Electrodes were automatically pre-localized in native and template space using the PaCER algorithm[3] (Husch et al., 2018) and then manually localized based on post-operative acquisitions using a tool specifically designed for this task (as implemented in Lead-DBS software, Horn and Kühn, 2015).

Analysis of LFP and MEG

MEG data were pre-processed with the temporal extension of Signal Space Separation method (Taulu and Simola, 2006) implemented in the MaxFilter software (Elekta Oy, Helsinki, Finland). The subsequent analyses were done in SPM12[4] (Litvak et al., 2011b) following the procedures described by Litvak et al. (2010, 2011a). LFP data from contacts located in the STN (see **Figure 1**) were converted to bipolar montage which gave one LFP channel per side. The data were high-pass filtered above 1 Hz and 50 Hz line noise and its harmonics were removed with notch filters (Butterworth 5th order, zero phase filters). The data were epoched into 3 s segments. Epochs containing deflections exceeding 20 μV in the LFP channels were removed from analysis which left 136 epochs of clean LFP data which was visually verified.

LFP spectra were computed using multi-taper spectral estimation method (Thomson, 1982). The power was averaged across trials, subjected to log-transform and normalized by subtracting a linear fit to the 55–95 Hz range from the whole spectrum. The aim of these steps was to be able to compare the spectra to our previous recordings done on different system (see below).

Significant cortico-STN coherence was identified by statistical comparison of scalp-frequency images of coherence in the 1–45 Hz range to surrogate images generated by shuffling the reference channel across trials. This procedure was described in detail by Litvak et al. (2011a). The identified significant coherence patterns were source localized for the corresponding frequency band and reference channel using Dynamic Imaging of Coherent Sources (DICS) beamforming (Gross et al., 2001) implemented in the Data Analysis in Source Space (DAiSS) toolbox for SPM[5]. This used a single shell forward model (Nolte, 2003) generated based on the patient's pre-operative T1 using standard SPM procedures (Mattout et al., 2007).

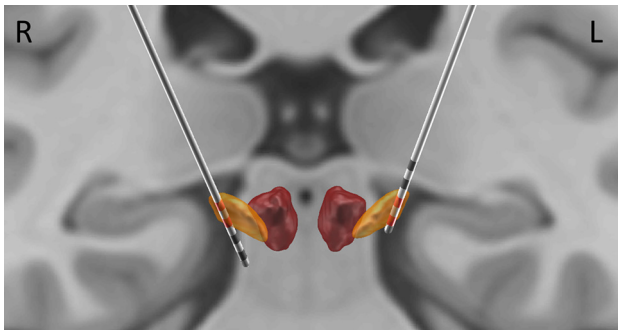

FIGURE 1 | Localization of electrode contacts. The localization was performed based on post-operative CT, coregistered to pre-operative magnetic resonance imaging (MRI). Subthalamic nucleus (STN) and the Red Nucleus are visualized based on DISTAL atlas (Ewert et al., 2018). The contacts used for bipolar derivations reported here (2, 3 on the right; 0, 1 on the left) are highlighted in red.

Comparison to PD Cohort

In order to examine the similarities and differences in STN spectra between the patient reported here and previously studied PD patients, we compared the results to those from a cohort previously reported by Litvak et al. (2011a). All the patients reported in the article were included except for patient 3 who was not responsive to dopaminergic medication.

RESULTS

The top two contacts (2 and 3) of the right electrode were localized inside the right STN; the bottom two contacts (0 and 1) of the left electrode were localized inside the left STN (**Figure 1**). The sensor level analysis revealed three significant clusters of coherence. We only report the frequency bands obtained from the sensor-level analysis here and **Figure 2** shows the corresponding source localizations. On the right side, two clusters were identified. The first cluster was in the theta-alpha band (4–12 Hz, **Figure 2A**) and localized to the deep frontal medial areas with the peak in the anterior cingulate cortex. The second cluster was in the beta band (28–35 Hz, **Figure 2B**) and localized to the ipsilateral pre-motor and motor cortices. A similar single beta cluster was found for the left STN channel with the same significant frequency range (**Figure 2C**) and localization to the corresponding areas on the left side.

Comparison of LFP power spectra to the previous PD cohort showed higher alpha-theta power for the dystonia patient and much lower power in the low beta range when compared

[1]http://www.lead-dbs.org/
[2]http://stnava.github.io/ANTs/
[3]http://adhusch.github.io/PaCER/
[4]https://www.fil.ion.ucl.ac.uk/spm/software/
[5]https://github.com/spm/daiss

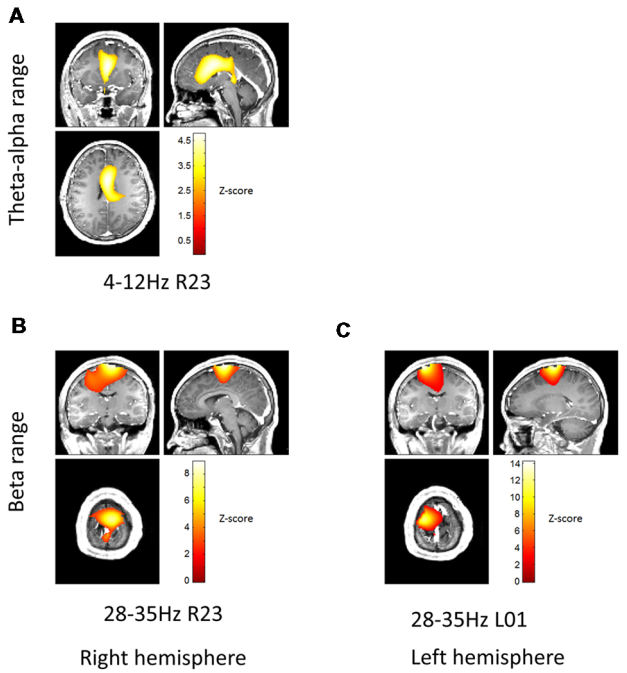

FIGURE 2 | Beamformer localization of significant coherent clusters. The frequency bands for each local field potentials (LFPs) channel were determined based on sensor-level test (see "Materials and Methods" section). Dynamic Imaging of Coherent Sources (DICS) coherence beamformer (Gross et al., 2001) was used for source analysis. For visualization purposes, the beamformer images were converted to *Z*-score across voxels, thresholded above 2.5 and overlaid on the patient's pre-operative T1 structural. Panel **(A)** shows localization of theta-alpha (4–12 Hz) coherence with the right STN. Panels **(B,C)** show localization of high beta (28–35 Hz) coherence with the right and left STN, respectively.

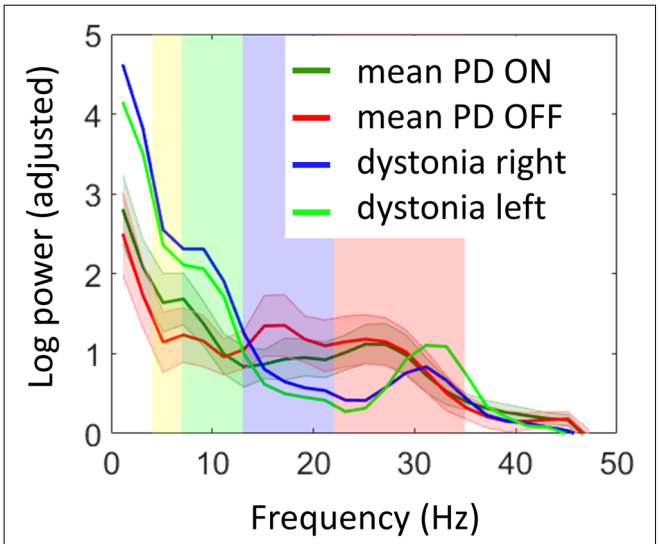

FIGURE 3 | Comparison of STN power spectra of the dystonia patient with the previously reported Parkinson's disease (PD) cohort (Litvak et al., 2011a). Log power was normalized by subtracting a linear fit to the spectrum in the 55–95 Hz range. The shaded error bars denote 95% confidence intervals for the mean of PD spectra. The background color shows the standard electrophysiological frequency bands: theta (yellow, 4–7 Hz), alpha (green, 7–13 Hz), low beta (purple, 13–22 Hz) and high beta (pink, 22–35 Hz). The dystonia patient showed increased power in theta and alpha bands and reduced power in low beta (see "Results" section for details).

to both ON and OFF dopamine states in PD (**Figure 3**). There was a distinct peak in power in the high beta band corresponding to the range of significant coherence between STN and the cortex which exceeded the mean values in this range for PD. In order to determine whether there were any significant differences between the dystonia patient and the PD cohort, we performed two sample *t*-tests between the two hemispheres of the dystonia patient and 22 hemispheres of the PD patients OFF drug assuming equal variance for power spectra averaged in pre-defined bands (shown in color in **Figure 3**). For theta (4–7 Hz) and alpha (7–13 Hz) the results were close to significance (M_{PD} = 1.15, M_{dyst} = 2.45, SD = 0.88, t = −2.01, p = 0.057 and M_{PD} = 1.12, M_{dyst} = 2.07, SD = 0.64, t = −2.01, p = 0.058 respectively) but without correction for multiple testing across bands. For low beta (13–22 Hz) and high beta (22–35 Hz) the differences were not significant (M_{PD} = 1.2, M_{dyst} = 0.68, SD = 0.66, t = 1.07, p = 0.29 and M_{PD} = 0.96, M_{dyst} = 0.66, SD = 0.6, t = 0.68, p = 0.5, respectively).

DISCUSSION

The present case report reproduces some of the previous findings regarding abnormal low-frequency oscillatory activity in dystonia and adds to the range of conditions for which cortico-subthalamic interactions have been studied with concurrent LFP-MEG recordings. It is now possible to discuss the commonalities and differences between PD (Hirschmann et al., 2011; Litvak et al., 2011a), OCD (Wojtecki et al., 2017) and dystonia. This gives a larger degree of confidence when speculating about the expected patterns of connectivity in the healthy state which cannot be assessed with invasive recording techniques.

LFP Power Spectra

The features of LFP power spectra we found are consistent with the majority of previous studies. Geng et al. (2017) reported a direct group comparison of STN LFP in dystonia and PD and their findings were very similar to ours: increased low-frequency power and reduced beta power in dystonia compared to PD. Neumann et al. (2012) report similar results for a single case. However, Wang et al. (2016), did not find significant differences between the two patient populations. Low-frequency activity has been shown to be a hallmark of dystonia in several studies of DBS patients with recordings in the GPi (Barow et al., 2014; Neumann et al., 2017). Furthermore, low-frequency power increase in the STN LFP was associated with induction of dyskinesia by dopaminergic drugs in PD (Alonso-Frech et al., 2006). Thus, it could be the case that this feature is associated with the symptom of hyperkinetic movements rather than a particular disease. Silberstein et al. (2003) compared pallidal LFP recorded intraoperatively between PD and dystonia and found exactly the same pattern as reported here: the 4–10 Hz power is highest in

dystonia, intermediate in PD on medication and lowest in PD off medication; 11–30 Hz power is highest in PD off medication, intermediate in PD on medication and lowest in dystonia. Low beta power has been demonstrated as a robust biomarker of clinical impairment induced by PD, particularly bradykinesia and rigidity. The symptoms of the patient reported here included right limb bradykinesia. However, the low beta power in the contralateral (left) STN was below that of the ipsilateral side. We, therefore, suggest that bradykinesia in dystonia might not necessarily be associated with increased low beta power in the STN. The left STN did show increased high beta power compared to the right STN but that was largely above the frequency range where beta power is increased in PD patients. High-beta power increase in the GPi was recently linked to hyperkinetic symptoms in Huntington's disease (Zhu et al., 2018) so beta activity could also be related to the patient's choreatic mouth movements. In order to determine whether and how high beta power increase is related to disease symptoms, observations in more patients are necessary.

Coherence in Dystonia, OCD and PD

Coherence in the high beta band (22–35 Hz) is common to all the studies of cortico-subthalamic interactions published to date (Lalo et al., 2008; Hirschmann et al., 2011; Litvak et al., 2011a; Oswal et al., 2016; Wojtecki et al., 2017; Belardinelli et al., 2019). In all the MEG studies where source localization was possible the cortical coherent sources localized to the ipsilateral mesial sensorimotor areas. These findings are also in line with simultaneous intraoperative cortical surface and STN LFP recordings (Whitmer et al., 2012). The cortical areas consistently shown as being coherent with the STN LFP in this band correspond well to those where the hyperdirect cortico-STN pathway is known to originate in humans (Lambert et al., 2012). The fact that high beta coherence is present in all the three clinical conditions: PD, dystonia and OCD suggests that it is likely to be present also in the healthy state. Whether and how the magnitude of high beta coherence is affected by disease is still an open question.

Our finding of theta-alpha coherence between the STN and anterior cingulate is very similar to the finding in OCD reported by Wojtecki et al. (2017). The frequency range of this coherence overlaps with that of theta-alpha power increase compared to the PD cohort. The two phenomena could, therefore, be related. Low frequency coherence between the STN and medial prefrontal cortex has been the subject of a number of recent studies where it has been shown to be involved in adjustment of decision thresholds for high conflict trials during decision-making tasks (Zavala et al., 2014, 2016, 2018; Herz et al., 2017; Hell et al., 2018; Kelley et al., 2018). Interestingly, despite the fact that all these studies were done on PD patients with STN-DBS, low-frequency coherence between the STN and medial prefrontal cortex was not observed at rest in PD (Hirschmann et al., 2011; Litvak et al., 2011a) and instead both studies reported coherence with temporo-parietal areas in the same band with Litvak et al. also reporting additional peak in the brainstem. There could be several possible explanations for these discrepancies. It could be the case that they reflect the differences between the three disorders. In that case, it would be likely that STN-prefrontal resting coherence is suppressed in PD because it is present in both OCD and dystonia. Alternatively, the differences could be due to different placement of the electrodes in the STN. This nucleus is commonly divided into motor, associative and limbic part which have different connectivity with the cortex (Lambert et al., 2012).

Limitations of the Study

To put the results of the single case recording reported here in context, we compare them to those from the previously reported PD patient cohort. However, it should be noted that those recordings were done using a different LFP amplifier. Although the spectra were normalized to minimize any contribution of the hardware differences and the results are in line with what could be expected, a comparison of LFPs recorded with the same hardware would, of course, be preferable. It would also be interesting to compare the coherence magnitude of the dystonia patient with the PD cohort but comparing the typical coherence values for patients from our cohort recorded on a CTF MEG system with those reported in the PD literature for the Neuromag system (Hirschmann et al., 2011, 2013) raised a suspicion that there is a systematic difference with Neuromag yielding lower values. We, therefore, opted to not include such a comparison in the present report as it could be misleading. Unfortunately, PD patients with STN electrodes are not available at our site for clinical reasons.

CONCLUSION

The present report extends the range of disorders for which cortico-subthalamic oscillatory connectivity has been studied. Our results support the suggestion that oscillatory coherent networks are not solely features of disease. However, whether these networks are affected by the disease and whether their modulation is causally related to disease pathophysiology remains an open question.

ETHICS STATEMENT

The study was approved by the local ethics committee of Ruijin hospital, Shanghai JiaoTong University, School of Medicine. The patient was informed about the aim and the scope of the study and gave written informed consent. The patient also consented to the publication of the present case report.

AUTHOR CONTRIBUTIONS

PH and TW did the MEG recording and collected clinical data. YW and HL recorded performed clinical video recordings. BS, SZ, WL, DL and YP performed the DBS surgery. CC and VL analyzed the data and wrote the article.

FUNDING

This work was supported by NSCF (Grant No. 81571346; National Natural Science Foundation of China). The Wellcome

Centre for Human Neuroimaging is supported by core funding from the Wellcome Trust (203147/Z/16/Z). UK MEG community is supported by UK MEG Partnership award from the Medical Research Council (MR/K005464/1).

ACKNOWLEDGMENTS

We would like to thank Dr Simon Farmer for his careful reading of the revised manuscript.

REFERENCES

Alonso-Frech, F., Zamarbide, I., Alegre, M., Rodríguez-Oroz, M. C., Guridi, J., Manrique, M., et al. (2006). Slow oscillatory activity and levodopa-induced dyskinesias in Parkinson's disease. *Brain* 129, 1748–1757. doi: 10.1093/brain/awl103

Avants, B. B., Epstein, C. L., Grossman, M., and Gee, J. C. (2008). Symmetric diffeomorphic image registration with cross-correlation: evaluating automated labeling of elderly and neurodegenerative brain. *Med. Image Anal.* 12, 26–41. doi: 10.1016/j.media.2007.06.004

Barow, E., Neumann, W.-J., Brücke, C., Huebl, J., Horn, A., Brown, P., et al. (2014). Deep brain stimulation suppresses pallidal low frequency activity in patients with phasic dystonic movements. *Brain* 137, 3012–3024. doi: 10.1093/brain/awu258

Belardinelli, P., Azodi-Avval, R., Ortiz, E., Naros, G., Grimm, F., Weiss, D., et al. (2019). Intraoperative localization of spatially and spectrally distinct resting-state networks in Parkinson's disease. *J. Neurosurg.* doi: 10.3171/2018.11.jns181684 [Epub ahead of print].

Brown, P., Oliviero, A., Mazzone, P., Insola, A., Tonali, P., and Di Lazzaro, V. (2001). Dopamine dependency of oscillations between subthalamic nucleus and pallidum in Parkinson's disease. *J. Neurosci.* 21, 1033–1038. doi: 10.1523/JNEUROSCI.21-03-01033.2001

Cao, C., Pan, Y., Li, D., Zhan, S., Zhang, J., and Sun, B. (2013). Subthalamus deep brain stimulation for primary dystonia patients: a long-term follow-up study. *Mov. Disord.* 28, 1877–1882. doi: 10.1002/mds.25586

Chabardès, S., Polosan, M., Krack, P., Bastin, J., Krainik, A., David, O., et al. (2013). Deep brain stimulation for obsessive-compulsive disorder: subthalamic nucleus target. *World Neurosurg.* 80, S31.e1–S31.e8. doi: 10.1016/j.wneu.2012.03.010

Crowell, A. L., Ryapolova-Webb, E. S., Ostrem, J. L., Galifianakis, N. B., Shimamoto, S., Lim, D. A., et al. (2012). Oscillations in sensorimotor cortex in movement disorders: an electrocorticography study. *Brain* 135, 615–630. doi: 10.1093/brain/awr332

Ewert, S., Plettig, P., Li, N., Chakravarty, M. M., Collins, D. L., Herrington, T. M., et al. (2018). Toward defining deep brain stimulation targets in MNI space: a subcortical atlas based on multimodal MRI, histology and structural connectivity. *Neuroimage* 170, 271–282. doi: 10.1016/j.neuroimage.2017.05.015

Fonov, V., Evans, A. C., Botteron, K., Almli, C. R., McKinstry, R. C., Collins, D. L., et al. (2011). Unbiased average age-appropriate atlases for pediatric studies. *Neuroimage* 54, 313–327. doi: 10.1016/j.neuroimage.2010.07.033

Friston, K. J., Ashburner, J., Kiebel, S., Nichols, T., and Penny, W. D. (2007). *Statistical Parametric Mapping: The Analysis of Funtional Brain Images.* Elsevier: Academic Press.

Friston, K. J., Bastos, A. M., Pinotsis, D., and Litvak, V. (2015). LFP and oscillations—what do they tell us? *Curr. Opin. Neurobiol.* 31, 1–6. doi: 10.1016/j.conb.2014.05.004

Geng, X., Zhang, J., Jiang, Y., Ashkan, K., Foltynie, T., Limousin, P., et al. (2017). Comparison of oscillatory activity in subthalamic nucleus in Parkinson's disease and dystonia. *Neurobiol. Dis.* 98, 100–107. doi: 10.1016/j.nbd.2016.12.006

Gross, J. (2014). Analytical methods and experimental approaches for electrophysiological studies of brain oscillations. *J. Neurosci. Methods* 228, 57–66. doi: 10.1016/j.jneumeth.2014.03.007

Gross, J., Kujala, J., Hamalainen, M., Timmermann, L., Schnitzler, A., and Salmelin, R. (2001). Dynamic imaging of coherent sources: studying neural interactions in the human brain. *Proc. Natl. Acad. Sci. U S A* 98, 694–699. doi: 10.1073/pnas.98.2.694

Harmsen, I. E., Rowland, N. C., Wennberg, R. A., and Lozano, A. M. (2018). Characterizing the effects of deep brain stimulation with magnetoencephalography: a review. *Brain Stimul.* 11, 481–491. doi: 10.1016/j.brs.2017.12.016

Hell, F., Taylor, P. C. J., Mehrkens, J. H., and Bötzel, K. (2018). Subthalamic stimulation, oscillatory activity and connectivity reveal functional role of STN and network mechanisms during decision making under conflict. *Neuroimage* 171, 222–233. doi: 10.1016/j.neuroimage.2018.01.001

Herz, D. M., Tan, H., Brittain, J.-S., Fischer, P., Cheeran, B., Green, A. L., et al. (2017). Distinct mechanisms mediate speed-accuracy adjustments in cortico-subthalamic networks. *Elife* 6:e21481. doi: 10.7554/elife.21481

Hirschmann, J., Özkurt, T. E., Butz, M., Homburger, M., Elben, S., Hartmann, C. J., et al. (2011). Distinct oscillatory STN-cortical loops revealed by simultaneous MEG and local field potential recordings in patients with Parkinson's disease. *Neuroimage* 55, 1159–1168. doi: 10.1016/j.neuroimage.2010.11.063

Hirschmann, J., Özkurt, T. E., Butz, M., Homburger, M., Elben, S., Hartmann, C. J., et al. (2013). Differential modulation of STN-cortical and cortico-muscular coherence by movement and levodopa in Parkinson's disease. *Neuroimage* 68, 203–213. doi: 10.1016/j.neuroimage.2012.11.036

Horn, A., and Kühn, A. A. (2015). Lead-DBS: a toolbox for deep brain stimulation electrode localizations and visualizations. *Neuroimage* 107, 127–135. doi: 10.1016/j.neuroimage.2014.12.002

Horn, A., Neumann, W.-J., Degen, K., Schneider, G.-H., and Kühn, A. A. (2017). Toward an electrophysiological "sweet spot" for deep brain stimulation in the subthalamic nucleus. *Hum. Brain Mapp.* 38, 3377–3390. doi: 10.1002/hbm.23594

Husch, A., V Petersen, M., Gemmar, P., Goncalves, J., and Hertel, F. (2018). PaCER—a fully automated method for electrode trajectory and contact reconstruction in deep brain stimulation. *Neuroimage Clin.* 17, 80–89. doi: 10.1016/j.nicl.2017.10.004

Kelley, R., Flouty, O., Emmons, E. B., Kim, Y., Kingyon, J., Wessel, J. R., et al. (2018). A human prefrontal-subthalamic circuit for cognitive control. *Brain* 141, 205–216. doi: 10.1093/brain/awx300

Lalo, E., Thobois, S., Sharott, A., Polo, G., Mertens, P., Pogosyan, A., et al. (2008). Patterns of bidirectional communication between cortex and basal ganglia during movement in patients with Parkinson disease. *J. Neurosci.* 28, 3008–3016. doi: 10.1523/JNEUROSCI.5295-07.2008

Lambert, C., Zrinzo, L., Nagy, Z., Lutti, A., Hariz, M., Foltynie, T., et al. (2012). Confirmation of functional zones within the human subthalamic nucleus: patterns of connectivity and sub-parcellation using diffusion weighted imaging. *Neuroimage* 60, 83–94. doi: 10.1016/j.neuroimage.2011.11.082

Limousin, P., Pollak, P., Benazzouz, A., Hoffmann, D., Le Bas, J. F., Broussolle, E., et al. (1995). Effect of parkinsonian signs and symptoms of bilateral subthalamic nucleus stimulation. *Lancet* 345, 91–95. doi: 10.1016/s0140-6736(95)90062-4

Little, S., Pogosyan, A., Neal, S., Zavala, B., Zrinzo, L., Hariz, M., et al. (2013). Adaptive deep brain stimulation in advanced Parkinson disease. *Ann. Neurol.* 74, 449–457. doi: 10.1002/ana.23951

Litvak, V., Eusebio, A., Jha, A., Oostenveld, R., Barnes, G. R., Penny, W. D., et al. (2010). Optimized beamforming for simultaneous MEG and intracranial local field potential recordings in deep brain stimulation patients. *Neuroimage* 50, 1578–1588. doi: 10.1016/j.neuroimage.2009.12.115

Litvak, V., Jha, A., Eusebio, A., Oostenveld, R., Foltynie, T., Limousin, P., et al. (2011a). Resting oscillatory cortico-subthalamic connectivity in patients with Parkinson's disease. *Brain* 134, 359–374. doi: 10.1093/brain/awq332

Litvak, V., Mattout, J., Kiebel, S., Phillips, C., Henson, R., Kilner, J., et al. (2011b). EEG and MEG data analysis in SPM8. *Comput. Intell. Neurosci.* 2011:852961. doi: 10.1155/2011/852961

Mattout, J., Henson, R. N., and Friston, K. J. (2007). Canonical source reconstruction for MEG. *Comput. Intell. Neurosci.* 2007:67613. doi: 10.1155/2007/67613

Meidahl, A. C., Tinkhauser, G., Herz, D. M., Cagnan, H., Debarros, J., and Brown, P. (2017). Adaptive deep brain stimulation for movement disorders: the long road to clinical therapy. *Mov. Disord.* 32, 810–819. doi: 10.1002/mds.27022

Miocinovic, S., de Hemptinne, C., Qasim, S., Ostrem, J. L., and Starr, P. A. (2015). Patterns of cortical synchronization in isolated dystonia compared

with Parkinson disease. *JAMA Neurol.* 72, 1244–1251. doi: 10.1001/jamaneurol.2015.2561

Mulders, A. E. P., Plantinga, B. R., Schruers, K., Duits, A., Janssen, M. L. F., Ackermans, L., et al. (2016). Deep brain stimulation of the subthalamic nucleus in obsessive-compulsive disorder: neuroanatomical and pathophysiological considerations. *Eur. Neuropsychopharmacol.* 26, 1909–1919. doi: 10.1016/j.euroneuro.2016.10.011

Neumann, W.-J., Huebl, J., Brücke, C., Ruiz, M. H., Kupsch, A., Schneider, G.-H. H., et al. (2012). Enhanced low-frequency oscillatory activity of the subthalamic nucleus in a patient with dystonia. *Mov. Disord.* 27, 1063–1066. doi: 10.1002/mds.25078

Neumann, W.-J., Horn, A., Ewert, S., Huebl, J., Brücke, C., Slentz, C., et al. (2017). A localized pallidal physiomarker in cervical dystonia. *Ann. Neurol.* 82, 912–924. doi: 10.1002/ana.25095

Neumann, W.-J., Jha, A., Bock, A., Huebl, J., Horn, A., Schneider, G.-H., et al. (2015). Cortico-pallidal oscillatory connectivity in patients with dystonia. *Brain* 138, 1894–1906. doi: 10.1093/brain/awv109

Nimmrich, V., Draguhn, A., and Axmacher, N. (2015). Neuronal network oscillations in neurodegenerative diseases. *Neuromolecular Med.* 17, 270–284. doi: 10.1007/s12017-015-8355-9

Nolte, G. (2003). The magnetic lead field theorem in the quasi-static approximation and its use for magnetoencephalography forward calculation in realistic volume conductors. *Phys. Med. Biol.* 48, 3637–3652. doi: 10.1088/0031-9155/48/22/002

Oswal, A., Beudel, M., Zrinzo, L., Limousin, P., Hariz, M., Foltynie, T., et al. (2016). Deep brain stimulation modulates synchrony within spatially and spectrally distinct resting state networks in Parkinson's disease. *Brain* 139, 1482–1496. doi: 10.1093/brain/aww048

Pavlides, A., Hogan, S. J., and Bogacz, R. (2015). Computational models describing possible mechanisms for generation of excessive beta oscillations in Parkinson's disease. *PLoS Comput. Biol.* 11:e1004609. doi: 10.1371/journal.pcbi.1004609

Piña-Fuentes, D., van Zijl, J. C., van Dijk, J. M. C., Little, S., Tinkhauser, G., Oterdoom, D. L. M., et al. (2019). The characteristics of pallidal low-frequency and beta bursts could help implementing adaptive brain stimulation in the parkinsonian and dystonic internal globus pallidus. *Neurobiol. Dis.* 121, 47–57. doi: 10.1016/j.nbd.2018.09.014

Rampoldi, L., Dobson-Stone, C., Rubio, J. P., Danek, A., Chalmers, R. M., Wood, N. W., et al. (2001). A conserved sorting-associated protein is mutant in chorea-acanthocytosis. *Nat. Genet.* 28, 119–120. doi: 10.1038/88821

Silberstein, P., Kühn, A. A., Kupsch, A., Trottenberg, T., Krauss, J. K., Wöhrle, J. C., et al. (2003). Patterning of globus pallidus local field potentials differs between Parkinson's disease and dystonia. *Brain* 126, 2597–2608. doi: 10.1093/brain/awg267

Taulu, S., and Simola, J. (2006). Spatiotemporal signal space separation method for rejecting nearby interference in MEG measurements. *Phys. Med. Biol.* 51, 1759–1768. doi: 10.1088/0031-9155/51/7/008

Thomson, D. J. (1982). Spectrum estimation and harmonic analysis. *Proc. IEEE* 70, 1055–1096. doi: 10.1109/proc.1982.12433

Wang, D. D., de Hemptinne, C., Miocinovic, S., Ostrem, J. L., Galifianakis, N. B., San Luciano, M., et al. (2018). Pallidal deep-brain stimulation disrupts pallidal beta oscillations and coherence with primary motor cortex in Parkinson's disease. *J. Neurosci.* 38, 4556–4568. doi: 10.1523/JNEUROSCI.0431-18.2018

Wang, D. D., de Hemptinne, C., Miocinovic, S., Qasim, S. E., Miller, A. M., Ostrem, J. L., et al. (2016). Subthalamic local field potentials in Parkinson's disease and isolated dystonia: an evaluation of potential biomarkers. *Neurobiol. Dis.* 89, 213–222. doi: 10.1016/j.nbd.2016.02.015

Whitmer, D., de Solages, C., Hill, B., Yu, H., Henderson, J. M., and Bronte-Stewart, H. (2012). High frequency deep brain stimulation attenuates subthalamic and cortical rhythms in Parkinson's disease. *Front. Hum. Neurosci.* 6:155. doi: 10.3389/fnhum.2012.00155

Wojtecki, L., Hirschmann, J., Elben, S., Boschheidgen, M., Trenado, C., Vesper, J., et al. (2017). Oscillatory coupling of the subthalamic nucleus in obsessive compulsive disorder. *Brain* 140:e56. doi: 10.1093/brain/awx164

Yoshida, F., Martinez-Torres, I., Pogosyan, A., Holl, E., Petersen, E., Chen, C. C., et al. (2010). Value of subthalamic nucleus local field potentials recordings in predicting stimulation parameters for deep brain stimulation in Parkinson's disease. *J. Neurol. Neurosurg. Psychiatry* 81, 885–889. doi: 10.1136/jnnp.2009.190918

Zavala, B., Jang, A., Trotta, M., Lungu, C. I., Brown, P., and Zaghloul, K. A. (2018). Cognitive control involves theta power within trials and beta power across trials in the prefrontal-subthalamic network. *Brain* 141, 3361–3376. doi: 10.1093/brain/awy266

Zavala, B., Tan, H., Ashkan, K., Foltynie, T., Limousin, P., Zrinzo, L., et al. (2016). Human subthalamic nucleus-medial frontal cortex theta phase coherence is involved in conflict and error related cortical monitoring. *Neuroimage* 137, 178–187. doi: 10.1016/j.neuroimage.2016.05.031

Zavala, B. A., Tan, H., Little, S., Ashkan, K., Hariz, M., Foltynie, T., et al. (2014). Midline frontal cortex low-frequency activity drives subthalamic nucleus oscillations during conflict. *J. Neurosci.* 34, 7322–7333. doi: 10.1523/JNEUROSCI.1169-14.2014

Zhan, S., Sun, F., Pan, Y., Liu, W., Huang, P., Cao, C., et al. (2018). Bilateral deep brain stimulation of the subthalamic nucleus in primary Meige syndrome. *J. Neurosurg.* 128, 897–902. doi: 10.3171/2016.12.jns16383

Zhu, G., Geng, X., Tan, Z., Chen, Y., Zhang, R., Wang, X., et al. (2018). Characteristics of globus pallidus internus local field potentials in hyperkinetic disease. *Front. Neurol.* 9:934. doi: 10.3389/fneur.2018.00934

Conflict of Interest Statement: The authors declare that the research was conducted in the absence of any commercial or financial relationships that could be construed as a potential conflict of interest.

The reviewer AM declared a shared affiliation, though no other collaboration, with one of the authors VL to the handling Editor.

frontiers in Neurology

BRIEF RESEARCH REPORT
published: 07 August 2019
doi: 10.3389/fneur.2019.00847

Hyperactivity of Basal Ganglia in Patients With Parkinson's Disease During Internally Guided Voluntary Movements

*Veronika Filyushkina[1], Valentin Popov[1,2], Rita Medvednik[1], Vadim Ushakov[3], Artem Batalov[2], Alexey Tomskiy[2], Igor Pronin[2] and Alexey Sedov[1,4]**

[1] Russian Academy of Sciences, Semenov Institute of Chemical Physics, Moscow, Russia, [2] Burdenko National Scientific and Practical Center for Neurosurgery, Moscow, Russia, [3] National Research Centre "Kurchatov Institute", Moscow, Russia, [4] Department of Physics of Living Systems, Moscow Institute of Physics and Technology, Moscow, Russia

The contribution of different brain areas to internally guided (IG) and externally triggered (ET) movements has been a topic of debate. It has been hypothesized that IG movements are performed mainly through the basal ganglia-thalamocortical loop while ET movements are through the cerebello-thalamocortical pathway. We hypothesized that basal ganglia activity would be modified in patients with Parkinson's disease during IG movement as compared with normal subjects. We used functional MRI (fMRI) to investigate the differences between IG and ET motor tasks. Twenty healthy participants and 20 Parkinson's disease patients (OFF-state) were asked to perform hand movements in response to sound stimuli (ET) and in advance of the stimuli (IG). We showed that ET movements evoked activation of a few large clusters in the contralateral motor areas: the sensorimotor and premotor cortex, supplementary motor area (SMA), insula, putamen, motor thalamus and ipsilateral cerebellum. IG movements additionally evoked activation of a large number of small clusters distributed in different brain areas including the parietal and frontal lobes. Comparison between the activity of Parkinson's disease patients and healthy volunteers showed few important differences. We observed that along with the activity of the posterior areas, an activation of the anterior areas of putamen was observed during IG movements. We also found hyperactivity of the ventral thalamus for both movements. These results showed that IG movements in PD patients were made with the involvement of both sensorimotor and associative basal ganglia-thalamocortical loops.

Keywords: fMRI, externally triggered movement, internally guided movement, basal ganglia, Parkinson's disease

OPEN ACCESS

Edited by:
Antonella Macerollo, University College London, United Kingdom

Reviewed by:
Pedro Ribeiro, Federal University of Rio de Janeiro, Brazil
Chon-Haw Tsai, China Medical University Hospital, Taiwan

***Correspondence:**
Alexey Sedov
Alexeys.sedov@gmail.com

Specialty section:
This article was submitted to Movement Disorders, a section of the journal Frontiers in Neurology

Received: *07 December 2018*
Accepted: *22 July 2019*
Published: *07 August 2019*

Citation:
Filyushkina V, Popov V, Medvednik R, Ushakov V, Batalov A, Tomskiy A, Pronin I and Sedov A (2019) Hyperactivity of Basal Ganglia in Patients With Parkinson's Disease During Internally Guided Voluntary Movements. Front. Neurol. 10:847. doi: 10.3389/fneur.2019.00847

INTRODUCTION

The internal-external control hypothesis proposed that the cerebellum, parietal lobe, and lateral premotor cortex (PMC) would dominate during externally-triggered (ET) movements, whereas the basal ganglia (BG) and supplementary motor area (SMA) would show a predominant involvement in internally-guided (IG) movements (1). More recent studies of functional brain imaging in humans and single cell recordings in monkeys showed preferential involvement of the medially located SMA in self-initiated movement and the lateral premotor cortex in externally

cued movement (2, 3). An event-related fMRI study showed activation within the basal ganglia, especially in putamen, during IG movements only (4). IG tasks were also characterized by significant interactions within the basal ganglia–thalamo–motor (BGTM) loop (5).

Clinical and experimental data has suggested that bradykinesia or slowness of movement initiation in Parkinson's disease may reflect an impaired connection between the supplementary motor area and putamen (6). Later neuroimaging studies have reported hypoactivation in the contralateral putamen and SMA (2, 7). In contrast, Yu et al. showed that putamen-SMA functional connectivity is enhanced in patients with PD (8). Neuroimaging studies have reported decreased percentage of activation in the regions within the BGTM during IG tasks and enhanced or preserved activation within the cerebello-cerebral (CC) loop during ET tasks in PD (9). Later disturbance in functional connectivity in the motor loop was found during IG but not ET movements in PD patients (7). On the other hand, electrophysiological studies in PD showed that BGTM circuit is involved in the preparation of both IG and ET movements but CC loop involved in the preparation of IG movement only (10).

Thus, the contribution of basal ganglia in various aspects of human movement remains unclear. Considering that in patients with Parkinson's disease the loss of dopamine is predominantly in the posterior putamen, associated with the control of habitual behavior (11), we hypothesized that basal ganglia activity pattern should be modified or displaced into associative areas during IG but not ET movement. The aim of the present study was to compare activation areas in the basal ganglia and thalamus during ET and IG motor tasks in normal and PD subjects.

METHOD

Twenty right-handed patients with Parkinson's disease (nine males, 11 females) and 20 age- and gender-matched right-handed healthy volunteers (11 males, nine females) participated in the study (**Supplementary Table 1**). The disease severity according to the unified Parkinson's disease rating scale (UPDRS)-III, without levodopa administration, ranged from 21 to 71 points, mean disease duration was 13.8 + 4.5 years. All patients did not take medicine for 12 h before the study (OFF-state). Informed consent was obtained from all subjects prior to their participation in the study. The study was approved by the Ethics Committee of the Burdenko National Medical Research Center of Neurosurgery (01/2018). We used a block design paradigm with two distinct ET and IG movements to investigate the differences between these conditions. Each condition lasted 30 s with 30 s rest and was repeated seven times in a session. In ET mode, subjects were asked to perform a simple repetitive movement (clenching a fist) in response to external audio stimuli with a constant period 0.75 s. In IG mode, subjects were asked to perform the same goal-directed movements in advance of the stimulus with a constant period 1.5 s. In this case, the stimuli serve as reward, and movements initiated by internal command. We chose a longer interval between stimuli to avoid automaticity of movements.

Imaging was performed on a 3-Tesla MR-scanner with an eight-channel head coil. The protocol included: (1) A T1-weighted sagittal 3D rapid gradient echo sequence for anatomical data (voxel size 1 × 1 × 1 mm), and (2) a T2 EPI echo planar sequence for functional images (voxel size 1.8 × 1.8 × 4 mm). fMRI and anatomical data analysis was performed with SPM software (http://www.fil.ion.ucl.ac.uk/spm/software/spm12/). First level analysis was performed using general linear models with contrasts: ET>Rest and IG>Rest (12). Second level analysis was calculated using a one-sample t-test ($p < 0.05$) corrected with FWE. For the comparison of activation between the tasks, a paired t-test model ($p < 0.001$) corrected with FDR was used. The fMRI analysis was performed at the whole-brain level. The basal ganglia and thalamus areas were analyzed with the mask using WFU PickAtlas SPM package (https://www.nitrc.org/projects/wfu_pickatlas/).

RESULTS

We observed that ET movements evoked activation in several brain areas: the contralateral pre-central and post-central gyri including the primary motor cortex (M1), the somatosensory cortex (PSC) and PMC (**Table 1**, **Supplementary Figure 1**). Cortical activation also affected the contralateral rolandic operculum (RO), insula, and SMA. Subcortical structures were represented mainly by the posterior putamen and ventral thalamus. In addition, we observed activation in both sides of the cerebellum. IG movements evoked activation within widely distributed networks in both hemispheres (**Table 1**, **Supplementary Figure 1**). Along with motor cortical areas, we observed activations in the ipsilateral inferior parietal lobule, supramarginal gyrus, superior frontal gyrus, insula, and frontal operculum. It is worth highlighting that there was activation of both sides of the SMA. Significant activations of subcortical structures were found in the ventral thalamic nuclei, pallidum, putamen, and anterior caudate. We also observed a few clusters of activation in the thalamus and putamen in the ipsilateral hemispheres as well as in the both sides of the cerebellum (**Table 1**, **Supplementary Figure 1**). IG>ET contrast indicated activation predominantly in the right hemisphere, with peak activation in the right insular area, SMA, superior frontal gyrus, frontal inferior operculum, and parietal inferior lobule as well as activation in the right cerebellar lobule VI (**Supplementary Figure 3**, **Supplementary Table 2**). Using opposite contrast we observed activation of several clusters in the contralateral pre-central and post-central gyri as well as in the cingulum and precuneus areas (**Supplementary Figure 3**).

ET movements evoked mostly the same clusters in PD patients (**Table 1**, **Supplementary Figure 2**). We observed activation in the contralateral pre-central and post-central gyri during ET movements in PD patients (**Table 1**, **Supplementary Figure 2**). It is worth highlighting that there was a smaller activity cluster volume in SMA. Activity clusters were also found in the centralis cingulate, RO, and supramarginal gyrus. Among the subcortical structures it is worth noting that there was activity of the contralateral ventral thalamus, pallidum, and posterior putamen.

TABLE 1 | Localization of activated areas during ET and IG movements in control group and PD patients.

Control subjects							PD patients						
Cluster	**N voxels**	**Peak MNI coordinates**			**Lable (aal)**	**Mean T**	**Cluster**	**N voxels**	**Peak MNI coordinates**			**Lable (aal)**	**Mean T**
		X	**Y**	**Z**					**X**	**Y**	**Z**		
ET MOVEMENT													
1	863	40	22	58	Pre-central L	7,4	1	634	37	29	50	Post-central L	7,0
					Post-central L							Pre-central L	
					Parietal Inf L							Parietal Inf L	
					Frontal Sup L		2	176	61	42	10	Temporal Sup L	5,9
2	419	41	29	18	Temporal Sup L	6,8						SupraMarginal L	
					Rolandic Oper L							Rolandic Oper L	
					SupraMarginal L							Temporal Mid L	
					Post-central L							Post-central L	
					Heschl L		3	159	5	9	54	Supp Motor Area L	6,6
					Insula L							Cingulum Mid L	
3	171	7	7	58	Supp Motor Area L	6,3						Supp Motor Area R	
					Supp Motor Area R		4	90	67	26	6	Temporal Sup R	5,8
4	58	41	3	14	Insula L	6,2						Temporal Mid R	
					Rolandic Oper L		5	201	16	24	2	Thalamus L	6,0
5	393	14	22	2	Thalamus L	6,7						Putamen L	
					Putamen L							Hippocampus L	
					Insula L							Pallidum L	
					Pallidum L		6	188	10	59	22	Cerebellum 4 5 R	6,6
6	819	18	48	26	Cerebellum 4 5 R	7,6						Vermis 4 5	
					Cerebellum 6 R							Cerebellum 6 R	
					Vermis 4 5							Vermis 6	
					Vermis 6							Cerebellum 3 R	
					Fusiform R								
					Lingual R								
					Cerebellum 3 R								
					Vermis 7								
					Vermis 8								
					Cerebellum 4 5 L								
					Cerebellum 8 R								
					Vermis 3								
7	82	40,44	2,96	14	Cerebellum 6 L	6,2							
IG MOVEMENT													
1	485	7	7	58	Supp Motor Area L	6,3	1	559	35	31	50	Post-central L	6,9
					Supp Motor Area R							Pre-central L	
					Frontal Sup R							Parietal Inf L	
					Cingulum Mid R		2	394	5	9	54	Cingulum Mid L	6,8
					Cingulum Mid L							Supp Motor Area L	
2	320	54	10	6	Insula R	6,3						Supp Motor Area R	
					Frontal Inf Oper R							Cingulum Mid R	
					Rolandic Oper R							Cingulum Ant L	
					Putamen R							Frontal Sup Medial L	
3	218	40	22	58	Pre-central L	6,4	3	347	31	16	2	Insula R	6,0
					Post-central L							Frontal Inf Oper R	
					Frontal Sup L							Pre-central R	
4	175	46	41	46	Parietal Inf R	6,4						Rolandic Oper R	
					SupraMarginal R							Putamen R	

(Continued)

TABLE 1 | Continued

Control subjects							PD patients						
Cluster	N voxels	Peak MNI coordinates			Lable (aal)	Mean T	Cluster	N voxels	Peak MNI coordinates			Lable (aal)	Mean T
		X	Y	Z					X	Y	Z		
					Parietal Sup R							Frontal Inf Tri R	
5	55	37	1	66	Frontal Mid R	5,9	4	196	54	44	34	Parietal Inf R	6,0
					Frontal Sup R							SupraMarginal R	
					Pre-central R							Angular R	
6	44	40	41	38	Parietal Inf L	5,9	5	162	35	42	30	Frontal Mid R	6,1
7	26	54	10	2	Frontal Inf Oper L	6,0						Frontal Inf Tri R	
					Rolandic Oper L		6	96	48	1	6	Rolandic Oper L	6,8
					Temporal Pole Sup L							Temporal Sup L	
					Insula L							Insula L	
8	15	42	1	6	Insula L							Temporal Pole Sup L	
					Rolandic Oper L							Frontal Inf Oper L	
9	16	40	35	26	Frontal Inf Tri R	6,0	7	71	54	26	22	Temporal Sup L	5,7
					Frontal Mid R	5,8						SupraMarginal L	
10	188	14	22	2	Thalamus L	6,1						Rolandic Oper L	
					Putamen L		8	66	61	42	10	Temporal Sup L	5,9
					Caudate L							Temporal Mid L	
11	499	18	48	22	Cerebellum 4 5 R	6,7	9	50	44	48	6	Frontal Mid R	6,1
					Vermis 4 5							Frontal Mid Orb R	
					Cerebellum 6 R							Frontal Inf Orb R	
					Vermis 6		10	26	67	27	6	Temporal Sup R	6,0
					Vermis 8							Temporal Mid R	
					Fusiform R		11	334	14	22	2	Thalamus L	6,2
					Vermis 7							Putamen L	
					Cerebellum 3 R							Pallidum L	
12	219	31	61	26	Cerebellum Crus1 L	6,9	12	31	14	22	10	Thalamus R	5,7
							13	140	12	59	22	Vermis 4 5	6,3
												Vermis 4 5	
												Cerebellum 6 R	
												Vermis 6	
												Cerebellum 4 5 L	

We also observed activity in the ipsilateral cerebellum. As in the control group, IG movements evoked a wider range of activation areas (**Table 1**, **Supplementary Figure 2**). We did not observe displacement of activity from the sensorimotor areas to SMA as seen in the control group. We also observed activation clusters in the angular gyrus and bilateral supramarginal gyrus. Subcortical structures were presented the in bilateral thalamus and contralateral putamen. Activity was also observed in both sides of the cerebellum. IG>ET contrast showed activity in the ipsilateral hemisphere in the parietal lobe, angular gyrus, supramarginal gyrus, inferior frontal gyrus, pre-central gyrus, insula, and SMA (**Supplementary Figure 3**, **Supplementary Table 2**). We also observed activation of the ipsilateral anterior putamen. Opposite contrast did not reveal any significant activation.

We observed a slight difference between basal ganglia and thalamic activities localization during ET movement and a robust localization difference during IG movements between PD and control. **Figure 1** (bottom) shows additional activation in the anterior putamen, ventral thalamus, and subthalamic area in PD patients during ET movements. We also observed activity in the dorsal putamen in controls only. IG movements were characterized by more pronounced differences between PD and controls (**Figure 1**, top). In PD patients we observed hyperactivity in the contralateral putamen, ventral thalamus, and subthalamic areas. An activation cluster was also observed in the ipsilateral thalamus. At the same time, we observed activity in the ipsilateral caudate in controls only.

DISCUSSION

Internally generated and externally triggered movements are associated with different cortical activation patterns (2, 3, 13, 14). We showed distinctions between ET and IG motor behavior concerned the localization and cluster size of

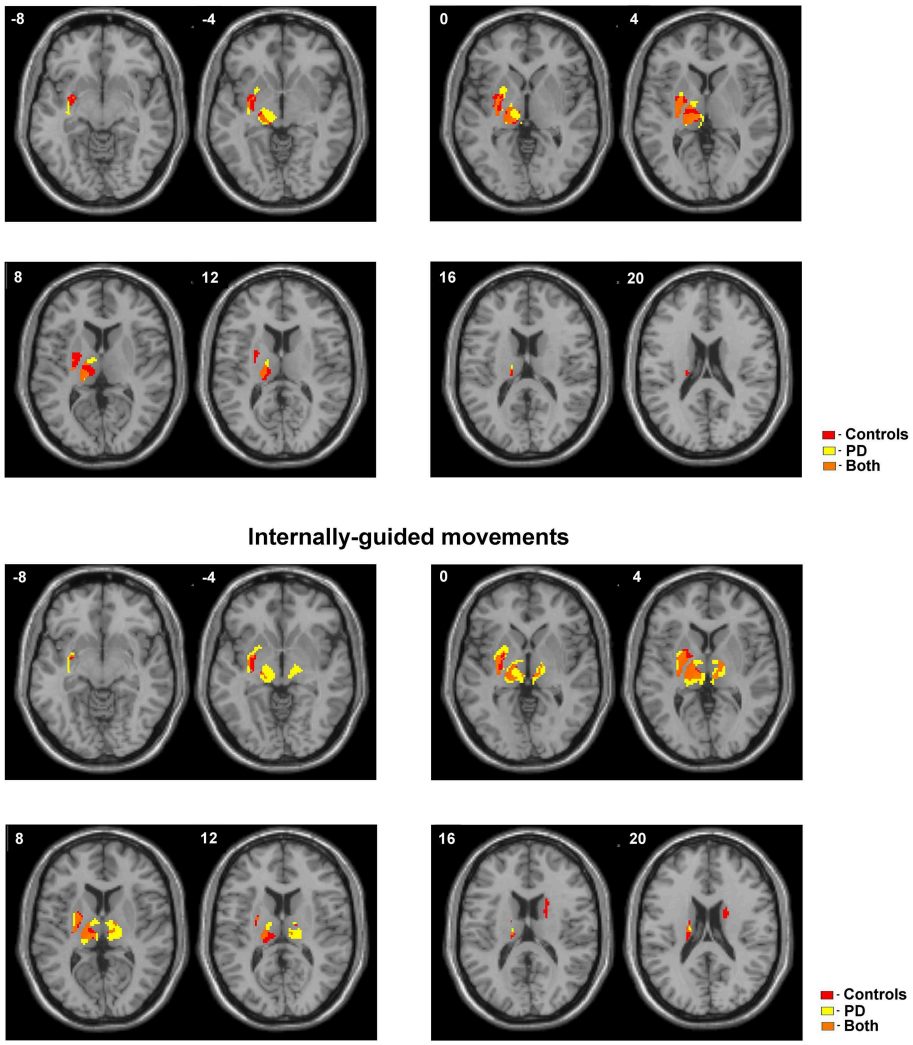

FIGURE 1 | Activated areas during ET and IG movements superimposed on anatomic slice of averaged brain in control group and PD patients.

activated brain areas in healthy group. ET movements only activate the executive circuits of the motor system, i.e., the sensorimotor cortex, basal ganglia, thalamus, and cerebellum. These regions belong to the closed sensorimotor loop which is thought to support motor actions that require neither complex motor programming or the associative control system based on a feedback loop (15). In contrast, execution of IG movements is supported by widely distributed networks in both hemispheres, reflecting the fact that the internal command for movement initiation requires wider brain activation. We initially observed significant activation of the bilateral SMA which is thought to play a role in the initiation of movement (16). These results is in accordance with electrophysiological data showed that the amplitude of pre-movement event-related potentials (ERPs) over midline frontal structures as well as the amount of active SMA neurons are increased during internally driven with respect to externally triggered motor acts (2). Furthermore, along with the motor cortex, associative frontal and parietal areas were also engaged in IG movement performance.

Activation of the prefrontal cortex reflects the cognitive processes that underlie complex motor behaviors such as planning, preparation, and performing actions, as well as the processes involved in anticipating, predicting, and interpreting the consequences of actions. These findings suggest that IG motor actions are associated with not only sensorimotor activation but also activation of the associative loop involving higher-order integrative cortical areas which are strongly interconnected with the anterior striatum (15).

Despite the fact that basal ganglia connections with various parts of the cerebral cortex are well-studied, the contribution of these areas in various aspects of human movement remains

unclear. Differences in participation of the basal ganglia and cerebellum loops are observed for planning and execution of IG and ET voluntary movements in healthy controls and PD patients (7, 10). Previous papers suggest disruption of cortico-striatal processing and preservation of relatively intact neural circuits that do not involve the basal ganglia in PD (5, 7). Electrophysiological study showed that deficit of self-initiated movement in PD patients is due to supplementary motor area underactivation (2).

We found activation in the main sensorimotor regions of the basal ganglia, namely the posterior putamen, pallidum, and ventrolateral thalamus, both during ET and IG movements in PD patients. At the same time, we found displacement of activation from the dorsolateral putamen in controls into the ventromedial direction in PD patients during ET movements. The most robust differences in basal ganglia were found during IG movements. We demonstrated hyperactivity in the putamen, including its anterior areas, and bilateral thalamus in PD patients. These results are contrary to previous data showed hypoactivation in the bilateral putamen in PD (7). According to the functional organization, anterior putamen with ventromedial prefrontal cortex are the part of the associative loop and play a significant role in goal-directed motor behavior (11, 17). On the other hand, the motor loop engages sensorimotor circuits and habitual performance, and includes the sensorimotor cortex and dorsolateral striatum, or posterior putamen. It has been theorized that imbalances of these two loops may lead to pathological conditions such as Parkinson's disease (11). We showed activation of both anterior and posterior putamen in PD patients unlike activation of only posterior putamen in the control group. We suppose that IG movements in PD could be controlled by an associative goal-directed network with the involvement of a wide range of cortical areas, which is activated in situations requiring non-routine decision making as in the self-initiated movements (2, 11). This could be a mechanism of compensation for disturbed sensorimotor control in PD patients. Further research of the SMA and basal ganglia network is needed for refinement of the pathological models of Parkinson's disease and improvement of treatment.

Our study has a limitation that should be mentioned. We used external reward stimuli in IG mode to unify paradigm. In the first few trials, some subjects could be wrong and performed movement with stimuli. We suppose that these trials do not significantly influence the results.

ETHICS STATEMENT

The study was approved by the Ethics Committee of the Burdenko National Medical Research Center of Neurosurgery (01/2018).

AUTHOR CONTRIBUTIONS

AS, AT, and IP contributed conception and design of the study. VF, VP, AB, and VU organized the database. VF and RM performed the statistical analysis. AS wrote the first draft of the manuscript. VF, VP, AT, and VU wrote sections of the manuscript. All authors contributed to manuscript revision, read, and approved the submitted version.

FUNDING

The reported study was funded by RFBR, project number 19-315-90097. This study was also supported by the Institute of Chemical Physics, Russian Academy of Sciences, in the framework of State Contract no. 0082-2014-0001, AAAA-A17-117040610310-6.

SUPPLEMENTARY MATERIAL

The Supplementary Material for this article can be found online at: https://www.frontiersin.org/articles/10.3389/fneur.2019.00847/full#supplementary-material

Supplementary Figure 1 | Statistical parametric maps of activated areas during externally triggered (ET) and internally guided (IG) movements in control groups. On the right—activated areas superimposed on anatomic slice of averaged brain.

Supplementary Figure 2 | Statistical parametric maps of activated areas during externally triggered (ET) and internally guided (IG) movements in PD patients. On the right—activated areas superimposed on anatomic slice of averaged brain.

Supplementary Figure 3 | Localization of activation areas using ET>IG and IG>ET contrast in control subjects and PD patients.

Supplementary Table 1 | Clinical characteristics of Parkinson's disease patients.

Supplementary Table 2 | Localization of activation areas using ET>IG and IG>ET contrast in control subjects and PD patients.

REFERENCES

1. Goldberg G. Supplementary motor area structure and function: review and hypotheses. *Behav Brain Sci.* (1985) 8:567–88. doi: 10.1017/S0140525X00045167
2. Jahanshahi M, Jenkins IH, Brown RG, Marsden CD, Passingham RE, Brooks DJ. Self-initiated versus externally triggered movements. I. An investigation using measurement of regional cerebral blood flow with PET and movement-related potentials in normal and Parkinson's disease subjects. *Brain.* (1995) 118 (Pt 4):913–933.
3. Debaere F, Wenderoth N, Sunaert S, Van Hecke P, Swinnen SP. Internal vs. external generation of movements: differential neural pathways involved in bimanual coordination performed in the presence or absence of augmented visual feedback. *NeuroImage.* (2003) 19:764–76. doi: 10.1016/S1053-8119(03)00148-4
4. Cunnington R, Windischberger C, Deecke L, Moser E. The preparation and execution of self-initiated and externally-triggered movement: a study of event-related fMRI. *NeuroImage.* (2002) 15:373–85. doi: 10.1006/nimg.2001.0976
5. Taniwaki T, Okayama A, Yoshiura T, Togao O, Nakamura Y, Yamasaki T, Ogata K, Shigeto H, Ohyagi Y, Kira J, et al. Functional network of the basal ganglia and cerebellar motor loops *in vivo*: different activation patterns between self-initiated and externally triggered movements. *NeuroImage.* (2006) 31:745–53. doi: 10.1016/j.neuroimage.2005.12.032
6. Marsden CD. Slowness of movement in Parkinson's disease. *Mov Disord.* (1989) 4:S26–37. doi: 10.1002/mds.870040505

7. Taniwaki T, Yoshiura T, Ogata K, Togao O, Yamashita K, Kida H, et al. Disrupted connectivity of motor loops in Parkinson's disease during self-initiated but not externally-triggered movements. *Brain Res.* (2013) 1512:45–59. doi: 10.1016/j.brainres.2013.03.027
8. Yu R, Liu B, Wang L, Chen J, Liu X. Enhanced functional connectivity between putamen and supplementary motor area in Parkinson's disease patients. *PLoS ONE.* (2013) 8:e59717. doi: 10.1371/journal.pone.0059717
9. Lewis MM, Slagle CG, Smith AB, Truong Y, Bai P, McKeown MJ, et al. Task specific influences of Parkinson's disease on the striato-thalamo-cortical and cerebello-thalamo-cortical motor circuitries. *Neuroscience.* (2007) 147:224–235. doi: 10.1016/j.neuroscience.2007.04.006
10. Purzner J, Paradiso GO, Cunic D, Saint-Cyr JA, Hoque T, Lozano AM, et al. Involvement of the basal ganglia and cerebellar motor pathways in the preparation of self-initiated and externally triggered movements in humans. *J Neurosci.* (2007) 27:6029–36. doi: 10.1523/JNEUROSCI.5441-06.2007
11. Redgrave P, Rodriguez M, Smith Y, Rodriguez-Oroz MC, Lehericy S, Bergman H, et al. Goal-directed and habitual control in the basal ganglia: implications for Parkinson's disease. *Nat Rev Neurosci.* (2010) 11:760–72. doi: 10.1038/nrn2915
12. Friston KJ, Holmes AP, Worsley KJ, Poline J-P, Frith CD, Frackowiak RSJ. Statistical parametric maps in functional imaging: a general linear approach. *Hum Brain Mapp.* (1994) 2:189–210. doi: 10.1002/hbm.460020402
13. Gerloff C. Functional coupling and regional activation of human cortical motor areas during simple, internally paced and externally paced finger movements. *Brain.* (1998) 121:1513–31. doi: 10.1093/brain/121.8.1513
14. Halsband U, Matsuzaka Y, Tanji J. Neuronal activity in the primate supplementary, pre-supplementary and premotor cortex during externally and internally instructed sequential movements. *Neurosci Res.* (1994) 20:149–155. doi: 10.1016/0168-0102(94)90032-9
15. Lanciego JL, Luquin N, Obeso JA. Functional Neuroanatomy of the Basal Ganglia. *Cold Spring Harb Perspect Med.* (2012) 2:a009621–a009621. doi: 10.1101/cshperspect.a009621
16. Cunnington R, Windischberger C, Deecke L, Moser E. The preparation and readiness for voluntary movement: a high-field event-related fMRI study of the Bereitschafts-BOLD response. *NeuroImage.* (2003) 20:404–12. doi: 10.1016/S1053-8119(03)00291-X
17. Nakano K, Kayahara T, Tsutsumi T, Ushiro H. Neural circuits and functional organization of the striatum. *J Neurol.* (2000) 247 (Suppl. 5):V1–15. doi: 10.1007/PL00007778

Conflict of Interest Statement: The authors declare that the research was conducted in the absence of any commercial or financial relationships that could be construed as a potential conflict of interest.

frontiers in Neurology

ORIGINAL RESEARCH
published: 18 September 2019
doi: 10.3389/fneur.2019.01001

Dopaminergic Modulation of Sensory Attenuation in Parkinson's Disease: Is There an Underlying Modulation of Beta Power?

Antonella Macerollo[1,2,3,4], *Patricia Limousin*[3,4], *Prasad Korlipara*[3], *Tom Foltynie*[3,4], *Mark J. Edwards*[5] *and James Kilner*[4]*

[1] The Walton Centre NHS Foundation Trust, Liverpool, United Kingdom, [2] School of Psychology, Faculty of Health and Life Sciences, University of Liverpool, Liverpool, United Kingdom, [3] National Hospital for Neurology and Neurosurgery, London, United Kingdom, [4] Institute of Neurology, University College of London, London, United Kingdom, [5] Department of Neurology, St George's University of London, London, United Kingdom

OPEN ACCESS

Edited by:
Salvatore Galati,
Neurocenter of Southern Switzerland (NSI), Switzerland

Reviewed by:
Antonella Conte,
Sapienza University of Rome, Italy
Isabella Berardelli,
Sapienza University of Rome, Italy

***Correspondence:**
James Kilner
j.kilner@ucl.ac.uk

Specialty section:
This article was submitted to Movement Disorders, a section of the journal Frontiers in Neurology

Received: 15 March 2019
Accepted: 02 September 2019
Published: 18 September 2019

Citation:
Macerollo A, Limousin P, Korlipara P, Foltynie T, Edwards MJ and Kilner J (2019) Dopaminergic Modulation of Sensory Attenuation in Parkinson's Disease: Is There an Underlying Modulation of Beta Power? Front. Neurol. 10:1001. doi: 10.3389/fneur.2019.01001

Background and Aims: Pathological high amplitude of beta oscillations is thought as the underlying mechanism of motor symptoms in Parkinson's disease (PD), in particular with regard to bradykinesia. In addition, abnormality in a neurophysiological phenomenon labeled sensory attenuation has been found in patients with PD. The current study explored the hypothesis that the abnormal sensory attenuation has a causal link with the typical abnormality in beta oscillations in PD.

Methods: The study tested sixteen right-handed patients with a diagnosis of PD and 22 healthy participants, which were matched by age and gender. Somatosensory evoked potentials were elicited through electrical stimulation of the median nerve at the wrist. Electrical activity was recorded at the scalp using a 128 channels EEG. Somatosensory evoked potentials were recorded in 2 conditions: at rest and at the onset of a voluntary movement, which was a self-paced abduction movement of the right thumb.

Results: Healthy participants showed a reduction of the N20-P25 amplitude at the onset of the right thumb abduction compared to the rest condition ($P < 0.05$). When patients were OFF medication, they showed mild reduction of the N20-P25 component at movement onset ($P < 0.05$). On the contrary, they did show greater attenuation of the N20-P25 component at the onset of movement compared to the rest condition when ON medication ($P < 0.05$). There was no significant evidence of a link between the degree of sensory attenuation and the change in beta oscillations in our cohort of patients.

Conclusion: These results confirmed a significant link between dopaminergic modulation and sensory attenuation. However, the sensory attenuation and beta oscillations were found as two independent phenomena.

Keywords: Parkinson's disease, sensory attenuation, beta power, bradykinesia, motor symptoms

INTRODUCTION

Several studies have showed that sensory afferents are reduced prior to and during movement (1–4). This phenomenon is denominated sensory attenuation (SA) or sensory gating.

A recent theoretical framework, labeled active inference, proposed that SA prior to and during active movement is an essential mechanism that allow to move (5).

This model of movement initiation hypothesizes that the brain needs to perceive when sensory information is uncertain and must down weight these external sensations to top-down predictions. In line with this hypothesis, the movement initiation is a consequence of fulfilling prior expectations about proprioceptive sensations. In other words, the movements are allowed by the transition from one sensory state to another. According to this model, an impairment to correctly initiate or maintain a voluntary movement might be due to an abnormality of SA (6).

It is still unknown if the pathophysiology of bradykinesia in Parkinson's disease (PD) is due to a deficit in SA. The latter is thought to be linked with pathology in reducing the precision of the somatosensory expectations (6).

The SA can be tested in two different fields: physiological and perceptual (7). The neurophysiological measure of SA is represented as a reduction in amplitude of somatosensory evoked potentials (SEPs) components at the onset of a voluntary movement compared with a rest condition (7).

SA is expected to be reduced in PD and improved with medical treatment. Indeed, SA prior to and during movement (as measured by a decrease in the amplitude of N20-P25 component of SEPs elicited by median nerve stimulation) has been found significantly reduced in PD patients OFF medication (8). Moreover, SA was normalized by dopaminergic medication (8). Of note, an attenuation of the N20-P25 component at the onset of voluntary movements in healthy participants (8).

This study aimed to replicate results of the previous study (8) in a completely naïve group of PD patients. The prediction was an interaction in the SEPs amplitude between group and time with the SEPs being more greatly attenuated in healthy controls at the onset of active movement than the patients' group in OFF state. Furthermore, it was predicted that there would not be any significant differences in SA between healthy participants and patients ON medication.

A second aim was to test whether SEPs attenuation was modulated as a function of disease and voluntary movement. In other words, it was tested if there was a correlation between the difference in N20-P25 amplitude between baseline and movement condition with measurements of bradykinesia using the Unified Parkinson's Disease Rating scale (UPDRS) (9) as well as parametric measures of the tapping through a cybernetic glove.

The prediction was that SEPs attenuation would correlate with movement such that the faster and more vigorous movements would be positively correlated with the degree of the SA. It was predicted that across subjects the lower (better) the UPDRS scores and the less slowing and decrement in amplitude of tapping measured by cyberglove, the greater the SA measured at movement onset. These results would be further support of the pathophysiological role of SA in the contest of bradykinesia.

Notably, the active inference theory makes more detailed predictions (10). It predicts that SA will be driven by a change in the precision of the sensory expectation, with lower precision leading to greater SEPs attenuation.

The second part of the study explored if SA modulations would be correlated with modulation in beta power in the sensorimotor cortex, which decrease prior to and during movement (11, 12).

Recently, Tan et al. (13) proposed a novel theory based on the functional role of sensorimotor post-movement beta synchronization (PMBS). This theory linked theoretical models of motor control related to a phenomenon called uncertainty and neurophysiological measures of sensorimotor activity. Indeed, voluntary movements stimulate peripheral sensory receptors providing sensory feedback of the movement action.

Adams et al. (10) tested a model hypothesizing that the predicted sensory consequences of a movement are compared to the actual sensory input. These authors calculated the prediction error by the difference between the predicted and actual sensory input. The prediction error is a measure used to make the forward model able to perform more accurate future predictions. Estimations of the uncertainty in the motor prediction and the uncertainty of the actual sensory input are required to calculate the importance of any prediction errors (14).

Tan et al. (13) have proposed modalities to manipulate the uncertainty. In addition, these authors predicted that PMBS would be correlate with the uncertainty rather than with the movement error. The PMBS amplitude over sensorimotor cortex was found to be characterized by negative correlation with the variable of uncertainty. Consequentially, this result supports a novel functional role of PMBS linking beta oscillations to the uncertainty of the parameters underlying the motor control. In other words, sensorimotor beta oscillatory power might be the neurophysiological mechanism allowing to estimate of uncertainty or causally modulating the uncertainty.

Palmer et al. (15) highlighted that this potential correlation between PMBS and sensory uncertainty might mean that beta oscillatory activity is a potential candidate for this sensory gating phenomenon. If beta oscillations modulation would be correlated with the time course of SEPs attenuation, this would be evidence that there might be a potential link between beta oscillatory activity and SA.

This finding is particularly relevant for the application of this theoretical account to explain akinesia and bradykinesia. In PD beta oscillations in the motor network and in the STN are higher during rest. Consequentially, pathological higher beta oscillations have been causally implicated in movement impairment rather than being just an epiphenomenon of the diseased state (16).

One theory therefore is that patients with PD have high sensory precision such that when they decide to move, they cannot attenuate this precision enough to allow the influence of top-down proprioceptive predictions to supersede. This theory is supported by our study, which has demonstrated decreased SA in patients diagnosed with PD compared to age-matched healthy controls (8, 17). Furthermore, dopaminergic treatment acted to

normalize SA in PD patients, which suggests this may be one of the mechanisms which can explain the improvement in motor symptoms under this class of medication (8).

Here, it was tested if the specific time course of the SA is correlated with modulations in beta power during movement execution. The prediction was that modulations in beta power will be positively correlated with the time course of SEPs modulation. If this is the case, it will establish a statistical dependency between beta power and SA.

METHODS

Sixteen patients diagnosed with idiopathic PD (10 males, 6 females; mean age, 68 years; range, 52–79 years; **Table 1**) and 22 age and sex matched healthy participants (14 males, 8 females; mean age, 67 years; range, 50–80 years) were involved in the study. Control subjects were recruited from a pool of healthy subjects of the University College of London. This group of participants were not diagnosed with any medical disorder and they were not on medication.

PD patients were recruited from the Movement Disorders Clinics at the National Hospital of Neurology and Neurosurgery.

Idiopathic PD was diagnosed according to the UK PD Society Brain Bank criteria (18) and further confirmed by abnormal dopamine transporter SPECT in all patients.

TABLE 1 | Clinical and demographic characteristics of patients with Parkinson disease (Mo, months; y, years; UPDRS, Unified Parkinson's Disease Rating Scale; SD, standard deviation; L, L-DOPA; D, Dopamine agonist).

	Age (y)	Gender	Disease duration (y)	Motor UPDRS upper limbs bradykinesia items OFF state	Motor UPDRS upper limbs bradykinesia items ON state	Treatments
1	72	M	11	11	6	L
2	75	F	4	9	5	L
3	61	M	2	6	3	L
4	75	M	5	11	5	L
5	77	F	10	9	5	L
6	68	F	4	6	3	L
7	56	M	4	8	3	L
8	70	F	6	6	3	L+D
9	69	M	6	9	4	L+D
10	79	F	12	10	6	L+D
11	68	F	10	12	6	L+D
12	52	M	10	12	6	L+D
13	62	M	3	8	3	L+D
14	68	M	8	12	9	L+D
15	72	M	5	8	3	L+D
16	68	M	5	8	3	L+D
Mean ± SD	68.1 ± 6.9	F8/M12	6.5 ± 2.9	9 ± 2	4.3 ± 1.7	

Participants did not have disabling tremor. None of the patients had cognitive decline. PD patients were on levodopa medication and/or on dopaminagonists.

Participants were right-handed.

The study was approved by the East of Scotland Research Ethics Service. Written informed consent was obtained from all participants.

Clinical disease severity was assessed with the motor section (items 3.1–3.18) of the UPDRS (9). The clinical assessment was performed in the ON as well as OFF state in each patient.

The amplitude and the frequency of a minute right hand tapping test with the Cyber Glove was recorded in both pharmacological states.

To reach the OFF state, patients were required not to take levodopa for at least 12 h and dopamine-agonists for at least 24 h prior to testing. Patients were assessed in the ON state 1 h after taking levodopa or 2 h after taking dopamine agonists (**Table 1**).

Procedure and Experimental Design

Participants were seated in a comfortable armchair with hands relaxed on the armrest of the chair and their eyes closed. Two electrodes were placed on the surface of the wrist. The anode was placed over the median nerve at the wrist and the cathode 2 cm proximal to the anode. SEPs were elicited by electrical stimulation of the median nerve at the right wrist using a constant current square-wave pulse (0.2 ms duration). The intensity of the stimulation at threshold (slight thumb twitch) was identified and then increased by 1 mA to produce a definite thumb twitch. The intensity remained the same throughout the experiment.

Electrical activity was recorded at the scalp using a 128 channels Biosemi ActiveTwo AD-box EEG. EEG was recorded at a sampling rate of 2,048 Hz.

Surface electromyography (EMG) of the right abductor pollicis brevis (APB) was monitored simultaneously.

SEPs were recorded in three conditions in a single session.

In the baseline condition, the subjects were relaxed and instructed not to react to the stimulus. The frequency of the median nerve stimulation was 0.5 Hz. Subjects received 500 stimulations in this condition.

In the movement condition, subjects were instructed to make a self-paced abduction movement of the right thumb with a frequency of around a movement every second. At the onset of the movement, the median nerve stimulus was automatically triggered. The frequency of movements was recorded. Participants made 500 thumb abductions.

In the rest condition, the subjects were relaxed and instructed not to react to the stimulus. In distinction to the baseline condition here the median nerve stimulations were given at precisely the same times as the self-paced movements recorded from the movement condition.

Data Analysis

Measure of SEPs Components and SA

EEG data analyses were performed in MATLAB 2013b (Math Works, Natick, MA, USA) using the software Statistical Parametric Mapping (SPM12, Wellcome Department of Imaging Neuroscience, London, UK).

The SEPs produced at movement onset has previously been employed to assess the degree of SA during active movement. Indeed, SEPs elicited by stimulation at this time point is not confounded by any possible effect of the afferent signal produced by the movement. The initial analysis was focused on modulations in the SEPs components, specifically the amplitude of the N20 and P25 as a function of group (PD patients ON medications, PD patients OFF medication and healthy participants). The peak-to-peak amplitude of the N20-P25 component was measured for each participant. EEG data were analyzed in SPM12.

The offline data were high-passed filtered at 0.1 Hz and, then, epoched to the time of the onset of the median nerve stimulation taking the 100 ms before stimulation and 250 ms after the stimulation. The data were baseline corrected by subtracting the average of the signal in a window from 20 to 5 ms prior to median nerve stimulation.

Artifacts exceeding 100 mV were manually rejected.

SEPs were averaged across the 500 trials of each condition. The baseline condition was the reference to select the appropriate channels to see N20 and P25. The electrodes over sensorimotor cortices were selected based on electrodes contralateral to the stimulated wrist that showed a negative peak at around 20 ms and a positive peak around 25–35 ms after the stimulus.

Then, the data from the selected channels were averaged and the amplitude and the time data points of N20 and P25 were measured. These electrodes and time points were used to calculate the amplitude of the N20 and P25 in the other two conditions—rest condition and movement condition. Note that the choice of electrodes and time points from an independent condition removed selection bias in the two experimental conditions of interest.

The SA was measured through the difference in the absolute amplitude of the peak N20-P25 between the rest and movement onset conditions was calculated.

Analysis of Parametric Measures of Tapping and Quantification of Bradykinesia

The finger-tapping performed using the cyber glove was recorded through a Matlab script. The amplitude and the frequency of each tapping movement in a minute of interval time were calculated using Welch's power spectral density estimate of the time series of the tapping as recorded by the CyberGlove. The data were then averaged, and the peak amplitude and frequency at the peak amplitude of the tapping was taken for each pharmacological state of each patient. These were the parametric measures of tapping.

The regression analysis between SA and parametric measures of tapping was performed to test the hypothesis of a correlation between dopaminergic modulation of SA and dopaminergic improvement of bradykinesia.

Analysis of Beta Power in Movement and Rest Condition

In healthy subjects, power in beta oscillations is expected to be attenuated prior to the thumb movement and augmented once the movement has ended (12).

After raw data conversion, EEG data were re-referenced by subtracting the average signal from two external electrodes attached to the subjects' earlobes from the signal from each EEG electrode. Data were high pass (0.1 Hz) filtered and down-sampled to 400 Hz.

A trigger was sent to the EEG system at the time of every median nerve stimulus. The data were epoched to the time of median nerve stimulation, taking the 1,000 ms before the onset and 1,000 ms after.

The different experimental blocks were merged into a single file.

For the time–frequency analysis, the power of the EEG signal at each frequency from 1 to 99 Hz in steps of 2 was estimated using the Morlet spectral estimation in SPM. The data were rescaled using a logarithmic transformation and averaged across all trials.

The time–frequency data were averaged over the same electrode channels selected for the SEPs analysis on the scalp map to investigate the modulation of beta power in each condition (rest and movement) for each subject and in each pharmacological state for each patient.

Subsequently, the time-frequency images for the rest condition for each subject were averaged across all subjects and three time' windows. The latter corresponded to the three phases of beta oscillations modulation with median nerve stimulation in the rest condition and were calculated as background (between 180 and 625 ms before the stimulus), suppression (between 165 and 378 ms after stimulus) and rebound (between 535 and 980 ms).

The beta power, obtained by averaging over the frequency of 15–25 Hz, was then averaged over each selected time window across subjects of each group to have a value of beta power for each time window per group per condition. Subsequently, a value of beta power modulation for each group and each time window was obtained through a subtraction of beta power value between rest and movement condition.

The value of beta power modulation was then regressed against the amplitude of SA per group per time window.

Finally, a regression analysis was performed between the amplitude of beta power and amplitude of SEPs for each group per time window per condition.

RESULTS

SEPs Components and SA

The averaged SEPs over our ROI (channels over the somatosensory cortex) across participants for PD patients OFF medication, ON medication, and control subjects are shown in **Figure 1**.

Repeated measures ANOVA with the group (ON vs. OFF) and condition (rest vs. movement) as factors showed a significant effect of the condition [$p < 0.05$; $F_{(1,30)} = 39.46$; $\text{Eta}^2 = 0.537$] and a significant interaction between condition and pharmacological state [$p < 0.05$; $F_{(1,30)} = 6.33$; $\text{Eta}^2 = 0.157$]. *Post-hoc* pairwise comparisons revealed a significant difference between N20-P25 peak to peak amplitude between the rest condition and movement condition [$p < 0.05$; $t_{(30)} = 5.85$].

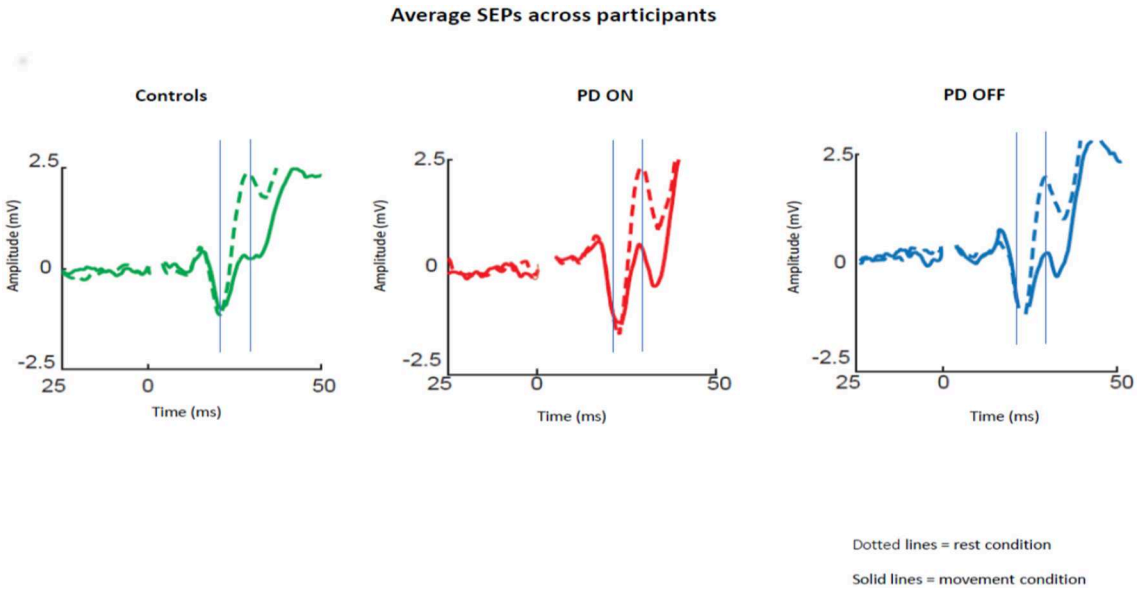

FIGURE 1 | Average SEPs across participants recorded from the left somatosensory cortex for PD patients OFF medication, ON medication, and control subjects. Solid lines show data for median nerve stimulation given at movement onset and dotted lines during baseline. The gray lines show the mean time of the peaks of the N20 and P25 components.

As expected, healthy participants showed attenuation of the N20-P25 amplitude at movement onset (2.13 ± 1.87) compared to the rest condition (4.8 ± 2.84) [$P < 0.05$; $t_{(21)} = 7.45$, **Figure 2A**].

PD patients OFF medication showed mild attenuation of the N20-P25 component at movement onset (3.99 ± 2.31) compared to rest condition (5.03 ± 3.29) [$P < 0.05$; $t_{(15)} = 2.52$; **Figure 2B**]. This group showed greater attenuation of the N20-P25 component at the onset of movement (2.59 ± 1.79) compared to the rest condition (5.02 ± 2.94) when ON medication [$P < 0.05$; $t_{(15)} = 5.95$; **Figure 2C**].

There was a significant difference in the amplitude of N20-P25 peak during the movement condition between OFF state (3.99 ± 2.31) and ON state (2.59 ± 1.79) [$p = < 0.05$; $t_{(15)} = 3.32$] with a smaller amplitude in the ON state.

There was no difference in the N20-P25 amplitude during the rest condition between OFF state (5.03 ± 3.29) and ON state (5.02 ± 2.94) [$p \geq 0.05$; $t_{(15)} = 0.017$].

The SA (defined as difference in the amplitude of N20-P25 peak between rest condition and movement condition) showed a significant difference between OFF (1.29 ± 1.55) and ON state (2.42 ± 1.55) in PD patients [$p \leq 0.05$; $t_{(15)} = -3.28$] with greater SA in ON state (**Figure 2D**).

There was no difference in the SA between PD patients in ON state (2.42 ± 1.55) and healthy subjects (2.74 ± 1.61) [$p \geq 0.05$, $t_{(36)} = -0.46$] (**Figure 2D**).

Having shown that SA was modulated by dopaminergic treatment and that SA was significantly attenuated in PD patients ON medication, it was tested if the severity of right arm bradykinesia was correlated with the degree of SA. In this regard, there was no statistically significant correlation between SA and UPDRS scores ($R^2 = 0.001$, $p = 0.893$ OFF medication (**Figure 3A**) and $R^2 = 0.001$, $p = 0.924$ ON medication (**Figure 4A**) as well as between SA and frequency of the fingers tapping ($R^2 = 0.059$, $p = 0.330$ OFF medication (**Figure 3B**) and $R^2 = 0.002$, $p = 0.867$ ON medication (**Figure 4B**) or amplitude of the fingers tapping ($R^2 = 0.06$, $p = 0.323$ OFF medication (**Figure 3C**) and $R^2 = 0.008$, $p = 0.718$ ON medication (**Figure 4C**).

After having tested the hypothesis of a potential correlation between SA and each measure of bradykinesia in the individual pharmacological state, a potential correlation between the dopaminergic modulation of SA and the dopaminergic modulation of each measure of bradykinesia was investigated. In other words, it was tested if there was a correlation between SA changes between OFF and ON states and changes of each measure of bradykinesia between OFF and ON states. There was no statistically significant correlation between dopaminergic modulation of SA and changes of UPDRS scores ($R^2 = 0.016$, $p = 0.616$) (**Figure 5A**). There was a significant correlation between dopaminergic modulation of SA and changes of frequency of the fingers tapping ($R^2 = 0.623$, $p < 0.001$) (**Figure 5B**). However, there was not significant correlation with the amplitude of the finger tapping at this frequency ($R^2 = 0.021$, $p = 0.562$) (**Figure 5C**).

Beta Oscillations Modulation

Having demonstrated that there was a modulation of SEPs over condition, the second aim was to test if the SA was correlated with modulations in beta oscillations over the sensorimotor cortex.

Firstly, it was tested the hypothesis that healthy controls and PD patients showed a modulation of beta power as function

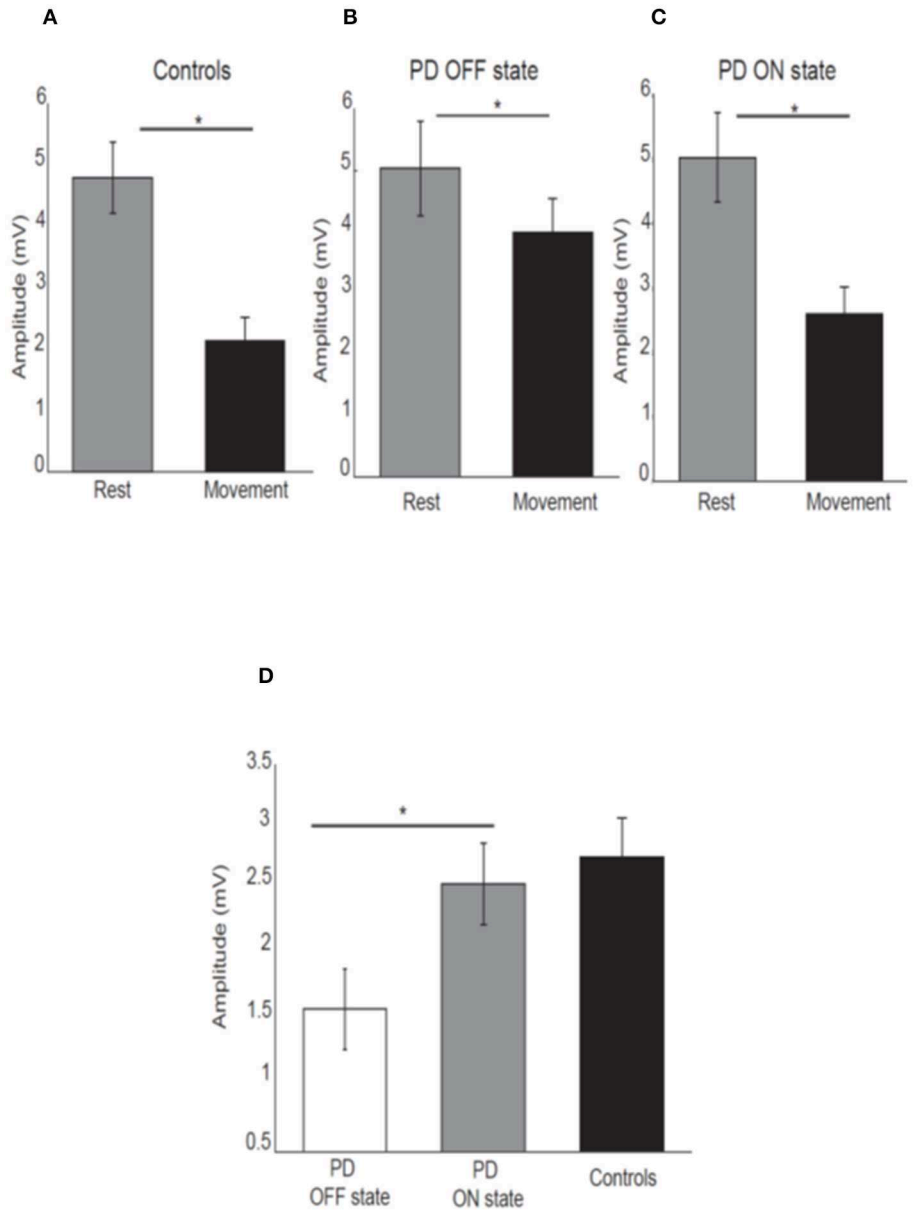

FIGURE 2 | Mean amplitude of the N20-P25 component for each condition for control subjects **(A)**, PD patients OFF medication **(B)**, ON medication **(C)**. Error bars show standard error of the means. Mean difference of the N20-P25 amplitude between rest condition and movement condition in PD patients OFF medication, ON medication and controls **(D)**. *$p < 0.05$.

of time in each experimental condition. The prediction was to find power in beta oscillations attenuated prior to the thumb movement and a rebound at the end of the movement. After averaging the time-frequency images across subjects for each group, the changes of the beta power spectrum (interval of frequency at 15–30 Hz) as function of time in each condition were showed. Beta power was clearly evident prior to movement in the baseline period, suppressed in the motor preparation and execution period and, finally, rebounded at the end of the thumb movement.

The modulation of beta oscillations in the rest condition averaged across subjects for each group is showed in the **Figure 6**.

Following the qualitative analysis, a quantitative analysis of the beta oscillations was performed in three time' windows selected as explained in the methods section. The three times windows corresponded to the three phases of beta oscillations modulation calculated as background (between 180 and 625 ms before the stimulus), suppression (between 165 and 378 ms after stimulus) and rebound (between 535 and 980 ms).

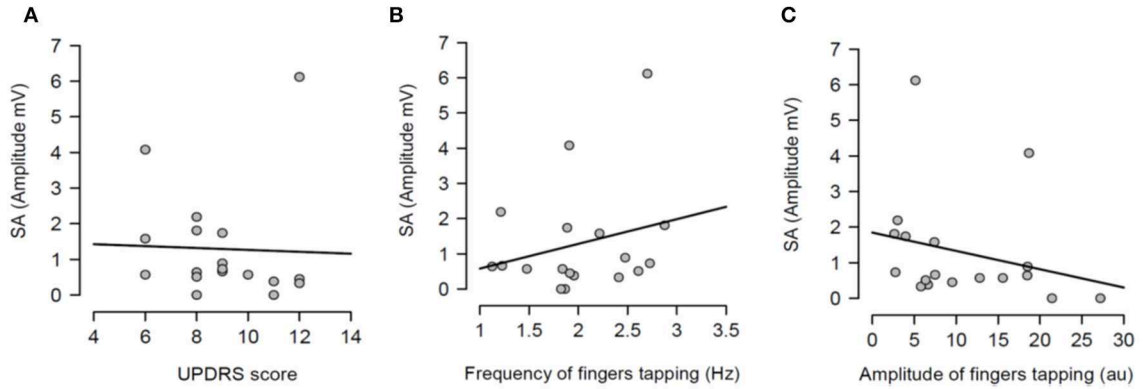

FIGURE 3 | Regression analysis between sensory attenuation (SA) and measures of bradykinesia [UPDRS score **(A)**, frequency of fingers tapping **(B)** and amplitude of fingers tapping **(C)**] in PD patients in OFF state.

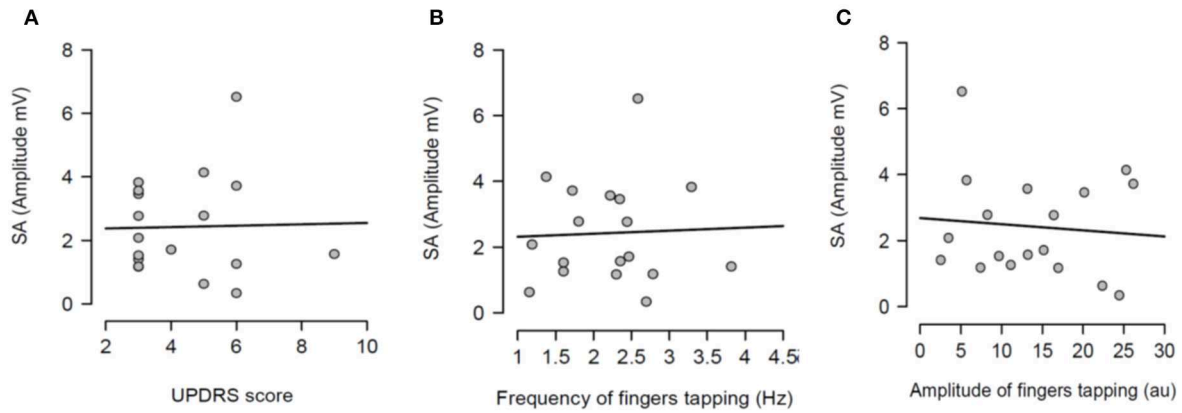

FIGURE 4 | Regression analysis between sensory attenuation (SA) and measures of bradykinesia [UPDRS score **(A)**, frequency of fingers tapping **(B)** and amplitude of fingers tapping **(C)**] in PD patients in ON state.

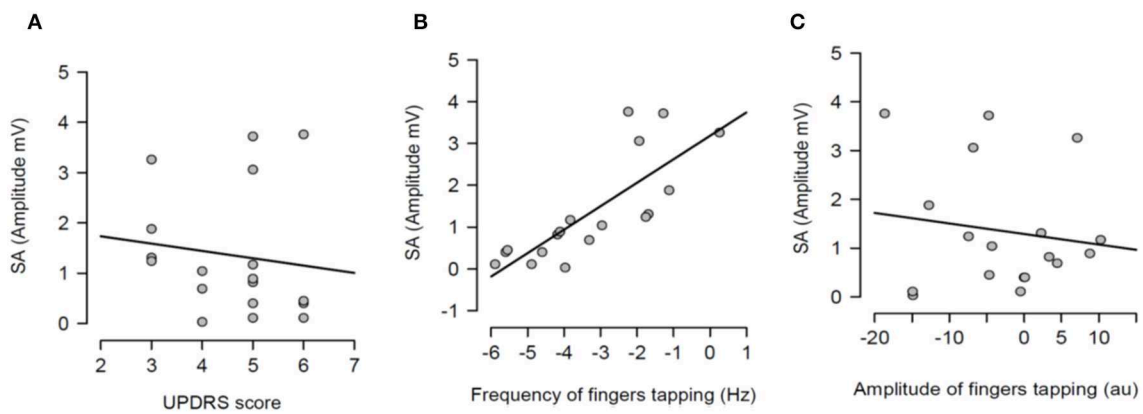

FIGURE 5 | Regression analysis between dopaminergic changes of sensory attenuation (SA) and dopaminergic changes of each measure of bradykinesia [UPDRS score **(A)**, frequency of fingers tapping **(B)** and amplitude of fingers tapping **(C)**]. The dopaminergic changes of each variable were calculated through the difference between OFF and ON values for each variable.

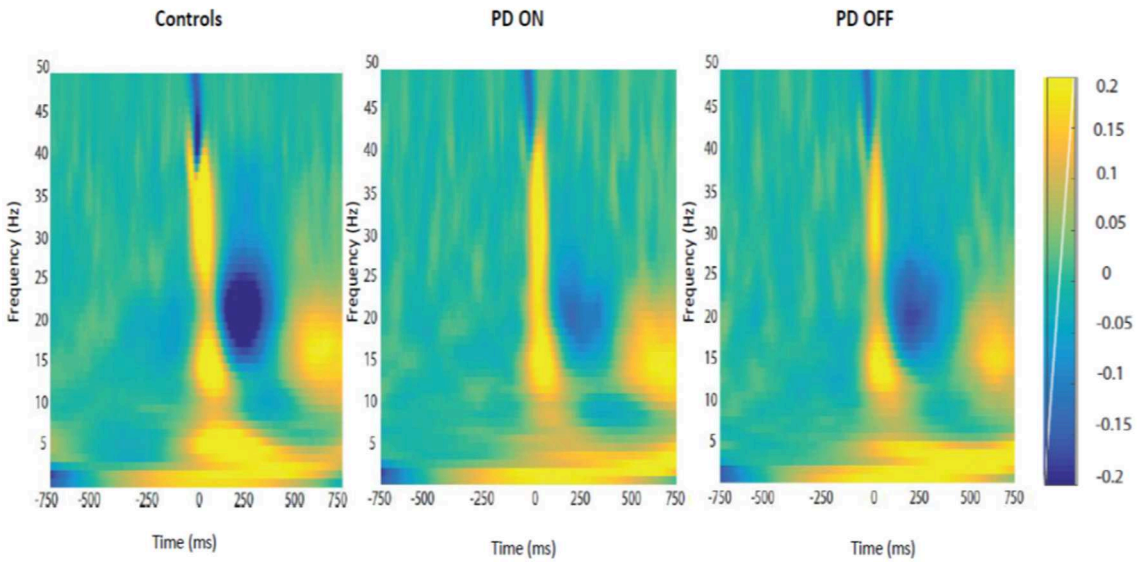

FIGURE 6 | Modulation of beta power changes as function of time at rest in each group of participants (PD ON, PD OFF, Healthy Subjects).

The quantitative analysis confirmed that the amplitude of beta oscillations was different as function of time. Indeed, beta oscillations amplitude showed a significant statistical difference in each group and in each condition over the 3 different timing windows (**Figure 7**).

Repeated measures 2 × 2 × 3 ANOVA with the group [healthy controls vs. patients (ON)], condition (rest vs. movement) and phase (background, suppression and rebound) as factors did not show a significant effect of group [$p > 0.05$; $F_{(1,36)} = 0.040$; $\text{Eta}^2 = 0.001$]. There was a significant effect of the condition [$p < 0.05$; $F_{(1,36)} = 34.88$; $\text{Eta}^2 = 0.493$] and a significant interaction between condition and group [$p < 0.05$; $F_{(1,36)} = 8.739$; $\text{Eta}^2 = 0.195$]. There was a significant effect of the phase [$p < 0.05$; $F_{(1,36)} = 91.185$; $\text{Eta}^2 = 0.717$]. There was no significant interaction between phase and group [$p > 0.05$; $F_{(1,36)} = 2.834$; $\text{Eta}^2 = 0.073$]. There was a significant interaction between condition and phase [$p < 0.05$; $F_{(1,36)} = 15.047$; $\text{Eta}^2 = 0.295$].

Post-hoc pairwise comparisons with Bonferroni corrections did not reveal significant difference between the two groups (healthy participants vs. PD ON state) in the rest condition in each phase: background [$p > 0.05$, $t_{(36)} = 1.090$], suppression [$p > 0.05$, $t_{(36)} = 0.491$] and rebound [$p > 0.05$, $t_{(36)} = 1.235$]. The two groups did not show significant difference neither in the movement condition in each phase: background [$p > 0.05$, $t_{(36)} = -0.645$], suppression [$p > 0.05$, $t_{(36)} = -0.579$] and rebound [$p > 0.05$, $t_{(36)} = -0.370$].

Furthermore, *post-hoc* pairwise comparisons showed significant differences between the rest and movement condition in the background phase [$p < 0.05$, $t_{(37)} = -5.356$], suppression [$p < 0.05$, $t_{(37)} = -4.156$] and rebound [$p < 0.05$, $t_{(37)} = -6.795$] over the two groups.

Repeated measures 2 × 2 × 3 ANOVA with the group [healthy controls vs. patients (OFF)], condition (rest vs. movement) and phase (background, suppression and rebound) as factors did not show an effect of the group [$p > 0.05$; $F_{(1,36)} = 0.0765$; $\text{Eta}^2 = 0.021$]. There was a significant effect of condition [$p < 0.05$; $F_{(1,36)} = 58.04$; $\text{Eta}^2 = 0.617$] and a significant interaction between condition and group [$p < 0.05$; $F_{(1,36)} = 7.931$; $\text{Eta}^2 = 0.181$]. There was a significant effect of the phase [$p < 0.05$; $F_{(1,36)} = 98.454$; $\text{Eta}^2 = 0.732$]. There was no significant interaction between phase and group [$p > 0.05$; $F_{(1,36)} = 2.366$; $\text{Eta}^2 = 0.062$]. There was a significant interaction between condition and phase [$p < 0.05$; $F_{(1,36)} = 20.392$; $\text{Eta}^2 = 0.362$].

Post-hoc pairwise comparisons with Bonferroni corrections did not reveal significant difference between the two groups (healthy participants vs. PD OFF state) in the rest condition in each phase: background [$p > 0.05$, $t_{(36)} = 1.446$], suppression [$p > 0.05$, $t_{(36)} = 1.125$] and rebound [$p > 0.05$, $t_{(36)} = 1.725$]. The two groups did not show significant difference neither in the movement condition in each phase: background [$p > 0.05$, $t_{(36)} = 0.112$], suppression [$p > 0.05$, $t_{(36)} = 0.217$] and rebound [$p > 0.05$, $t_{(36)} = 0.484$].

Furthermore, *post-hoc* pairwise comparisons showed significant differences between the rest and movement condition in the background phase [$p < 0.05$, $t_{(37)} = -6.739$], suppression [$p < 0.05$, $t_{(37)} = -5.002$] and rebound [$p < 0.05$, $t_{(37)} = -8.876$] over the two groups.

Having found a modulation of beta oscillations amplitude as function of time, the subsequent aim was to test if there was a

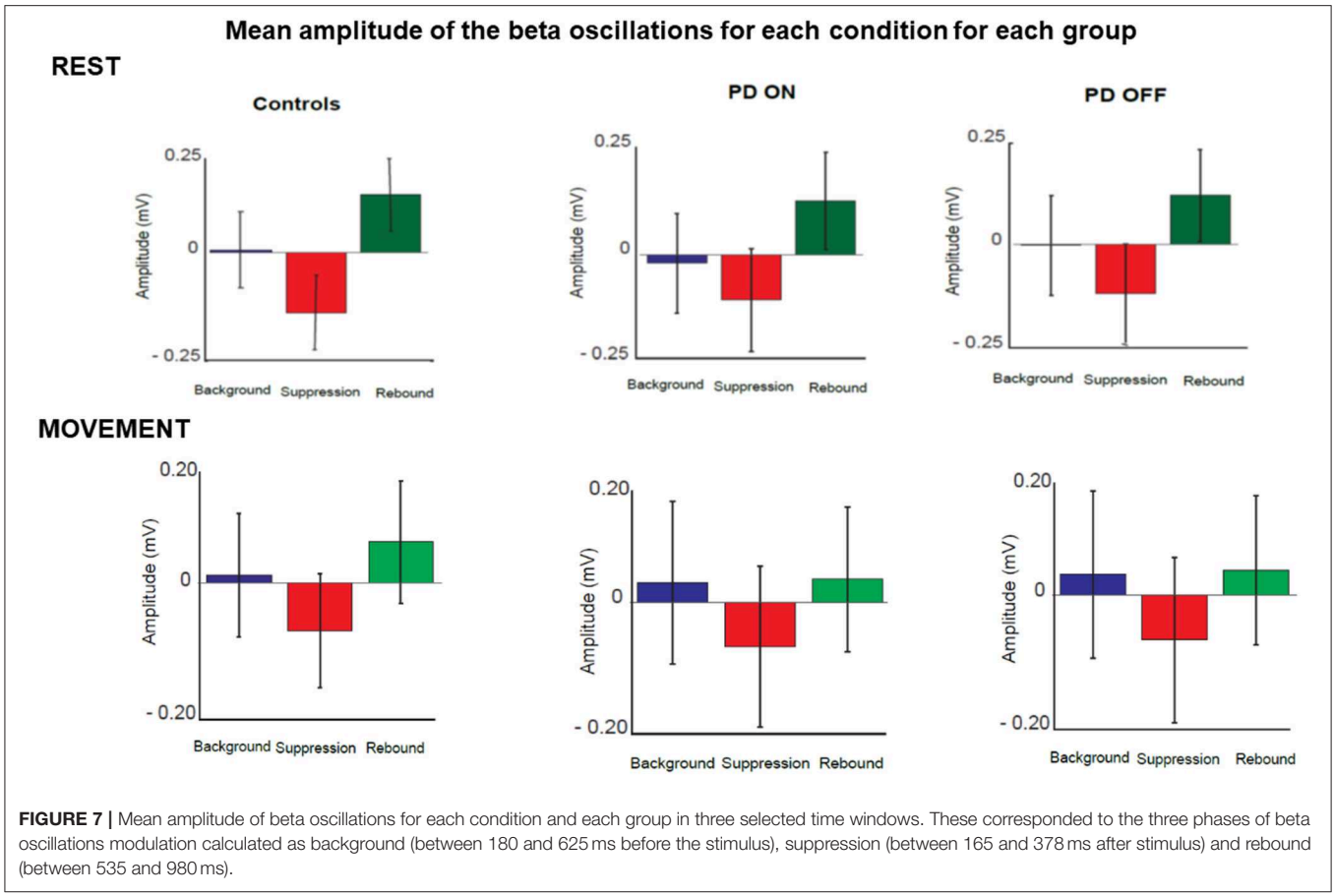

FIGURE 7 | Mean amplitude of beta oscillations for each condition and each group in three selected time windows. These corresponded to the three phases of beta oscillations modulation calculated as background (between 180 and 625 ms before the stimulus), suppression (between 165 and 378 ms after stimulus) and rebound (between 535 and 980 ms).

correlation between beta oscillations amplitude changes across the two conditions and SEPs changes across the two conditions, which was the measure of SA.

This correlation analysis was performed separately for each time window in each group of participants.

There was no evidence that SA and beta oscillations amplitude modulation were correlated in PD patients ON state and healthy subjects. Indeed, healthy participants did not show a significant correlation between beta oscillations amplitude modulation and SA in background phase ($R^2 = 0.04$, $p = 0.51$), suppression phase ($R^2 = 0.08$, $p = 0.24$) or the rebound phase ($R^2 = 0.06$, $p = 0.37$). The absence of a correlation between these two neurophysiological phenomena was evident also in the PD patients group in ON (background phase, $R^2 = 0.11$, $p = 0.56$; suppression phase, $R^2 = 0.07$, $p = 0.73$; rebound phase, $R^2 = 0.14$, $p = 0.43$) as well as in OFF state (background phase, $R^2 = 0.005$, $p = 0.41$; suppression phase, $R^2 = 0.003$, $p = 0.31$; rebound phase, $R^2 = 0.006$, $p = 0.15$) (**Figure 8**).

Having not found evidence for a relationship between the degree of SA and the changes in beta power, it was tested if there was a relationship between beta oscillations amplitude and SEPs amplitude. The two measures were measured as a general phenomenon and not as function of the group. Therefore, we investigated if beta oscillations amplitude and SEPs amplitude were correlated in two groups: healthy subjects + PD in OFF state and healthy subjects + PD in ON state.

In the first analyzed group including healthy and PD patients OFF medication, a positive correlation between beta power magnitude and SEPs amplitude was found in the rest condition in all selected time windows (background phase, $p = 0.02$, $R^2 = 0.139$; suppression phase, $p = 0.01$, $R^2 = 0.162$; rebound phase, $p = 0.00$, $R^2 = 0.220$). In other words, lower amplitude of SEPs was correlated with lower beta power amplitude.

However, this positive correlation seemed to be driven by the PD patients OFF medication. Indeed, when the two groups of participants were analyzed separately, healthy subjects did not show any correlation between beta oscillations amplitude and SEPs amplitude at rest in each time window (background phase, $p = 0.21$, $R^2 = 0.07$; suppression phase, $p = 0.16$, $R^2 = 0.09$; rebound phase, $p = 0.06$, $R^2 = 0.159$). Whereas, the PD OFF medication showed a significant correlation between the two measures at rest in all time windows (background phase, $p = 0.02$, $R^2 = 0.304$; suppression phase, $p = 0.01$, $R^2 = 0.335$; rebound phase, $p = 0.01$, $R^2 = 0.371$) (**Figure 9**).

In the movement condition the group including healthy subjects and PD OFF patients still showed a significant correlation between the two conditions in the background timing window ($p = 0.03$, $R^2 = 0.113$) and a statistical trend in the

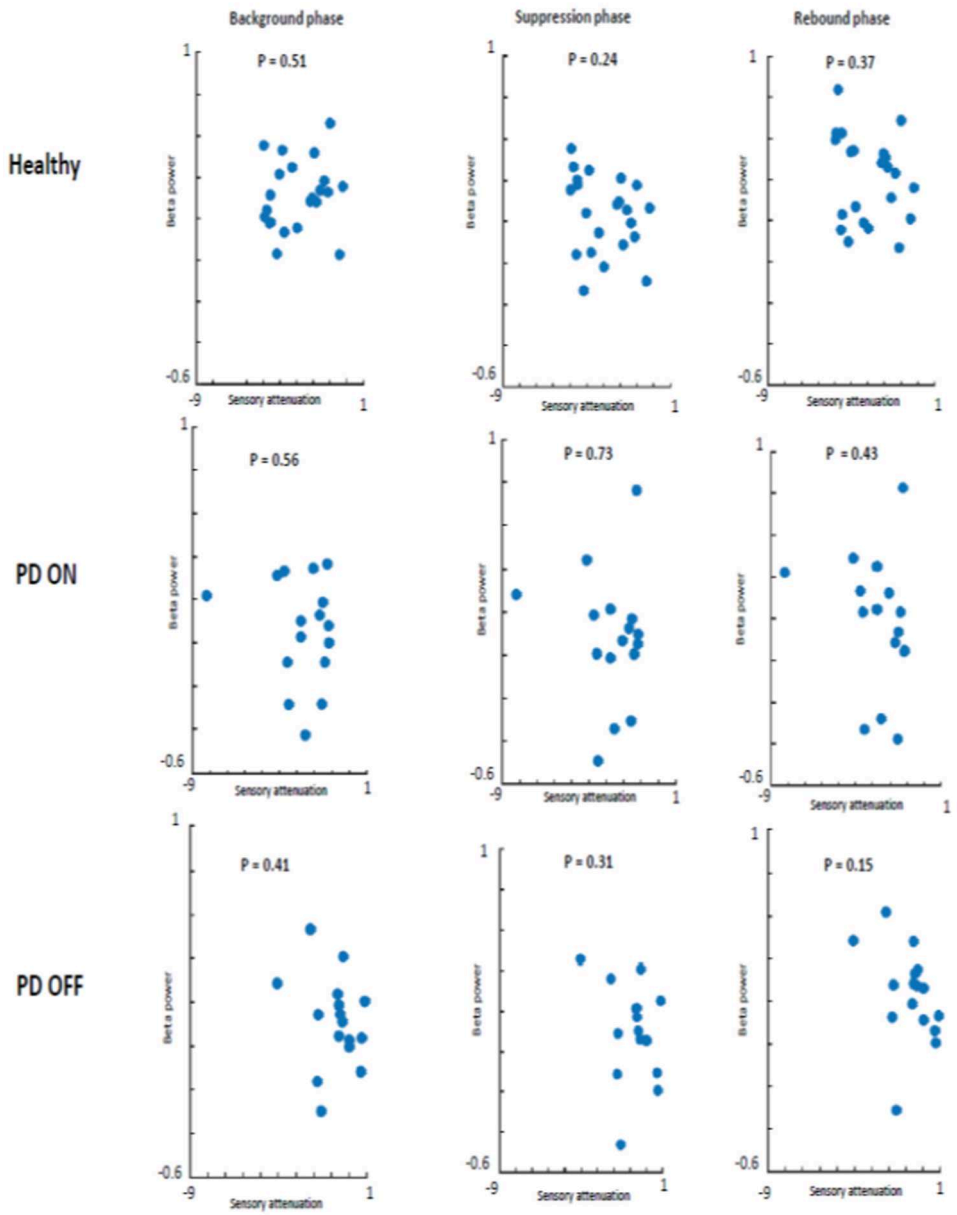

FIGURE 8 | Correlation analysis beta power modulation and sensory attenuation individually in the three groups of participants.

suppression phase ($p = 0.08$, $R^2 = 0.08$) and in the rebound phase ($p = 0.08$, $R^2 = 0.08$). Interestingly, this correlation was driven by the PD OFF patients. Indeed, when the two groups of participants were analyzed separately the significant correlation was kept only by PD OFF medication. The control group did not show any correlation in all time windows (background phase, $p = 0.41$, $R^2 = 0.03$; suppression phase, $p = 0.69$, $R^2 = 0.008$; rebound phase, $p = 0.46$, $R^2 = 0.02$), whereas PD OFF medication showed significant correlation between beta oscillations modulations and SA in the three time windows (background phase, $p = 0.01$, $R^2 = 0.363$; suppression phase, $p = 0.01$, $R^2 = 0.351$; rebound phase, $p = 0.01$, $R^2 = 0.354$).

In the second analyzed group including healthy participants and PD patients ON medication a statistical trend of the correlation between beta oscillations amplitude and SEPs amplitude was found in the first two times windows (background phase, $p = 0.09$, $R^2 = 0.07$; suppression phase, $p = 0.07$, $R^2 = 0.08$) and a significant correlation in the rebound window in the rest condition ($p = 0.01$, $R^2 = 0.144$). However, it is likely that this result was driven by the power of this bigger sample.

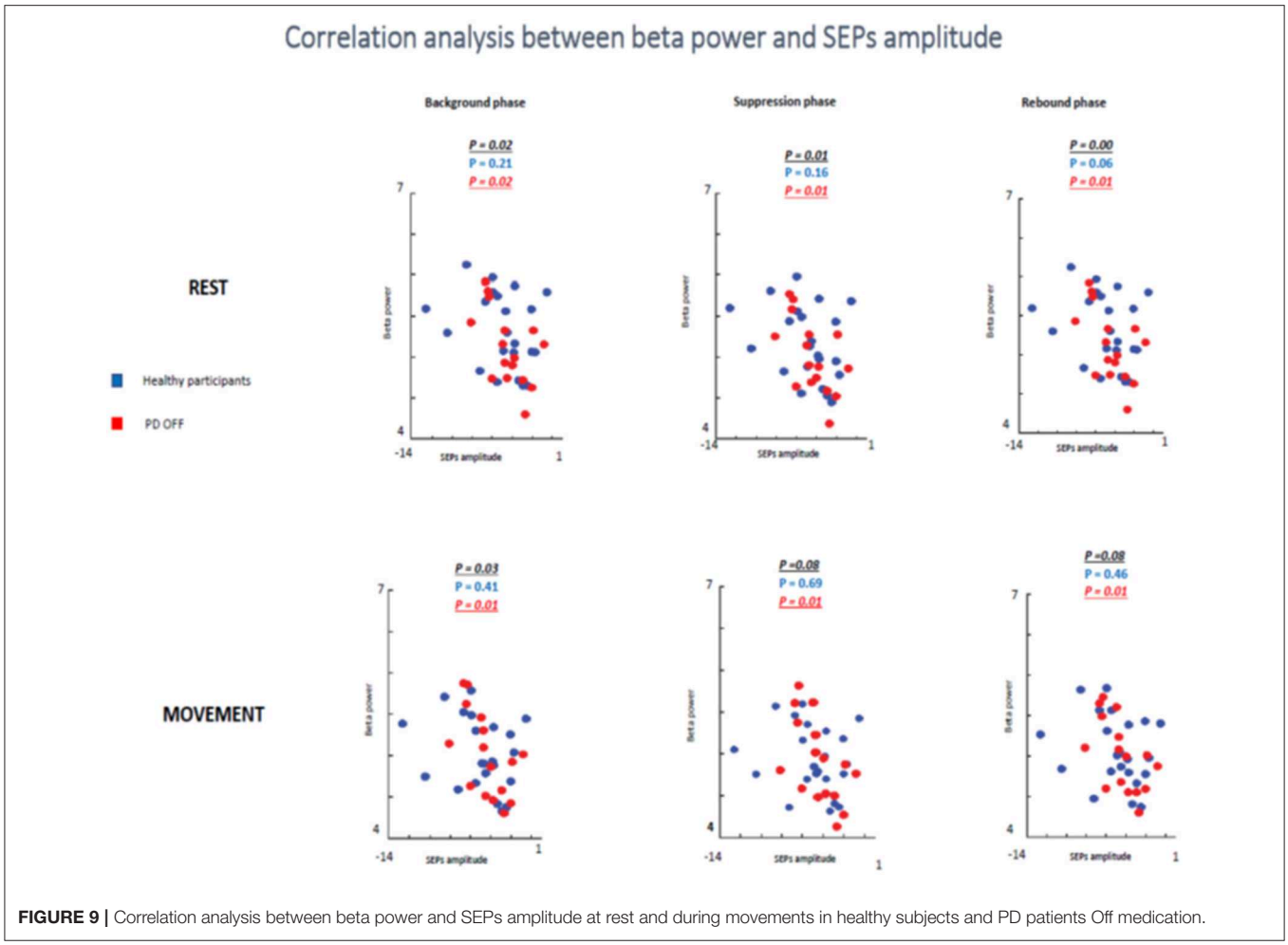

FIGURE 9 | Correlation analysis between beta power and SEPs amplitude at rest and during movements in healthy subjects and PD patients Off medication.

When the two groups of participants were analyzed separately, neither groups showed any significant correlations between the two measures in the rest condition in any time windows. Healthy subjects did not show a significant correlation in the background phase ($p = 0.21$, $R^2 = 0.07$) or in the suppression phase ($p = 0.16$, $R^2 = 0.09$). There was a statistical trend in the rebound window ($p = 0.06$, $R^2 = 0.159$). PD patients ON medication did not show significant correlation in background phase ($p = 0.62$, $R^2 = 0.08$), suppression phase ($p = 0.44$, $R^2 = 0.06$) and rebound phase ($p = 0.40$, $R^2 = 0.137$) (**Figure 10**).

In the movement condition, there was no significant correlation in all analysis (healthy participants + PD ON patients and separately healthy subjects and PD ON). The combination of healthy controls and PD patients in ON state showed the following results: background phase, $p = 0.69$, $R^2 = 0.04$; suppression phase, $p = 0.87$, $R^2 = 0.001$; rebound window in the rest condition, $p = 0.88$, $R^2 = 0.001$).

When the two groups of participants were analyzed separately, neither groups showed any significant correlations between the two measures in the rest condition in any time windows. Healthy subjects' group did not show a significant correlation in the background phase ($p = 0.41$, $R^2 = 0.034$) or in the suppression phase ($p = 0.69$, $R^2 = 0.008$). There was a statistical trend in the rebound window ($p = 0.46$, $R^2 = 0.027$). PD patients ON medication did not show significant correlation in background phase ($p = 0.62$, $R^2 = 0.017$), suppression phase ($p = 0.44$, $R^2 = 0.043$) and rebound phase ($p = 0.40$, $R^2 = 0.050$) (**Figure 10**).

These results might be explainable by the presence of SEPs attenuation in both groups at the onset of the movement. Therefore, SEPs amplitude was lower at the onset of the movement compared to the magnitude at rest but beta does not change as function of condition, therefore the correlation was not significant.

DISCUSSION

These results confirmed our previous study (8). A significant link was found between dopaminergic modulation and SA. Indeed, at movement onset PD patients off medication showed a lower SA compared to PD patients ON medication. The mean difference of the N20-P25 amplitude between rest condition and movement condition was significantly different between PD patients OFF medication and ON medication.

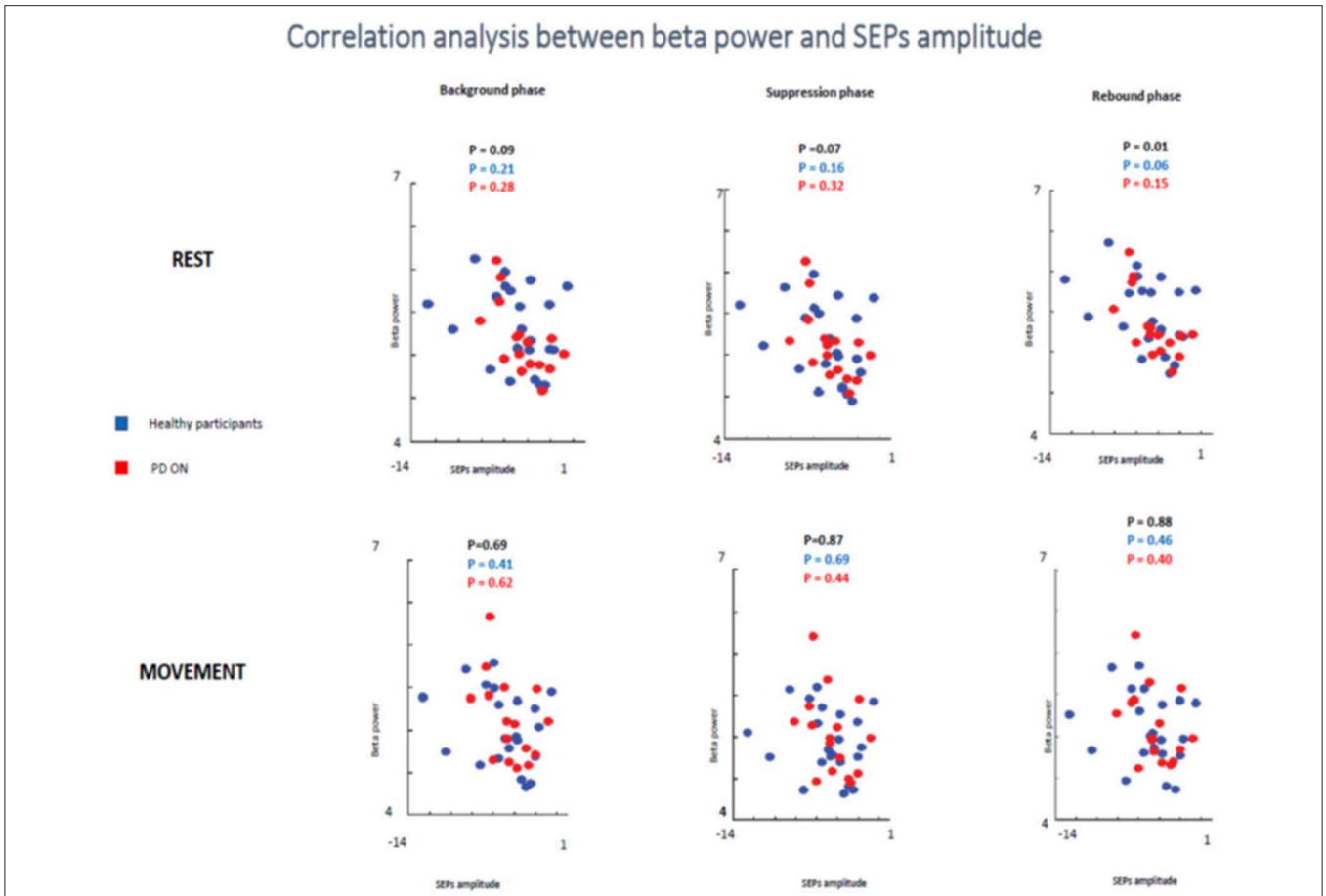

FIGURE 10 | Correlation analysis between beta power and SEPs amplitude at rest and during movements in healthy subjects and PD patients ON medication.

This result of lower SA in PD patients OFF medication is in line with previous studies that have shown abnormal SA in PD (19, 20). It is important to consider that there were critical differences in the task design. In previous studies (19, 20), patients were tested making vigorous wrist flexion and extension movements. In addition, SEPs were recorded during continuous movement. In our study, subjects performed a movement of the thumb and the median nerve stimuli was delivered at the onset of the voluntary movement. Our results supported the hypothesis that a failure in SA prior to movement onset contributes to the difficulties in movement initiation in PD.

In line with previous studies (12, 21), healthy subjects showed changes in beta oscillations as attenuated prior the voluntary movement and augmented once the movement has ended.

A potential correlation of SA with cortical beta oscillations in the cohort of PD patients and age-matched healthy subjects was hypothesized. The study was focused in understanding the functional role of beta oscillations as it is well-known that PD patients have a pathologically higher power of beta oscillations, both in the cortex (16) and sub-cortically in the subthalamic nucleus (16, 22–24). Of note, levodopa treatment (22, 23) and subthalamic deep brain stimulation for PD (22, 23, 25, 26) are associated with a decrease in beta power. On the other hand, it is well known that stimulation of the subthalamic nucleus at the beta frequency (15–30 Hz) causes a slowing of movement in patients with PD (27). Consequentially, the high amplitude of beta oscillations in PD was proposed as a cause of bradykinesia (16). However, the mechanism underlying this hypothesis is still not clear.

This study provided evidence that physiological SA could be the neurophysiological mechanism underlying the bradykinesia. Therefore, if both these mechanisms (physiological SA and high beta oscillations) have been hypothesized as underlying the bradykinesia, a correlation between these two mechanisms was proposed. Specifically, it was tested whether the modulation of SA was correlated with the modulation of beta oscillations during voluntary movements.

Our results did not show significant evidence of a modulation of cortical beta oscillations driven by the sensory-motor cortex on SA. This finding can be interpreted in two ways, either that the cortical beta oscillations are not involved in modulation of SA or that our groups' size was not enough to reach the statistical power.

Regarding the first possibility, although there is no direct evidence of a potential link between cortical beta oscillations and

SA, it is known that the beta oscillations plays important role on the modulation of motor control. In particular, it has been shown that the modulation of beta oscillations shows a particular pattern during voluntary movements (12). This modulation of beta oscillations takes place at the onset of voluntary movement, when SA is also present. Consequentially, there is a rationale to explore if the SA modulation is correlated with beta oscillations modulation over the sensorimotor cortex. On the other hand, the beta oscillations are present not only at the cortical level but also at the subcortical level as in the basal ganglia, which were not explored in this study. From the above, it was not possible to determine whether or not subcortical beta oscillations play a modulatory role on SA. In order to address this issue further, it would be necessary to investigate SA in PD patients with STN-DBS to test if there is a correlation with the abnormal beta oscillations in STN, typically seen in this group of patients.

Regarding the second possibility, it is well known that a major fault of scientific studies (including ours) is inadequate statistical power. A larger number of subjects were required to adequate power the studies because of increased variability of SA as well as cortical beta oscillations in the patient population. Although this is a major limitation for any conclusion about the mean of potential link between SA and beta oscillations in patients with PD, the fact that SA was replicated to be reduced in patients with PD OFF dopaminergic treatment is noteworthy on its own. Increased variability may have important implications in the design and interpretation of future studies and may indeed be related to pathophysiological mechanisms of PD.

The results of this study did not support the theory suggesting that the modulation of physiological SA and modulation of beta oscillations over the sensorimotor cortex are related. However, it was confirmed the modulation of the two parameters during voluntary movements. In particular, the two groups of participants showed reduced beta power just prior to and during the period of movement and transiently increased subsequent to the end of the movement. This result is in line with previous studies (28, 29). Furthermore, several studies showed evidences that beta oscillations play a role in sensorimotor processing (30–33). In this regard, Baker et al. (31) found that beta frequency showed a coherence between proprioceptive afferents (Ia muscle spindles) and forearm muscle activity, suggesting that beta oscillations may have a role mainly in proprioceptive processing. On the contrary, there was no coherence between muscle activity and afferents relate to cutaneous receptors. However, Witham et al. (33) did not find a difference in coherence with M1 between areas 1 and 3b, which are associated to cutaneous receptive fields, and areas 3a and 2, which are associated with proprioception (areas 3a and 2). Therefore, this study provided evidence for a close link between the sensory and motor systems via oscillatory synchronization and support previous hypotheses that this pattern of activity may be important in coordinating the processing of somatosensory information within its motor context (32, 33).

The current study did not confirm a role of beta pattern activity in coordinating the somatosensory integration at least in terms of SA.

This study did not show a significant different amplitude in the cortical beta oscillations between PD ON and healthy controls as well as between PD OFF and healthy controls. Therefore, these results bring under discussion the pathological role of sensorimotor beta oscillations in PD. There is a need to be a replication of the study on a larger group of PD patients to confirm these results. Additionally, further studies are needs to test a potential correlation between physiological SA and beta oscillations generated in the basal ganglia with the aim to test if modulation of SA is correlated with this other pattern of beta activity.

DATA AVAILABILITY

The raw data supporting the conclusions of this manuscript will be made available by the authors, without undue reservation, to any qualified researcher.

ETHICS STATEMENT

The study was approved by the local institutional ethics committee, which was the East of Scotland Research Ethics Service. Written informed consent was obtained from all participants.

AUTHOR CONTRIBUTIONS

AM: design of the study, collecting data, EEG analysis, statistical analysis, writing manuscript. PL, PK, TF, and ME: design of the study, reviewing of the manuscript. JK: design of the study, EEG analysis, statistical analysis, reviewing manuscript.

FUNDING

The study has been funded by the Medical Research Council (MRC) Grant (Reference No. MRC 520092).

ACKNOWLEDGMENTS

Oral presentation at third conference of the European Academy of Neurology (Amsterdam, Netherlands, June 24-27, 2017): Sensory attenuation phenomena: Is it the neurophysiological mechanism underlying modulation of beta oscillations? A. Macerollo, P. Limousin, L. Korlipara, T. Foltynie, M. Edwards, J. Kilner. European Journal of Neurology 2017. Volume 24, Supplement 1: S767.

REFERENCES

1. Voss M, Ingram JN, Haggard P, Wolpert DM. Sensorimotor attenuation by central motor command signals in the absence of movement. *Nat Neurosci*. (2006) 9:26–7. doi: 10.1038/nn1592
2. Angel RW, Malenka RC. Velocity-dependent suppression of cutaneous sensitivity during movement. *Exp Neurol*. (1982) 77:266–74. doi: 10.1016/0014-4886(82)90244-8
3. Rushton DN, Rothwell JC, Craggs MD. Gating of somatosensory evoked potentials during different kinds of movement in man. *Brain*. (1981) 104:465–91. doi: 10.1093/brain/104.3.465

4. Milne RJ, Aniss AM, Kay NE, Gandevia SC. Reduction in perceived intensity of cutaneous stimuli during movement: a quantitative study. *Exp Brain Res*. (1988) 70:569–76. doi: 10.1007/BF00247604
5. Friston KJ, Daunizeau J, Kilner J, Kiebel SJ. Action and behavior: a free-energy formulation. *Biol Cybern*. (2010) 102:227–60. doi: 10.1007/s00422-010-0364-z
6. Brown H, Adams RA, Parees I, Edwards M, Friston K. Active inference, sensory attenuation and illusions. *Cogn Process*. (2013) 14:411–27. doi: 10.1007/s10339-013-0571-3
7. Blanchard DC, Defensor EB, Meyza KZ, Pobbe RL, Pearson BL, Bolivar VJ., et al. Physiological and perceptual sensory attenuation have different underlying neurophysiological correlates. *J Neurosci*. (2016) 36:10803–12. doi: 10.1523/JNEUROSCI.1694-16.2016
8. Macerollo A, Chen JC, Korlipara P, Foltynie T, Rothwell J, Edwards MJ., et al. Dopaminergic treatment modulates sensory attenuation at the onset of the movement in Parkinson's disease: a test of a new framework for bradykinesia. *Mov Disord*. (2016) 31:143–6. doi: 10.1002/mds.26493
9. Goetz CG, Tilley BC, Shaftman SR, Stebbins GT, Fahn S, Martinez-Martin P., et al. Movement Disorder Society-sponsored revision of the Unified Parkinson's Disease Rating Scale (MDS-UPDRS): scale presentation and clinimetric testing results. *Mov Disord*. (2008) 23:2129–70. doi: 10.1002/mds.22340
10. Adams RA, Shipp S, Friston KJ. Predictions not commands: active inference in the motor system. *Brain Struct Funct*. (2013) 218:611–43. doi: 10.1007/s00429-012-0475-5
11. Gastaut H. Electrocorticographic study of the reactivity of rolandic rhythm. *Rev Neurol*. (1952) 87:176–82.
12. Pfurtscheller G. Lopes da Silva FH. Event-related EEG/MEG synchronization and desynchronization: basic principles. *Clin Neurophysiol*. (1999) 110:1842–57. doi: 10.1016/S1388-2457(99)00141-8
13. Blanchard DC, Defensor EB, Meyza KZ, Pobbe RL, Pearson BL, Bolivar VJ., et al. Post-movement beta activity in sensorimotor cortex indexes confidence in the estimations from internal models. *J Neurosci*. (2016) 36:1516–28. doi: 10.1523/JNEUROSCI.3204-15.2016
14. Kording KP, Wolpert DM. Bayesian integration in sensorimotor learning. *Nature*. (2004) 427:244–7. doi: 10.1038/nature02169
15. Palmer C, Zapparoli L, Kilner JM. A new framework to explain sensorimotor beta oscillations. *Trends Cogn Sci*. (2016) 20:321–3. doi: 10.1016/j.tics.2016.03.007
16. Little S, Brown P. The functional role of beta oscillations in Parkinson's disease. *Parkinsonism Relat Disord*. (2014) 20(Suppl. 1):S44–8. doi: 10.1016/S1353-8020(13)70013-0
17. Macerollo A, Chen JC, Parees I, Sadnicka A, Kassavetis P, Bhatia KP., et al. Abnormal movement-related suppression of sensory evoked potentials in upper limb dystonia. *Eur J Neurol*. (2016) 23:562–8. doi: 10.1111/ene.12890
18. Hughes AJ, Daniel SE, Kilford L, Lees AJ. Accuracy of clinical diagnosis of idiopathic Parkinson's disease: a clinico-pathological study of 100 cases. *J Neurol Neurosurg Psychiatry*. (1992) 55:181–4. doi: 10.1136/jnnp.55.3.181
19. Cheron G, Piette T, Thiriaux A, Jacquy J, Godaux E. Somatosensory evoked potentials at rest and during movement in Parkinson's disease: evidence for a specific apomorphine effect on the frontal N30 wave. *Electroencephalogr Clin Neurophysiol*. (1994) 92:491–501. doi: 10.1016/0168-5597(94)90133-3
20. Insola A, Le Pera D, Restuccia D, Mazzone P, Valeriani M. Reduction in amplitude of the subcortical low- and high-frequency somatosensory evoked potentials during voluntary movement: an intracerebral recording study. *Clin Neurophysiol*. (2004) 115:104–11. doi: 10.1016/j.clinph.2003.08.003
21. Pfurtscheller G, Stancak A Jr, Edlinger G. On the existence of different types of central beta rhythms below 30 Hz. *Electroencephalogr Clin Neurophysiol*. (1997) 102:316–25. doi: 10.1016/S0013-4694(96)96612-2
22. Giannicola G, Marceglia S, Rossi L, Mrakic-Sposta S, Rampini P, Tamma F., et al. The effects of levodopa and ongoing deep brain stimulation on subthalamic beta oscillations in Parkinson's disease. *Exp Neurol*. (2010) 226:120–7. doi: 10.1016/j.expneurol.2010.08.011
23. Jenkinson N, Brown P. New insights into the relationship between dopamine, beta oscillations and motor function. *Trends Neurosci*. (2011) 34:611–8. doi: 10.1016/j.tins.2011.09.003
24. Moran RJ, Mallet N, Litvak V, Dolan RJ, Magill PJ, Friston KJ., et al. Alterations in brain connectivity underlying beta oscillations in Parkinsonism. *PLoS Comput Biol*. (2011) 7:e1002124. doi: 10.1371/journal.pcbi.1002124
25. Selber P, Kerr Graham H, Gage J. Does suppression of oscillatory synchronisation mediate some of the therapeutic effects of DBS in patients with Parkinson's disease? *Front Integr Neurosci*. (2012) 6:47. doi: 10.3389/fnint.2012.00047
26. Kühn AA, Kempf F, Brücke C, Gaynor Doyle L, Martinez-Torres I, Pogosyan A., et al. High-frequency stimulation of the subthalamic nucleus suppresses oscillatory beta activity in patients with Parkinson's disease in parallel with improvement in motor performance. *J Neurosci*. (2008) 28:6165–73. doi: 10.1523/JNEUROSCI.0282-08.2008
27. Eusebio A, Chen CC, Lu CS, Lee ST, Tsai CH, Limousin P., et al. Effects of low-frequency stimulation of the subthalamic nucleus on movement in Parkinson's disease. *Exp Neurol*. (2008) 209:125–30. doi: 10.1016/j.expneurol.2007.09.007
28. Baker SN, Kilner JM, Pinches EM, Lemon RN. The role of synchrony and oscillations in the motor output. *Exp Brain Res*. (1999) 128:109–17. doi: 10.1007/s002210050825
29. Baker SN, Olivier E, Lemon RN. Coherent oscillations in monkey motor cortex and hand muscle EMG show task-dependent modulation. *J Physiol*. (1997) 501(Pt 1):225–41. doi: 10.1111/j.1469-7793.1997.225bo.x
30. Baker SN. Oscillatory interactions between sensorimotor cortex and the periphery. *Curr Opin Neurobiol*. (2007) 17:649–55. doi: 10.1016/j.conb.2008.01.007
31. Baker SN, Chiu M, Fetz EE. Afferent encoding of central oscillations in the monkey arm. *J Neurophysiol*. (2006) 95:3904–10. doi: 10.1152/jn.01106.2005
32. Riddle CN, Baker SN. Manipulation of peripheral neural feedback loops alters human corticomuscular coherence. *J Physiol*. (2005) 566(Pt 2):625–39. doi: 10.1113/jphysiol.2005.089607
33. Witham CL, Baker SN. Network oscillations and intrinsic spiking rhythmicity do not covary in monkey sensorimotor areas. *J Physiol*. (2007) 580(Pt.3):801–14. doi: 10.1113/jphysiol.2006.124503

Conflict of Interest Statement: The authors declare that the research was conducted in the absence of any commercial or financial relationships that could be construed as a potential conflict of interest.

frontiers in Systems Neuroscience

REVIEW
published: 30 October 2019
doi: 10.3389/fnsys.2019.00061

The Cortico-Basal Ganglia-Cerebellar Network: Past, Present and Future Perspectives

Demetrio Milardi[1,2†], Angelo Quartarone[1†], Alessia Bramanti[2], Giuseppe Anastasi[1], Salvatore Bertino[1], Gianpaolo Antonio Basile[1], Piero Buonasera[2], Giorgia Pilone[2], Giuseppe Celeste[3], Giuseppina Rizzo[1], Daniele Bruschetta[1] and Alberto Cacciola[1*]*

[1]Department of Biomedical, Dental Sciences and Morphological and Functional Images, University of Messina, Messina, Italy, [2]IRCCS Centro Neurolesi "Bonino Pulejo", Messina, Italy, [3]I.S.A.S.I.E. Caianello, National Research Council, Messina, Italy

Much of our present understanding of the function and operation of the basal ganglia rests on models of anatomical connectivity derived from tract-tracing approaches in rodents and primates. However, the last years have been characterized by promising step forwards in the *in vivo* investigation and comprehension of brain connectivity in humans. The aim of this review is to revise the current knowledge on basal ganglia circuits, highlighting similarities and differences across species, in order to widen the current perspective on the intricate model of the basal ganglia system. This will allow us to explore the implications of additional direct pathways running from cortex to basal ganglia and between basal ganglia and cerebellum recently described in animals and humans.

Keywords: cerebellum, connectomics, globus pallidus, substantia nigra, tractography

OPEN ACCESS

Edited by:
Preston E. Garraghty, Indiana University Bloomington, United States

Reviewed by:
Martin Bares, Masaryk University, Czechia
Ellen J. Hess, Emory University, United States
Kate Roman, Emory University, Unites States, in collaboration with reviewer EH

***Correspondence:**
Angelo Quartarone
aquartar65@gmail.com
Alberto Cacciola
alberto.cacciola0@gmail.com

†These authors have contributed equally to this work

Received: *23 April 2019*
Accepted: *08 October 2019*
Published: *30 October 2019*

Citation:
Milardi D, Quartarone A, Bramanti A, Anastasi G, Bertino, S, Basile GA, Buonasera P, Pilone G, Celeste G, Rizzo G, Bruschetta D and Cacciola A (2019) The Cortico-Basal Ganglia-Cerebellar Network: Past, Present and Future Perspectives. Front. Syst. Neurosci. 13:61. doi: 10.3389/fnsys.2019.00061

INTRODUCTION

The brain is a complex network consisting of a huge number of neurons ($\sim 10^{11}$) segregated in spatial regions with similar cytoarchitecture and functional features. Identifying anatomical physical pathways between the various structures of the brain has always been a major challenge in neuroscience. Neuronal connectivity patterns can be investigated at different levels of scale: (i) the microscale allows to study single synaptic connections linking two or more individual neuronal cells, providing a detailed anatomical description of the basic substrates of the cerebral microcircuits; (ii) at the mesoscale level, where brain connectivity is investigated at the level of columns and mini-columns; and (iii) at macroscale level that explore large-scale anatomical connectivity patterns focusing on the inter-regional white matter pathways connecting distinct neuronal populations (Sporns, 2011).

The current knowledge about the short-, medium- and long-range neuroanatomical connections of the basal ganglia system comes from both invasive and non-invasive experimental techniques applied respectively in animals and humans.

The basal ganglia are a group of subcortical nuclei which integrate information from widespread cortical areas and in turn project their outputs back to the cerebral cortex (Alexander et al., 1990). Considering their pivotal role in motor and non-motor functions, the basal ganglia have been a main topic of interest in the field of basic and clinical neurosciences. Basal ganglia

connections have been widely studied and different models of basal ganglia circuitry have undergone major revisions during the last decades (Nelson and Kreitzer, 2014).

The present review aims at providing a comprehensive overview on the interactions between the cerebral cortex, the basal ganglia and the cerebellum in order to better understand how such interplay contributes to specific attributes of motor and non-motor behavior and to the pathophysiology of basal ganglia disorders.

We will first discuss the most common invasive and non-invasive techniques to study brain connectivity respectively in animals and humans. We will then review the traditional models of basal ganglia anatomy and circuitry highlighting similarities and differences across species. Finally, we will widen the current perspective on basal ganglia connectomics providing a new challenging, comprehensive and integrated cortico-basal ganglia-cerebellum model.

HISTORY OF BASAL GANGLIA CONCEPT

The presence of structures at the basis of the human brain had already raised the attention of many scientist from the antiquity to the 19th century; early anatomical depictions of the basal ganglia appear in the works of classical anatomists such as Galenus or Vesalius; the use of the term "corpus striatum," to refer to the large subcortical masses located nearby the cerebral ventricles, is attested early in Thomas Willis *"Cerebri Anatome"* (1664) (Parent, 2017). Most of the actual nomenclature used to describe basal ganglia structures comes from authors of late 18th and early 19th century; in particular, terms such as "globus pallidus," "external capsule," "internal capsule," "lenticular nucleus" are introduced in the classical treatise of Karl Friedrich Burdach (Parent, 2013). In the same period, structures such as the substantia nigra and the subthalamic nucleus (Luys, 1868) were described. The term *Basal Ganglia* has been originally proposed by Sir David Ferrier in a highly challenging and comprehensive masterpiece of the 19th century on the yet unraveled brain structure and function, "The functions of the brain" (1887). In this treatise, Ferrier writes that "the basal ganglia—the *corpora striata* and *optic thalami*—are ganglionic masses, intercalated in the course of the projection system of fibers which connect the cortex with the *crura cerebri*, and through these with the periphery. The corpora striata are the "ganglia of interruption" of the projection system of the foot or basis of the crus, an anatomical indication of their motor signification" (Ferrier, 1887).

After that, a wide corpus of research has been focused on basal ganglia structure and function both in health and in disease. The last half of the 20th century has seen the rise of neuroanatomical tracing techniques, that allowed for a complete description of basal ganglia anatomy and connectivity in different animal species. In the last 20 years, these techniques have been paralleled by neuroimaging techniques focused at reconstructing white matter anatomy of the human brain. An overview of strengths and limitations of such techniques will be provided below.

INVASIVE AND NON-INVASIVE APPROACHES TO STUDY ANATOMICAL CONNECTIVITY

Traditional Anterograde and Retrograde Tract Tracing

Despite several efforts have been made to study brain and basal ganglia functional anatomy, the most recent breakthroughs occurred with the development of various powerful neuronographic methods, introduced in late 20th century, which have allowed to describe the close interrelation between the core structures of the basal ganglia and to set the ground basements of the current ideas on the basal ganglia circuits.

Degeneration and tract-tracing approaches are among the most common methods applied in animal studies. Highly localized lesions, leading to Wallerian degeneration, combined with stains that selectively color degenerating neuronal cell bodies and axons have been helpful in the past to trace neural pathways (Johnson, 1961; Afifi et al., 1974). However, degeneration techniques are limited by the low accuracy to determine the exact location of axonal terminals and by the fact that not all the neurons show marked degeneration after a lesion. Taking into account such limitations, the second half of the 20th century has been characterized by a methodological innovation based on the axonal transport of tracers. Anterograde tract-tracing allows to identify the axons terminations by injecting chemical tracers and dyes which are incorporated into macromolecules by the neuronal cell bodies and then carried to the end of the axons. Another widely used tract-tracing strategy is retrograde tracing: a molecular marker (i.e., horseradish peroxidase enzyme) injected into the area of axonal terminations is carried *via* the retrograde axonal transport towards the cell body thus revealing the origin of the neuronal pathway (Köbbert et al., 2000; Raju and Smith, 2006; Schofield, 2008). Regardless of the transport direction, time must be considered to allow the tracer reaching its destination and then to proceed with tracer detection using fluorescent light or immunohistochemistry. Although the astonishing findings revealed by experimental tract-tracing in animals, this technique did not have successful application in the post-mortem human brain due to slow rate of diffusion (Beach and McGeer, 1987; Haber, 1988). In addition, both anterograde and retrograde tract-tracing are prone to limitations, considering different potential sources of false-positive and false-negative results. As a matter of fact, it is possible that tracer injections may spread beyond the target or involve adjacent pathways; also, it is possible that retrograde tracers are uptaken by fibers of passage, producing false-positive results (Reiner et al., 2000; Van Haeften and Wouterlood, 2000). Furthermore, when using biotinylated dextran amine (BDA) for anterograde tracing care should be taken due to the possible retrograde trafficking and the subsequent anterograde transport into neuronal collaterals (Reiner et al., 2000).

On the other hand, false-negative findings may derive considering the inability to label all neurons in a population in any given study. Another potential source of false-negative

findings is that it might not be possible to identify the colocalization of markers especially when the neuronal structures are tiny, due to either imperfect antibody penetration or disproportional concentration of antigens (Reiner et al., 2000; Van Haeften and Wouterlood, 2000). Despite the outstanding historical importance of tract-tracing and its actual advantages, these limitations led to the development of new, more precise tracing methods.

Neuronal Tracing by Neurotropic Viruses

Beyond conventional tracers, neurotropic viruses have the great potential to exploit the connectivity of neural circuits; viral replication amplifies the signal at each step of the process; moreover, viral tracers are able to traverse multisynaptic pathways. These features allow a more precise individuation of anatomical connections and to distinguish between direct and indirect projections. Albeit several neurotropic viruses exist, only two major classes, the herpes and rabies viruses, have been traditionally employed to experimentally track neuronal pathways. While such classes of viruses are substantially different, they do share an envelope structure and the ability to infect neurons and to spread along the nervous system. Ugolini et al. (1987) demonstrated for the first time ever that the herpes simplex virus type 1 (HSV 1) could be used to trace neural connections across at least two synapses in rodents, thus paving the way for further development of virus tracing in non-human primates (Hoover and Strick, 1993; Middleton and Strick, 1994). As major limitations, HSV 1 induces rapid neuronal degeneration and may spuriously spread to glial and other neuronal cells. As a consequence, attempts to limit the local spread do not allow to trace further than second-order neurons (Kaplitt and Loewy, 1995). By contrast, rabies viruses do not induce neuronal degeneration and are able to detect neuronal connections across an unlimited number of synapses (Ugolini, 2011). However, major drawbacks in using viruses to label multisynaptic connections are the low speed of the viral transport, paralleled by their fast-lethal effects on the experimental animal, that dies for the infection after a short time. Consequently, and considering that at least 2 days are needed to label first-order neurons, higher-order neurons are labeled only after 12 h or more from that time (Aston-Jones and Card, 2000). Therefore, tracking a neuronal network consisting of, e.g., seven synapses, could take approximately up to 1 week.

However, despite all the above-mentioned limitations virus transneuronal tracing still remains the gold standard approach to map axonal connections in animals. On the other hand, the application of such invasive tracking methods is elusive when applied to the human brain.

Non-invasive Neuroimaging Approaches for the Human Brain

The great success of neuroanatomical tracing has boosted the research on neuronal connectivity based on animal models. However, translating such findings from animals to the human brain posits some non-negligible theoretical issues: it forces the assumption that brain structures of interest are relatively conserved in the human brain, and it does not account for inter-specific differences. During the last decades, the progress of magnetic resonance imaging (MRI) has allowed the development of neuroimaging approaches as an alternative modality to assess morphological neuronal connectivity patterns in living humans. Diffusion-weighted magnetic resonance imaging (DWI) and tractography have been successfully employed to model and infer white matter bundles' trajectory of white matter bundles together with their microstructural properties (Milardi et al., 2016b, 2017; Cacciola et al., 2017a,c; Calamuneri et al., 2018; Rizzo et al., 2018; Arrigo et al., 2019). Despite these techniques have lower spatial resolution than chemical and virus tract-tracing and they are not able to estimate the directionality of neural pathways, they do provide the only chance to explore anatomical connectivity *in vivo* and non-invasively in the human brain (Chung et al., 2011).

DWI allows to measure water molecules diffusion along different directions. Considering the impermeable nature of axons, water diffusivity is highly directional (anisotropic) being constrained to the main axonal direction; therefore DWI indirectly evaluates white matter microstructure (Basser et al., 1994, 2000). Assuming that such local diffusion is explained by a three-dimensional Gaussian process, the main axis of the diffusion ellipsoid corresponds to principal diffusion direction and its fractional anisotropy corresponds to the degree to which diffusion is preferred along this direction over other directions. Therefore, by computing the principal local diffusion direction within the single voxels and attempting to infer specific spatial axonal trajectories, tractography can be used to map and reconstruct main fiber bundles at a system level (Alexander et al., 2007). Classical diffusion-weighted images used for tractographic reconstruction usually have a voxel resolution of $2 \times 2 \times 2$ mm^3 which is notably higher than the axonal diameter (Jbabdi and Johansen-Berg, 2011), whilst traditional anatomical tracers can track the projections of single axons. Another major drawback of tractography is the inability to determine the polarity of a given connection and thus to establish whether a given fiber pathway is afferent or efferent (Parker et al., 2013).

In addition, simple diffusion signal modeling approaches cannot reliably disentangle the complex white matter architecture consisting of twisting, bending, crossing and kissing fibers thus failing in representing any of their orientations. To overcome this issue, "model-free" approaches have been developed in the last decade, such as Diffusion Spectrum Imaging (DSI; Wedeen et al., 2005), Q-ball Imaging (Tuch et al., 2003) and Constrained Spherical Deconvolution (Tournier et al., 2007).

Despite the above-mentioned limitations, DWI and tractography are the only existing techniques able to investigate anatomical connectivity in the human brain *in vivo* and non-invasively. Indeed diffusion tractography has been extensively recognized as the first "*in vivo* dissection" approach to map the major fiber bundles in the human brain with extreme precision as well as to show the existence of new associative pathways that have been subsequently replicated using the traditional post-mortem Klingler dissection (Klingler, 1935; Klingler and Gloor, 1960). For instance, the increasing use of tractography has boosted our understanding of the morphological shape

of the major long-range white matter pathways (Catani et al., 2005; Parker et al., 2005; Yagmurlu et al., 2016), consequently confirmed by post-mortem dissection in the human brain (Lawes et al., 2008; Yagmurlu et al., 2016). Last but not least, tractography has allowed to develop several atlas of the human brain (Mori and van Zijl, 2007; Oishi, 2011; Catani and Thiebaut de Schotten, 2012). As a final remark, the anatomical validity and reproducibility of DWI tractography have been assessed *in vitro* in a highly gyrated model of the porcin brain, demonstrating that tractography is able to reliably detect specific white matter pathways and therefore to be a powerful tool in investigating anatomical brain connectivity (Dyrby et al., 2007).

INTER-SPECIES COMMONALITIES AND DIFFERENCES IN THE BASAL GANGLIA NETWORK

Despite the basic basal ganglia anatomy and connectivity are well preserved across most species, from rodents to non-human and human primates (Reiner et al., 1998; Stephenson-Jones et al., 2012), some meaningful interspecific topographical and functional variations need to be carefully addressed. The basal ganglia have been observed in all amniote species; the basic organization of these telencephalic nuclei seems to be phylogenetically conserved, since evidences of a remarkable similarity between lampreys, the oldest now-living vertebrates, and mammals have been carefully described (Grillner and Robertson, 2016). This supported the view according to which rudimentary basal ganglia were already present in the vertebrate's common ancestor.

In mammals, the basal ganglia demonstrate a much more extensive interaction with the cerebral cortex (Reiner et al., 1998). Furthermore, the basal ganglia seem to maintain the same circuit organization, namely the presence of input nuclei, output nuclei and modulatory stations through which information is funneled and processed (Gerfen et al., 1987a,b; Smith and Parent, 1988; Alexander et al., 1990). Indeed, several neuroanatomical and neurophysiological insights gained studying rodents have been lately confirmed in primates. However, some remarkable differences both in the macroscopic and microscopic anatomy need to be addressed.

From the gross anatomy perspective, the striatum could be divided into a dorsal and a ventral compartment; these two divisions lack of a clear boundary but greatly differ in their connectivity profiles (Haber and Knutson, 2010). In rodents, the dorsal striatum is named neostriatum and it could be divided into a dorsomedial and a dorsolateral part, whilst in monkeys and humans it is divided into caudate nucleus and putamen (Grillner and Robertson, 2016). Structural separation of the striatum into caudate nucleus and putamen by the internal capsule in primates does provide a clear functional distinct segregation of the cortical inputs to these two main structures. Although the caudate nucleus is traditionally associated with cognitive functions and the putamen with motor functions, both structures receive widespread afferents from the cerebral cortex, see Haber (2016) for an extensive review. Rodents, instead, lack of such structural separation within the dorsal striatum.

In parallel, the same considerations could be made for the difference in the Globus Pallidus (GP) gross anatomy between rodents and primates. Both in human and non-human primates, the internal (GPi) and external (GPe) segments of the GP are structurally divided by the internal lamina and are placed close to each other. On the other hand, in rodents, the GPi functional homologous, termed entopeduncular nucleus, is mostly embedded in the internal capsule (Carter and Fibiger, 1978) whilst the GPe homolog is termed simply as GP.

Moreover, a striking difference between primates and rodents is represented by the cerebral cortex, which constitutes one of the main interacting systems with the basal ganglia. In primates, the need for more complex motor tasks and sensory integration has allowed the development of large and architecturally complex association areas (Preuss and Goldman-Rakic, 1989, 1991). According to recent works, this difference would make the old world monkeys the most valuable animal model to study function and disease of the basal ganglia (Smith and Galvan, 2018).

A main difference is that in rodents, cortico-spinal pyramidal neurons directly synapse on the striatum; in primates, on the other hand, cortico-spinal and cortico-striatal descending systems are totally segregated (Parent and Parent, 2006; Kita and Kita, 2012; Smith et al., 2014).

Moreover, differences in volume, distribution and number of neurons of the basal ganglia among mammals have been described, underlining substantial differences between rats and non-human primates and subtle variations between humans and monkeys (Hardman et al., 2002).

Despite such morphological differences, the organization of the main afferent and efferent systems of the basal ganglia network is almost similar across species. With some limitations, and paying attention to inter-species differences, rodents still constitute a valuable model to study basal ganglia in physiology and disease (Hooks et al., 2018; Miyamoto et al., 2019).

TRADITIONAL CIRCUITS OF THE BASAL GANGLIA NETWORK

The most basic circuit model of basal ganglia function involving the "direct" and "indirect" pathways has been originally proposed by Albin et al. (1989) and it has represented the cornerstone of our knowledge on basal ganglia function for two decades (**Figure 1**). More recently, DeLong and Wichmann (2007) have suggested that the output nuclei—the GPi and the SNr—exert a tonic firing to the intralaminar and ventral motor nuclei of the thalamus which in turn regulate motor-related areas in the cerebral cortex (DeLong and Wichmann, 2007) influencing desired and unwanted behaviors.

A third fundamental pathway, the so-called "hyperdirect pathway" of the basal ganglia circuitry has been recently identified. Although the subthalamic nucleus (STN) has been considered for many decades one of the relevant nodes of the "indirect" pathway, it also receives direct signals from the cerebral cortex (Nambu et al., 2000).

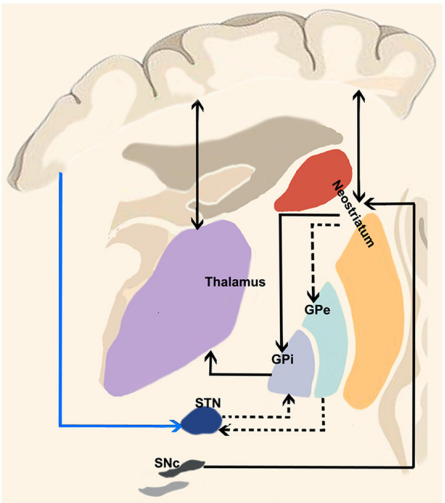

FIGURE 1 | "Classical" cortico-basal ganglia-cerebellar pathways. The most basic circuit model of basal ganglia function involving the "direct" and "indirect" pathways originally proposed by Albin et al. (1989). Red lines highlight the "direct" pathway funneling information from the cerebral cortex to the striatum and then to internal segment of the globus pallidus/pars reticulata of the substantia nigra (GPi/SNr) *via* GABAergic inhibitory projections thus selectively reducing GPi/SNr activity and releasing the thalamocortical circuits involved in motor pattern generators. The dotted black lines depict the "indirect" pathway: when excited by the glutamatergic inputs of the cerebral cortex, striatal medium spiny neurons (expressing D2 receptors) allow the cells of the striatal matrix to send inhibitory signals to the GPe, thus exerting its tonic GABAergic inhibition on the subthalamic nucleus (STN). Therefore, the glutamatergic neurons of the STN can excite the GPi/SNr thus suppressing thalamic activity on the cerebral cortex and increasing inhibitory influences on the upper motor neurons. More recently, a "hyperdirect" pathway has been described (blue line between the cerebral cortex and STN), conveying excitatory stimuli from motor, associative and limbic brain areas on the STN, bypassing the "indirect" inhibitor circuit and leading to excited GPi/SNr activity.

When a given motor pattern is computed by cortical motor areas, it is first conveyed to the basal ganglia *via* glutamatergic projections with the purpose of releasing the intended movement and suppressing the unintended ones. The "direct" pathway funnels information from the striatum to internal segment of the globus pallidus/pars reticulata of the substantia nigra (GPi/SNr) *via* GABAergic inhibitory projections thus selectively reducing GPi/SNr activity and releasing firing from thalamocortical neurons.

Along with the initial signal to the striatum, the cerebral cortex suppresses surrounding or competing motor patterns. This activity is known to be mediated by the "indirect" and "hyperdirect" pathways. When excited by the glutamatergic inputs of the cerebral cortex, striatal D2 receptors allow the cells of the striatal matrix to send inhibitory signals to the GPe which normally exerts a tonic GABAergic inhibition on the STN. Therefore, the glutamatergic neurons of the STN can then excite the GPi/SNr thus suppressing thalamic activity on the cerebral cortex and increasing inhibitory influences on the upper motor neurons (DeLong and Wichmann, 2007, 2009; Stinear et al., 2009; Noorani and Carpenter, 2014). Moreover, the glutamatergic "hyperdirect" pathway, conveying excitatory stimuli from motor, associative and limbic brain areas on the STN (Nambu et al., 2002) triggers GPi/SNr activity (**Figure 1**) bypassing the indirect pathway. This latter view is supported by the fact that cortical neurons projecting to GPe appear to be in a different group than those projecting to STN (Kita and Kita, 2012). The following inhibition of the thalamocortical projections suggests therefore a major role of the hyperdirect pathway in holding back movements (Wessel et al., 2016).

NEUROPHYSIOLOGICAL INSIGHTS ON BASAL GANGLIA FUNCTION

A possible electrophysiological correlate of basal ganglia activity in the human brain is the Bereitschaft potential, also known as readiness potential (RP), a slow negative electroencephalographic (EEG) activity that usually precedes self-paced movements (Shibasaki and Hallett, 2006). The RP has been initially considered as an electrical phenomenon originating from cortical activity which occurs before both simple and complex motor tasks (Rektor et al., 1994, 1998, 2001a). However different evidences suggest that RP may be recorded also from subcortical structures such as striatum and thalamic nuclei (ventral intermediate nucleus VIM, ventroposterior nucleus VP; Rektor et al., 2001c). In particular, latencies of RP recorded in the putamen precedes those recorded by electrodes implanted in cortical motor areas (Rektor et al., 2001a). Following investigations conducted on patients implanted in caudate nucleus, putamen and GPi demonstrated that these regions are potential substrates for RP generation (Rektor et al., 2001b); this is in line with previous evidences of disrupted RPs after lesions in the basal ganglia (Dick et al., 1989) and suggests that cortico-basal ganglia-thalamo-cortical reverberating circuits may be involved in the generation of RP. Moreover, a P3-like activity has been recorded in basal ganglia and in cortical motor and premotor areas during a multimodal evoked related potential (ERP) stimulation paradigm aimed at investigating electrical activity related to cognitive processing of sensorial stimuli (Rektor et al., 2003). This suggests a possible interplay of cortical areas and basal ganglia during cognitive processing.

BEYOND THE DIRECT, INDIRECT AND HYPERDIRECT PATHWAYS

One of the main aims of the present review is to widen the current perspective on basal ganglia connectomics providing a new challenging, comprehensive and integrated basal ganglia model. As previously mentioned, most of our knowledge on the basal ganglia is mainly based on invasive tract-tracing studies conducted on animals, whilst the available data on humans come from clinical evidences of patients with movement disorders and from pioneering neuroimaging studies.

The last 10 years have been characterized by the growing idea that, in addition to the direct, indirect and hyperdirect pathways, several other feedback and reverberating circuits can contribute to modulate basal ganglia output. Numerous studies have indeed pointed out that the basal ganglia directly integrate signals from

widespread cortical areas and are part of an extensive network involving also the cerebellum (**Figure 2**).

The Cortico-Pallidal Pathway

In a traditional textbook of anatomy, the French anatomist Testut remarked that "Ascending and descending cortico-caudatal, cortico-putaminal, and cortico-pallidal connections do exist. Cortico-caudatal and cortico-putaminal fibers are indicated together as cortico-striatal pathway: they are less than cortico-pallidal fibers. The cortico-pallidal fibers are prevalently but not exclusively cortico-fugal (efferent). These fibers (demonstrated both by anatomic dissection and by neuronography), originate from area 6" (Testut and Latarjet, 1971). Over the subsequent decades, the cortico-pallidal fibers almost disappeared from the literature. Early degeneration studies have described the possible existence of a direct cortico-pallidal projection in monkeys (Leichnetz and Astruc, 1977), leaving an open window to provide more conclusive evidences on the topic. By using BDA anterograde tract-tracing in rodents, Naito and Kita (1994) showed for the first time the existence of direct, topographically-organized connections between the medial and lateral precentral cortices and the GPe (Naito and Kita, 1994). Although it could be argued that these projections could represent passing fibers (that it is well known to be massively present in the GP), it is worthy to note that the BDA approach used in the study labeled with great precision fine fibers and boutons thus allowing to disentangle them from pallidal passing fibers. The existence of such fibers of passage could furthermore explain why retrograde tract-tracing techniques are not able to the show the presence of this cortico-pallidal pathway. Supporting evidences for the existence of such direct pattern of connectivity come from recent studies showing cholinergic and GABAergic neurons within the GPe that in turn send direct signals to the cerebral cortex (Chen et al., 2015; Saunders et al., 2015).

More recently, evidence supporting the likely existence of a direct cortico-pallidal pathway was provided by Milardi et al. (2015) using CSD-based tractography, thus being the first to characterize the cortico-pallidal connectivity patterns in the living human brain. More recently, Cacciola et al. (2017b) provided a quantitative connectomic analysis revealing that the pallidal network mainly involves the sensorimotor areas (i.e., precentral and postcentral gyri), the superior frontal and paracentral gyri, with less representative widespread connectivity patterns with other important cortical areas (Cacciola et al., 2017b). These findings have been further corroborated by other diffusion tractography studies (da Silva et al., 2017; Grewal et al., 2018; Middlebrooks et al., 2018; Cacciola et al., 2019).

Indirect evidences supporting a tight interplay between GP and frontal cortex in humans come also from PET studies in patients with focal lesions of the GP which have demonstrated reduced metabolism in frontal cortical areas as well as psychiatric symptoms reminiscent of patients with frontotemporal lobe damage. Taken together these findings strongly indicate a disrupted functional interaction between the GP and the frontal lobe (Laplane et al., 1989). In addition, by using a promising approach of simultaneous magnetoencephalography-local field potentials (MEG-LFP) recording in dystonic patients with deep brain stimulation (DBS) electrodes in the GPi, Neumann et al. (2015) demonstrated that the GPi is interconnected with several brain regions in spatial- and frequency-specific functional networks. In particular, MEG-LFP coherence analysis revealed oscillatory pallidal connectivity with the temporal cortex in the theta band (4–7 Hz), with the sensorimotor regions in the beta band (10–30 Hz) and with the cerebellum in the alpha band (6–13 Hz).

Therefore, the oscillatory drive of information flow between the motor-related areas and the GPi could be gathered either indirectly *via* the corticostriatal pathway or through a direct cortico-pallidal connection. The cortico-pallidal pathway could represent a possible anatomical substrate of the robust beta-band oscillatory activity in the cerebral-basal ganglia feedback loops involved in motor control (Cacciola et al., 2016b; **Figure 3**).

In addition, it has been reported in dystonic implanted patients, that single-pulse GPi-DBS may modulate motor cortical excitability at a relatively short latency suggesting the possibility of a direct cortical-GPi connection in humans (Cacciola et al., 2018; Ni et al., 2018b).

Recently, Cacciola et al. (2019) by using whole-brain tractography-based segmentation unveiled that the basal ganglia system is topographically organized in functionally segregated and integrated circuits within the GPi and GPe. In particular, the topographical organization of the cortico-pallidal pathway within the GP resulted in an antero-dorsal associative region and a posterior sensorimotor region, despite it was not possible to identify a well-defined limbic territory, thus suggesting that the cortico-pallidal fibers may provide only a relative contribution to the limbic territories in the GP. On the other hand, the most represented connectivity patterns to the GPi derived from sensorimotor regions suggesting a possible role of such pathway in sensorimotor integration. From a more practical point of view, this topographical segmentation of the GP applied to DBS, focused-ultrasound and radiosurgery interventions could improve patient's outcome by minimizing side effects at the same time (Cacciola et al., 2019; Strafella, 2019).

Although the direct and indirect evidences on the possible existence of a monosynaptic pathway between the cerebral cortex and the GPi are continuously growing, its exact functional meaning is still not clear and speculative (Cacciola et al., 2018; Ni et al., 2018a,b).

The Cortico-Nigral Pathway

Along with the GPi, the SNr is a key hub of the basal ganglia circuitry, involved in motor control (Friend and Kravitz, 2014), cognition (Simpson et al., 2010) and learning (Sesack and Grace, 2010), receiving both inhibitory and excitatory inputs from the striatum, GPe and STN, respectively (Kita and Kitai, 1987; Chevalier and Deniau, 1990; Smith et al., 1990). GABAergic neurons located in the SNr mainly target the peduncolopontine nucleus and the superior colliculi, thus suggesting SNr involvement in eyes, head and neck movements. In addition, SNr sends GABAergic inputs to the thalamic intralaminar nuclei that in turn send back projections to the striatum as well as to nuclei that send inputs to the cerebral cortex. In rodents, the ventromedial and paralaminar medial

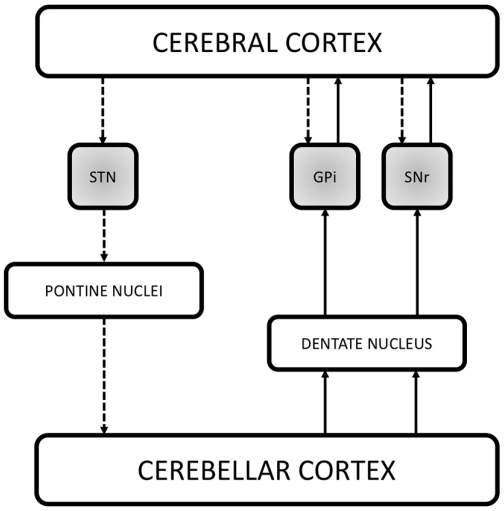

FIGURE 2 | Schematic illustration of the recently demonstrated anatomical connections in the basal ganglia network. The figure reports the three direct systems running between the cerebral cortex and the basal ganglia (STN, GPi and SNr, shaded gray boxes), providing a fast route of connection by passing the striatum and the thalamus. Recent studies have also demonstrated that the basal ganglia communicate with the cerebellum. Retrograde transneuronal transport of rabies virus in monkeys revealed a disynaptic pathway from the STN passing through the pontine nuclei to the granule cells of the cerebellar cortex. Additional findings suggest the existence of reciprocal cerebellar output on the basal ganglia *via* the dentate nucleus. Indeed, it has been demonstrated both in animals and humans that the dentate nucleus is connected with the GPi and SNr thus directly influencing the output stations of the basal ganglia in the timing of actions as well as in action selection. The dashed lines represent the cerebral cortex output on the basal ganglia and the information flow from the basal ganglia to the cerebellum. The solid lines instead represent the cerebellar output on the output nuclei of the basal ganglia which in turn communicates with the cerebral cortex. STN, subthalamic nucleus; GPi, internal segment of the globus pallidus; SNr, pars reticulata of the substantia nigra.

dorsal thalamic nuclei are the main target of GABAergic SNr inputs and in turn provide widespread projections to frontal cortical areas, including the equivalent eye field areas in primates. On the other hand, the principal targets of the SNr are the ventral anterior and paralaminar medial dorsal nuclei which instead project to more discrete organized frontal areas (Bentivoglio et al., 1979; Hoover and Strick, 1999).

By contrast, both in rodents and in primates, SNc provides extensive dopaminergic innervation to dorsal and ventral striatum (Beckstead et al., 1979; Haber, 2014). From striatum in turn, originates a set of reciprocating GABA-ergic connections to SNc (Szabó, 1979; Haber et al., 2000). In addition to these projections, SNc receives excitatory glutamatergic afferents from the STN, and GABA-ergic projections from GPi and SNr (Smith and Kieval, 2000; Watabe-Uchida et al., 2012).

Therefore, both the SNc and SNr receive disynaptic inhibitory and excitatory inputs from the cerebral cortex *via* the neostriatum and STN respectively. In addition, several anatomical studies have indicated a direct connection between the cortex and the SN (**Figure 3**). Although the majority of these studies have clearly shown the existence of a direct cortico-SN pathway, the topographical arrangement, the extent of the cortical regions involved in the projection and the morphological characteristics of the fibers and boutons were not well clarified until the mid-nineties. In an anterograde tracing study with BDA in rats, Naito and Kita (1994) addressed this issue by showing that the SNc received orderly arranged, but sparse connections from the entire prefrontal cortex; the density of boutons in SNc was much less than the ones of the striatum. More recently, Frankle et al. (2006) injected anterograde tracers into the orbital (OFC), cingulate and dorsolateral prefrontal (dlPFC) cortices, demonstrating direct connections from OFC and dlPFC to SN in the macaque monkey.

In human, the SN is involved in an extensive sub-cortical network (Düzel et al., 2009; Menke et al., 2010; Chowdhury et al., 2013), despite less is known about the possible existence of a human homologous of the direct cortico-nigral connections demonstrated in animals. In this regard, by using dMRI and tractography, Cacciola et al. (2016a) have recently reconstructed a white matter pathway linking the superior frontal, inferior frontal, precentral, postcentral gyri and the paracentral lobule with the SN bypassing the caudate nucleus, the putamen, the GP and the STN in the human brain (Cacciola et al., 2016a). In addition, in line with previous findings, the same authors demonstrated that the SN is extensively connected with many sensorimotor and associative cortical areas as well as with subcortical structures, including the cerebellum (Cacciola et al., 2017b).

In conclusion, the basal ganglia connectome seems to be more complex than expected; non-canonical pathways such as the cortico-pallidal and cortico-nigral pathways may have a role in basal ganglia physiology and pathophysiology of basal ganglia disorders. However, their functions remain speculative and need more investigation to be completely understood.

THE CEREBELLUM AND BASAL GANGLIA INTERPLAY

Along with the fundamental role in motor control, the cerebellum and basal ganglia are involved in several aspects of behavior, from cognition to emotion (Middleton and Strick, 1994; Schmahmann and Caplan, 2006). The involvement of the cerebellum in so many functions could be explained by taking into account that it works in strict connection with the cerebral cortex and the basal ganglia, which in turn play both a pivotal role in a variety of motor and non-motor functions.

According to the traditional view, the cerebellum and basal ganglia interact at the level of the cerebral cortex. However, the last decades have been characterized by increasing evidences showing a direct cerebello-basal ganglia interplay forming an integrated building block involved in several complex tasks.

Anterograde and retrograde studies demonstrated that neurons of the central lateral nucleus of thalamus, which projects both to motor cortex and to laterodorsal part of the striatum, receive inputs from the lateral cerebellar nucleus (Ichinohe et al., 2000). These findings were extended to non-human primates in a study conducted on macaques by means of retrograde transneuronal transport of rabies virus (Hoshi et al., 2005),

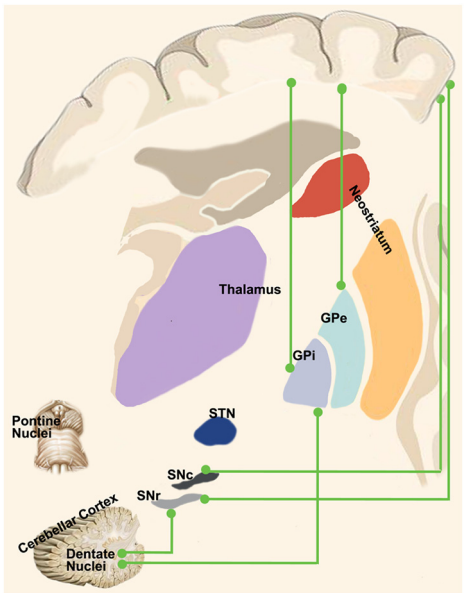

FIGURE 3 | "Novel" cortico-basal-ganglia-cerebellar pathways. Highlight the newly identified connections between the cerebral cortex, GPi, GPe and SN as well as the complementary circuits between the dentate nucleus and such nuclei as described in recent tractographic studies in humans.

showing a pathway linking primarily the dentate nucleus (but also the interpositus and fastigial nuclei) to the contralateral striatum through ventral anterior (VA), ventral lateral (VL) and intralaminar nuclei (CM/Pf) and finally reaching the external part of the globus pallidus (**Figure 3**). Labeled neurons in the dentate nucleus belonged both to its motor and non-motor domains (Dum et al., 2002), suggesting that the interplay of these subcortical structures is crucial for motor, cognitive and emotional processing.

A few years later, Bostan et al. (2010) employed the same experimental setting to investigate the presence of a pathway projecting from basal ganglia to cerebellum. The retrograde transport revealed that first-order neurons were located in the pedunculopontine nucleus while second-order neurons were found to be topographically organized in the STN (**Figure 3**). These fascinating studies provided new insights on the roles of basal ganglia and cerebellum showing that their interplay may be more complex than expected. Virus tracing is not the only technique which has been employed to study connectivity between these two subcortical structures. Converging evidences coming from electrophysiological experiments and human neuroimaging studies will be discussed below.

ELECTROPHYSIOLOGICAL INSIGHT INTO CEREBELLAR-BASAL GANGLIA INTERACTIONS

Electrophysiological investigations, conducted on anesthetized cats to assess the latency of basal ganglia-cerebellum activation, failed in finding strong evidences of a rapid-gated cerebellum-basal ganglia communication. The long latencies (50–350 ms) found made the hypothesis of rapidly funneling stimuli from cerebellum to basal ganglia neglectable (Ratchetson and Li, 1969). This assumption has been recently challenged by Chen et al. (2014) in a optogenetic study on freely moving rats, which revealed short-latency activation (10 ms) of basal ganglia after optogenetic stimulation of dentate nucleus, thus accounting for a rapid communication between cerebellum and basal ganglia leading to fine coordination of their respective outputs. Moreover, when the electrical stimulation of dentate nucleus is delivered simultaneously to high frequency stimulation of cerebral cortex, the overall result is a direction change of synaptic plasticity, reverting long term depression (LTD) in long term potentiation (LTP; Chen et al., 2014). These findings do provide new insight on the role of basal ganglia-cerebellum communication in learning phenomena. The synergic role of cerebellum and basal ganglia in learning processes is not new considering the pioneer studies of the early 2000 showing that the cerebral cortex, cerebellum and basal ganglia are involved in specific learning paradigms: unsupervised, error-based (supervised) and reward-based learning (Doya, 1999, 2000). The recent anatomical findings of the two- and tri-synaptic pathways linking the cerebellum and basal ganglia, together with the evidence of a short latency communication, led Caligiore et al. (2017) to consider their computational role and to update the previous model of the cortico-basal ganglia-cerebellum loops. The possible computational role of the dento-thalamo-striatal pathway is to convey the predicted outcome of a candidate action, processed in the cerebellum to the striatum where the outcome itself is evaluated (*forward model*). On the other hand, the computational role of the subthalamic-ponto-cerebellar pathway is not clear at all; nevertheless, considering the involvement of the subthalamic nucleus in the indirect pathway and aversive learning phenomena, it is tempting to speculate that it would prevent the new *forward models* to be conveyed to the striatum (Caligiore et al., 2017).

POSSIBLE DIRECT CEREBELLAR-BASAL GANGLIA CONNECTIONS

In addition to the dento-thalamo-striatal and subthalamo-ponto-cerebellar pathways, Milardi et al. (2016a) reconstructed a white matter pathway linking the dentate nucleus both to the GPi and to the SN *via* the superior cerebellar peduncles and bypassing the red nucleus, thalamus and striatum (Milardi et al., 2016a; **Figure 3**).

Although its physiological meaning is still unknown, the dento-nigral pathway, reconstructed in human by means of dMRI and tractography, could represent the phylogenetical equivalent of the pathway observed *via* tract-tracing in cats and rats (Snider et al., 1976) allowing a fine-tuning of a fast cerebellar influence of one of the output nuclei of the basal ganglia system. In addition, release of dopamine in caudate nucleus and incremented dopamine production in substantia nigra were found after unilateral stimulation of the dentate nucleus in cats (Nieoullon et al., 1978) suggesting that direct connections

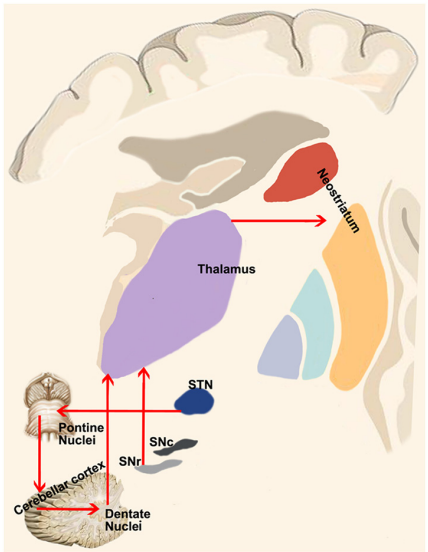

FIGURE 4 | Cerebellum-basal ganglia interplay. This panel shows the connections between the cerebellum and basal ganglia as revealed by retrograde tracing studies in monkeys. Red lines indicate the output of the cerebellum on the basal ganglia *via* the dentate-thalamo-striatal pathway as well as the control of basal ganglia on the cerebellum *via* the STN-ponto-cerebellar cortex pathway.

from deep cerebellar nuclei could exert a modulatory role on dopaminergic tone in the basal ganglia.

Recent evidences of a direct route connecting dentate nucleus to globus pallidus, on human side, comes from a MEG-LFP study (Neumann et al., 2015), showing a functional oscillatory connectivity in the alpha band (7–13 Hz) between the cerebellum and globus pallidus in dystonic patients with an electrode implanted in the GPi. In addition, it was also found a negative correlation between the alpha band of coherence and symptoms severity as measured by Toronto Western Spasmodic Torticollis Rating Scale suggesting a compensatory role of the cerebellum in dystonic patients.

These direct connections between the dentate nucleus and GPi and SNr are very intriguing considering the presence of a direct cortico-pallidal and cortico-SN pathways bypassing the striatum in humans (Milardi et al., 2015; Cacciola et al., 2016a) and in monkeys (Leichnetz and Astruc, 1977; Frankle et al., 2006). Hence, it is tempting to speculate on the existence of 3 direct systems running between the cortex, the basal ganglia (STN, GPi and SNr) and the cerebellum, providing a fast route of connection bypassing the striatum and the thalamus (**Figure 4**). These considerations are not necessarily in conflict with the consensus position of Caligiore et al. (2017) if we postulate the appearance, in the evolutionary scale in humans, of a new phylogenetic fast system connecting cerebellum and basal ganglia which may complement the disynaptic or trisynaptic projections from the dentate nucleus, passing through the thalamus and reaching the putamen or the GPe. This new fast system would be necessary to support the manual dexterity which is an exquisite feature of human specimens.

FUNCTIONAL SIGNIFICANCE OF CEREBELLAR-BASAL GANGLIA INTERACTION IN MOVEMENT DISORDERS

The basal ganglia and the cerebellum have been often conceived separately as structures involved in different neurological syndromes. However, evidences concerning the co-operation of cerebellum and basal ganglia in movement disorders are currently growing. Thus, the above-described scenario could open an entirely new perspective into the pathophysiology of basal ganglia and cerebellum disorders (Coenen et al., 2011; Husárová et al., 2014).

Different aspects of movement disorders could be gathered by cerebellum-basal ganglia interface. Cerebellum and basal ganglia have been involved in time computation: the former should be accounted for millisecond-range intervals whilst the latter would work mainly on the second-ranges (Ivry, 1996; Buhusi and Meck, 2005; Wiener et al., 2010). Functional MRI (fMRI) studies revealed hypoactivation of basal ganglia and cerebellar cortex during early stages of Parkinson's Disease (PD) compared to healthy controls, during an interception task. A direct causal modeling analysis revealed differential modulation of effective connectivity strength between basal ganglia and cerebellum in performing a motor timing task (Husárová et al., 2013, 2014). This would suggest an involvement of cerebello-basal ganglia circuits in motor and perceptual timing alterations, that are typical of PD.

Although the involvement of basal ganglia in the pathophysiology of dystonia is indisputable, the mechanisms producing dystonia are incompletely understood, with recent evidence pointing to the involvement of a variety of brain areas including the cerebellum (Quartarone and Hallett, 2013; Jinnah et al., 2017). As it is possible that the etiological heterogeneity of dystonias reflects the relative importance of different nodes in this extended motor network, one major challenge is determining first, the role and contribution of the different brain regions in the various forms of dystonia with a comprehensive model; second, if there is a final common pathway for all dystonias (Quartarone and Ruge, 2018).

Anomalies in the cerebellum and basal ganglia have been widely investigated in both animal and human studies of dystonia (Filip et al., 2013; Tewari et al., 2017). Different cases of secondary dystonia emerging from cerebellar lesions are described in humans (Alarcón et al., 2001; LeDoux and Brand, 2003; Shen et al., 2016). In a murine model of cerebellar-induced dystonia, a cerebellar outflow interruption has been causally linked to burst firing activity in basal ganglia, which is a prominent feature of dystonia (Chen et al., 2014).

Moreover, also primary dystonia, such as cervical dystonia has also been conceptualized as deriving from alterations in neural integration for head and eye movements, involving cerebellum and basal ganglia in association with oculomotor structures (Shaikh et al., 2016). In line with this hypothesis, in a fMRI study during a visuospatial task, Filip et al. (2017) observed cerebellum-basal ganglia hypoconnectivity in patients with cervical dystonia.

The pathway linking the STN to cerebellum could be involved in motor symptoms of PD. In particular, STN pathological activity, characterized by burst activity and higher firing rates, may in turn be responsible for hyperactivity of cerebellar cortex leading to alterations in the cerebello-thalamo-cortical circuits (Bostan et al., 2010; Bostan and Strick, 2018). It can be therefore hypothesized that DBS of the STN could exert its positive effects on motor learning by stimulating the pathway linking the STN to the cerebellum. Supporting this hypothesis, a recent fMRI study on 20 PD patients implanted with DBS of the STN found that functional connectivity between active contact and contralateral cerebellum is strongly predictive of improvement in motor learning (de Almeida Marcelino et al., 2019). It would be tempting to speculate that suppression of STN aberrant activity, promoted by DBS, could lead to improved cerebellar function and, by consequence, to improvement in motor learning.

CONCLUSIONS

In conclusion, further experimental and challenging studies should be fostered to characterize the full extent of the interplay between the cerebral cortex, the basal ganglia and the cerebellum. However, several evidences have already suggested that the system is more intricated than initially assumed. In the present review, we discussed the invasive and non-invasive techniques to investigate the anatomy and the extrinsic and intrinsic connections of the basal ganglia network. We illustrated the neuroanatomical findings obtained in non-human species that have inspired a paradigmatic shift in this scenario, providing evidences that the cortico-basal ganglia circuits constitute a complex system. Finally, we provide further support coming from neuroimaging studies that these pathways may exist in humans and may exert a meaningful role in basal ganglia disorders. Taken together, these observations suggest that the cerebral cortex, the basal ganglia and the cerebellum form an integrated and segregated network acting on multiple motor and non-motor functions. Although such complex interplay has not yet been explored in detail, we hope it will be a focus of new-generation optogenetic, physiologic, behavioral and neuroimaging studies.

The proposed scenario, with the presence of parallel direct and indirect projections running between the cortex, basal ganglia and cerebellum, complements new ideas that view movement disorders as disorders of a complex motor network rather than a limited disruption of individual nuclei in the basal ganglia.

AUTHOR CONTRIBUTIONS

DM: writing of the first draft of the manuscript, conception, organization, and execution of the research project, data analysis and interpretation, literature research, and critically revised the manuscript. AQ: writing of the first draft of the manuscript, conception, organization, and execution of the research project, data analysis and interpretation, literature research, critically revised the manuscript, and Guarantor and supervisor of the research project. GA: conception, organization, and execution of the research project, data interpretation, critically revised the manuscript, Guarantor and supervisor of the research project. AC: conception, organization, and execution of the research project, data analysis and interpretation, writing of the first draft and revision of the final version of the manuscript, and Guarantor and supervisor of the research project. AB, SB, GB, PB and GP: data analysis and interpretation, writing of the first draft and literature research. GC: data analysis and interpretation, revised the manuscript and literature research. GR and DB: data analysis and interpretation and literature research.

REFERENCES

Afifi, A. K., Bahuth, N. B., Kaelber, W. W., Mikhael, E., and Nassar, S. (1974). The cortico-nigral fibre tract. An experimental Fink-Heimer study in cats. *J. Anat.* 118, 469–476.

Alarcón, F., Tolosa, E., and Muñoz, E. (2001). Focal limb dystonia in a patient with a cerebellar mass. *Arch. Neurol.* 58, 1125–1127. doi: 10.1001/archneur.58.7.1125

Albin, R. L., Young, A. B., and Penney, J. B. (1989). The functional anatomy of basal ganglia disorders. *Trends Neurosci.* 12, 366–375. doi: 10.1016/0166-2236(89)90074-x

Alexander, G. E., Crutcher, M. D., and Delong, M. R. (1990). Basal ganglia-thalamocortical circuits: parallel substrates for motor, oculomotor, "prefrontal" and "limbic" functions. *Prog. Brain Res.* 85, 119–146. doi: 10.1016/s0079-6123(08)62678-3

Alexander, A. L., Lee, J. E., Lazar, M., and Field, A. S. (2007). Diffusion tensor imaging of the brain. *Neurotherapeutics* 4, 316–329. doi: 10.1016/j.nurt.2007.05.011

Arrigo, A., Calamuneri, A., Milardi, D., Mormina, E., Gaeta, M., Corallo, F., et al. (2019). Claustral structural connectivity and cognitive impairment in drug naïve Parkinson's disease. *Brain Imaging Behav.* 13, 933–944. doi: 10.1007/s11682-018-9907-z

Aston-Jones, G., and Card, J. P. (2000). Use of pseudorabies virus to delineate multisynaptic circuits in brain: opportunities and limitations. *J. Neurosci. Methods* 103, 51–61. doi: 10.1016/s0165-0270(00)00295-8

Basser, P. J., Mattiello, J., and LeBihan, D. (1994). MR diffusion tensor spectroscopy and imaging. *Biophys. J.* 66, 259–267. doi: 10.1016/s0006-3495(94)80775-1

Basser, P. J., Pajevic, S., Pierpaoli, C., Duda, J., and Aldroubi, A. (2000). *In vivo* fiber tractography using DT-MRI data. *Magn. Reson. Med.* 44, 625–632. doi: 10.1002/1522-2594(200010)44:4<625::aid-mrm17>3.0.co;2-o

Beach, T. G., and McGeer, E. G. (1987). Tract-tracing with horseradish peroxidase in the postmortem human brain. *Neurosci. Lett.* 76, 37–41. doi: 10.1016/0304-3940(87)90188-1

Beckstead, R. M., Domesick, V. B., and Nauta, W. J. H. (1979). Efferent connections of the substantia nigra and ventral tegmental area in the rat. *Brain Res.* 175, 191–217. doi: 10.1016/0006-8993(79)91001-1

Bentivoglio, M., van der Kooy, D., and Kuypers, H. G. J. M. (1979). The organization of the efferent projections of the substantia nigra in the rat. A retrograde fluorescent double labeling study. *Brain Res.* 174, 1–17. doi: 10.1016/0006-8993(79)90800-x

Bostan, A. C., Dum, R. P., and Strick, P. L. (2010). The basal ganglia communicate with the cerebellum. *Proc. Natl. Acad. Sci. U S A* 107, 8452–8456. doi: 10.1073/pnas.1000496107

Bostan, A. C., and Strick, P. L. (2018). The basal ganglia and the cerebellum: nodes in an integrated network. *Nat. Rev. Neurosci.* 19, 338–350. doi: 10.1038/s41583-018-0002-7

Buhusi, C. V., and Meck, W. H. (2005). What makes us tick? Functional and neural mechanisms of interval timing. *Nat. Rev. Neurosci.* 6, 755–765. doi: 10.1038/nrn1764

Cacciola, A., Calabrò, R. S., Costa, A., Naro, A., Milardi, D., and Bruschetta, D. (2017a). Enlarged Virchow-Robin spaces in a young man: a constrained spherical deconvolution tractography study. *Acta Biomed.* 88, 319–324. doi: 10.23750/abm.v88i3.5181

Cacciola, A., Calamuneri, A., Milardi, D., Mormina, E., Chillemi, G., Marino, S., et al. (2017b). A connectomic analysis of the human basal ganglia network. *Front. Neuroanat.* 11:85. doi: 10.3389/fnana.2017.00085

Cacciola, A., Milardi, D., Calamuneri, A., Bonanno, L., Marino, S., Ciolli, P., et al. (2017c). Constrained spherical deconvolution tractography reveals cerebello-mammillary connections in humans. *Cerebellum* 16, 483–495. doi: 10.1007/s12311-016-0830-9

Cacciola, A., Milardi, D., Anastasi, G. P., Basile, G. A., Ciolli, P., Irrera, M., et al. (2016a). A direct cortico-nigral pathway as revealed by constrained spherical deconvolution tractography in humans. *Front. Hum. Neurosci.* 10:374. doi: 10.3389/fnhum.2016.00374

Cacciola, A., Milardi, D., and Quartarone, A. (2016b). Role of cortico-pallidal connectivity in the pathophysiology of dystonia. *Brain* 139:e48. doi: 10.1093/brain/aww102

Cacciola, A., Milardi, D., Anastasi, G., and Quartarone, A. (2018). Cortico-pallidal connectivity: lessons from patients with dystonia. *Ann. Neurol.* 84:158. doi: 10.1002/ana.25255

Cacciola, A., Milardi, D., Bertino, S., Basile, G. A., Calamuneri, A., Chillemi, G., et al. (2019). Structural connectivity-based topography of the human globus pallidus: implications for therapeutic targeting in movement disorders. *Mov. Disord.* 34, 987–996. doi: 10.1002/mds.27712

Calamuneri, A., Arrigo, A., Mormina, E., Milardi, D., Cacciola, A., Chillemi, G., et al. (2018). White matter tissue quantification at low b-values within constrained spherical deconvolution framework. *Front. Neurol.* 9:716. doi: 10.3389/fneur.2018.00716

Caligiore, D., Pezzulo, G., Baldassarre, G., Bostan, A. C., Strick, P. L., Doya, K., et al. (2017). Consensus paper: towards a systems-level view of cerebellar function: the interplay between cerebellum, basal ganglia, and cortex. *Cerebellum* 16, 203–229. doi: 10.1007/s12311-016-0763-3

Carter, D. A., and Fibiger, H. C. (1978). The projections of the entopeduncular nucleus and globus pallidus in rat as demonstrated by autoradiography and horseradish peroxidase histochemistry. *J. Comp. Neurol.* 177, 113–123. doi: 10.1002/cne.901770108

Catani, M., and Thiebaut de Schotten, M. (2012). *Atlas of Human Brain Connections.* Oxford, UK: Oxford University Press.

Catani, M., Jones, D. K., and ffytche, D. H. (2005). Perisylvian language networks of the human brain. *Ann. Neurol.* 57, 8–16. doi: 10.1002/ana.20319

Chen, C. H., Fremont, R., Arteaga-Bracho, E. E., and Khodakhah, K. (2014). Short latency cerebellar modulation of the basal ganglia. *Nat. Neurosci.* 17, 1767–1775. doi: 10.1038/nn.3868

Chen, M. C., Ferrari, L., Sacchet, M. D., Foland-Ross, L. C., Qiu, M. H., Gotlib, I. H., et al. (2015). Identification of a direct GABAergic pallidocortical pathway in rodents. *Eur. J. Neurosci.* 41, 748–759. doi: 10.1111/ejn.12822

Chevalier, G., and Deniau, J. M. (1990). Disinhibition as a basic process in the expression of striatal functions. *Trends Neurosci.* 13, 277–280. doi: 10.1016/0166-2236(90)90109-n

Chowdhury, R., Lambert, C., Dolan, R. J., and Düzel, E. (2013). Parcellation of the human substantia nigra based on anatomical connectivity to the striatum. *Neuroimage* 81, 191–198. doi: 10.1016/j.neuroimage.2013.05.043

Chung, H. W., Chou, M. C., and Chen, C. Y. (2011). Principles and limitations of computational algorithms in clinical diffusion tensor MR tractography. *Am. J. Neuroradiol.* 32, 3–13. doi: 10.3174/ajnr.a2041

Coenen, V. A., Mädler, B., Schiffbauer, H., Urbach, H., and Allert, N. (2011). Individual fiber anatomy of the subthalamic region revealed with diffusion tensor imaging: a concept to identify the deep brain stimulation target for tremor suppression. *Neurosurgery* 68, 1069–1076. doi: 10.1227/NEU.0b013e31820a1a20

da Silva, N. M., Ahmadi, S. A., Tafula, S. N., Cunha, J. P. S., Bötzel, K., Vollmar, C., et al. (2017). A diffusion-based connectivity map of the GPi for optimised stereotactic targeting in DBS. *Neuroimage* 144, 83–91. doi: 10.1016/j.neuroimage.2016.06.018

de Almeida Marcelino, A. L., Horn, A., Krause, P., Kühn, A. A., and Neumann, W.-J. (2019). Subthalamic neuromodulation improves short-term motor learning in Parkinson's disease. *Brain* 142, 2198–2206. doi: 10.1093/brain/awz152

DeLong, M. R., and Wichmann, T. (2007). Circuits and circuit disorders of the basal ganglia. *Arch. Neurol.* 64, 20–24. doi: 10.1007/978-1-4615-1235-6_2

DeLong, M., and Wichmann, T. (2009). Update on models of basal ganglia function and dysfunction. *Park. Relat. Disord.* 15, S237–S240. doi: 10.1016/s1353-8020(09)70822-3

Dick, J. P. R., Rothwell, J. C., Day, B. L., Cantello, R., Buruma, O., Gioux, M., et al. (1989). The bereitschaftspotential is abnormal in Parkinson's disease. *Brain* 112, 233–244. doi: 10.1093/brain/112.1.233

Doya, K. (1999). What are the computations of the cerebellum, the basal ganglia and the cerebral cortex? *Neural Netw.* 12, 961–974. doi: 10.1016/S0893-6080(99)00046-5

Doya, K. (2000). Complementary roles of basal ganglia and cerebellum in learning and motor control. *Curr. Opin. Neurobiol.* 10, 732–739. doi: 10.1016/s0959-4388(00)00153-7

Dum, R. P., Li, C., and Strick, P. L. (2002). Motor and nonmotor domains in the monkey dentate. *Ann. N Y Acad. Sci.* 978, 289–301. doi: 10.1111/j.1749-6632.2002.tb07575.x

Düzel, E., Bunzeck, N., Guitart-Masip, M., Wittmann, B., Schott, B. H., and Tobler, P. N. (2009). Functional imaging of the human dopaminergic midbrain. *Trends Neurosci.* 32, 321–328. doi: 10.1016/j.tins.2009.02.005

Dyrby, T. B., Søgaard, L. V., Parker, G. J., Alexander, D. C., Lind, N. M., Baaré, W. F. C., et al. (2007). Validation of *in vitro* probabilistic tractography. *Neuroimage* 37, 1267–1277. doi: 10.1016/j.neuroimage.2007.06.022

Ferrier, D. (1887). *The Functions of the Brain.* London: Smith, Elder & Co.

Filip, P., Gallea, C., Lehéricy, S., Bertasi, E., Popa, T., Mareček, R., et al. (2017). Disruption in cerebellar and basal ganglia networks during a visuospatial task in cervical dystonia. *Mov. Disord.* 32, 757–768. doi: 10.1002/mds.26930

Filip, P., Lungu, O. V., and Bareš, M. (2013). Dystonia and the cerebellum: a new field of interest in movement disorders? *Clin. Neurophysiol.* 124, 1269–1276. doi: 10.1016/j.clinph.2013.01.003

Frankle, W. G., Laruelle, M., and Haber, S. N. (2006). Prefrontal cortical projections to the midbrain in primates: evidence for a sparse connection. *Neuropsychopharmacology* 31, 1627–1636. doi: 10.1038/sj.npp.1300990

Friend, D. M., and Kravitz, A. V. (2014). Working together: basal ganglia pathways in action selection. *Trends Neurosci.* 37, 301–303. doi: 10.1016/j.tins.2014.04.004

Gerfen, C. R., Baimbridge, K. G., and Thibault, J. (1987a). The neostriatal mosaic: III. Biochemical and developmental dissociation of patch-matrix mesostriatal systems. *J. Neurosci.* 7, 3935–3944. doi: 10.1523/JNEUROSCI.07-12-03935.1987

Gerfen, C. R., Herkenham, M., and Thibault, J. (1987b). The neostriatal mosaic: II. Patch- and matrix-directed mesostriatal dopaminergic and non-dopaminergic systems. *J. Neurosci.* 7, 3915–3934. doi: 10.1523/JNEUROSCI.07-12-03915.1987

Grewal, S. S., Holanda, V. M., and Middlebrooks, E. H. (2018). Corticopallidal connectome of the globus pallidus externus in humans: an exploratory study of structural connectivity using probabilistic diffusion tractography. *Am. J. Neuroradiol.* 39, 2910–2935. doi: 10.3174/ajnr.a5816

Grillner, S., and Robertson, B. (2016). The basal ganglia over 500 million years. *Curr. Biol.* 26, 1088–1100. doi: 10.1016/j.cub.2016.06.041

Haber, S. (1988). Tracing intrinsic fiber connections in postmortem human brain with WGA-HRP. *J. Neurosci. Methods* 23, 15–22. doi: 10.1016/0165-0270(88)90017-9

Haber, S. N. (2014). The place of dopamine in the cortico-basal ganglia circuit. *Neuroscience* 282, 248–257. doi: 10.1016/j.neuroscience.2014.10.008

Haber, S. N. (2016). "Corticostriatal circuitry," in *Neuroscience in the 21st Century: From Basic to Clinical*, 2nd Edn. eds D. Pfaff and N. Volkow (New York, NY: Springer), 1721–1741.

Haber, S. N., Fudge, J. L., and McFarland, N. R. (2000). Striatonigrostriatal pathways in primates form an ascending spiral from the shell to the dorsolateral striatum. *J. Neurosci.* 25, 2369–2382. doi: 10.1523/JNEUROSCI.20-06-02369.2000

Haber, S. N., and Knutson, B. (2010). The reward circuit: linking primate anatomy and human imaging. *Neuropsychopharmacology* 35, 4–26. doi: 10.1038/npp.2009.129

Hardman, C. D., Henderson, J. M., Finkelstein, D. I., Horne, M. K., Paxinos, G., and Halliday, G. M. (2002). Comparison of the basal ganglia in rats, marmosets, macaques, baboons and humans: volume and neuronal number for the output, internal relay, and striatal modulating nuclei. *J. Comp. Neurol.* 445, 238–255. doi: 10.1002/cne.10165

Hooks, B. M., Papale, A. E., Paletzki, R. F., Feroze, M. W., Eastwood, B. S., Couey, J. J., et al. (2018). Topographic precision in sensory and motor corticostriatal projections varies across cell type and cortical area. *Nat. Commun.* 9:3549. doi: 10.1038/s41467-018-06928-1

Hoover, J. E., and Strick, P. L. (1993). Multiple output channels in the basal ganglia. *Science* 259, 819–821. doi: 10.1126/science.7679223

Hoover, J. E., and Strick, P. L. (1999). The organization of cerebellar and basal ganglia outputs to primary motor cortex as revealed by retrograde transneuronal transport of herpes simplex virus type 1. *J. Neurosci.* 19, 1446–1463. doi: 10.1523/JNEUROSCI.19-04-01446.1999

Hoshi, E., Tremblay, L., Féger, J., Carras, P. L., and Strick, P. L. (2005). The cerebellum communicates with the basal ganglia. *Nat. Neurosci.* 8, 1491–1493. doi: 10.1038/nn1544

Husárová, I., Lungu, O. V., Mareček, R., Mikl, M., Gescheidt, T., Krupa, P., et al. (2014). Functional imaging of the cerebellum and basal ganglia during predictive motor timing in early Parkinson's disease. *J. Neuroimaging* 24, 45–53. doi: 10.1111/j.1552-6569.2011.00663.x

Husárová, I., Mikl, M., Lungu, O. V., Mareček, R., Vaníček, J., and Bareš, M. (2013). Similar circuits but different connectivity patterns between the cerebellum, basal ganglia and supplementary motor area in early Parkinson's disease patients and controls during predictive motor timing. *J. Neuroimaging* 23, 452–462. doi: 10.1111/jon.12030

Ichinohe, N., Mori, F., and Shoumura, K. (2000). A di-synaptic projection from the lateral cerebellar nucleus to the laterodorsal part of the striatum *via* the central lateral nucleus of the thalamus in the rat. *Brain Res.* 880, 191–197. doi: 10.1016/s0006-8993(00)02744-x

Ivry, R. B. (1996). The representation of temporal information in perception and motor control. *Curr. Opin. Neurobiol.* 6, 851–857. doi: 10.1016/s0959-4388(96)80037-7

Jbabdi, S., and Johansen-Berg, H. (2011). Tractography: where do we go from here? *Brain Connect.* 1, 169–183. doi: 10.1089/brain.2011.0033

Jinnah, H. A., Neychev, V., and Hess, E. J. (2017). The anatomical basis for dystonia: the motor network model. *Tremor Other Hyperkinet. Mov.* 7:506. doi: 10.7916/D8V69X3S

Johnson, T. N. (1961). Fiber connections between the dorsal thalamus and corpus striatum in the cat. *Exp. Neurol.* 3, 556–569. doi: 10.1016/s0014-4886(61)80005-8

Kaplitt, M. G., and Loewy, A. D. (1995). *Viral Vectors: Gene Therapy and Neuroscience Applications.* San Diego, CA: Academic Press.

Kita, H., and Kitai, S. T. (1987). Efferent projections of the subthalamic nucleus in the rat: light and electron microscopic analysis with the PHA-L method. *J. Comp. Neurol.* 260, 435–452. doi: 10.1002/cne.902600309

Kita, T., and Kita, H. (2012). The subthalamic nucleus is one of multiple innervation sites for long-range corticofugal axons: a single-axon tracing study in the rat. *J. Neurosci.* 32, 5990–5999. doi: 10.1523/JNEUROSCI.5717-11.2012

Klingler, J. (1935). Erleichterung der makroskopischen Präparation des Gehirn durch den Gefrierprozess. *Schweiz. Arch. Neurol. Psychiat.* 36, 247–256.

Klingler, J., and Gloor, P. (1960). The connections of the amygdala and of the anterior temporal cortex in the human brain. *J. Comp. Neurol.* 115, 333–369. doi: 10.1002/cne.901150305

Köbbert, C., Apps, R., Bechmann, I., Lanciego, J. L., Mey, J., and Thanos, S. (2000). Current concepts in neuroanatomical tracing. *Prog. Neurobiol.* 62, 327–351. doi: 10.1016/s0301-0082(00)00019-8

Laplane, D., Levasseur, M., Pillon, B., Dubois, B., Baulac, M., Mazoyer, B., et al. (1989). Obsessive-compulsive and other behavioural changes with bilateral basal ganglia lesions: a neuropsychological, magnetic resonance imaging and positron tomography study. *Brain* 112, 699–725. doi: 10.1093/brain/112.3.699

Lawes, I. N., Barrick, T. R., Murugam, V., Spierings, N., Evans, D. R., Song, M., et al. (2008). Atlas-based segmentation of white matter tracts of the human brain using diffusion tensor tractography and comparison with classical dissection. *Neuroimage* 39, 62–79. doi: 10.1016/j.neuroimage.2007.06.041

LeDoux, M. S., and Brand, K. A. (2003). Secondary cervical dystonia associated with structural lesions of the central nervous system. *Mov. Disord.* 18, 60–69. doi: 10.1002/mds.10301

Leichnetz, G. R., and Astruc, J. (1977). The course of some prefrontal corticofugals to the pallidum, substantia innominata, and amygdaloid complex in monkeys. *Exp. Neurol.* 54, 104–109. doi: 10.1016/0014-4886(77)90238-2

Luys, J. (1868). *Recherches sur le Systeme Nerveux Cérébro-Spinal; sa structure, ses fonctions, ses maladies; par, J. Luys, Médecin des Hôpitaux de Paris.* Paris: Bailliére.

Menke, R. A., Jbabdi, S., Miller, K. L., Matthews, P. M., and Zarei, M. (2010). Connectivity-based segmentation of the substantia nigra in human and its implications in Parkinson's disease. *Neuroimage* 52, 1175–1180. doi: 10.1016/j.neuroimage.2010.05.086

Middlebrooks, E. H., Tuna, I. S., Grewal, S. S., Almeida, L., Heckman, M. G., Lesser, E. R., et al. (2018). Segmentation of the globus pallidus internus using probabilistic diffusion tractography for deep brain stimulation targeting in Parkinson disease. *AJNR Am. J. Neuroradiol.* 39, 1127–1134. doi: 10.3174/ajnr.a5641

Middleton, F. A., and Strick, P. L. (1994). Anatomical evidence for cerebellar and basal ganglia involvement in higher cognitive function. *Science* 266, 458–461. doi: 10.1126/science.7939688

Milardi, D., Arrigo, A., Anastasi, G., Cacciola, A., Marino, S., Mormina, E., et al. (2016a). Extensive direct subcortical cerebellum-basal ganglia connections in human brain as revealed by constrained spherical deconvolution tractography. *Front. Neuroanat.* 10:29. doi: 10.3389/fnana.2016.00029

Milardi, D., Cacciola, A., Cutroneo, G., Marino, S., Irrera, M., Cacciola, G., et al. (2016b). Red nucleus connectivity as revealed by constrained spherical deconvolution tractography. *Neurosci. Lett.* 626, 68–73. doi: 10.1016/j.neulet.2016.05.009

Milardi, D., Cacciola, A., Calamuneri, A., Ghilardi, M. F., Caminiti, F., Cascio, F., et al. (2017). The olfactory system revealed: non-invasive mapping by using constrained spherical deconvolution tractography in healthy humans. *Front. Neuroanat.* 11:32. doi: 10.3389/fnana.2017.00032

Milardi, D., Gaeta, M., Marino, S., Arrigo, A., Vaccarino, G., Mormina, E., et al. (2015). Basal ganglia network by constrained spherical deconvolution: a possible cortico-pallidal pathway? *Mov. Disord.* 30, 342–349. doi: 10.1002/mds.25995

Miyamoto, H., Tatsukawa, T., Shimohata, A., Yamagata, T., Suzuki, T., Amano, K., et al. (2019). Impaired cortico-striatal excitatory transmission triggers epilepsy. *Nat. Commun.* 10:1917. doi: 10.1038/s41467-019-09954-9

Mori, S., and van Zijl, P. (2007). Human white matter atlas. *Am. J. Psychiatry* 164:1005. doi: 10.1176/ajp.2007.164.7.1005

Naito, A., and Kita, H. (1994). The cortico-pallidal projection in the rat: an anterograde tracing study with biotinylated dextran amine. *Brain Res.* 653, 251–257. doi: 10.1016/0006-8993(94)90397-2

Nambu, A., Tokuno, H., Hamada, I., Kita, H., Imanishi, M., Akazawa, T., et al. (2000). Excitatory cortical inputs to pallidal neurons *via* the subthalamic nucleus in the monkey. *J. Neurophysiol.* 84, 289–300. doi: 10.1152/jn.2000.84.1.289

Nambu, A., Tokuno, H., and Takada, M. (2002). Functional significance of the cortico-subthalamo-pallidal 'hyperdirect' pathway. *Neurosci. Res.* 43, 111–117. doi: 10.1016/s0168-0102(02)00027-5

Nelson, A. B., and Kreitzer, A. C. (2014). Reassessing models of basal ganglia function and dysfunction. *Annu. Rev. Neurosci.* 37, 117–135. doi: 10.1146/annurev-neuro-071013-013916

Neumann, W. J., Jha, A., Bock, A., Huebl, J., Horn, A., Schneider, G. H., et al. (2015). Cortico-pallidal oscillatory connectivity in patients with dystonia. *Brain* 138, 1894–1906. doi: 10.1093/brain/awv109

Ni, Z., Hallett, M., and Chen, R. (2018a). Reply to "Corticopallidal connectivity: lessons from patients with dystonia". *Ann. Neurol.* 84:159. doi: 10.1002/ana.25253

Ni, Z., Kim, S. J., Phielipp, N., Ghosh, S., Udupa, K., Gunrai, C. A., et al. (2018b). Pallidal deep brain stimulation modulates cortical excitability and plasticity. *Ann. Neurol.* 83, 352–362. doi: 10.1002/ana.25156

Nieoullon, A., Cheramy, A., and Glowinski, J. (1978). Release of dopamine in both caudate nuclei and both substantia nigrae in response to unilateral stimulation of cerebellar nuclei in the cat. *Brain Res.* 148, 143–152. doi: 10.1016/0006-8993(78)90384-0

Noorani, I., and Carpenter, R. H. S. (2014). Basal ganglia: racing to say no. *Trends Neurosci.* 37, 467–469. doi: 10.1016/j.tins.2014.07.003

Oishi, K. (2011). *MRI Atlas of Human White Matter.* San Diego, CA: Academic Press.

Parent, A. (2013). The history of the basal ganglia: the contribution of Karl Friedrich Burdach. *Neurosci. Med.* 03, 374–379. doi: 10.4236/nm.2012.34046

Parent, A. (2017). "The history of the basal ganglia: the nuclei," in *Handbook of Basal Ganglia Structure and Function*, eds H. Steiner and K. Y. Tseng (Cambridge, MA: Academic Press), 37–39.

Parker, G. J. M., Luzzi, S., Alexander, D. C., Wheeler-Kingshott, C. A. M., Ciccarelli, O., and Lambon Ralph, M. A. (2005). Lateralization of ventral and dorsal auditory-language pathways in the human brain. *Neuroimage* 24, 656–666. doi: 10.1016/j.neuroimage.2004.08.047

Parker, G. D., Marshall, D., Rosin, P. L., Drage, N., Richmond, S., and Jones, D. K. (2013). A pitfall in the reconstruction of fibre ODFs using spherical deconvolution of diffusion MRI data. *Neuroimage* 65, 433–448. doi: 10.1016/j.neuroimage.2012.10.022

Parent, M., and Parent, A. (2006). Single-axon tracing study of corticostriatal projections arising from primary motor cortex in primates. *J. Comp. Neurol.* 496, 202–213. doi: 10.1002/cne.20925

Preuss, T. M., and Goldman-Rakic, P. S. (1989). Connections of the ventral granular frontal cortex of macaques with perisylvian premotor and somatosensory areas: anatomical evidence for somatic representation in primate frontal association cortex. *J. Comp. Neurol.* 282, 293–316. doi: 10.1002/cne.902820210

Preuss, T. M., and Goldman-Rakic, P. S. (1991). Architectonics of the parietal and temporal association cortex in the strepsirhine primate Galago compared to the anthropoid primate Macaca. *J. Comp. Neurol.* 310, 475–506. doi: 10.1002/cne.903100403

Quartarone, A., and Hallett, M. (2013). Emerging concepts in the physiological basis of dystonia. *Mov. Disord.* 28, 958–967. doi: 10.1002/mds.25532

Quartarone, A., and Ruge, D. (2018). How many types of dystonia? pathophysiological considerations. *Front. Neurol.* 9:12. doi: 10.3389/fneur.2018.00012

Raju, D. V., and Smith, Y. (2006). Anterograde axonal tract tracing. *Curr. Protoc. Neurosci.* 1:1.14. doi: 10.1002/0471142301.ns0114s37

Ratchetson, R. A., and Li, C. (1969). Effect of dentate stimulation on neuronal activity in the globus pallidus. *Exp. Neurol.* 24, 298–309. doi: 10.1016/0014-4886(69)90023-5

Reiner, A., Medina, L., and Veenman, C. L. (1998). Structural and functional evolution of the basal ganglia in vertebrates. *Brain Res. Rev.* 28, 235–285. doi: 10.1016/s0165-0173(98)00016-2

Reiner, A., Veenman, C. L., Medina, L., Jiao, Y., Del Mar, N., and Honig, M. G. (2000). Pathway tracing using biotinylated dextran amines. *J. Neurosci. Methods* 103, 23–37. doi: 10.1016/s0165-0270(00)00293-4

Rektor, I., Bareš, M., Kaňovský, P., and Kukleta, M. (2001a). Intracerebral recording of readiness potential induced by a complex motor task. *Mov. Disord.* 16, 698–704. doi: 10.1002/mds.1123

Rektor, I., Bareš, M., and Kubová, D. (2001b). Movement-related potentials in the basal ganglia: a SEEG readiness potential study. *Clin. Neurophysiol.* 112, 2146–2153. doi: 10.1016/s1388-2457(01)00662-9

Rektor, I., Kanovsky, P., Bares, M., Louvel, J., and Lamarche, M. (2001c). Event-related potentials, CNV, readiness potential, and movement accompanying potential recorded from posterior thalamus in human subjects. A seeg study. *Neurophysiol. Clin.* 31, 253–261. doi: 10.1016/s0987-7053(01)00262-3

Rektor, I., Fève, A., Buser, P., Bathien, N., and Lamarche, M. (1994). Intracerebral recording of movement related readiness potentials: an exploration in epileptic patients. *Electroencephalogr. Clin. Neurophysiol.* 90, 273–283. doi: 10.1016/0013-4694(94)90145-7

Rektor, I., Kaňovský, P., Bareš, M., Brázdil, M., Streitová, H., Klajblová, H., et al. (2003). A SEEG study of ERP in motor and premotor cortices and in the basal ganglia. *Clin. Neurophysiol.* 114, 463–471. doi: 10.1016/s1388-2457(02)00388-7

Rektor, I., Louvel, J., and Lamarche, M. (1998). Intracerebral recording of potentials accompanying simple limb movements: a SEEG study in epileptic patients. *Electroencephalogr. Clin. Neurophysiol.* 107, 277–286. doi: 10.1016/s0013-4694(98)00073-x

Rizzo, G., Milardi, D., Bertino, S., Basile, G. A., Di Mauro, D., Calamuneri, A., et al. (2018). The limbic and sensorimotor pathways of the human amygdala: a structural connectivity study. *Neuroscience* 385, 166–180. doi: 10.1016/j.neuroscience.2018.05.051

Saunders, A., Oldenburg, I. A., Berezovskii, V. K., Johnson, C. A., Kingery, N. D., Elliott, H. L., et al. (2015). A direct GABAergic output from the basal ganglia to frontal cortex. *Nature* 521, 85–89. doi: 10.1038/nature14179

Schmahmann, J. D., and Caplan, D. (2006). Cognition, emotion and the cerebellum. *Brain* 129, 290–292. doi: 10.1093/brain/awh729

Schofield, B. R. (2008). Retrograde axonal tracing with fluorescent markers. *Curr. Protoc. Neurosci.* 1:1.17. doi: 10.1002/0471142301.ns0117s43

Sesack, S. R., and Grace, A. A. (2010). Cortico-basal ganglia reward network: microcircuitry. *Neuropsychopharmacology* 35, 27–47. doi: 10.1038/npp.2009.93

Shaikh, A. G., Zee, D. S., Crawford, J. D., and Jinnah, H. A. (2016). Cervical dystonia: a neural integrator disorder. *Brain* 139, 2590–2599. doi: 10.1093/brain/aww141

Shen, G., Nan, G., Shin, C. W., Park, H., Lee, K. Y., and Jeon, B. (2016). Combined focal myoclonus and dystonia secondary to a cerebellar hemorrhage: a case report. *BMC Neurol.* 16:228. doi: 10.1186/s12883-016-0745-6

Shibasaki, H., and Hallett, M. (2006). What is the bereitschaftspotential? *Clin. Neurophysiol.* 117, 2341–2356. doi: 10.1016/j.clinph.2006.04.025

Simpson, E. H., Kellendonk, C., and Kandel, E. (2010). A possible role for the striatum in the pathogenesis of the cognitive symptoms of schizophrenia. *Neuron* 65, 585–596. doi: 10.1016/j.neuron.2010.02.014

Smith, Y., Bolam, J. P., and von Krosigk, M. (1990). Topographical and synaptic organization of the GABA-containing pallidosubthalamic projection in the rat. *Eur. J. Neurosci.* 2, 500–511. doi: 10.1111/j.1460-9568.1990.tb00441.x

Smith, Y., and Galvan, A. (2018). Non-human primate research of basal ganglia and movement disorders: advances and challenges. *J. Neural Transm.* 125, 275–278. doi: 10.1007/s00702-018-1849-5

Smith, Y., and Kieval, J. Z. (2000). Anatomy of the dopamine system in the basal ganglia. *Trends Neurosci.* 23, S28–S33. doi: 10.1016/s1471-1931(00)00023-9

Smith, Y., and Parent, A. (1988). Neurons of the subthalamic nucleus in primates display glutamate but not GABA immunoreactivity. *Brain Res.* 453, 353–356. doi: 10.1016/0006-8993(88)90177-1

Smith, Y., Wichmann, T., and DeLong, M. R. (2014). Corticostriatal and mesocortical dopamine systems: do species differences matter? *Nat. Rev. Neurosci.* 15:63. doi: 10.1038/nrn3469-c1

Snider, R. S., Maiti, A., and Snider, S. R. (1976). Cerebellar pathways to ventral midbrain and nigra. *Exp. Neurol.* 53, 714–728. doi: 10.1016/0014-4886(76)90150-3

Sporns, O. (2011). The human connectome: a complex network. *Ann. N Y Acad. Sci.* 1224, 109–125. doi: 10.1111/j.1749-6632.2010.05888.x

Stephenson-Jones, M., Ericsson, J., Robertson, B., and Grillner, S. (2012). Evolution of the basal ganglia: dual-output pathways conserved throughout vertebrate phylogeny. *J. Comp. Neurol.* 520, 2957–2973. doi: 10.1002/cne.23087

Stinear, C. M., Coxon, J. P., and Byblow, W. D. (2009). Primary motor cortex and movement prevention: where stop meets go. *Neurosci. Biobehav. Rev.* 33, 662–673. doi: 10.1016/j.neubiorev.2008.08.013

Strafella, A. P. (2019). Imaging tools to map *in vivo* the human brain. *Mov. Disord.* 34, 931–933. doi: 10.1002/mds.27732

Szabó, J. (1979). Strionigral and nigrostriatal connections anatomical studies. *Appl. Neurophysiol.* 42, 9–12. doi: 10.1159/000102324

Testut, L., and Latarjet, A. (1971). *Anatomia Umana.* 5th Edn. Torino: UTET.

Tewari, A., Fremont, R., and Khodakhah, K. (2017). It's not just the basal ganglia: cerebellum as a target for dystonia therapeutics. *Mov. Disord.* 32, 1537–1545. doi: 10.1002/mds.27123

Tournier, J. D., Calamante, F., and Connelly, A. (2007). Robust determination of the fibre orientation distribution in diffusion MRI: non-negativity constrained super-resolved spherical deconvolution. *Neuroimage* 35, 1459–1472. doi: 10.1016/j.neuroimage.2007.02.016

Tuch, D. S., Reese, T. G., Wiegell, M. R., and Wedeen, V. J. (2003). Diffusion MRI of complex neural architecture. *Neuron* 40, 885–895. doi: 10.1016/s0896-6273(03)00758-x

Ugolini, G. (2011). Rabies virus as a transneuronal tracer of neuronal connections. *Adv. Virus Res.* 79, 165–202. doi: 10.1016/B978-0-12-387040-7.00010-X

Ugolini, G., Kuypers, H. G. J. M., and Simmons, A. (1987). Retrograde transneuronal transfer of Herpes simplex virus type 1 (HSV 1) from motoneurones. *Brain Res.* 422, 242–256. doi: 10.1016/0006-8993(87)90931-0

Van Haeften, T., and Wouterlood, F. G. (2000). Neuroanatomical tracing at high resolution. *J. Neurosci. Methods* 103, 107–116. doi: 10.1016/s0165-0270(00)00300-9

Watabe-Uchida, M., Zhu, L., Ogawa, S. K., Vamanrao, A., and Uchida, N. (2012). Whole-brain mapping of direct inputs to midbrain dopamine neurons. *Neuron* 74, 858–873. doi: 10.1016/j.neuron.2012.03.017

Wedeen, V. J., Hagmann, P., Tseng, W. Y. I., Reese, T. G., and Weisskoff, R. M. (2005). Mapping complex tissue architecture with diffusion spectrum magnetic resonance imaging. *Magn. Reson. Med.* 54, 1377–1386. doi: 10.1002/mrm.20642

Wessel, J. R., Ghahremani, A., Udupa, K., Saha, U., Kalia, S. K., Hodaie, M., et al. (2016). Stop-related subthalamic β activity indexes global motor suppression in Parkinson's disease. *Mov. Disord.* 31, 1846–1853. doi: 10.1002/mds.26732

Wiener, M., Turkeltaub, P., and Coslett, H. B. (2010). The image of time: a voxel-wise meta-analysis. *Neuroimage* 49, 1728–1740. doi: 10.1016/j.neuroimage.2009.09.064

Yagmurlu, K., Middlebrooks, E. H., Tanriover, N., and Rhoton, A. L. (2016). Fiber tracts of the dorsal language stream in the human brain. *J. Neurosurg.* 124, 1396–1405. doi: 10.3171/2015.5.JNS15455

Conflict of Interest: The authors declare that the research was conducted in the absence of any commercial or financial relationships that could be construed as a potential conflict of interest.

Advantages of publishing in Frontiers

OPEN ACCESS
Articles are free to read for greatest visibility and readership

FAST PUBLICATION
Around 90 days from submission to decision

HIGH QUALITY PEER-REVIEW
Rigorous, collaborative, and constructive peer-review

TRANSPARENT PEER-REVIEW
Editors and reviewers acknowledged by name on published articles

Frontiers
Avenue du Tribunal-Fédéral 34
1005 Lausanne | Switzerland

Visit us: www.frontiersin.org
Contact us: info@frontiersin.org | +41 21 510 17 00

REPRODUCIBILITY OF RESEARCH
Support open data and methods to enhance research reproducibility

DIGITAL PUBLISHING
Articles designed for optimal readership across devices

FOLLOW US
@frontiersin

IMPACT METRICS
Advanced article metrics track visibility across digital media

EXTENSIVE PROMOTION
Marketing and promotion of impactful research

LOOP RESEARCH NETWORK
Our network increases your article's readership